Addis Ababa University

Addis Ababa Institute of Technology

School of Electrical and Computer Engineering (SECE)

Development of Power System Dynamic Security Analysis Tools Based on the Most Current Snapshot from SCADA Data

By: Teshome Lindi E-mail: teshelindi@gmail.com

Supervisor: Dr.Ing. Fekadu Shewarega

(University of Duisburg-Essen, Duisburg, Germany)

A PHD Dissertation

Submitted to the

School of Electrical and Computer Engineering Addis Ababa Institute of Technology Addis Ababa University

in Partial fulfillment the requirement of the

Degree Doctor of Philosophy

In

Electrical Power Engineering

Mar. 2025

Addis Ababa, Ethiopia

Approval Page

SCHOOL OF ELECTRICAL AND COMPUTER ENGINEERING

ADDIS ABABA INSTITUTE OF TECHNOLOGY

ADDIS ABABA UNIVERSITY

I hereby declare that this Ph.D. Research/ Dissertation contain no material that has been submitted previously, in whole or in part, for the award of any other academic degree. Except where otherwise indicated, this Ph.D. Research/ Dissertation are my own original work.

Teshome Lindi	_____	_____
Ph.D. Student	*Signature*	*Date*

As thesis research advisor, I hereby notify that I read and evaluated this Ph.D. Dissertation prepared, under my guidance by Teshome Lindi Development of Power System Dynamic Security Analysis Tools Based on the Most Current Snapshot from SCADA Data. I recommend that it be accepted as fulfilling the dissertation requirement.

Dr. Ing Fekadu Shewarega		*17.06.2025*
Advisor	*Signature*	*Date*

As members of the examining board of the PhD dissertation presentation, we certify that we have read and evaluated the Ph.D. Dissertation prepared by Teshome Lindi, recommended that ***it be accepted as fulfilling the dissertation requirement.***

_____	_____	
Name of chairman Signature		*Date*

_____	_____	
Name of internal examiner Signature		*Date*

_____	_____	
Name of external examiner Signature		*Date*

_____	_____	
Post Graduate Associate Director	*Signature*	*Date*

Declaration

I hereby declare that this Ph.D. Research/Dissertation contains no material that has been submitted previously, in whole or in part, for the award of any other academic degree. Except where otherwise indicated, this Ph.D. Research/Dissertation is my own original work.

Ph.D Dissertation

Submitted by:

Teshome Lindi _____ _____

Signature Date

Approved by:

Supervisor: Dr. Ing. Fekadu Shewarega 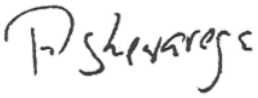 17.06.2025

Signature Date

Abstract

Currently power systems become increasingly complex, driven by the continuous increasing load demands and growing interconnection of stochastic generations. Furthermore, the introduction of demand response mechanisms to balance generation and consumption is under active investigation. These developments make system operating conditions less predictable, leading to significant challenges in ensuring operational security. To address these challenges, both static and dynamic security analysis tools are essential. However, until recently, efforts in security analysis have predominantly emphasized static methods. The focuses of this thesis is to develop effective and robust tools and techniques for dynamic security analysis in near real-time environments.

One of the core elements of near real-time dynamic security assessment tools is contingency screening and ranking. Fast power system contingency screening and ranking technique has been developed in this thesis, and its performance is evaluated using benchmark test cases. The approach analyzes the transient stability of the power system against a specified list of credible contingencies. Based on the most current snapshot from Supervisory Control and Data Accusation (SCADA) data transient stability is simulated for each credible contingency and Transient Stability Index (TSI) is evaluated as the normalized weighted sum of squares of error at every simulation time step based on both machine's state variables such as rotor angle deviations, rotor angular speed, etc and machine's bus complex bus voltages (magnitude V and angle θ). Finally contingencies are ranked based on these TSI and the worst contingency is identified for the next detail assessment. This proposed method not only reduces the time performances but also improves the accuracy of resulting indices. The method is tested on IEEE 9bus and 11bus test systems. Test results reveal that the proposed method is faster, robust and can be used in near real-time dynamic security assessment tools. .

Determining if all synchronous generators remain in synchronism after subjected to large disturbance is significantly important to maintain power system transiently stable. To achieve this requirement, the transient stability assessment tool that estimate the systems distance to transient stability boundary for the contingency under consideration is required. In this thesis critical clearing time (CCT) is used to estimate the distance at a given particular operating point from transient stability boundary. Using the proposed contingency screening and ranking technique the worst contingency is identified based on their TSI. Then critical clearing time

(CCT) is evaluated for this contingency to represent the systems distance to transient stability boundary. CCT is normally calculated by uniformly increasing the fault clearing time until the system instability using traditional PTDS. A novel transient stability assessment (TSA) tool that avoids the time-consume due to the repetitive step increase fault duration and high computational burden resulting from using traditional numerical integration method and classical differential transformation method is developed and introduced in this thesis. This tool combines PTDS based on Adaptive step-size Differential Transformation Method (AsDTM) by cross cut technique to evaluate CCT for the worst contingency. Its performance efficiency and accuracy is assessed and validated using two standard test cases.

Effective dynamic security analysis (DSA) tools can identify harmful or insecure operating conditions and recommend preventive control actions to restore stability and security within the system. Fast and robust tools that check and enhance power system dynamic performance based on combined power system time domain simulation (PTDS) and particle swarm optimization (PSO) is proposed here. The method aims at modifying the operating conditions of a power system so as to make it able to withstand severe contingency that would drive it to instability. Conventional time domain simulation method requires high computational efforts however, to support control room operators in taking preventive measures required within timeframe, time domain simulation with improved performance efficiency is needed. A novel power system time domain simulation method which is based on adaptive order and step-size differential transformation (AOSDTM) with significantly better performance efficiency is proposed. The worst contingency is identified based on the proposed contingency screening and ranking technique. Transient stability criteria are checked for this worst contingency by the system operators maintaining system constraints. The critical fault clearing time is used as key feature for monitoring power system transient stability during generation rescheduling process. The proposed and developed tools are tested and validated by using standard IEEE test systems. The test results show that the proposed method is fast and robust and can be used in a near real time power system DSA tools

Key words Dynamic security analysis, Time domain simulation, Transient stability assessment, Contingency screening, Differential transformation method, Preventive control

Acknowledgment

First and foremost, I thank Saint Mary with her begotten Son for all the blessings and giving me the strength and ability to complete this long journey.

Beginning with my earliest years, without my family ability to teach me, I would not be here today. Thus, I would like to express my heartfelt gratitude to my parents for their unflinching love and genuine interest in my education during a time when educational opportunities were scarce. Not only at that time, even in the present situation has it seemed like a dream. Without their genuine interest and inspiration in those years, I am confident that I would not be where I am today. Therefore, I could reach this stage of my life primarily because of my mother and father's absolute unconditional love, hard work, and sacrifice.

My sincere thanks go to my advisor, Dr.Ing.Fekadu Shewarega, who has introduced me with the idea of working on the area of dynamic security assessment. In addition, I would like to pass my deepest gratitude for his valuable guidance, immediate responses, constructive comments, encouragement and professional expertise without which this work could have not been completed.

I am forever grateful to my wife Buzayehu Andualem and my daughters Henoke, Dagim, Abay, Amanueal, and Yohans for their unconditional support and constant encouragement. I dedicate everything that I have accomplished to them. Words fail me in expressing my love to them. In particular, I owe my deepest thanks to my lovely wife, Buzayehu, for her endless love, countless sacrifices, and timely encouragement.

I would like to express my appreciation and gratitude to my true brother Mr. Shemelis R, and his beloved families for their kind, unconditional, and continuous support and encouragement throughout the course of my study.

Last but not least, I want to thank my friends, particularly Mr. Abebe A., Dr. Teweligne K., Mr. Mengesha H., and Mr. Damot T., for their continuous support and encouragement throughout the course of my study.

Table of Contents

List of Figure

List of Tables

List of Abbreviations

GHz Giga Hertz

Rk4 Fourth Order Rangkuta

List of Acronyms

AsDTM Adaptive step-size Differential Transformation method

AOSDTM Adaptive Order & Step-size Differential Transformation method

CPU Central Processing Unit

DAE Differential Algebraic Equations

DSA Dynamic Security Assessment

DT Differential Transformation

DTM Differential Transformation method

TS Transient Stability

SCADA Supervisory Control And Data Acquisition

GB Giga Bite

RAM Random Access Memory

RES Renewable Energy Source

ZIP Constant impedance, Constant current, Constant power Load

PTDS Power system time domain simulation

TSS Transient stability simulation

CCT Critical Clearing Time

EMS Energy Management System

TSO Transmission System Operators

TEF Transient Energy Function

EEP Ethiopian Electric Power

SIME Single Machine Equivalent

PMU Phasor Measurement Unit

MDO Minimum Damping of Oscillation

OAS Oscillatory Stability Assessment

ANN Artificial Neural Network

WAMS Wide Area Monitoring System

IEEE Institute of Electrical Electronic Engineering

PES Power Engineering Society's

DSAPS Dynamic Security Assessment Processing System

FACTS Flexible Alternating Current Transmission System

ACS Anticipatory Computing System

List of Symbols

E Local error estimate

EE Estimate of the maximum of power system state variable's &bus voltage's last order coefficient terms

T Simulation Period

D Damping constant

E'd D-axis machine internal voltage

E'q Q-axis machine internal voltage

Efd Field excitation voltage

H Machine inertia constant

Id d-axis stator current

Iq q-axis stator current

KA Amplifier gain

KE Exciter constant

P Active power

PC Speed governor input power setting

PCH Output power of steam chest

PSV Output power of steam valve

Q Reactive power

Rf Rate feedback in exciter

RD Speed regulation quantity (droop)

S Complex power

SE Saturation constant

TM Mechanical torque

T Time

V Bus voltage magnitude

VR Exciter input

Vref Input reference voltage

X Reactance

Y Admittance

Z Impedance

θ Bus voltage angle

ω Angular speed

ωs Nominal angular speed

δ Machine rotor angle

List of Publications

The publications that emanate from this PHD research are listed as follows

[1.] Teshome.L. Kumissa and F. Shewarega, "Fast Power System Transient Stability Simulation," Energies, vol. 16, 2023.

[2.] Kumissa, T.L.; Shewarega, F. Transient Stability-Based Fast Power System Contingency Screening and Ranking. Electricity 2024, 5, 947–971. **https://doi.org/10.3390/** electricity 5040048

[3.] Teshome Lindi & Fekadu Shewarega (13 Jun 2024): Adaptive order and step-size differential transformation method-based power system transient stability simulation, Australian Journal of Electrical and Electronics Engineering, DOI: 10.1080/1448837X.2024.2359210

CHAPTER ONE: Introduction

1.1. Background

Reliable electricity supply is foundational to all economic and societal activities in modern societies [**1**]. The consequences of large blackouts therefore are all too obvious to merit any further elaboration. Ensuring secure operation of the system during widely varying loading scenarios or following possible unforeseen events represents an immense challenge to the system operator. To assess the security risk correctly and to initiate any necessary corrective measures, the operator needs to have situational awareness at all times, know the stability margins and find the most effective solution in the event of stability problems often under stressful situations in which every split second counts.

The power system worldwide has undergone major structural and organizational changes in the past decades, which, on the one hand, resulted in a significant operational efficiency but, on the other hand, created immense challenges in terms of operational security [**2**]. Many power system networks now cover large geographic areas sometime spanning whole continents. This interconnection has offered a number of benefits, such as sharing reserves both for a normal operation and during emergency conditions, dividing the responsibility for the frequency regulation among larger number of generators and possibility to generate the power in the economically optimum areas. These operational benefits come at the expense of some new problems, for example, the resulting additional vulnerability due to the risk of a disturbance spreading over large distances and thus affecting vast service areas.

Another change which affects all countries (but developing countries to a larger extent) is the continuously growing load demand. This has forced power systems to operate more and closer to stability limits, thus reducing the security margin. Power systems operated near their stability limits may lead to the appearance of power system oscillations and instabilities during large disturbances. The increase in distributed generation, renewable energies-based power generation, smart grid technologies and the deployment of new transmission equipment is the other new development [**3**]. The result is that two conflicting trends can be observed in almost any country of the world: one positive and the other negative. The increasing number of active network elements opens-up new possibilities for remedial actions in case of stability problems [**3**]. At the same time, this coupled with the ongoing liberalization of the electricity industry and with it the

entry into the scene of new non-utility actors, which consider electricity just another commodity to be traded, increase the risk of blackouts.

Security analysis refers to the analysis and quantification of the degree and risk in a power system's ability to survive imminent disturbances (contingencies) without interruption to customer service [**4**] [**5**].The security analysis of power systems includes steady-state security analysis (SSSA) and dynamic security analysis (DSA). SSSA analyses the system steady state operating points between dynamic transitions, whereas DSA focuses on the security of system dynamics in various timescales, from transients of several seconds to slow dynamics of several minutes or even hours. DSA is defined in [**4**] as evaluation necessary to determine if a power system can satisfy established reliability and security standards during both transient and steady-state conditions for a selected list of contingencies.

Whilst security monitoring until recently focused only on static security assessments, these new developments forced system operators to deploy more and more dynamic security assessment tools that monitor problems such as an uncontrollable voltage decline, generator over-speed (loss of synchronism), or un-damped oscillatory behavior. Power systems steady state stability and its margin is one of the basic problems ensuring the security of power system operation. Because steady state stability analysis always calculates a large number of cases with different flow and network configuration, the estimated stability limit is usually too conservative to normal states, and at some abnormal state it may lead to incorrect result [**6**]. Hence to guarantee all aspects of security, both steady-state and dynamic security analysis tools should be deployed in system operation and planning environment.

Dynamic security analysis tools are not state of the art in conventional energy management systems (EMS) [**7**]. A lack of accurate dynamic models, missing guidelines how to use DSA information for system operation, unfamiliarity of control room operators about power system dynamics, and missing concepts how to apply dynamic stability limits are the main hindering aspects for a wider adoption by TSOs [**7**]. The identification of the power system critical limits and instabilities, and determining and application of fast and correct remedial/ preventive actions are keys for realizing the power grid security [**1**]. The objective of the security monitoring subsystem shown in Figure 1-1 is to monitor the system state for a defined list of contingencies in terms of operational security. Power system security can be identified from the power flow change and physical, operating and economic limits. To guarantee all aspects of security, both

steady-state and dynamic security must be combined to address the increasing challenges and state of the art, as depicted in Figure 1-1. It is therefore vital that DSA tools should be deployed to provide the system operator with up to date information on time or on demand. This implies that the need for dynamic security analysis tools is increasing throughout the world [**5**]. In DSA, many security aspects of power system are analyzed, including transmission line thermal loading, voltage, rotor angles and frequency deviation, which is very computationally burdensome.

In DSA tools, many security aspects of power system are analyzed, including transmission line thermal loading, voltage, rotor angles and frequency deviation, which very computationally burdensome and require many efforts [**2**]. Dynamic security analysis (DSA) can be performed both in off-line and in near real time environments [**2**] [**6**]. It is generally computationally intensive due to the numerical integration involved in evaluating the transient behavior of the system during major disturbances. The analysis may be based on full simulation approach or an approximated approach [**8**] [**9**] [**10**].

In off-line DSA tools, detailed time-domain stability analysis is performed for all credible contingencies and a variety of operating conditions. Off-line DSA is usually used to determine limits of power transfers across important transfer corridors to be used in an operating environment. Since the analysis is performed off-line, there is no severe constraint in terms computation time and therefore detailed analysis can be done for a wide range of conditions and contingencies.

Near real time dynamic security analysis tools consider the most current system operating state from SCADA data. Whenever contingency study is required, the most current snapshot from the SCADA data is used as the basis. A basic near real time DSA framework includes essentially two steps [**5**]. The first involves a rapid screening process to limit the number of contingencies that must be evaluated in detail. This rapid screening process might base on direct methods that do not use numerical integration or computational intelligence or other methods. In addition to giving fast stability evaluation, these methods inherently include a mechanism for assessing the severity of a contingency. That is, if a system is determined to be stable, the applied methods also provide evidence that shows the stability status of the system. This could be usually provided in the form of energy margin or critical fault clearing time (CCT). The process includes a ranking strategy based on these energy margins or CCT. The decision process in which

contingencies are studied in greater detail is included in this first step. Next power system time-domain simulation based on extensive numerical integration to reveal swing trajectories and voltage variations is performed. This is conducted on limited lists of sever contingencies identified during the screening process.

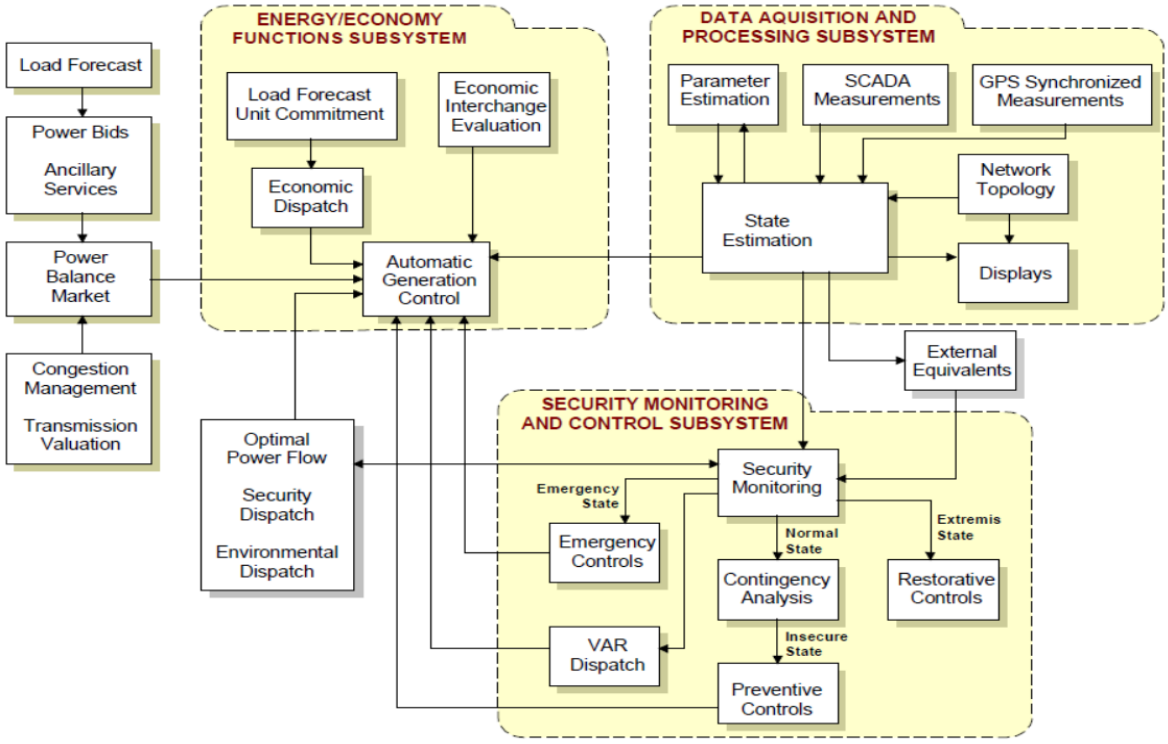

Figure 1-1 Modern energy management system with Combined SSSA and DSA process

1.2. Problem statement

To ensure the continuous secure operation of a system, it is essential to keep system variables, such as line flow ranges and generator loading rates, within acceptable operating limits. If these limits are significantly violated, the system could experience instability related to frequency, voltage, or rotor angle fluctuations in machines. For reliable operation, near real-time tools are necessary to monitor system security, capable of handling a diverse range of network connectivity and generation dispatches during both normal and abnormal conditions [**11**] [**12**]. Given the increasing complexity of power systems due to rising load demands and the growing integration of stochastic generation sources, traditional steady-state security verification is inadequate for ensuring system integrity in all scenarios [**7**].

Power system blackouts such as the case of 2003 incident in the northeastern United States Ontario, and Canada can have significant economic repercussions. This blackout impacted

around 50 million individuals and remains up to four days, resulting in approximated economic destruction ranging from $4 billion to $10 billion (U.S. dollars). [**13**] and blackouts on the EEP national grid from January 2013 to mid-of May 2016, [**14**] has resulted in tremendous societal consequences and substantial economic loss due to the unnerved energy, which accounts for 1,943,431.018 USD for the 38 blackouts during those three and half years. As documented in [**13**] and [**15**] the principal cause of these blackouts was the lack .of situational awareness. Deploying a near real-time DSA tools can aware the system situation at all time and significantly reduce the risk of blackout.

Due to the complexity in modeling and interactions between individual elements or system equipment as well as the computational structure for describing more recent power systems DSA is characterized by complex dynamic behavior. In order to analyze power system dynamic security, complex mathematical model equations are used to represent system components. The representation consists of both static and dynamic characteristics and can be expressed by Differential Algebraic Equations (DAE) (described in Chapter 2). A comprehensive analysis techniques have been evolved, that can split in to 2 major classes as power system time domain simulation method (includes: direct method (such as TEF), numerical integration approach, probabilistic methods, and differential transformation method) and automatic learning technique [**5**].

Most of the existing DSA tools and methods are somewhere in between these two groups. Since power systems consists of thousands of components, dynamical simulation is very time consuming. Commercially available DSA tools solves differential equations by a numerical integration method, and the algebraic network equations by a numerical iteration at each integration step [**16**] [**17**] [**8**]. These methods may suffer from huge computation burdens caused by the iterations after each integration step for the convergence of the network equations and the large number of integration steps to ensure the accuracy and numerical stability of solving the differential equations. Moreover, the computation speed can further deteriorate when system states change significantly, or the system model has strong nonlinearity since the network equation is more difficult or even fails to converge by numerical iteration methods. The computation time could be further increased if a more detailed system model is considered.

Approaches relying on offline databases offer a level of general conclusion, may not consistently and accurately assess security and stability [**18**]. Therefore, techniques that depend on data

mining (DM), DTs, or automated training methods are excluded from consideration in this thesis. Modern power system incorporates a large number stochastic generations (which are based on renewable energy sources) and this makes difficult to predict the system condition. Similarly, approaches such as energy function method and sensitivity analysis proposed by [**19**] [**20**] [**21**] [**22**] [**23**] [**24**] provide a quantitative measure which indicate the degree of system stability based on energy margin or stability indices but these required computational efforts and restrictions regarding modeling details. However, DSA tools with improved performance efficiency and accuracy is significantly demanding in today's power system operational planning.

Even though, DSA tools developed based on time domain simulation by using conventional numerical integrations method is relatively robust, the method still require advancement in their computational burden and speed to be applied as efficient and robust near real-time analysis tools [**18**]. Improved performance efficiency and accuracy are possibly achieved only with advanced in conventional PTDS methods and use of system model details, through advanced programs and technics those relatively better to provide accurate simulation of different system conditions as power flow, dynamic stability, short circuit analysis and protective relays coordination [**15**]. Results from time domain analysis can also help to decide on a time scale for the instabilities and control strategies, but it is difficult to find a best control strategy from simulations alone, an optimization method may pave the way for a theoretical solution with rigorous justification.

The aim of this thesis is to develop fast and robust dynamic security analysis and monitoring tools based on the most current snapshot from the SCADA data. Fast dynamic security analysis tools with advanced in power system time domain simulation based on differential transformation method, which can perform in the timeframe is developed. The developed tools include efficient and robust tools for power system contingency screening and ranking, detail transient stability assessment (TSA) and transient stability based dynamic security enhancement, which are verified as a core elements of fast and robust dynamic security analysis tools in [**5**]. Dynamic security analysis deals with different types of power system stability conditions. However, this thesis investigates and develops dynamic security analysis tools that only analyzes and recommend possible preventive measures to maintain secure operation with respect to transient stability phenomena.

1.3. Research objectives

1.3.1. General objective

The main objective of this thesis is to develop fast and relatively accurate DSA tools that help the system operators to check and make sure that at every given operating condition, for every credible contingency the system will survive or if the system is transitioning into insecure state and recommend proper preventive control measures if required.

Therefore, main objective is to develop efficient and robust DSA tools that can

- Read the most current snapshot form SCADA data
- Perform power flow analysis and initialize the dynamic system
- Perform transient stability simulation based power system contingency screening and ranking
- Perform power system transient stability assessment
- Perform PSO based optimal generation rescheduling to recommend remedial measures that enhance power system dynamic security, if any

1.3.2. Specific objectives

- To organize and structure dynamic and static data for power system analysis.
- To develop a dynamic modeling framework for near real-time power system Dynamic Security Assessment (DSA).
- To create current balance models for steady-state power system analysis.
- To utilize MATLAB and MATPOWER software packages in developing tools for assessing static and dynamic behaviors of power systems.
- To implement MATLAB algorithms for transient stability analysis, including DTM, Rk4, AsDTM, and AOSDTM methods, ensuring modular and efficient code organization.
- To design algorithms for interfacing MATPOWER, solvers, dynamic/static data, and models within the MATLAB environment.
- To develop a contingency screening and ranking tool for early identification of the most critical scenarios.
- To create AsDTM and AOSDTM-based tools for transient stability simulation in power systems.
- To design a dynamic analysis tool that recommends remedial measures to enhance transient stability.
- To prepare and apply standard IEEE test systems for benchmarking and validation.
- To rigorously test and validate the developed DSA tools using standard IEEE test systems.

1.4. Literature review

All economic and social activities of modern societies are very dependent on the availability of electric supply system and therefore, reliable electricity supply is significantly linked to the modern society's life. To supply this continuously growing demand, the size and complexity of the power supply systems with stochastic generation (due to Renewables energy system) is increasing. This pushes power systems to operate more and more closely to stability limits [**25**]. Inability to detect system instability behavior in a sufficient time interval to launch the corrective actions could result in a system failure at one location on system that can quickly degenerate in to cascading failures, which is usually mechanism for large collapses or blackout of the system. Fast and accurate analysis of system security is of great significance for safe and stable operation of power system. To identify any insecure contingency before it happens, time domain

simulation is expected to be transitioned from offline or day-ahead studies to the real time operation environment. The power industry and the research community are seeking next generation tools which are more powerful for power system dynamic security analysis.

According to the report by [**5**]. Traditionally achieved security solely through off-line analyses using forecasted information has proven inadequate and often impractical in the new environment as a result, on-line DSA has emerged in which a snapshot of the current system is obtained and is used to conduct security assessment, which reduces the need for prediction of system conditions and therefore is expected to provide more accurate assessments. However, since all data must be assimilated in near-real-time, and computations must be conducted automatically with little or no human intervention (and in a tightly constrained cycle time),

This report has documented some fifteen DSA tools, state-of-the-art installations and the existence of numerous others which are either in-service or under development, that include assessment of voltage security, transient security, and small signal security with the range of assessment capabilities as determination of critical contingencies, transfer limits, and determination of remedial measures necessary to ensure security. It also indicates that the computational methods used for each type of security assessment depends on the specific requirements (speed, accuracy, reliability), system characteristics(large, small, meshed, radial, etc) and, in some cases, the techniques available in the state-of the-art tools used.

In [**26**], the authors discuss the advanced functions of the dynamic security analysis tools implemented in Brazil's ONS. As noted in [**26**], this system employs both detailed TDS and direct techniques. Traditionally, assessing stability through TDS necessitates visual inspection of results. However, the authors have replaced this inspection requirement by using numerical energy functions alongside a modified SIME approaches to calculate stability margins, identify instability, and allow termination of simulations before expected time. The enhancements to the dynamic security analysis functions primarily focus on the transient stability assessment technics, where the earliest SIME approach has been refined. This modified SIME version enhances both the speed and accuracy of stability assessments for stable cases. However modified version of SIME is still depends on model simplification and full TDS is not conducted. These limit the robustness of the proposed method.

In [**27**], recent achievements in research on dynamic security analysis based on the TEF methods are discussed. They presented updated near real-time DSA tools and implement at TEPCO in Japan. This updated DSA tools consists of 2 core functions. The first function is responsible to perform filtering of power system contingency under known operating condition. Contingencies are then categorized, and harmless contingencies are eliminated from further consideration. Harmful cases are transferred to the second function that conducts detailed TDS. To effectively filter and categorize the potential contingencies as whole, the authors introduced an enhanced version of the boundary of stability region based control of unstable equilibrium point classifiers [**28**]. Every classifier is tailored to screen out contingencies based on specific features, such as their severity. The second function performs boundary of stability region based control of unstable equilibrium point led TDS for each harmful/uncertain contingency, as elaborated by [**29**]. The method involves executing detailed TDS, with the output used to assess stability and determine stability margins.

A novel method for dynamic security analysis based on the measured data by PMU along with DT created offline is introduced by [**30**]. This approach processes near real time data for the upcoming 24 hours, which includes various operating conditions linked to load profiles and generation patterns based on unit commitments. These datasets facilitate comprehensive TDS of N−1 and credible N−K contingencies. The results from these simulations are stored in a database to train DT. Potential attributes (PAs) that reflect the system's dynamic behavior are identified using this DT. Additionally, thresholds for the PAs are established based on the simulation data and the DT. Unlike the conventional terminal node based DT approach, the authors propose a path-based DT method. In this method, insecurity scores are calculated for each path within the DT, and acceptable limits for these scores are defined. During real-time operation, phasor measurements units are employed to assess the critical attributes and these values are used to trace corresponding paths in the decision tree. If any insecurity score surpasses the set threshold and the related contingency is deemed likely, appropriate preventive actions can be planned and implemented.

An innovative DTs based approach for dynamic security analysis and preventive control technique is presented by [**31**]. This methodology involves training of 2 decision trees daily, utilizing a database of power system simulations and forecasted data for a day. The first decision tree, called the observation decision tree, employs measurable variables to supervise the system's

condition and select series security threats. The second tree, known as the preventive decision tree, focuses on controllable variables to provide real-time decision support for preventive measures. During online operations, real-time measurements are compared against predefined thresholds in the ODT. If a threshold is breached, the data are directed to the preventive decision tree, which determines the most effective preventive control strategy concerning generation shifts. System security is assessed using straightforward security indices, including transient security indices based on the maximum angular separation of generators. Additionally, a third approach utilizing DT is presented in [**32**]. Emphasis is given for mitigating the impacts of missed PMU measurements. In this method, multiple small decision trees are trained offline and subsequently re-evaluated with new cases in near real-time. During real-time operation, the method employs wide-area PMU measurements, acknowledging that some measurements may be absent. A boosting algorithm is used to assign weights to the viable small decision trees before they are combined.

Moreover, the authors of [**33**] presented a linear method for risk-based dynamic security analysis. They introduce a tool that quantifies total system risk, calculated as the sum of risks associated with each contingency. The risk for a specific contingency is computed by multiplying the probability of its occurrence, the probability related to its stability margin, and its severity. Severity is defined by a linear function that relates to the ratio of critical fault clearing time to actual fault clearing time. The stability margin probability is influenced by uncertainties, such as those stemming from power consumption forecasts. The results indicate that this linear approach significantly outperforms other risk assessment methods in terms of computational efficiency.

The authors of [**34**] developed a methodology for on-line identification of power system dynamic signature based on incoming system responses from Phasor Measurement Units (PMUs) in Wide Area Measurement Systems (WAMS). This Author also used a data mining techniques in the methodology to convert real-time monitoring data into transient stability information and the pattern of system dynamic behavior in the event of instability.

The authors of [**35**]developed algorithm to determine Transient stability margin using power swing-based energy margin (SM), which is a stability margin based on the energy exchange in each power swing during transients and the determination of stability while computing CCT can be based on either SM .they were also suggested E-SIME techniques for closed loop real time

emergency control. The author of [**36**] proposed an energy function approach to assess power system transient stability impacts following increased penetration of asynchronous generation plants. In this paper asynchronous wind farm generation was considered as an equivalent conventional synchronous generator with negligible inertia. Based on this approach he assessed single machine infinite system and three machine nine bus test system to compute critical energy and critical fault clearing time using potential energy boundary surface method and evaluated the result gained. He also developed a new representation of plotting contours of critical clearing times on inertia space to enables estimation of additional inertia required for a system due to inertia reduction from asynchronous generators.

A periodic method of analyzing small-signal rotor angle stability, which is utilized to supervise the stability boundary and calculate the stability margin of a given generator, is presented by authors of [**37**]. If the stability margin of a specific generator drops lower than specified security limit, the approach determines generation re-scheduling measure to bring back the system to normal operation state.

The author of [**38**] proposed the architecture of dynamic security assessment processing system (DSAPS) to address dynamic security assessment (DSA) giving a special focus on low-probability, high-consequence events. He introduced a trajectory sensitivity analysis and reviewed its applications in power system. To assess transient voltage dips quantitatively using trajectory sensitivities, it presented an index. Then the framework of anticipatory computing system (ACS) for cascading defense is presented as an important function of DSAPS. ACS addresses various security problems and the uncertainties in cascading outages. Corrective control design is automated to mitigate the system stress in cascading progressions. The corrective controls introduced in the dissertation include corrective security constrained optimal power flow, a two-stage load control for severe under-frequency conditions, and transient stability constrained optimal power flow for cascading outages.

The authors of [**37**] proposed SIME method is further improved through reduction of model detail for synchronous generator and by developing a new coupling coefficient to identifying critical machine cluster and used reliably to evaluate the first swing transient stability of a power system in its present state, considering a defined list of credible contingencies.

The authors of [**39**] proposed a decision support tool for transient stability preventive control contributing to increased situation awareness of control room operators by providing additional information about the state of the power system in terms of transient stability, time domain approach is used to assess the transient stability for potentially critical faults. Potential critical fault locations are identified by a critical bus screening through analysis of pre-disturbance steady-state conditions.

The author of [**40**] developed a tool for assessment of power system stability and design a framework for enhancing system stability based on the investigation of the dynamic behavior of the system and a market based rescheduling strategy that increases the stability margin was proposed. System stability is investigated by simulating a set of critical contingencies to determine whether the disturbances will result in any unsafe operating conditions and extract the necessary information to classify system states. The classification is based on the computation of CCT for transient stability assessment (TSA) and the minimum damping of oscillation (MDO) for power system oscillatory stability assessment (OSA). An artificial neural network (ANN) is designed to serve as accurate and fast tool for dynamic stability assessment (DSA). Fast response of ANN allows system operators to take suitable control actions to enhance the system stability and to forestall any possible impending breakup of the system. Particle swarm optimization is used as an optimization tool to search for the optimal solution to enhance the system stability with a minimum cost. The handling of all system constraints including stability constraints is achieved using a self-adaptive penalty function. However, since this method relies on offline databases, it faces challenges due to the huge array of possible operating conditions and also due to the increasing complexity, stochastic and highly non-linear behaviors of the power system network, there exists many uncertainties.

The author of [**41**] proposed a novel non-iterative and fully analytical method to solve power system differential algebraic equations (DAEs) to simulate power system dynamic behavior. This is based on the differential transformation method, a mathematical tool that can obtain power series coefficients by transformation rules instead of calculating high order derivatives. This method approximates the solution of complex power system differential algebraic model equations as a truncated power series of time. The approach is flexible in handling power system with any model detail without limitations. It also requires less computation effort and simulation time cost. However, differential transformation method gives a good approximation to the true

solution in a very small region. To extend the region of solution convergence and improve accuracy of the results, DTM is applied at equal and fixed time interval as proposed by [**42**] [**43**] [**44**], up to the end of simulation period. In some cases, a very small sub division of interval is required with this method, which results in more computational effort and increased simulation time cost.

Table 1-1 Summary of the Literature Reviews (strengths and limitations)

Authors of [26], [27],[35], [36]	DSA technic	Strength	Limitation
	Employ numerical energy functions along with an adapted single machine equivalent technique to calculate stability margins.	Provide fast quantitative measure which indicate the degree of system stability based on energy margin or stability indices	Required extensive computational efforts and restrictions regarding modeling details.
Authors of [28],[29]	Detailed TDS analysis is conducted, and the results are utilized to assess stability.	Provide accurate solution and suitable for offline analysis	Computational intensive so cannot be used in near real-time DSA
Authors of [30], [31], [32], [34], [39]	Proposed dynamic security assessment and determine preventive measures that incorporate PMU and DTs developed offline.	Relatively faster assessment approach	Since this method relies on offline databases, it is challenged by the extensive range of operating conditions
Authors of [33]	Probabilistic method of DSA	Fast assessment method	As the system complexity increases robustness of the method significantly reduces
Authors of [35]	Developed algorithm to determine Transient stability margin using power swing-based energy margin and also suggested E-SIME techniques for closed loop real time emergency control	Provide fast quantitative measure which indicate the degree of system stability based on energy margin or stability indices	Required extensive computational efforts and restrictions regarding modeling details.
Authors of [37]	Proposed a periodic small signal rotor angle stability assessment using SIME method	Provide relatively fast quantitative measure which indicate the degree of system stability	Has restrictions regarding modeling details
Authors of [38]	introduced a trajectory sensitivity analysis	Provide fast quantitative measure which indicate	Has restrictions regarding modeling details

		the degree of system stability	
Authors of [40]	DSA based on ANN	Relatively faster assessment method	Since this method relies on offline databases, it is challenged by the extensive range of operating conditions
Authors of [41]	Proposed TDS based on differential transformation method	Non-iterative and fully analytical method	Gives a good approximation to the true solution in a very small region
Authors of [42],[43], and [44]	Proposed TDS based on multi-step differential transformation method	Extend the region of solution convergence and improve accuracy of the results	Results in more computational effort and increased simulation time cost.

1.5. Researches gaps

Most of the researchers/Authors mentioned in the literature review above are primarily concentrate on improving the performance efficiency of dynamic security analysis such as methods trained on off-line database with or without PMU, direct methods as sensitivity and updated SIME methods and differential transformation methods as described in the Table 1.1 above. As the limitations of each method described in the limitation column of the literature review summary table above no one tries to optimize between performance efficiency (speed) and robustness of DSA methods.

1.6. Research methodology

In order to meet the stated objectives and accomplish this thesis work successfully the following methodology was followed.

- A literature survey of new analytical developments and novel concepts in near real time transient stability based dynamic security analysis, and comparison in terms of accuracy and computational burden.
- Power system transient stability analysis based on differential transformation method (DTM) is studied and investigated.
- Novel algorithm that automatically varies the step size and order adaptively with the resulting truncation error is developed and based on this novel algorithm, fast and robust power system transient stability simulation tools (AsDTM and AOSDTM) are developed.

- Overview the current state-of-the-art in the area of near real time DSA
- MATLAB software package is used to develop the proposed DSA tools. Here power flow analysis software package, Matpower is installed within MATLAB to perform power flow analysis.
- Develop a framework for building a dynamic system model using equipment parameters, network topology and latest snapshot data from the SCADA.
- Model files are created and power system models with different details are developed stored. The controller libraries for synchronous generators have been built,
- Standard power system test systems and cases are identified and prepared for testing and validating the developed power system dynamic simulation and analysis (DSA) tools.
- Static and dynamic data for each test case system are identified and stored in separate and labeled data file (database). Finally

  - ❖ Fault scenarios (contingencies) have been selected for the purpose of testing and validation of the developed DSA tools. A scenario is then defined on the basis of the fault location and the fault case.
  - ❖ Transient stability based fast power system contingency screening and ranking tool is developed, tested and validated
  - ❖ Efficient and robust power system transient stability assessment tool which is based on AsDTM and AOSDTM power system time domain simulation by bisection method is developed.
  - ❖ Efficient and robust method that identify and group synchronous generators as critical machines (CM) group and non-critical machines (NCM) group during unstable system conditions is developed, tested and validated
  - ❖ Fast and robust method of evaluating stability indicators (CCT) is developed and used to evaluate the impact of each contingency. Qualitative conclusions about the robustness of the system state are also made on the basis of the limit of this CCT
  - ❖ Using these tools in combination with particle swarm optimization (PSO), dynamic security analysis tools that can recommend preventive mechanisms to enhance transient stability is developed, tested and validated.

1.7. Research contributions

The main contributions of this dissertation are as listed below :

- Fast and robust power system transient stability simulation methods and tools
- Fast and robust contingency screening and ranking tool is developed
- Fast and robust power system transient stability assessment tool is developed
- A tool that enables power system operators to early recognize the noncritical and critical generator groups depending on the most current snapshot from the SCADA data under a list of credible contingencies.
- A DSA tools that incorporates tools mentioned in 2 up to 4 above combined with particle swarm optimization (PSO), that can perform contingency screening and ranking, detail transient stability analysis, and determines remedial action to enhance transient stability (rotor angle instability).

1.8. Thesis organization

In the previous subsections of Chapter one, problem statement, research objectives, and research methodology are briefly discussed. The first chapter was wounded up with a summary of the contributions of this thesis work, along with an outline of the thesis structure. The next five Chapters provide an overview of the tasks related to the five core topics covered in the thesis.

Chapter two describes the model requirements and different power system dynamic security analysis methods, explain the proposed fast and robust PTDS method, which is used throughout this thesis, and presents description of the overall framework of the developed DSA tools. The third chapter presents descriptions of the developed transient stability based fast and robust contingency screening and ranking tool. Testing and validation of the proposed and developed tool for contingency screening and ranking is presented using different standard IEEE test systems. The fourth chapter presents descriptions of the developed transient stability analysis tool. Testing and validation of the developed tool for transient stability assessment is explained using different IEEE test systems.

The fifth chapter presents the proposed and developed tool for transient stability based dynamic security enhancement based on optimal generation rescheduling using PSO is presented and described. Testing and validation of this tool is presented using different IEEE test systems. The last chapter (chapter six) presents conclusion and outlook. This chapter summarizes the general

framework and the performance efficiency and robustness achieved by the proposed and developed DSA tools. Further investigation needed for improving the performance and robustness of the developed DSA tools are identified and listed to be considered as future research need in this regard.

CHAPTER TWO: Power System DSA Based on TDS and Overall Framework of the Developed DSA tools

2.1. Introduction

Power system security is concerned with the technical performance and quality of service when a disturbance causes a change in system conditions. When changes occur, the various components of the power system respond and hopefully reach a new equilibrium condition that is acceptable according to the required security criteria. Mathematical analysis of these responses and new equilibrium condition is called security analysis. If the analysis evaluates only the expected post disturbance equilibrium condition (steady-state operating point), this is called static security analysis (SSA). If the analysis evaluates the transient performance of the system as it progresses after the disturbance, this is called dynamic security analysis (DSA). DSA has been formally defined by the Institute of Electrical and Electronics Engineers (IEEE), Power Engineering Society's (PES), working group on DSA as

"Dynamic Security Analysis is a mathematical analysis made to evaluate the ability of a certain power system to withstand a defined set of contingencies and to survive the transition to an acceptable steady-state condition".

During network disturbances, the power generators have to provide immediate support by changing the currently generated power supplied to the grid. The immediate change is restricted by the power system inertia during the initial few hundred milliseconds. Most turbines are unable to yield the fast torque response required to act in such small level in transient stability. Thus dynamic behavior investigation and preparing the proper actions that improve system response during contingencies are important aspects during power system operation and control. The analysis of power system dynamics have been characterized by complex dynamic behavior due to the modeling complexity and interactions/interrelations among individual components as well as the computational structure for describing modern power systems. In order to analyze any power system dynamic performance, a mathematical model is used to represent the system.

2.2. Power System Models

Power system incorporated large number of electrical equipment in it. The complexity of modern power systems become more as they are enhanced with new devices such as Flexible AC Transmission System devices (FACTs) and distributed stochastic generation. It is very important to understand the various power system models before applying them. In this subsection, power

system models are described for a variety of power system components. The representation consists of both static and dynamic behaviors of power system. Based on representation for each component, a generic mathematical expression is given for the purpose of power system DSA. The following subsections provide overview of the mathematical models of power system used throughout this thesis.

2.2.1. Load Flow Analysis

Power flow is the model for the network and power system variables are studied from a set of algebraic equations. The vector space representation of the power flow equations is as follows [**5**].

$$0 = h(p) \tag{2-1}$$

In the Equation (2.1), algebraic variables ***p*** represents the solution of power flow analysis and ***h*** represents network equations. At each bus of the power system, power or current injections are balanced. For instance, considering both real power and reactive power balance, the expansion of the function ***h*** *in* nonlinear form can be given as follows.

$$\begin{cases} 0 = P_{gi} - P_{Li} - P_{totali} \\ 0 = Q_{gi} - Q_{Li} - Q_{totali} \end{cases} \tag{2-2}$$

Where

P_{gi} : Real power generation at bus i

P_{li} : Real power load at bus i

P_{ti} : Net real power injection at bus i

Q_{gi} : Reactive power generation at bus i

Q_{li} : Reactive power load at bus i

Q_{ti} : Net reactive power injection at bus i

Generations is estimated based on the inherent characteristics of the generator. Loads are determined from system load characteristics. The physical characteristics of the system constrain the total reactive and real power injections which can be expressed as follows.

$$\begin{cases} P_{totali} = \sum_{i=1}^{n} V_i V_k Y_{ik} \cos(\theta_i - \theta_k - \varphi_{ik}) \\ Q_{totali} = \sum_{i=1}^{n} V_i V_k Y_{ik} \sin(\theta_i - \theta_k - \varphi_{ik}) \end{cases} \quad (2\text{-}3)$$

Where V and θ are bus voltage and angle respectively, and these variables belong to the unknown variables $\boldsymbol{p}$ in Equation (2-1) for power flow analysis. The variables Y and φ are given parameters from power system model representing bus connections. In the power flow analysis, it is usually bus voltages and angles for slack bus, active power generation and bus voltage magnitude for PV buses, and active and reactive power for load buses are given. By solving a set of nonlinear equations, power system static states such as buses voltages and angles for load buses, reactive power generation and bus voltage angle for PV buses can be determined from power flow analysis.

2.2.2. Synchronous Generator Model

For power system dynamic simulation synchronous generators can be modeled with different depth of detail. The main concern of the work is to develop DSA tools that analysis power system stability due to large disturbances (transient stability). The phenomena and timescales of interest are in the range of transient electromechanical oscillations due to large disturbances so ordinary differential equations are considered sufficient. Therefore, fourth order generator models are used to describe synchronous generator [**1**], [**45**] [**46**]. The expression of the synchronous machine model is given as:

$$\begin{cases} \dfrac{d\delta_i}{dt} = (\omega_i - \omega_s) \\ \dfrac{d\omega_i}{dt} = \dfrac{\omega_s}{2*H}\left[P_{mi} - D_i(\omega_i - \omega_s) - \left(E'_{qi} - X'_{di} I_{di}\right) I_{qi} - \left(E'_{di} + X'_{qi} I_{qi}\right) I_{di} \right] \\ \dfrac{dE'_{qi}}{dt} = \dfrac{1}{T'_{d0i}}\left[E_{fdi} - E'_{qi} - \left(X_{di} - X'_{di}\right) I_{di} \right] \\ \dfrac{dE'_{di}}{dt} = \dfrac{1}{T'_{q0i}}\left[-E'_{di} + \left(X_{qi} - X'_{qi}\right) I_{qi} \right] \end{cases} \quad (2\text{-}4)$$

Where $\boldsymbol{\delta}$ is the generator angle, ω is the generator angular speed; $\boldsymbol{E_d'}$ and E_q' are transient direct axis (d axis) and quadrature axis (q axis) EMF respectively. The variables $\boldsymbol{I_d}$ and $\boldsymbol{I_q}$ are d axis and q axis current respectively, and the parameter variables T_{d0} and $\boldsymbol{T_{q0}}$ are d axis and q axis open circuit time constants. $\boldsymbol{X_d}$ and $\boldsymbol{X_q}$ represent synchronous d axis and q axis reactances; $\boldsymbol{X_d'}$ and $\boldsymbol{X_q'}$

represent synchronous d axis and q axis transient reactance's; $\boldsymbol{H_i}$ is the machine inertia constant and $\mathbf{D_i}$ is the machine damping constant.

Interface voltage equations to the network are given as follows:

$$E'_{qi} = V_i \cos(\delta_i - \theta_i) + R_{si} I_{qi} + X'_{di} I_{di}$$
$$E'_{di} = V_i \sin(\delta_i - \theta_i) + R_{si} I_{qi} + X'_{qi} I_{qi} \qquad (2\text{-}5)$$

Where $\boldsymbol{V}$ and $\boldsymbol{\theta}$ are bus voltage and angle, and *Rs* is armature resistance of the machine. The machine currents ***Id*** and ***Iq*** can be eliminated by solving the generator interface equations to the network. Hence,

$$\begin{bmatrix} I_{di} \\ I_{qi} \end{bmatrix} = \begin{pmatrix} R_{si} & -X'_{qi} \\ X'_{di} & R_{si} \end{pmatrix}^{-1} \left(\begin{bmatrix} E'_{di} \\ E'_{qi} \end{bmatrix} - \begin{bmatrix} v_{di} \\ v_{qi} \end{bmatrix} \right) \qquad 2\text{-}6$$

$$\begin{bmatrix} I_{xi} \\ I_{yi} \end{bmatrix} = \begin{pmatrix} \sin\delta & \cos\delta \\ -\cos\delta & \sin\delta \end{pmatrix} \begin{pmatrix} R_{si} & -X'_{qi} \\ X'_{di} & R_{si} \end{pmatrix}^{-1} \left(\begin{bmatrix} E'_{di} \\ E'_{qi} \end{bmatrix} - \begin{pmatrix} \sin\delta & -\cos\delta \\ \cos\delta & \sin\delta \end{pmatrix} \begin{bmatrix} v_{di} \\ v_{qi} \end{bmatrix} \right) \qquad (2\text{-}7)$$

Power system network is modeled as a real equation of generator and load bus current injections to the network in this study. For the admittance matrix expressed in rectangular coordinates as

$$Y_{ij} = G_{ij} + jB_{ij} \qquad (2\text{-}8)$$

The current injection at each node *i* can be written as

$$I_i = I_{xi} + jI_{iy} = \sum_{j=1}^{N/2} Y_{ij} V_j = \sum_{j=1}^{N/2} \left(G_{ij} + jB_{ij} \right) \left(V_{xj} + jV_{yj} \right) \qquad (2\text{-}9)$$

Where N = twice the number of buses

Separating real and imaginary parts gives

$$I_{xi} = \sum_{j=1}^{N/2} \left(G_{ij} V_{xj} - B_{ij} V_{yj} \right)$$
$$I_{yi} = \sum_{j=1}^{N/2} \left(G_{ij} V_{yj} + B_{ij} V_{xj} \right) \qquad (2\text{-}10)$$

$$\begin{bmatrix} I_{x1} \\ I_{y1} \\ \vdots \\ I_{xi} \\ I_{yi} \\ \vdots \\ I_{xN} \\ I_{yN} \end{bmatrix} = \begin{pmatrix} Y_{11} & \cdots & Y_{1i} & \cdots & Y_{1N} \\ \vdots & \ddots & \vdots & & \vdots \\ Y_{1i} & \cdots & Y_{ij} & \cdots & Y_{iN} \\ \vdots & & \vdots & \ddots & \vdots \\ Y_{N1} & \cdots & Y_{Nj} & \cdots & Y_{NN} \\ & & & & \end{pmatrix} \begin{bmatrix} V_{x1} \\ V_{y1} \\ \vdots \\ V_{xi} \\ V_{yi} \\ \vdots \\ V_{xN} \\ V_{yN} \end{bmatrix} \quad I = YV \tag{2-11}$$

Where all the elements are now real sub matrices of the form

$$Y_{ij} = \begin{pmatrix} G_{ij} & -B_{ij} \\ B_{ij} & G_{ij} \end{pmatrix}, I = \begin{bmatrix} I_{x1} \\ I_{y1} \\ \vdots \\ I_{xi} \\ I_{yi} \\ \vdots \\ I_{xN} \\ I_{yN} \end{bmatrix} V = \begin{bmatrix} V_{x1} \\ V_{y1} \\ \vdots \\ V_{xi} \\ V_{yi} \\ \vdots \\ V_{xN} \\ V_{yN} \end{bmatrix} \tag{2-12}$$

Y_{ij} : admittance of the transmission line between bus I & j

B_{ij} : suspentance of the transmission line between bus I & j

G_{ij} : conductance of the transmission line between bus I & j

I_{xi} and I_{iy} : rectangular components of current injected at bus i

V_{xi} and V_{yi} : rectangular components of voltage at bus i

N: 1,2,3,...,2* total number of buses

2.2.3. Excitation System Model

The mathematical models of simplified IEEE type DC-1 excitation system shown by Figure 2-1 is used to represent excitation system in this thesis.

$$\begin{cases} \dfrac{dE_{fdi}}{dt} = \dfrac{1}{T_{ei}}\left[V_{ri} - \left(K_{ei} + S_{ei}\left(E_{fdi}\right)\right)\right] * E_{fdi} \\ \dfrac{dV_{ri}}{dt} = \dfrac{1}{T_{ai}}\left[-V_{ri} + K_{ai} * \left(V_{refi} - V_i - V_{fi}\right)\right] \\ \dfrac{dV_{fi}}{dt} = \dfrac{1}{T_{fi}}\left[-V_{fi} - \left(K_{ei} + S_{ei}\left(E_{fdi}\right)\right)K_{fi}E_{fdi} \Big/ T_{ei} + K_{fi}V_{ri} \Big/ T_{ei}\right] \end{cases} \quad (2\text{-}13)$$

Where V_{ref} is the reference voltage of the automatic voltage regulator (AVR) V_r and R_f are the outputs of the AVR and exciter soft feedback; E_{fd} is the voltage applied to generator field winding; T_a , T_e and T_f are AVR, exciter and feedback time constants; K_a , K_e and K_f are gains of AVR, exciter and feedback; $V_{r,min}$ and $V_{r,max}$ are the lower and upper limits of V_{rt}

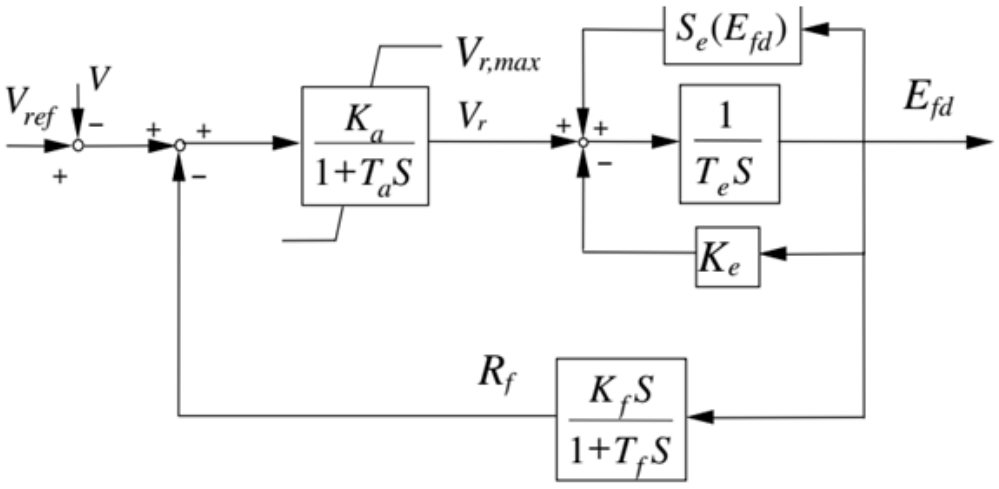

Figure 2-1 IEEE Type DC-1 Excitation System [18]

2.2.4. Governor Model

A simplified prime mover and speed governor is shown by Figure 2-2. Two differential equations are used to describe the dynamics of the governor [**18**].

$$\begin{cases} \dfrac{dP_{sui}}{dt} = 1 \Big/ T_{Gi}\left(P_{refi} - P_{sui} - \left(\omega_i - \omega_s \Big/ R_i\right)\right) \\ \dfrac{dP_{mi}}{dt} = 1 \Big/ T_{CHi}\left(P_{refi} - P_{mi}\right) \end{cases} \quad (2\text{-}14)$$

Where P_{refi} is represents real power generation; P_{mi} is the mechanical power of the prime mover and P_{sui} is the steam valve or water gate opening; R_i is the governor regulation constant representing the inherent speed-droop characteristic; ω_s is the governor reference speed; T_{CHi} and T_{Gi} are the time constants related to the prime mover and speed governor respectively; $P_{sui-\min}$ and $P_{sui-\max}$ are the lower and upper limits of P_{sui}.

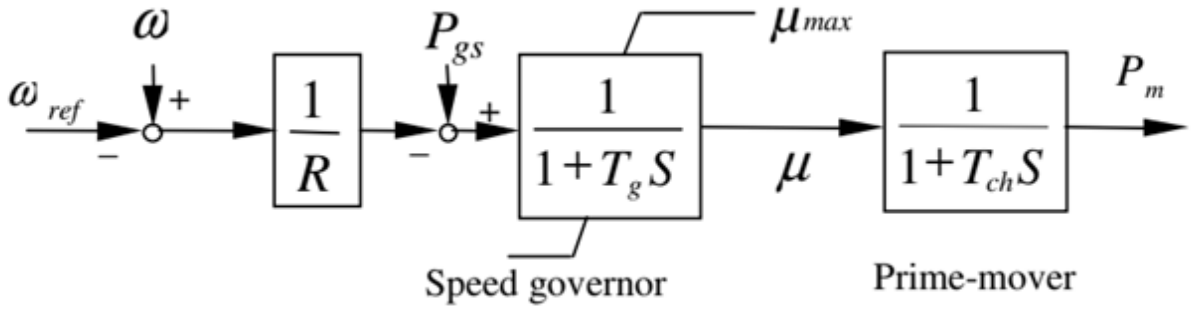

Figure 2-2 Simplified Speed Governor and Prime Mover [18**]**

2.2.5. Load Model

Load model may be voltage and frequency dependent. In power system analysis, common load models can be constant power model, constant current model, and constant impedance model. The representation for these load models are shown as follows [**18**].

Constant Power Load:

$$P_{li} = P_{li0} \qquad Q_{li} = Q_{li0} \tag{2-15}$$

Constant Current Load:

$$P_{li} = P_{li0}\left(V_i / V_{i0}\right) \qquad Q_{li} = Q_{li0}\left(V_i / V_{i0}\right) \tag{2-16}$$

Constant Impedance Load:

$$P_{li} = P_{li0}\left(V_i / V_{i0}\right)^2 \qquad Q_{li} = Q_{li0}\left(V_i / V_{i0}\right)^2 \tag{2-17}$$

2.2.6. Power System DAE Model

Since power systems are represented by both differential equations and algebraic equations, i.e. differential algebraic equations (DAE) , their mathematical formulation is as follows [**18**].

$$\begin{cases} \dfrac{dx}{dt} = f(x, p) \\ 0 = h(x, p) \end{cases} \tag{2-18}$$

The differential equation ***f*** represents governing dynamics of power systems, which is associated with generators, excitation systems, and speed governor. The differential variables ***x*** consist of the states of dynamic components. The algebraic equation ***h*** represents the network power or current balance of power systems. The algebraic states ***y*** includes bus voltages and bus phase angles. The values of the algebraic variables can be changed instantaneously, while differential variables cannot jump from one state value to another state value without transition time.

During power system analysis the control and parameter variables should be incorporated and the DAE system in (2-18) can be rewritten as the following form [**18**]:

$$\begin{cases} \dfrac{dx}{dt} = f(x, p, u) \\ 0 = h(x, p, u) \end{cases} \tag{2-19}$$

In the above equations, variable ***u*** is the control and parameter variable which may be used to control or tune power system performance. Power system dynamic security problems are studied based on the mathematical model. The study of dynamic responses subject to the disturbances can be achieved through dynamical simulation, or time domain simulation of the power system mathematical model. The control strategies for power system dynamics are also based on the mathematical model.

2.3. Dynamic phenomenon of interest for DSA

DSA requires the mathematical models of the synchronous machines and other distributed generations with their controllers, FACT devices, connected loads, transmission system networks, and e.t.c. to analyze the system responses to the contingency under consideration.

Theoretically, this would require detailed modeling of a wide array of devices with different response rates and characteristics due to the high dimensionality and complexity of the problem. However, this approach is not purposeful. It is essential to make simplifying assumptions and to study specific class of problems using the right degree of detail. For finding a suitable modeling detail, therefore, it is necessary to identify the dynamic phenomena of interest first. While there are numerous phenomena that may be of interest in dynamic analyses, typical DSA programs focus primarily on transient stability, voltage transients and oscillatory stability.

2.3.1. Transient stability

The cardinal requirement in alternating current interconnection is that all synchronously rotating generators must maintain intact with one another in steady state. Any disturbance, such as a grid short circuit, impacts more or less all interconnected machines, but the severity depends on their relative electrical distance to the fault location. Although the increasing number and size of renewable based generation plants and links with converter interface are steadily altering the picture, the dynamics of power systems is still largely determined by the behavior of synchronous generators connected to the network. The phrase “transient stability” characterizes the behavior of individual synchronous generators or more precisely their rotor angles with respect to the synchronously rotating common reference frame. Should any generator leave the synchronous operation mode and start to run asynchronously then one speaks of transient instability.

When a fault occurs in the system, the electrical power output of some generators (usually those near the fault) will tend to decrease. Since the turbine power input does not change instantaneously to match this, these generators will first accelerate above the nominal synchronous speed. During this instant, generation of other remote generators may increase as a result of the primary control action, resulting in deceleration below the synchronous speed. Deciding whether all generators remain stable or some generators become unstable following a contingency is the most significant task in DSA analysis, and all current DSA programs focus primarily on this type of stability and its associated constraints on system operation.

2.3.2. Voltage transients

Voltage transients are important as voltage values outside acceptable limits can cause operation failure or damage to equipment. During large disturbances for instance three phase short circuit faults the system quantities such as voltages and currents can change over a wide margin that can

impact voltage-sensitive loads and result in conditions that may be unacceptable even though the generators remain in synchronism after the contingency. This may further resulted in voltage levels where recovery to nominal levels is impossible. Furthermore deterioration of the system results in voltage collapses conditions which may initiates additional relay action or trip out of generator in the aftermath of the contingency. The extent to which such phenomena can be detected in DSA programs depends on the level of modeling detail for control systems, relays, and the accuracy of load models in the simulation.

Normally the effects of under / overvoltage transients are not included in the large-scale DSA simulation programs, and the automatic tripping or relay operation associated with under/overvoltage are not normally modeled as part of the simulation used for DSA [**2**]. Since these possible actions are not explicitly modeled, the programs simply monitor voltage levels as the transient process progresses.

2.3.3. Oscillatory stability

Oscillatory stability (small signal stability) refers to the damping behavior of the rotor angles of individual synchronous generators or groups of generators when subjected to oscillations. The machines may oscillate together in groups or against each other through the electrical network to which they are connected. If the oscillations caused by small disturbances (for example, load changes) experience damping, i.e. the oscillations of the system variables remain small, the power system is stable. If, on the other hand, the magnitude of oscillations continues to increase or is sustained over a lengthy period of time with significant amplitude of oscillation, then the system is determined to be unstable.

It is inevitable that a power system is subjected to small disturbances (load changes) during the course of operation. A power system capable of normal operation must, in principle, be stable in terms of small-signal stability. However, the small-signal stability phenomenon is influenced by several factors, including initial operating conditions, strength of electrical connections to the other generators in the system, characteristics of various control devices, etc. As a result, the conclusion regarding the oscillatory stability behavior of the system at a given operating point is valid only at that operating condition. This fact makes oscillatory stability analysis at regular intervals as part of DSA necessary.

For performing oscillatory stability analysis, the system is initially assumed to be at an equilibrium point in normal operation mode. A small disturbance is introduced, and then the free

movement of the system after the disappearance of the disturbance is analyzed. The basic approach for the analysis is to linearize the system equations around the operating point and then to use the Lyapunov method to draw conclusions about the local stability of the nonlinear system around that equilibrium point. In other words, the assumption is that a movement of a nonlinear system over a small range should have similar properties to its linearized approximation. However this dissertation is concentrated only on TSA.

2.4. Methods of dynamic security analysis

The ultimate goal of DSA is to generate the operating guidelines for defining the areas of secure operation. Generating the operating guidelines includes selecting contingencies, performing a detailed stability study, analyzing the results for violations, and then considers the control strategy required to restore post disturbance system equilibrium. Power system response to large disturbances is typically studied by time domain simulation, but such simulations are time consuming for large power systems, and developing a fast simulation method is often quite a challenging problem.

Existing time domain simulation (TDS) methods are:

- Numerical integration methods
- Direct or Lyapunov methods
- Probabilistic methods, and
- Differential transformation methods

2.4.1. Numerical integration

The differential algebraic equations (DAE) presented in equations (2-11) to (2-14) from the previous subsection can be addressed using numerical integration. There are two main approaches for solving DAEs: simultaneous and partitioned methods [**46**]- [**47**]. In the simultaneous method, both the differential and algebraic equations are solved together at each iteration step. In contrast, the partitioned method first addresses the differential equations using numerical integration, followed by the resolution of the algebraic equations, with this process repeating until the simulation concludes. Consider the following DAE equations Equation (2-20) and in the following subsequent subsections this equation is solved by using one of the numerical integration method as shown by Equations (2-21)- (2-25)

$$\frac{dx}{dt} = f\left(x, I_{d-q}, \overline{V}, u\right)$$
$$I_{d-q} = h\left(x, \overline{V}\right)$$
$$0 = g\left(x, I_{d-q}, \overline{V}\right) \qquad (2\text{-}20)$$

Where

$$x = \left[x_1^T \ldots x_{n_g}^T\right]^T, u = \left[u_1^T \ldots u_1^T\right]^T, I_{d-q} = \left[I_{d=q1}^T \ldots I_{d=qn_g}^T\right]^T$$
$$x_i = \left[\delta_i, \omega_i, E_{di}^{'}, E_{qi}^{'}, E_{fi}, V_{ri}, V_{fi}, P_{mi}, P_{svi}\right]^T$$
$$u_i = \left[V_{ref}, P_{ref}\right]^T$$
$$I_{d-qi} = \left[I_{di}, I_{qi}\right]^T$$
$$\overline{V} = \left[\overline{V}_1 \ldots \overline{V}_n\right]^T = \left[V_1 e^{j\theta} \ldots V_n e^{j\theta}\right]^T \qquad (2\text{-}21)$$

These equations (Equation 2-21) are solved by numerical integration through the implicit method called trapezoidal method as

$$x_{n+1} = x_n + \int_{t_n}^{t_{n+1}} f\left(x, I_{d-q}, \overline{V}, u\right)$$
$$x_{n+1} = x_n + \frac{\Delta t}{2}\left(f\left(x_{n+1}, I_{d-q_{n+1}}, \overline{V_{n+1}}, u_{n+1}\right) + f\left(x_n, I_{d-q_n}, \overline{V_n}, u_n\right)\right) \qquad (2\text{-}22)$$

$$I_{d-q_{n+1}} - h\left(x_{n+1}, \overline{V_{n+1}}\right) = 0$$
$$g\left(x_{n+1}, I_{d-q_{n+1}}, \overline{V_{n+1}}\right) = 0 \qquad (2\text{-}23)$$

Equations (2-22 & 2-23) can be solved by Newton-Raphson method where the variables are x_{n+1} , $I_{d-q\ n+1}$,$V_{\ n+1}$,u_{n+1} with initial conditions x_n , I_{d-qn} ,V_n ,u_n . Since the variables at n^{th} integration step are not explicitly required for finding the solution of Equations (2-22 & 2-23) this method is also called as simultaneous implicit method.

Using explicit methods such as Euler's, Modified Euler's and Runga-Kutta methods the integration of equation (2-21) can be solved. In this case the differential equations and algebraic equations are solved explicitly. For instance, using Euler's method the integration of equation (2-21) at n^{th} integration step is given as

$$x_{n+1} = x_n + \frac{\Delta t}{2}\left(f\left(x_n, I_{d-q_n}, \overline{V_n}, u_n\right)\right) \tag{2-24}$$

Where, Δt integration time step and should be less than the least time constant of the system in order to have a stable numerical method. Once, the variables x_{n+1} at n^{th} integration step are found then the algebraic equations can be solved by solving the following algebraic equations using Newton-Raphson or any other alternative methods.

$$\begin{aligned} I_{d-q_{n+1}} - h\left(x_{n+1}, \overline{V_{n+1}}\right) &= 0 \\ g\left(x_{n+1}, I_{d-q_{n+1}}, \overline{V_{n+1}}\right) &= 0 \end{aligned} \tag{2-25}$$

While each numerical integration method has its own strengths and weaknesses, both approaches yield solutions that pertain to the system's stability, depending on the complexity of the models used. This method is commonly applied in offline environments; however, it is typically too computationally intensive for real-time applications.

To overcome these limitations, a variable time-step-based power system transient stability simulation based on numerical integration method was proposed by [**48**] [**49**]. The integration time step control is performed based on the system behavior during the course of simulation. The method uses small time steps when the system variables are changing rapidly and large time steps when the system variables do not exhibit rapid variations. Solution error is estimated and the time step is adjusted to meet the specified tolerance threshold at each iteration step. This reduces the number of iterations and can also be used with more complex integration schemes. However, (1) at each iteration step, if the estimated solution error is greater than the specified tolerance threshold, the current solution is rejected and the solution procedures are repeated again using the new step size, which increases simulation time cost. (2) Still, algebraic equations are solved by iteration after each integration steps; this also has an impact on total simulation time cost.

An adaptive time step approach to dynamical simulation based on monitoring the conservation of energy was proposed by [**50**]. The method considers a physical object's velocity and positions error estimate to determine the next time step. Using this method, numerical stability and computational efficiency (speed) were improved when compared with the traditional fixed-step

numerical integration method. However, the method is independent of the system model equations describing its dynamic behaviors.

2.4.2. Direct Lyapunov method

The Direct Lyapunov method, often referred to as the Transient Energy Function (TEF) approach, replaces numerical integration with stability criteria. In this technique, the value of a specifically designed Lyapunov function, V, is calculated at the point of the last switching event within the system and then compared to a pre-determined critical value, Vcr. If V is found to be less than Vcr, the post-fault transient process is considered stable [24].

Despite its theoretical appeal, this method has practical challenges and limitations. The efficiency of the approach depends heavily on simplifying the system variables. Determining the critical value for stability assessment requires incorporating the fault into the system equations. Moreover, designing an appropriate Lyapunov function that accurately reflects the system's internal characteristics is a complex task. The method is also only rigorously valid when the operating point lies within the estimated stability region.

2.4.3. Probabilistic methods

In probabilistic methods, stability analysis is approached as a probabilistic issue rather than a deterministic one, as the type and location of faults, along with pre-contingency system conditions, inherently involve uncertainties. This method seeks to establish probability distributions for power system stability, evaluating the likelihood that the system will remain stable in response to specific disturbances. It considers a wide range of faults at various locations and with differing fault-clearing times. To achieve statistically significant results, substantial computation time is necessary, making this method more suitable for planning purposes.

2.4.4. Differential transformation methods

The theory of differential transformation method is originally established to derive approximate solutions of nonlinear differential equations [**24**] and defined as bellow. Next it is developed by researchers in the fields of mathematics and physics to obtain semi-analytical solutions of various nonlinear dynamic systems. In [**51**] [**52**] [**53**] [**54**] this method has been examined for real-life complex network systems like power systems modeled by high-order nonlinear differential equations.

Definition: Consider a function x(t) of a real continuous variable t. The Differential Transformation (DT) of x(t) is defined by Equation (1), and the inverse DT of X(k) is de-fined by Equation (2), where k is the order [**24**] [**51**] [**52**] [**53**] [**54**]

$$X(k)=\frac{1}{k!}\left[\frac{d^k x(t)}{dt^k}\right]_{(t=0)} \qquad (2\text{-}26)$$

$$x(t)=\sum_{k=1}^{\infty} x(k)t^k \qquad (2\text{-}27)$$

The DT method provides various transformation rules for numerous generic functions, for both linear and nonlinear functions and for both simple and compositional functions, such that a differential equation in a continuous set about the variable t (time) is converted to a new set of difference equations in a discrete set about the variable k (the power series order).

In power system simulation, DTM can be used as an explicit, fast, and robust solver of power system complex differential algebraic equations (DAEs). It is proved that the performance efficiency of a DTM is much better than that of the traditional numerical integration methods, because when using the DTM method, the iteration to solve algebraic equations after each integration step is eliminated and has a higher radius of convergence. To solve multi-machine power system DAE models using the DTM method, the process is as follows: (1) transform power system DAE equations, (2) calculate the coefficients of state and algebraic variables, and (3) perform inverse transformation to determine state and algebraic variables as a function of time. Details of these procedures are presented in the following subsection.

A differential transformation method (DTM)-based transient stability simulation algorithm is fully analytical method. This method approximates the solution of complex power system differential algebraic model equations as a truncated power series of time. The approach is flexible in handling power system with any model detail without limitations. It also requires less computation effort and simulation time cost. However, differential transformation method gives a good approximation to the true solution in a very small region. To extend the region of solution convergence and improve accuracy of the results, DTM is applied at equal and fixed time interval up to the end of simulation period. In some cases, a very small sub division of interval is

required with this method, which results in more computational effort and increased simulation time cost.

2.5. The proposed fast and robust power system Transient Stability Simulation method

2.5.1. Introduction

In this thesis, an adaptive step size differential transformation method (AsDTM)-based power system transient stability simulation method [**55**] is proposed. This work introduces a novel step-size control algorithm based on local convergence error results at the end of each simulation time step by using the differential transformation method (DTM). The proposed novel power system transient stability simulation algorithm (1) is relatively robust and accurate, because it is flexible in handling power systems with any model detail and complexity without limitations; (2) improves simulation speed and accuracy based on control of local convergence error at each time step; (3) local solution error is estimated from only the last coefficient terms of the state and algebraic variables without any further calculations as in the variable step-size algorithm using traditional numerical integration methods; and (4) the solution obtained for the current simulation time step can be used during the next simulation time step without any limitations, such that the number of steps required to complete the transient stability simulation process reduces. These enable the proposed simulation scheme to be applied as an online transient stability simulation tool in small and medium-sized power systems.

2.5.2. Description of the proposed power system transient stability simulation method

For practical implementation of numerical methods of solving differential algebraic equations, the use of variable step-size length is a crucial issue because it allows us to automate the control of error. The proposed simulation method solves complex power system DAE models using the differential transformation method at variable time steps. The step size is varied based on the local truncation error control algorithm. The automatic controls of step-size length are performed based on the following principles:

- Reduce the time step length when the error is above the tolerable error limit, to improve the accuracy of simulation.
- Increase the time step length when the error is below the tolerable error limit, to avoid unnecessary computational burden and improve the overall efficiency.

Figure 2-3 shows a flowchart of the proposed AsDTM-based transient stability simulation algorithm. Each block of the proposed method of power system transient stability simulation is described step-by-step below.

Consider a power system with n bus and m machine DAE models in which synchronous machines are designated by a two-axis model with Type_1 automatic voltage regulator and primary speed control systems, as given by Equations (2-11) –(2-14) in the previous subsections, and all system loads are represented by constant impedance loads with both the network and stator algebraic equations represented by real matrices (expressed in rectangular form). Consider also the state space representation of the power system DAE model equations as given by Equation (2-28), where x is the state vector, v is the vector of bus voltages, f represents a vector field determined by differential equations on dynamic devices such as synchronous generators and associated controllers, i is the vector valued function on current injections from all generators and load buses, and Y_{bus} is the network admittance matrix.

$$\frac{dx_j}{dt} = f(x_j, v_j)$$
$$Y_{bus} v_j = i(x_j, v_j) \qquad (2\text{-}28)$$

where x(t) represents $\delta_j(t), \omega_j(t), E'_{qj}(t), E'_{dj}(t), V_{rj}(t), V_{fj}(t), E_{fj}(t), P_{chj}(t), and\ P_{svj}(t)$ and j = 1, 2, 3 … m, represent machine number.

Step 1 Derive DTs of power system DAEs:

Apply the differential transformation to functions given by Equation (2-28) on both sides, by using transformation to obtain Equation (2-29):

$$(k+1)X(k+1) = F(X(m), V(m)), m = 0.....k \quad (a)$$
$$Y_{bus} V(k) = I(X(m), V(m)), m = 0.....k \quad (b) \qquad (2\text{-}29)$$

where X represents $\delta_j, \omega_j, E'_{qj}, E'_{dj}, V_{rj}, V_{fj}, E_{fj}, P_{chj}, and\ P_{svj}$.

The vector valued function $i(x, v)$ in Equation (2-28) represents both generators and load current injections. But here, for this specific case, constant impedance loads are considered and are included in the network admittance matrix Y_{bus}.

The differential transformation of the stator algebraic equation, Equation (2-30), can be derived and represented by Equation (2-32).

Let $y_a = \begin{pmatrix} r_a & -x'_q \\ x'_d & r_a \end{pmatrix}^{-1}$, $r = \begin{pmatrix} \sin\delta & \cos\delta \\ -\cos\delta & \sin\delta \end{pmatrix}$, $\tau = r y_a$, $\gamma = r y_a r'$, and the generator current injection equation is

$$\begin{bmatrix} I_x \\ I_y \end{bmatrix} = \left(\tau \begin{bmatrix} E'_d \\ E'_q \end{bmatrix} - \gamma \begin{bmatrix} V_x \\ V_y \end{bmatrix} \right) \quad (2\text{-}30)$$

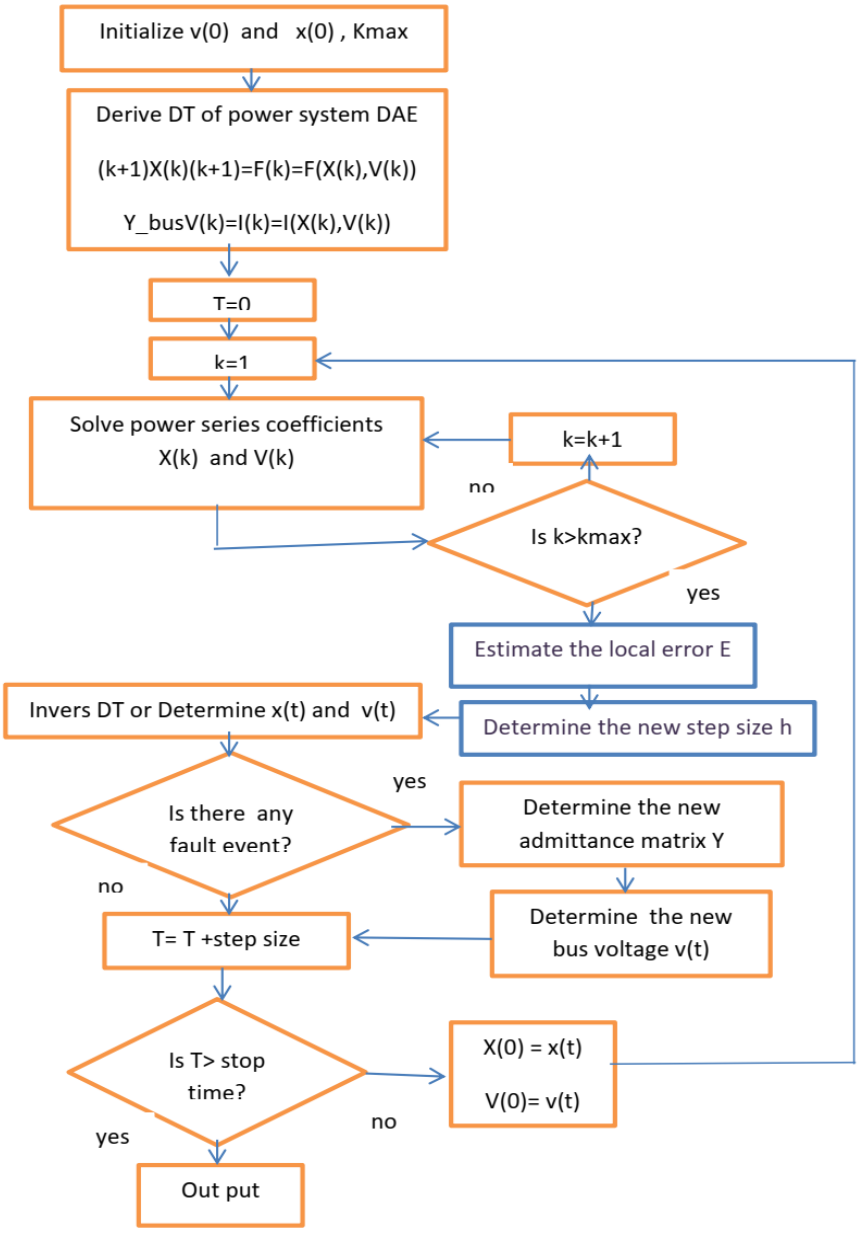

Figure 2-3 **Flowchart of AsDTM-based fast power system transient stability simulation method.**

Differential transformations of r, γ, and τ are given as

$$R(k) = \begin{pmatrix} \varphi(k) & \alpha(k) \\ -\alpha(k) & \varphi(k) \end{pmatrix}$$

where $\tau(k) = R(k)y_a,\ \gamma(k) = R(k)y_aR(k)'$.
Therefore, the differential transformation of the generator current injection equation is

$$\begin{bmatrix} I_x(k) \\ I_y(k) \end{bmatrix} = \left(\sum_{m=0}^{k} \tau(m) \begin{bmatrix} E'_d(k-m) \\ E'_q(k-m) \end{bmatrix} - \sum_{m=0}^{k} \gamma(m) \begin{bmatrix} V_x(k-m) \\ V_y(k-m) \end{bmatrix} \right) \tag{2-31}$$

The load current injection at each bus is represented by

$$\begin{bmatrix} I_x(k) \\ I_y(k) \end{bmatrix} = zeros(2,1)$$

Finally, DTs of the network algebraic equation are given as Equation (24):

$$\begin{bmatrix} I_{x1}(k) \\ I_{y1}(k) \\ \vdots \\ I_{xi}(k) \\ I_{yi}(k) \\ \vdots \\ I_{xN}(k) \\ I_{yN}(k) \end{bmatrix} = \begin{pmatrix} Y_{11} & \cdots & Y_{1i} & \cdots & Y_{1N} \\ \vdots & \ddots & \vdots & & \vdots \\ Y_{1i} & \cdots & Y_{ij} & \cdots & Y_{iN} \\ \vdots & & \vdots & \ddots & \vdots \\ Y_{N1} & \cdots & Y_{Nj} & \cdots & Y_{NN} \\ & & & & \end{pmatrix} \begin{bmatrix} V_{x1}(k) \\ V_{y1}(k) \\ \vdots \\ V_{xi}(k) \\ V_{yi}(k) \\ \vdots \\ V_{xN}(k) \\ V_{yN}(k) \end{bmatrix} \quad I(k) = YV(k) \tag{2-32}$$

Where

$$Y_{ij} = \begin{pmatrix} G_{ij} & -B_{ij} \\ B_{ij} & G_{ij} \end{pmatrix}, I(k) = \begin{bmatrix} I_{x1}(k) \\ I_{y1}(k) \\ \vdots \\ I_{xi}(k) \\ I_{yi}(k) \\ \vdots \\ I_{xN}(k) \\ I_{yN}(k) \end{bmatrix} V(k) = \begin{bmatrix} V_{x1}(k) \\ V_{y1}(k) \\ \vdots \\ V_{xi}(k) \\ V_{yi}(k) \\ \vdots \\ V_{xN}(k) \\ V_{yN}(k) \end{bmatrix}$$

Step 2 Solve power series coefficients:

This step is initialized by the initial values of bus voltage V(0) and state variables X(0). The main task here is to solve power series coefficients X(k) and V(k) from the (k−1)th-order coefficients, as indicated by the two circled numbers in Figure 2.4. Thus, any order coefficients are solvable from X(0),V(0).

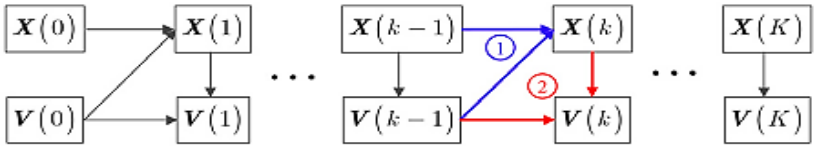

Figure 2-4 Recursive process to solve power series coefficients (source: [60]), where X(k) represents $\delta_j(k), \omega_j(k), E'_{qj}(k), E'_{dj}(k), V_{rj}(k), V_{fj}(k), E_{fj}(k), P_{chj}(k), and\ P_{svj}(k)$ **and j = 1, 2, 3 … m. [41]**

The coefficients of state variables X(k) for differential equations are derived from Equation (2-29a) recursively from X(1) up to X (k), as shown in Figure 2-4. But when solving the coefficients of algebraic variables, bus voltage V(k) is not straightforward since V(k) appears on both sides, as we can observe from Equation (2-29b). If ZIP load models are considered the current injunction equations for constant power, and constant current load portions of the ZIP load are nonlinear and will be turned into linear in terms of their coefficients, the proof is given by [57]. Since constant impedance load is considered in this dissertation, the DT of the generator current injection equation given by Equations (2-31) can be rewritten as Equation (2-33) below.

$$\begin{bmatrix} I_x(k) \\ I_y(k) \end{bmatrix} = \left(\sum_{m=0}^{k} \tau(m) \begin{bmatrix} E'_d(k-m) \\ E'_q(k-m) \end{bmatrix} - \sum_{m=1}^{k} \gamma(m) \begin{bmatrix} V_x(k-m) \\ V_y(k-m) \end{bmatrix} \right) - \gamma(0) \begin{bmatrix} V_x(k) \\ V_y(k) \end{bmatrix} \tag{2-33}$$

And let

$$B_g = \sum_{m=0}^{k} \tau(m) * \begin{bmatrix} E'_d(k-m) \\ E'_q(k-m) \end{bmatrix} - \sum_{m=1}^{k} \gamma(m) * \begin{bmatrix} V_x(k-m) \\ V_y(k-m) \end{bmatrix}$$

$$\begin{bmatrix} I_x(k) \\ I_y(k) \end{bmatrix} = A_g \begin{bmatrix} V_x(k) \\ V_y(k) \end{bmatrix} + B_g \ i.e\ I(k) = A_g V(k) + B_g$$

Since the load current injection is zero, letting A_l represent zeros (2,2), B_l represent zeros (2,1) at each of the n buses, $A = A_g + A_l$ & $B = B_g + B_l$ for machine buses, and $A = A_l$ & $B = B_l$ at (n – m) buses, then A represents (2×n) by (2×n) matrixes and B represents (2×n) by 1 column vector. Therefore, the current injections into the network from all the buses can be

$$I(k) = AV(k) + B \tag{2-34}$$

where

$$I(k) = \begin{bmatrix} I_{x1}(k) \\ I_{y1}(k) \\ \vdots \\ I_{xi}(k) \\ I_{yi}(k) \\ \vdots \\ I_{xN}(k) \\ I_{yN}(k) \end{bmatrix} \quad V(k) = \begin{bmatrix} V_{x1}(k) \\ V_{y1}(k) \\ \vdots \\ V_{xi}(k) \\ V_{yi}(k) \\ \vdots \\ V_{xN}(k) \\ V_{yN}(k) \end{bmatrix}$$

The detailed derivation of matrix A and B for other types of load model is not the focus of this paper but it is available in [**54**]. Considering constant impedance loads, the coefficients of bus voltages V(k) for all the network buses and coefficients of state variables X(k) are solved from Equations (2-35) from a–c recursively from X(1) up to X(k) and V(1) up to V (k).

$$\begin{aligned} X(k) &= \frac{1}{k} F(X(m), V(m)), \quad m = 0 \ldots k-1 \quad (a) \\ Y_{bus}\, V(k) &= AV(k) + B \quad (b) \\ V(k) &= (Y_{bus} - A)^{-1} B \quad (c) \end{aligned} \tag{2-35}$$

Step 3 Determine the new step size (h_{new}):

As described in the previous subsections, the proposed simulation method solves complex power system DAE models using the differential transformation method at variable time steps. The step size is varied based on the local truncation error control algorithm. The main term of this local truncation error is known in the form of $|Y(k)|t^k$, [**42**], where t is the local time variable in subinterval $[t_m, t_{m+1}]$ and m is the number of subintervals between [0,T]. In this paper, the series term $|Y(k)|t^k$ is used as a local truncation error estimate of the power series of degree k. Therefore, without any further calculation, we can estimate the simulation step size that ensures the prescribed local admissible error by using just one of the coefficient terms [**42**] [**56**]. The equation to calculate the step size (h) adopted and applied for power system transient stability simulation, as described below.

Let Mst, EXst, and TGst be matrix of generators, exciters, and turbine governor state variable, respectively. If m and N represent the number of machines and state variables, respectively, the size of each matrix is equal to **m** × **N**. Consider also the tolerable local solution error $\partial > 0$. The order of DTM, k, is given and fixed at the beginning of simulation. Therefore, since all order coefficient terms of state variables and all the network bus voltages are known at this stage, the new step size (h_{new}) will be determined as follows:

In this thesis an admissible local solution error of $\partial = 10^{-6}$ per unit is considered. Therefore, we can calculate the new step size h using the following two steps:

- Determine the maximum of absolute value of the last coefficient terms of all the variables as in Equation (2-36):

$$E = \max[\max(\max(|Mst(k)|), \max(\max(|EXst(k)|), \max(\max(|TGst(k)|), \max(|V(k)|)] \quad (2\text{-}36)$$

- Evaluate the new step size h_{new} by using Equation (2-37):

$$h_{new} = \left(\left(\frac{\partial}{E} \right)^{\frac{1}{k}} \right) \leq \text{max step size (hmax)} \quad (2\text{-}37)$$

Step 4 Inverse DT on X(k) and V(k).

Apply inverse DT to X(k) and V(k) to obtain the DTM-based solution of power system DEA in (2-38) a and b,

$$x_j(t) = \sum_{m=0}^{k} X_j(m) h_{new}{}^m \quad (a)$$
$$v_j(t) = \sum_{m=0}^{k} V_j(m) h_{new}{}^m \quad (b) \quad (2\text{-}38)$$

where x(k) represents $\delta_j(k), \omega_j(k), E'_{qj}(k), E'_{dj}(k), V_{rj}(k), V_{fj}(k), E_{fj}(k), P_{chj}(k), and\ P_{svj}(k)$.

Step 5 Check for disturbance or event, and if any, determine the new $(Y)_{matrix}$ and reinitialize bus voltages.

Step 6 Increment the simulation time t as $t_i + 1 = t_i + h_{new}$ (where i represents the number of time nodes, separated by the length of every time window).

Step 7 Using the time domain solutions x(t) and v(t) (step 4, above) as initial values of the state variables and bus voltages for the next simulation time window, respectively, repeat steps 2 to 6 until the end of the simulation period (T).

2.5.3. Simulation Results and Validation

For validating the proposed AsDTM-based power system transient stability simulation, three-phase short-circuit faults on bus 2 of IEEE 9 bus and on bus 31 of 39 bus test systems at 0.6 s and cleared after 0.2 s were simulated. In each case, the accuracy and performance of the proposed method was validated using the transient stability simulation results based on the traditional numerical method (fourth-order Range–Kutta (Rk4) with step size h = 0.001 s) and

total time cost (time for TS simulation) as benchmarks. For this simulation purpose, differential transformation (DT) order k = 7 for IEEE 9 bus and k = 10 for 39 bus test systems were used with both DTM and AsDTM simulation methods.

Figure 2-6 shows the step-size variation of the AsDTM-based transient stability simulation under admissible local error of 10−6. The step size varies adaptively between hmin = 0.00425 s and hmax = 0.2 s. The average step size h is equal to 0.01. For the DTM-based simulation, this average h = 0.01 was used as a fixed step size, shown in Figure 2-6.

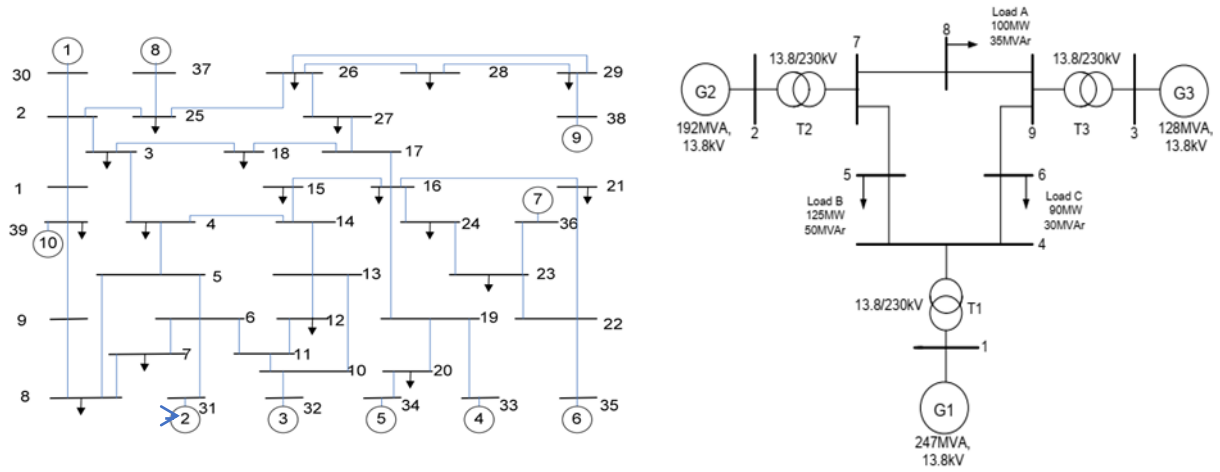

(**a**) (**b**)

Figure 2-5 **One-line diagram of (a) New England 39 bus system; (b) IEEE 9 bus system [18].**

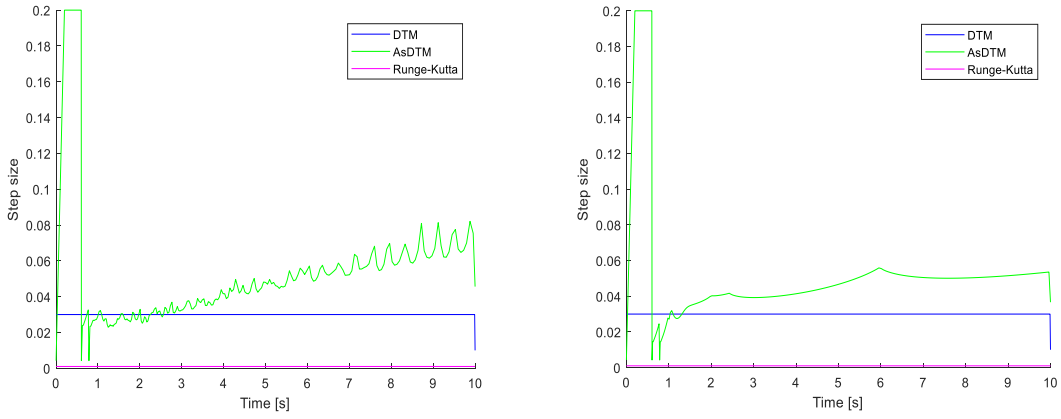

(**a**) (**b**)

Figure 2-6 **Step-size variations during simulation for IEEE (a) 9 bus and (b) 39 bus test systems.**

From Figures 2-7a,b and 2-8a,b, we can observe the number of iterations and simulation time requirement relationships among AsDTM, DTM, and Rk4 simulation methods, respectively. The total number of iterations for simulating three-phase fault cleared after 0.2 s using Rk4, DTM,

and AsDTM methods are 9995, 2345, and 1582 for the IEEE 9 bus test system and 9984, 3320, and 2260 for the IEEE 39 bus test system, respectively. Similarly, the total simulation time cost for the same case using Rk4, DTM, and AsDTM methods are 16.54 s, 2.331 s, and 1.292 s, for the IEEE 9 bus test system and 45.57 s, 9.614 s, and 7.692 for the IEEE 39 bus test system, respectively, from the simulation results shown in Figures 2-7 and 2-8.

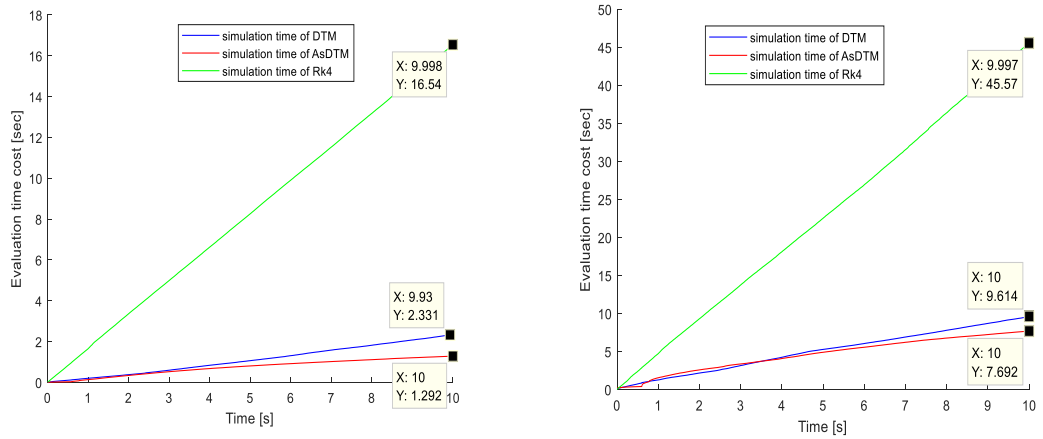

(**a**) (**b**)

Figure 2-7 Simulation time cost for IEEE (a) 9 bus and (b) 39 bus test systems.

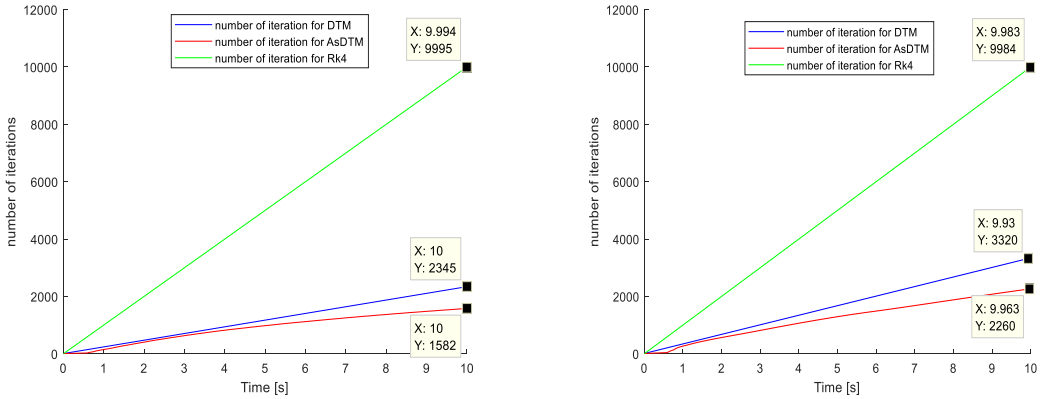

(**a**) (**b**)

Figure 2-8 Number of iterations for IEEE (a) 9 bus and (b) 39 bus test systems.

DTM-based simulation: The proposed AsDTM improved/reduced the total simulation time cost and total number of iterations by 20% and 31.93% for the IEEE 39 bus test system and improved/reduced the total simulation time cost and total number of iterations by 44.57% and 32.54% for the IEEE 9 bus test system, respectively.

Rk4-based simulation: The proposed AsDTM improved/reduced the total simulation time cost and total number of iterations by 83% and 77.36% for the IEEE 39 bus test system and

improved/reduced the total simulation time cost and total number of iterations by 92% and 84% for the IEEE 9 bus test system, respectively.

Therefore, we can conclude that the proposed AsDTM-based power system transient stability simulation method increases simulation speed by 20–44.57% and 83–92% when compared with the DTM- and Rk4-based simulations, respectively.

Figures 2-9a,b and 2-10a,b, show the rotor angle and speed errors simulation results. Error results relationships among AsDTM and DTM simulation methods are given in Table 2-1 below.

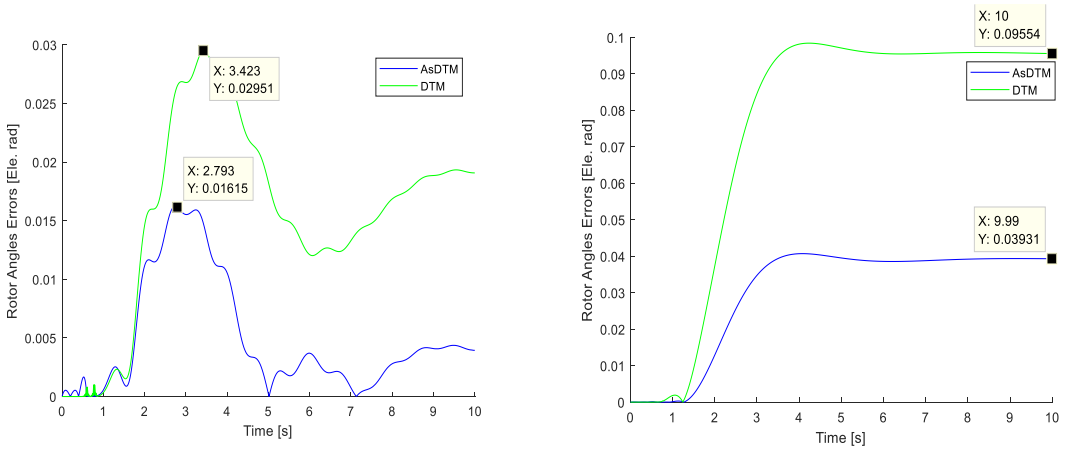

(**a**) (**b**)

Figure 2-9 **Rotor angle error for IEEE (a) 9 bus and (b) 39 bus test systems.**

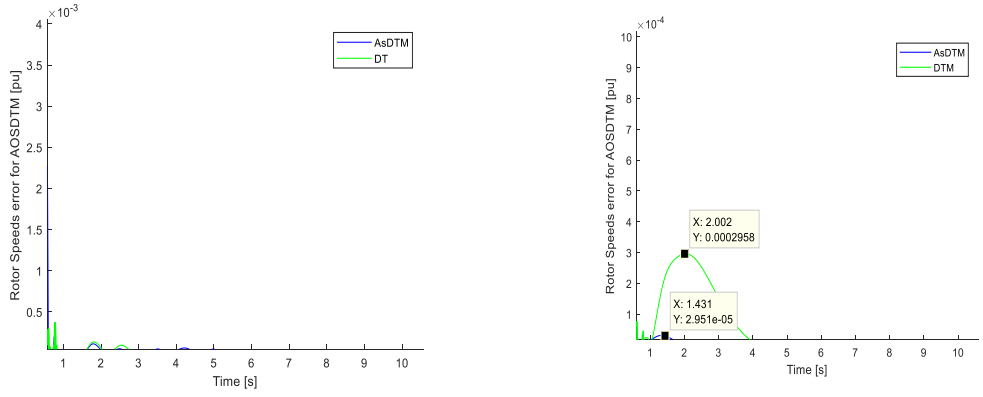

(**a**) (**b**)

Figure 2-10 Rotor speed error for IEEE (a) 9 bus and (b) 39 bus test systems.

Table 2-1 Rotor angle and speed errors simulation results relationships

Method	Max Error			
	IEEE 9	IEEE 39	IEEE 9	IEEE 39
	Rotor Angle (rad)		Rotor Speed (pu)	
AsDTM	0.01615	0.03931	0.00005	0.00002951

DTM	0.02951	0.09554	0.0005	0.0002958

From the simulation results of Figures 2-9a,b and 2-10a,b, and Table 2-1, compared with the DTM-based simulation, the proposed AsDTM-based power system transient stability simulation improves rotor angle error by 45.27% and 58.85% and improves rotor speed error by 90% for IEEE 9 and IEEE 39 test systems, respectively.

Figures 2-11a,b and 2-12a,b, represent the rotor angle and speed simulation results, where the quality of results obtained with AsDTM and DTM methods used the convergence criterion, the measure of which is the concurrency time of curves corresponding to two compared solutions. The best convergence was found for the AsDTM results. This implies that the AsDTM-based simulation gives more accurate results. However, since the shapes of the trajectories obtained by both DTM and AsDTM methods were the same as the reference trajectory obtained by the Rk4 method, we can conclude that both DTM and AsDTM methods are numerically stable.

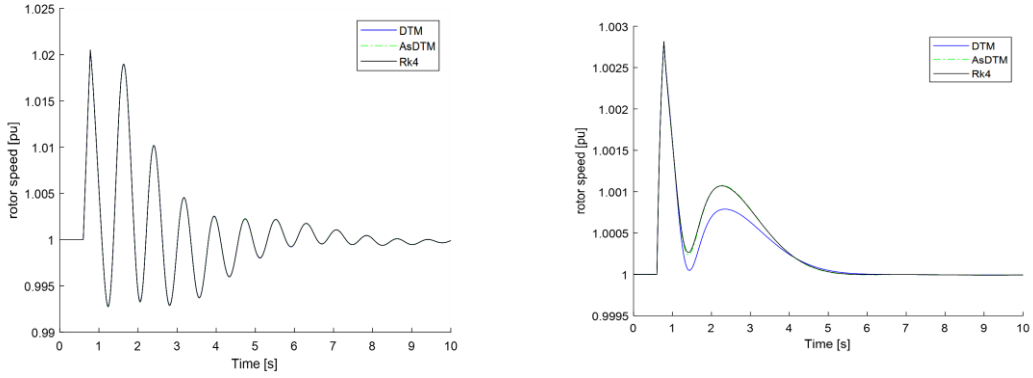

Figure 2-11 **Rotor speed simulation for IE(a) 9 bus and (b) 39 bus test systems.**

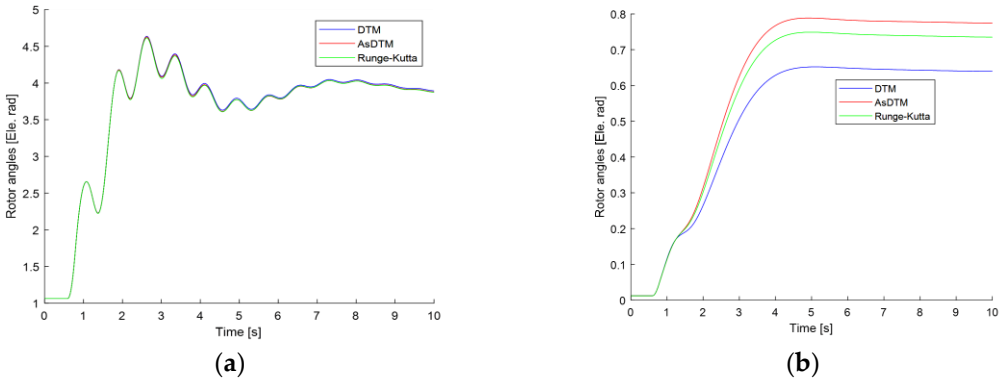

Figure 2-12 **Rotor angle simulation for IEEE (a) 9 bus and (b) 39 bus test systems.**

2.6. Control method

In security monitoring, we should check and make sure that at every given operating condition for an assumed (hypothetical) contingency (fault or equipment outage), the system will survive. If we find out that the system is transitioning into (insecure state) we should initiate "preventive control" measures in an offline or online bases.

Offline preventive measures::

- Re-dispatching (shift load from one generator to another, etc.)
- Mobilizing reserves
- Mobilize additional var resources to provide voltage support
- **Reduction of transmission system reactance:** This can be accomplished by adding extra parallel transmission circuits, implementing series compensation on existing circuits, and utilizing transformers with lower leakage reactance.
- **Connecting dynamic braking resistors:** These can be installed at generator and substation terminals to counteract electromechanical acceleration during faults. Additionally, shunt resistors can be activated to create an artificial load after a fault, enhancing the damping of accelerated generators[**40**]

Online remedial and preventive measures include:

- Transient excitation boosting
- HVDC link (if available) rapid power ramping
- Generator tripping
- Online Transformer tap-changer blocking
- Generation fast valving
- Automatic Load shedding

In this thesis, generation rescheduling is viewed as a practical preventive control measure to enhance system security during contingencies. To effectively prepare the appropriate level of generation rescheduling, a fast and robust tool for assessing system dynamic behavior is essential. This ensures timely and effective actions can be taken to maintain system stability. Detail of the proposed assessment of preventive control measures is given in Chapter 5.

2.7. General framework of the developed dynamic security analysis tools

The overall framework of the proposed dynamic security analysis tools are illustrated in Figure 2 13. These tools are developed using MATLAB codes in MATLAB environment. To perform a dynamic simulation, three input m-files have been defined: one for static (power flow) data, second for dynamic data, and third for event (disturbance/fault) data. Matpower format has been used for power flow data. The dynamic data consist of generator data, exciter data, and governor data. The event data file defines three matrices: event, bus-change, and line-change. These tools also accept an option vector as an optional fourth input argument, **mdoption**s. The option vectors used are solving method, tolerance, minimum and maximum step size, output, and plots. Output data consist of matrixes of state and non-state variables.

These tools have three basic functional parts. The first function is a function for contingency screening and ranking. In this section, system post-disturbances behavior is studied based on power system transient stability simulation during all credible contingencies and transient stability indices (TSI) are evaluated for the contingencies, and ranked. Finally the worst contingency is identified. Detail descriptions of the analysis method used in building this function is presented in Chapter 3. The next function is a function for Transient stability assessment (TSA) through evaluation of CCT. In this part power system transient stability is assessed for the worst contingency identified in the previous part and critical and noncritical machines clusters are identified based on system dynamic performance simulation with respect to Center of Angle (COA) including generator's sensitivity factors. The algorithm and analysis method used in this functional part is presented in Chapter 4.

The third functional part is a function where PSO based optimal generation rescheduling to enhance power system dynamic security satisfying operational constraints with minimum loss is performed. The mathematical formulation of the necessary conditions is a system dynamic performance analysis based on Adaptive Order and Step-size based Differential Transformation Methods (AOSDTM). The output is the best control strategy with which to mitigate instabilities. Description of the algorithm and analysis method used is given in Chapter 5.

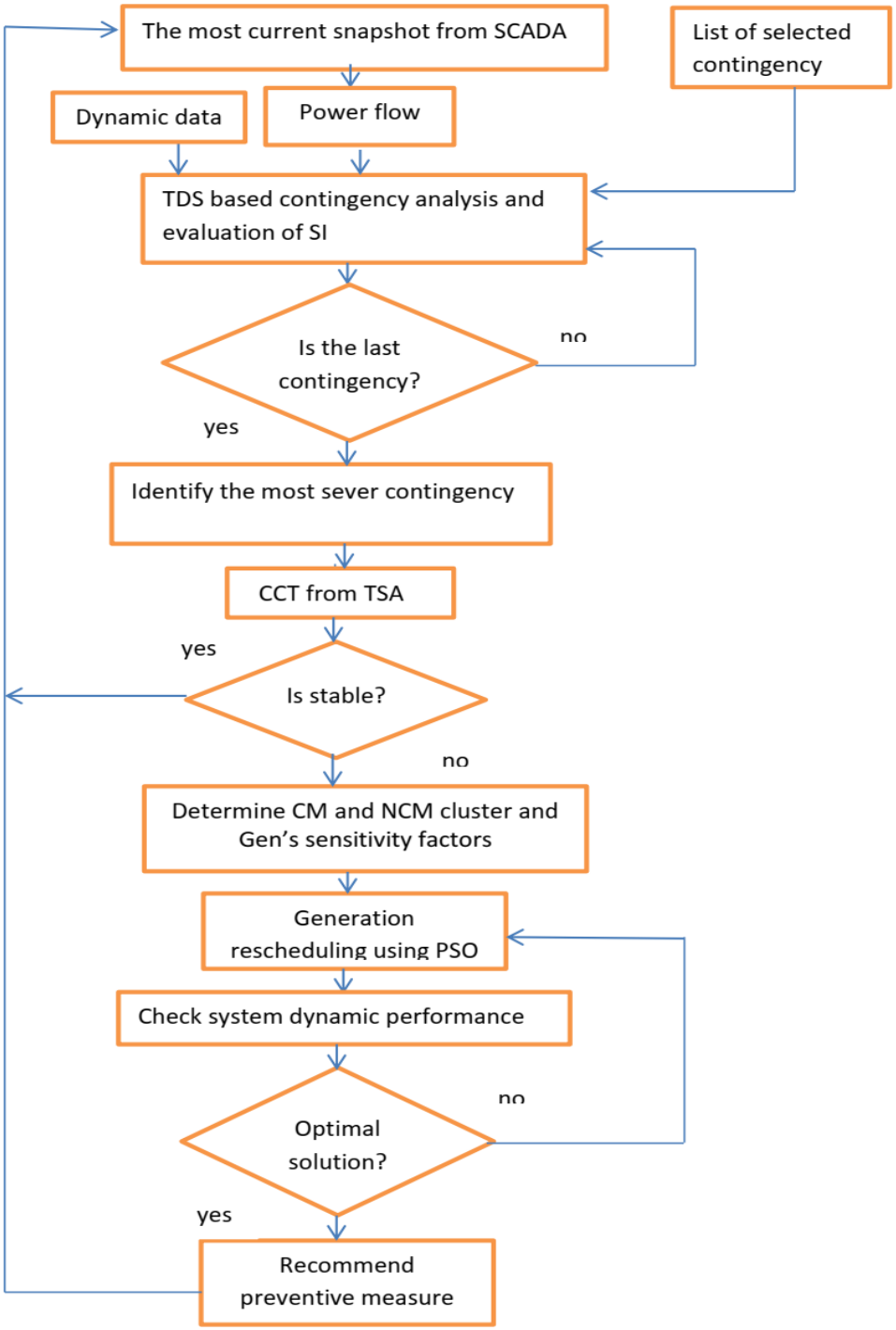

Figure 2-13 The schematic diagram of the proposed dynamic security analysis tools framework

CHAPTER THREE: Fast and Robust Power System Contingency Screening and Ranking

3.1. Introduction

The purpose of contingency screening and ranking is to identify and list potentially sever contingencies for detail evaluation of the power system due to the fact that every credible contingency will not bring instability problem to the power system. Conformation of critical contingencies list is created according to the comparisons of the performance of power system [**57**] [**58**] [**59**]. The performance of power system after being subject to each contingency are evaluated with respect to capacities of network equipment's, operating constraints, etc. During contingency screening, contingencies with small influence on power system operation are removed. Their exclusion from critical contingencies achieves a significant reduction of information for near real-time operation, i.e. only few potentially severe contingencies are considered to undergo detailed evaluation. This detailed analysis is usually performed using TDS from which the severity of each contingency is determined so that possible preventative actions may be determined.

During contingency screening, the instability aspects of the power system should be analyzed and specified to perform detailed assessment for security violations and stability problems. The impacts of contingencies are mostly measured in terms of severity indices (SI) such as transient stability indices (TSI). Various methods of contingency screening and ranking have been proposed and applied, but ensuring a balance between assessment speed and accuracy still remains challenging. Contingency screening methods for thermal overloading or voltage declines may be much easier to apply than those for stability, in which complex dynamics and nonlinearities of the system may render simplified screening methods unreliable.

Contingency screening and ranking methods used in commercially available Dynamic Security Analysis tools (DSA) generally categorized as direct transient stability analysis method (such as TEF), detail time domain simulation or numerical integrations method, and severity or stability indicators [**60**]Authors of [**61**]- [**62**] proposed some indices for contingency screening and ranking However, they often require numerical integration for a significant interval after the fault clearance. [**62**] Proposes heuristic individual and global transient instabilities indices based on combined numerical integration and direct methods (hybrid technic) of filtering contingency in near real time DSA session. Approaches based on simplified modeling with assumptions,

presented by [**63**] can result in substantial simulation errors. A transient stability simulation based indices for contingency screening and ranking are proposed by [**64**], which solves both differential and algebraic equations of a power system numerically by MATLAB ODE solver.

Approaches, such as numerical integration, direct (energy function methods) and combination of both methods are explored by [**65**] [**35**] [**66**]. The conventional numerical integration based methods are accurate but requires intensive computations but direct methods are the reverse. Multiple severity indices for DSA and contingent disturbance event ranking are proposed by [**67**] . To assess the severity of a contingent disturbance event, they suggest multiple indices that rely on dot products of specific system states, transient energy conversion (TEC), and coherency. They also presented an amalgamated index which, allocate different weights to the previously described indices and aggregates their contributions. This approach involves conducting a detailed TDS after the fault is cleared for up to 500 ms and the indices are calculated to evaluate stability and rank the respective contingent disturbance event. However, many of these indices are unable to distinguish between harmless and harmful (unstable) scenarios while tested using with a particular test case. Power system contingency screening and ranking utilizing techniques such as TEF was presented by [**68**]. The proposed approach has garnered significant attention, and analysis based on such technics has been continuously refined.

Hybrid methods, like SIME [**35**], improve transient stability simulation speed but with simplified modeling and assumptions which can result in substantial errors.. This approach is divided into 2 components. The first component screens out harmless contingent disturbance events, while the second component ranks and evaluates the rest potentially sever contingent disturbance events based on their evaluated CCTs. This requires carrying out one or two TDS per contingent disturbance event. Fast power system contingency screening technique based on SIME was presented by [**69**]. A new index has been introduced for grouping generators, along with contingent disturbance event classification relying on the power angle shape of the one machine infinite bus (OMIB) equivalent. For this purpose, the proposed approach conducts one up to three TDS per contingency, by changing the fault clearing time. Alternatively, contingent disturbance event screening methods, which are executed periodically, deployment of wide-area measurement systems in power systems enabled transient stability prediction utilizing real time synchronized phasor measurements.

A contingent disturbance event filtering technique based on the EEAC as presented in [**70**] was proposed by [**71**]. EEAC enhances the original equal area criterion (EAC) to extend its application with multi-machine systems. A set of procedure to eliminate harmless cases from a list of multiple contingent disturbance events was also formulated. To select and screen these harmless cases, the stability margins are calculated immediately after the fault is cleared using both static and dynamic EEAC, as presented in detail by Authors of [**72**] [**73**]. Subsequently, the established procedures are applied to determine whether a case is harmless and should be excluded. However, approaches such as power system TDS based on energy function, numerical integrations, and probabilistic methods described above provide quantitative measures which indicate the degree of system stability based on energy margin or stability indices but the required computational efforts and restrictions regarding modeling details. Therefore, there is an urgent need to improve and develop time domain simulation method for more robust and efficient power system contingency screening and ranking

3.2. The proposed contingency screening and ranking method

Power system contingency screening is expected to be executed periodically several times per day. It filters contingency to ensure system stability considering set of credible contingent disturbance events. TSI based efficient and robust power system contingency screening and ranking methods is introduced in this thesis. Based on the most current snapshot from the SCADA data, transient stability is simulated for each credible contingency and TSI is evaluated as the normalized weighted sum of squares of error at every simulation time step from the simulation results of both state variables and complex bus voltages. The TS indices evaluated based on the simulation results of machine's state variables are represented as machine's state variables indices (SI) and those evaluated based on the simulation results of machine's bus complex bus voltages are represented as algebraic indices (AI). Finally contingencies are ranked based on these two indices and the worst contingency is identified for the next detail assessment. The proposed method (1) is accurate because it is flexible in handling power systems with any model detail and complexity without limitations; (2) has improved computation speed. These enable the proposed power system contingency screening and ranking method to be applied in a near real-time DSA tools sessions.

Figure 3.1 indicates flowchart of the proposed contingency screening technique. The following subsections gives description of each parts of the proposed algorithm

3.2.1. System Snapshot

The most current system snapshots consisting of complex power flows through transmission lines, complex power injections (generation or demand at buses), and bus voltage magnitudes are read from Supervisory Control and Data Acquisition (SCADA) data.

3.2.2. Update Power System Models

The obtained most current system snapshot and the model database provide the required dynamic and static data and parameters of each component. Based on these power system models representing current system state including the admittance matrix Y is constructed.

3.2.3. Power flow and Dynamic system initialization

Power system models categorized based on model details/complexity level and stored in files with independent addresses. The model databases provide the required dynamic and static data and parameters of each component. Based on these power system models representing current system state including the admittance matrix Y is constructed. Using these power system models and Matpower software package, perform power flow analysis which is considered to represent the system's pre-fault steady state conditions and hence initialize the power system transient stability simulations. Further, a list of credible contingencies is generated here.

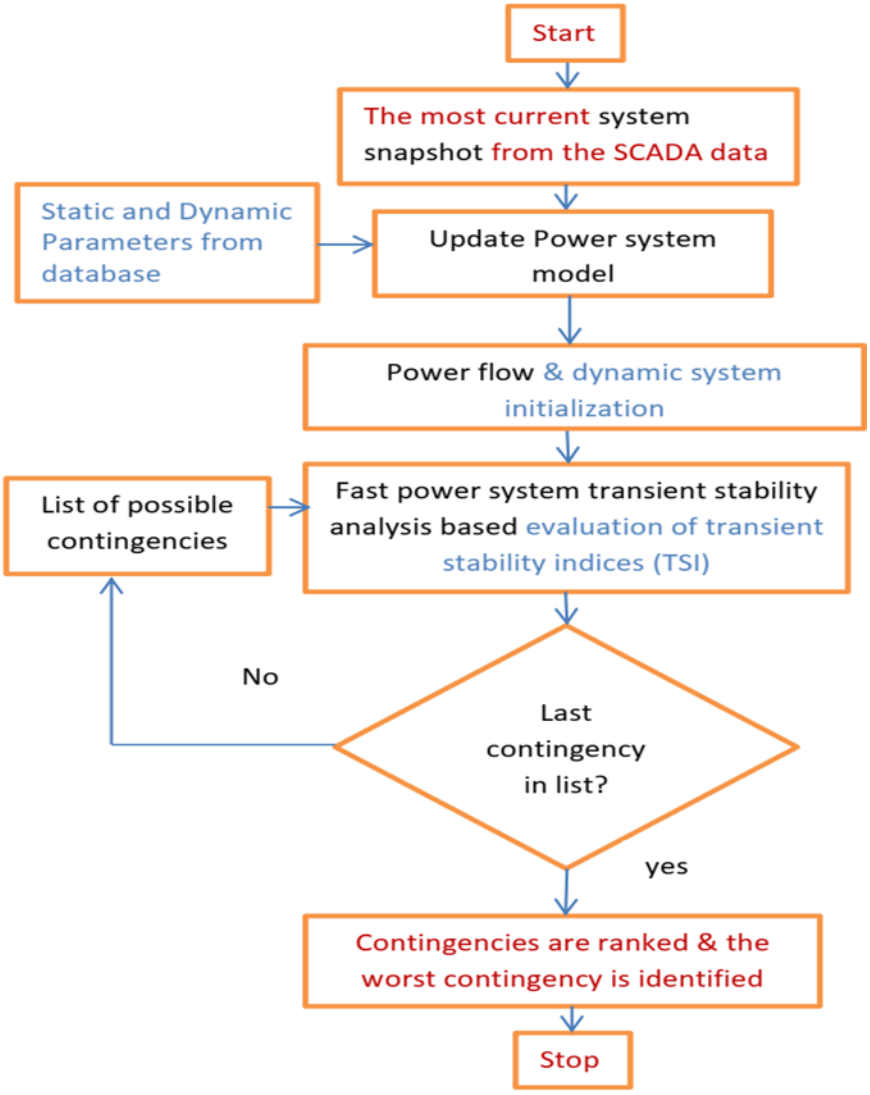

Figure 3-1 Flowchart diagram of the proposed power system contingency screening

3.2.4. Transient Stability Analysis Based TSI Evaluations

Power system transient stability analysis is one of the most critical functions of dynamic security analysis (DSA) tools. Traditional numerical integration method is commonly used in commercially available power system transient stability simulation tools. Speed of computation remains the most critical challenge for its application in near real-time transient stability assessment. It was proved that the DTM-based transient stability simulation method reduces the impact of computation burden. For near real-time application, the DTM-based simulation method still requires further improvement regarding its accuracy and performance efficiency. The main focuses of this subsection is to develop new, fast and robust methods of evaluating transient stability indices. The developed method is based the power system transient stability

analysis algorithm given by the flowchart shown in Figure 2-3. Detail descriptions of each steps of the applied power system transient stability simulation given by flowchart Figure 2-3 is presented in Chapter 2 Section 2.3.

Transient stability analysis-based TS indices evaluation of the scenario is triggered after the fault/event parameters (parameters that represent each credible contingency) have been determined for all credible contingencies listed and the power system model is initialized. The TSI of each considered contingency is determined in terms of the dynamic performance response at each machine bus. The dynamic performance response at each machine bus is determined in terms of the machine state and algebraic variable values deviation from their respective steady-state conditions. When a power system is subjected to a large disturbance, the algebraic variables change instantly while the machine state variables may need some transient time to change values. Upon clearing, the variables are expected to return to their initial operating values or new and acceptable steady state values. However, this is not always the case due to the severity of that disturbance.

In this dissertation, severity index values, such as SI and AI representing the machine related state variables and machine bus complex voltage deviations from steady state conditions respectively are used to identify and list contingencies according to their severity. For each contingency in the list, these deviations are expressed as weighted sum of squares of error of the machine state and non-state variables, complex bus voltages at each simulation time step as defined by Equation (3-1). Where ψ (k) = DT of ψ(t) and V(k)=DT of v(t).

$$SI_{new} = SI_{prev} + \left(\frac{\sum_{i=1}^{m}\sum_{j=1}^{l} W_{ij}(\psi_{ij}(t) - \psi_{ij}(t_0))^2}{m} \right) * h$$

$$AI_{new} = AI_{prev} + \left(\frac{\sum_{i=1}^{m}\sum_{j=1}^{l} W_{ij}(v_{ij}(t) - v_{ij}(t_0))^2}{m} \right) * h \qquad (3\text{-}1)$$

Where ψ(t) represents δ_i(t), ω(t) $_i E'_{qi}$(t) , E'_{di}(t) , V, (t) V_{fi}(t) , P_{chi}(t) , P_{svi}(t) and E_{fi}(t) & i =1,2,3……m, represent machine number

h= the new step-size

SI_{new} = new severity index values of machine related state variables

SI_{prev} = previous severity index values of machine related state variables

AI_{new} = new severity index values of machine bus complex voltage

AI_{prev} = previous severity index values of machine bus complex voltage

W_{ij} = weight associated with the state and algebraic variables

l = the number of the state or algebraic variables.

Finally, indices evaluated for all listed credible contingencies are related by normalizing them with the largest of all.

The values of state and algebraic variables ψ and $\bar{v}$ respectively and the step-size (h) in the above equations are obtained from the transient stability analysis results based on AsDTM method, described in Section 2.3 of Chapter 2. These indices can be evaluated at any time required during the simulation period.

3.2.5. Contingencies are ranked and the worst contingency is identified

For each considered contingency case, respective severity index is evaluated. Finally each of the severity indexes normalized with the largest of all the indices and listed in descending order. The

contingency in the upper top position is the most critical contingency identified and the contingency in the bottom position is the least critical contingency.

3.3. Case studies and results

3.3.1. Test system, cases and setup

3.3.2. Test system

Two test systems are employed to validate the proposed screening approach. The first test system is the IEEE 9-bus system, which consists of 9 bus and 3 machines. The second test system is the IEEE 39-bus system, which consists of 39 bus and 10 machines. Constant impedance load model is used with the TDS. A two axis model is used to represent synchronous generators, each with Type_1 automatic voltage regulation and primary speed control systems.

3.3.3. Test cases

A list of credible contingencies are identified for testing the proposed fast and robust techniques of screening and ranking power system contingency, For both systems three phase bus faults are considered. This faults are located at 6 buses (non-generator buses) for the first test system and 29 buses (similarly, non-generator buses) for the second test system. A susceptance of 10^{-10} is considered enough to bring zero impedance bus faults [**74**]. This fault is added to the network admittance matrix for every non-generator buses in sequential order (one after the other). In this work the fault is cleared only by removing the added fault parameters from the respective bus admittance matrix without isolating the faulted bus itself so that the network structure is not changed..

3.3.4. Test setup

The tests are carried out on standard personal computer(PC) with the following properties: Intel(R) Core(TM) i5-5200U CPU @ 2.20GHz 2.20 GHz, 8GB RAM, running on 64-bit operating system, x64-based processor. The TDS are conducted using the simulation tools/codes developed based on proposed AsDTM on MATLAB R2017b [**75**]. MATPOWER [**76**] is used for solving power flow. The CPU times include all steps of the contingency screening and ranking.

3.3.5. Assessment Results and Discussion

To validate the proposed contingency screening and ranking method, three-phase short-circuit faults located at 6 buses (non-generator buses) for IEEE 9-bus test system and 29 buses (similarly, non-generator buses) for the 39-bus test system are used. To analyze their impacts, each fault is triggered at 0.6 s and cleared at two different fault clearing times. TSI for each faulted bus is evaluated, first by considering the 0.15 s (150 ms) fault clearing time and next by considering the 0.25 s (250 ms) fault clearing time. During both scenarios, the evaluated TSI are ranked and plotted. In both cases, the accuracy and performance of the proposed method are validated using the assessment results based on the traditional numerical method (fourth-order Range–Kutta (Rk4) with step size h = 0.001 s) as benchmarks. For this purpose, the differential transformation (DT) order k = 14 is used for both test systems with both DTM and AsDTM simulation methods.

Two types of TS indices are evaluated for each credible contingency during transient stability analysis at each assessment time step. These indices were evaluated based on the machine's state variables (as rotor angle deviations(δ),angular speed(ώ), etc.); analysis results are represented as state variable indices (SI) and those evaluated based on the machine's bus complex bus voltages (such as bus voltage magnitude (V) and voltage angle(θ)) analysis results are represented as algebraic variable indices (AI)..

3.3.5.1. Validation of the accuracy of the proposed method

In the following sub-section, the accuracy of the proposed method is validated with respect to the TS indices evaluated using transient stability analysis based on a traditional numerical method (fourth order Range–K utta (Rk4))) as a benchmark. Tests are per-formed considering two scenarios. During the first scenario, contingencies are analysed and ranked considering a 150 ms fault clearing time and the next scenario by considering a 250 ms fault clearing time. The TSI evaluated based on a fourth order Range–K utta Rk4 (reference method), the proposed AsDTM, and the classical DTM methods using both test systems are plotted as shown by Figures 3-2a,b and 3-3a,b below. The TSI results evaluated based on the proposed method, and those evaluated from the classical DTM method (with a fixed step-size of h = 0.0125 s) are ranked and compared with the benchmark results as given in Tables 3–1 to 3-4 below. As one can clearly observe from the plots given by Figures 3-2a,b and 3-3a,b, the TSI (AI and SI) results evaluated based on the proposed method for the 150 ms fault clearing time indicate that the most and least critical situations are when there is a three phase short-circuit fault at buses 22 and 12, respectively, for

the 39-bus test system and at buses 8 and 5, respectively, for the 9-bus test system. These results strongly agree with the most and least critical buses identified based on the Rk4 (benchmark) for both test cases as shown by Figures 3-2a,b and 3-3a,b below. But the plots of the TSI evaluated based on the classical DTM method indicate that the most and least critical situations are when there is a three-phase short-circuits fault at buses 22 and 9, respectively, for the 39-bus test system. This result shows that the least critical situation identified by using the classical DTM method is completely different from the benchmark result..

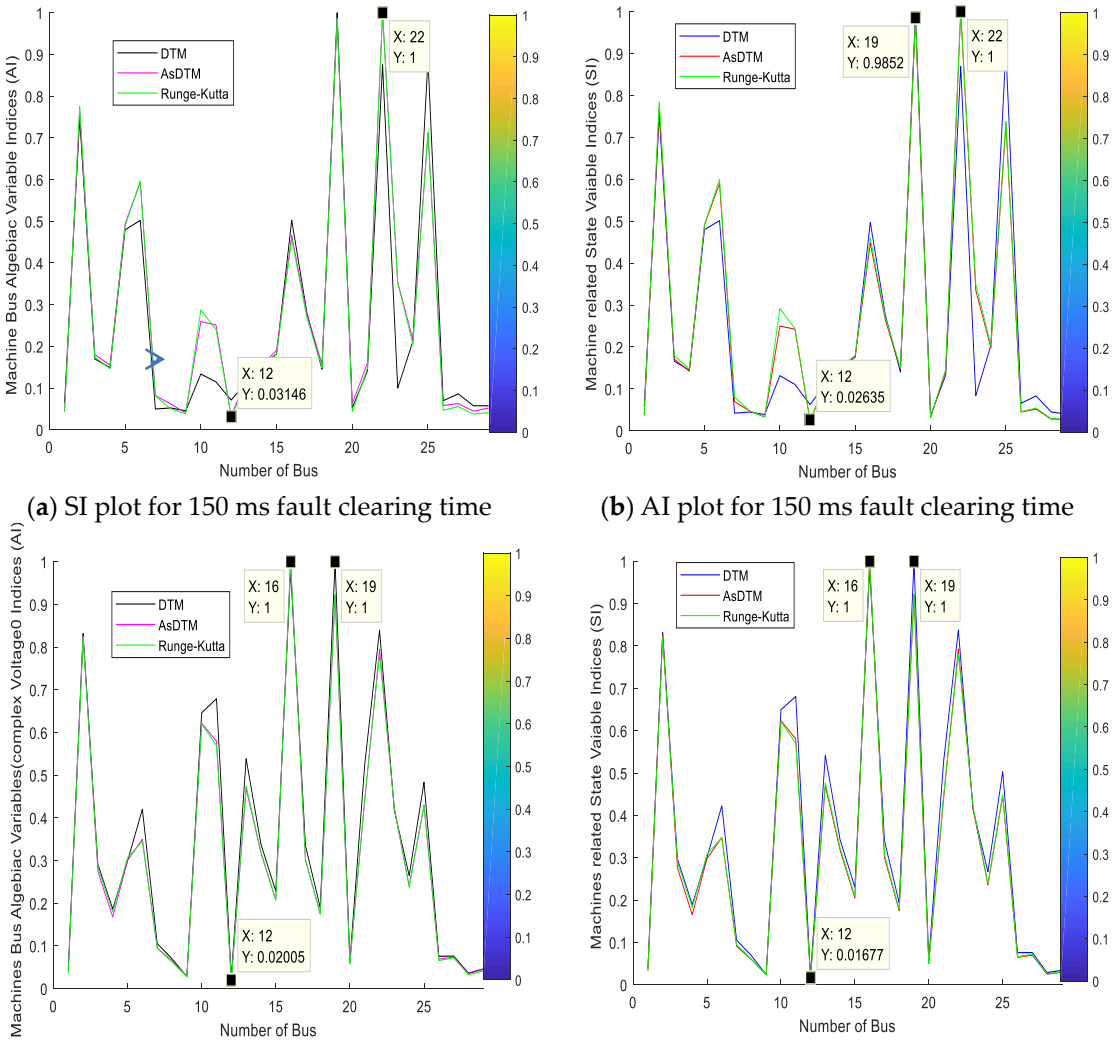

(**a**) SI plot for 150 ms fault clearing time (**b**) AI plot for 150 ms fault clearing time

(**c**) SI plot for 250 ms fault clearing time (**d**) AI plot for 250 ms fault clearing time

Figure 3-2 SI and AI plots of 39-bus test system

Similarly, from the plots given by Figures 3-2c,d and 3-3c,d, the TSI (AI and SI) evaluated based on the proposed method for the 250 ms fault clearing time indicate that the most and least critical situations are when there is a three-phase short-circuit fault at buses 16 and 12, respectively, for

the 39-bus test system and at buses 8 and 5, respectively, for the 9-bus test system. These results again strongly agree with the most and least critical buses identified based on the reference method for both test cases. But the plots of the TSI based on the classical DTM method indicate that the most and least critical situations are when there is a three-phase short-circuit fault at buses 19 and 12, respectively, for the 39-bus test system and at buses 8 or 9 and 4, respectively, for the 9-bus test system. These results show that the most and least critical situations identified by using the classical DTM method are different from those identified by the benchmark method. Therefore, more accurate results are found by using the proposed contingency screening and ranking method.

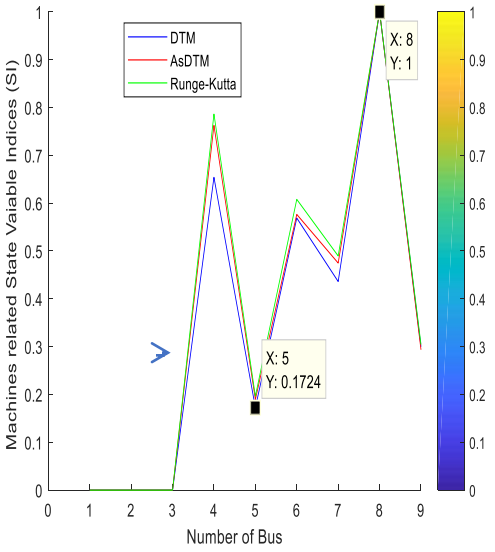

(**a**) SI plot for 150 ms fault clearing time

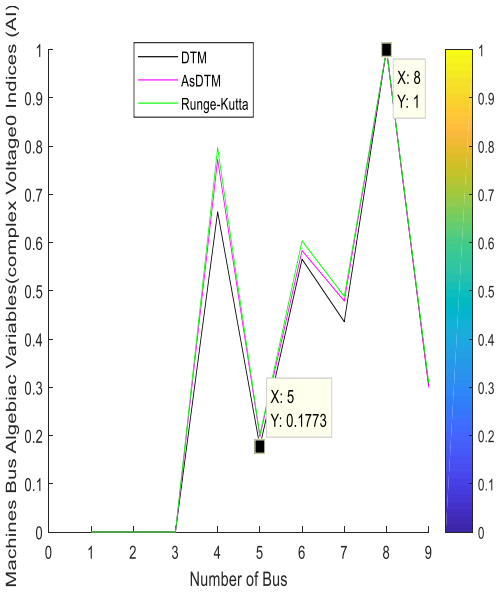

(**b**) AI plot for 150 ms fault clearing time

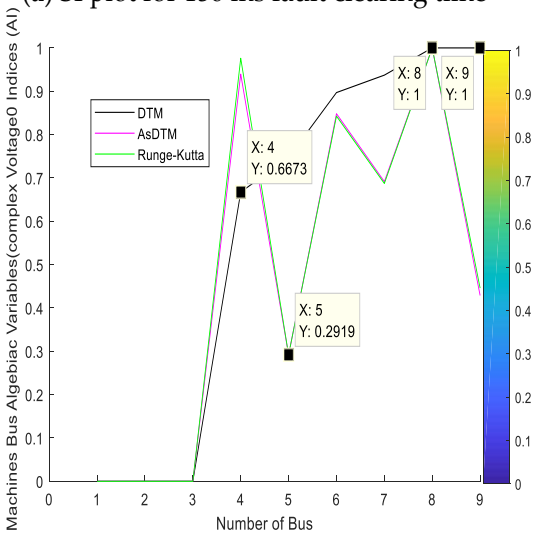

(**c**) SI plot for 250 ms fault clearing time

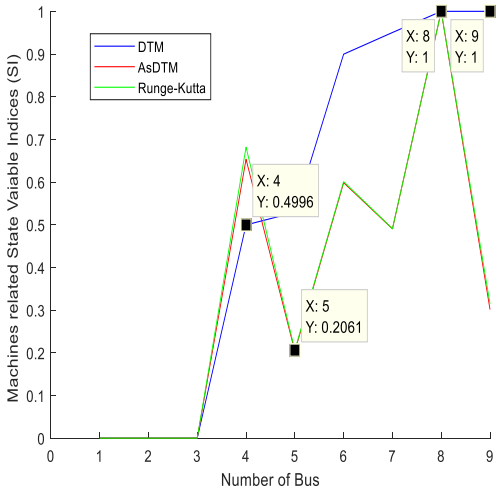

(**d**) SI plot for 250 ms fault clearing time

Figure 3-3 SI and AI plots of 9-bus test system

In addition, Figures 3-2a–d and 3-3a–d representing the SI and AI plots, where the quality of the plot results obtained with the AsDTM and DTM methods used the convergence criterion, the measure of which is the concurrency of trajectories rout corre-sponding to two compared solutions. The best convergence was found for the AsDTM-based SI and AI plots. This implies that the AsDTM-based TSI evaluation gives more accurate results. On the other hand, since the shapes of the trajectories obtained by both the DTM and AsDTM methods were the same as the reference trajectory for the first scenario (Figures 3-2a,b and 3-3a,b) we can conclude that both the DTM and AsDTM methods are numerically stable. However, when we observe the TSI plots for the second scenario (for the 250 ms fault clearing time), specially Figure 3-3c,d show that the DTM method is not numerically stable as the network complexity decreases and fault clearing time increases.

Tables 3–1 to 3-4 below give contingencies ranked using their respective TSI evaluated based on the benchmark, classical DTM and the proposed AsDTM methods considering both 150 ms and 250 ms fault clearing by using both test systems. From the summary and the results given in Table 3-5, in all cases the proposed AsDTM-based contingency screening and ranking method provides 93% accurate results.

Table 3-1 TS indices error magnitude relationship among AsDTM and DTM assessment methods

Cont. Ranked Using TSI Evaluated Based on Numerical Integration Method (Benchmarks)		**Cont. Ranked Using TSI Evaluated Based on AsDTM Method**		**Con. Ranked Using TSI Evaluated Based on DTM Method**	
Bus No	Rank	Bus No	Rank	Bus No	Rank
Bus 22	1	Bus 22	1	Bus 22	1
Bus 19	2	Bus 19	2	Bus 19	2
Bus 2	3	Bus 2	3	Bus 2	3
Bus 25	4	Bus 25	4	Bus 25	4
Bus 6	5	Bus 6	5	Bus 6	5
Bus 5	6	Bus 5	6	Bus 16	6
Bus 16	7	Bus 16	7	Bus 5	7
Bus 23	8	Bus 23	8	Bus 23	8
Bus 10	9	Bus 10	9	Bus 10	9
Bus 17	10	Bus 17	10	Bus 17	10
Bus 11	11	Bus 11	11	Bus 15	11
Bus 24	12	Bus 24	12	Bus 11	12
Bus 15	13	Bus 15	13	Bus 24	13
Bus 3	14	Bus 3	14	Bus 3	14

Bus 14	15	Bus 18	15	Bus 21	15
Bus 18	16	Bus 14	16	Bus 18	16
Bus 4	17	Bus 4	17	Bus 14	17
Bus 21	18	Bus 21	18	Bus 4	18
Bus 13	19	Bus 13	19	Bus 13	19
Bus 7	20	Bus 7	20	Bus 27	20
Bus 27	21	Bus 27	21	Bus 26	21
Bus 8	22	Bus 8	22	Bus 8	22
Bus 26	23	Bus 26	23	Bus 1	23
Bus 1	24	Bus 1	24	Bus 7	24
Bus 9	25	Bus 9	25	Bus 29	25
Bus 20	26	Bus 20	26	Bus 28	26
Bus 28	27	Bus 28	27	Bus 12	27
Bus 29	28	Bus 29	28	Bus 20	28
Bus 12	29	Bus 12	29	Bus 9	29

Table 3-2 Three-phase short-circuit on each non-generator buses of 9-bus test system and each cleared after 150 ms

Cont. Ranked Using TSI Evaluated Based on Numerical Integration Method (Benchmarks)		**Cont. Ranked Using TSI Evaluated Based on AsDTM Method**		**Con. Ranked Using TSI Evaluated Based on DTM Method**	
Bus No	Rank	Bus No	Rank	Bus No	Rank
Bus 8	1	Bus 8	1	Bus 8	1
Bus 4	2	Bus 4	2	Bus 4	2
Bus 6	3	Bus 6	3	Bus 6	3
Bus 7	4	Bus 7	4	Bus 7	4
Bus 9	5	Bus 9	5	Bus 9	5
Bus 5	6	Bus 5	6	Bus 5	6

Table 3-3 Three-phase short-circuit on each non-generator buses of 39-bus test system and each cleared after 250 ms.

Cont. Ranked Using TSI Evaluated Based on Numerical Integration Method (Benchmarks)		**Cont. Ranked Using TSI Evaluated Based on AsDTM Method**		**Con. Ranked Using TSI Evaluated Based on DTM Method**	
Bus No	Rank	Bus No	Rank	Bus No	Rank
Bus 16	1	Bus 16	1	Bus 19	1
Bus 19	2	Bus 19	2	Bus 16	2
Bus 2	3	Bus 2	3	Bus 22	3
Bus 22	4	Bus 22	4	Bus 2	4
Bus 10	5	Bus 10	5	Bus 11	5
Bus 11	6	Bus 11	6	Bus 10	6

Bus 13	7	Bus 13	7	Bus 13	7
Bus 25	8	Bus 25	8	Bus 21	8
Bus 21	9	Bus 21	9	Bus 25	9
Bus 23	10	Bus 23	10	Bus 6	10
Bus 6	11	Bus 6	11	Bus 23	11
Bus 14	12	Bus 14	12	Bus 14	12
Bus 5	13	Bus 5	13	Bus 17	13
Bus 17	14	Bus 17	14	Bus 12	14
Bus 3	15	Bus 3	15	Bus 3	15
Bus 24	16	Bus 24	16	Bus 24	16
Bus 15	17	Bus 15	17	Bus 15	17
Bus 4	18	Bus 18	18	Bus 18	18
Bus 18	19	Bus 4	19	Bus 4	19
Bus 7	20	Bus 7	20	Bus 24	20
Bus 27	21	Bus 27	21	Bus 27	21
Bus 26	22	Bus 26	22	Bus 26	22
Bus 8	23	Bus 8	23	Bus 8	23
Bus 20	24	Bus 20	24	Bus 20	24
Bus 1	25	Bus 1	25	Bus 1	25
Bus 29	26	Bus 29	26	Bus 29	26
Bus 28	27	Bus 28	27	Bus 28	27
Bus 9	28	Bus 9	28	Bus 9	28
Bus 12	29	Bus 12	29	Bus 12	29

Table 3-4 Three-phase short-circuit on each non-generator buses of 9-bus test system and each cleared after 250 ms.

Cont. Ranked Using TSI Evaluated Based on Numerical Integration Method (Benchmarks)		Cont. Ranked Using TSI Evaluated Based on AsDTM Method		Con. Ranked Using TSI Evaluated Based on DTM Method	
Bus No	Rank	Bus No	Rank	Bus No	Rank
Bus 8	1	Bus 8	1	Bus 8 & Bus 9	1
Bus 4	2	Bus 4	2	Bus 7	2
Bus 6	3	Bus 6	3	Bus 6	3
Bus 7	4	Bus 7	4	Bus 5	4
Bus 9	5	Bus 9	5	Bus 4	5
Bus 5	6	Bus 5	6	-	6

Compared with the benchmark results, the range of accuracy of assessment results based on the proposed AsDTM and the classical DTM methods are summarized as given in Table 3-5 below.

Table 3-5 Summary of the accuracy of the ranked contingencies based on DTM and the proposed AsDTM methods compared with the benchmark results.

Fault Cleared	Accuracy of Contingencies Ranked Using TSI Evaluated Based on AsDTM Method in %		Accuracy of Contingencies Ranked Using TSI Evaluated Based on DTM Method in %	
	For 39-Bus Test System	**For 9-Bus Test System**	**For 39-Bus Test System**	**For 9-Bus Test System**
150 ms	93	100	41.38	100
250 ms	93	100	44.82	16.67

From the results summary given in Table 3-5 above, we can conclude that the proposed contingency screening and ranking method is more accurate compared with the DTM method. The increase in the fault clearing time also has no influence on the accuracy of the proposed AsDTM method. Further, as the complexity or sizes of the network decrease the proposed method is as accurate as the reference method. But we can simply observe from the assessment results given in Tables 3-1 to 3-5 that as the network size as well as the fault clearing time increase the probability that the classical DTM method can identify the most critical contingency is almost null.

Even though the most and least critical buses screened out based on the proposed method are the same as the benchmark results (evaluated based on the Rk4 method) in all cases, the magnitudes of the evaluated TS indices (SI and AI) for the three-phase short-circuit at all non-generator buses for both test cases are not the same as the benchmark results. Figures 3-4a–d and 3-5a–d below show the error plots of the AsDTM- and DTM-based evaluated transient stability indices. As can be seen from Figures 3-4 and 3-5 a to d, the magnitudes of the generated SI and AI error by the DTM-based evaluation method are 0.1664 and 0.1619, respectively, for the 39-bus test system and 0.1327 for the 9-bus test system, when the fault is cleared after 150 ms in both cases. Similarly, the magnitudes of the generated SI and AI error by the proposed AsDTM-based evaluation method are 0.0418 and 0.02753, respectively, for the 39-bus test system and 0.03145 and 0.02427, respectively, for the 9-bus test system when the fault is cleared after 150 ms in both cases.

Similarly, when the fault is cleared after 250 ms, the magnitudes of the generated SI and AI error by the proposed AsDTM-based evaluation method are 0.01701 and 0.01254, respectively, for the 39-bus test system and 0.03661 and 0.02842, respectively, for the 9-bus test system and the

magnitudes of the generated SI and AI error by the DTM-based evaluation method are 0.1098 for the 39-bus test system and 0.685 and 0.5542 for the 9-bus test system, respectively.

Compared to the proposed method, the magnitude of the SI and AI error generated by the classical DTM-based evaluation method is relatively greater. This shows that more accurate indices are evaluated based on the proposed AsDTM method. A summary of the TS indices error magnitude resulted from using AsDTM and DTM assessment methods relative to the benchmark results are given in Table 3-6 below.

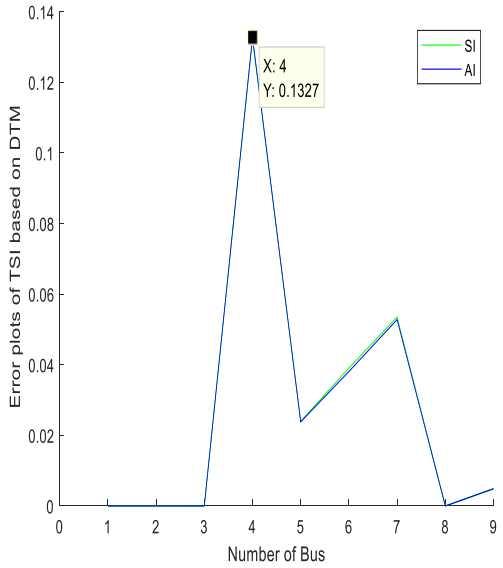

(**a**) Plots TSI evaluated based on DTM for fault clearing time of 150 ms

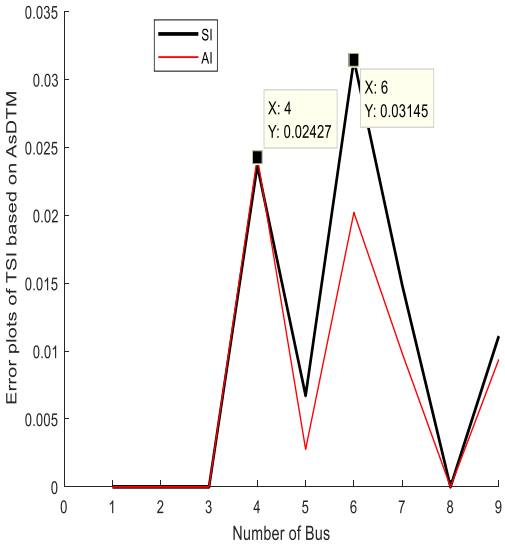

(**b**) Plots TSI evaluated based on AsDTM for fault clearing time of 150 ms

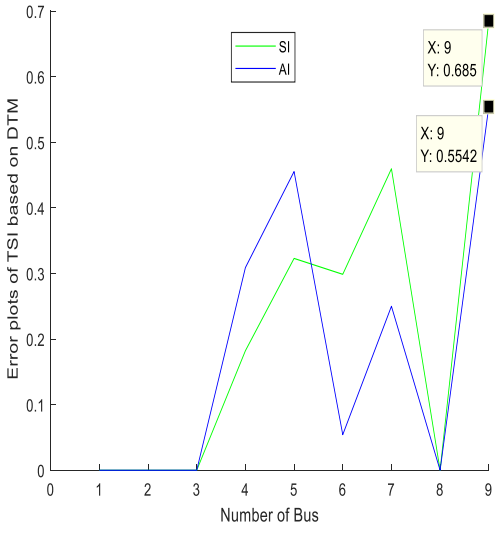

(**c**) Plots TSI evaluated based on DTM for fault clearing time of 250 ms

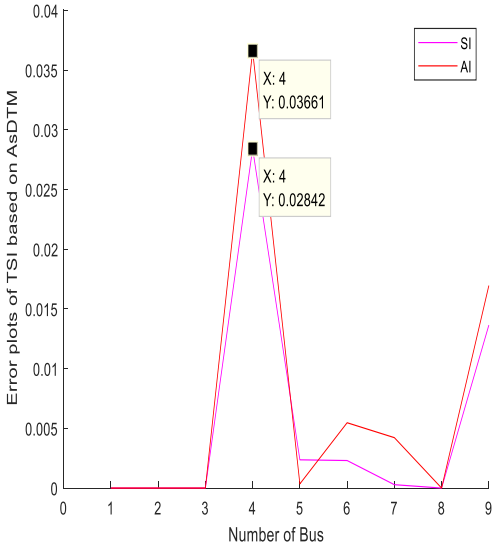

(**d**) Plots TSI evaluated based on AsDTM for fault clearing time of 250 ms

Figure 3-4 DTM- and AsDTM-based SI and AI error plots for 9-bus test system.

Table 3-6 TSI error by AsDTM and DTM methods relative to the benchmark results.

Test System	Fault Cleared After	Assessment Method	Maximum TSI Error	
			SI	**AI**
9 bus	150 ms	AsDTM	0.03145	0.02427
		DTM	0.1327	0.1327
	250 ms	AsDTM	0.03661	0.02842
		DTM	0.685	0.5542
39 bus	150 ms	AsDTM	0.0418	0.02753
		DTM	0.1664	0.1619
	250 ms	AsDTM	0.01701	0.01254
		DTM	0.1098	0.1098

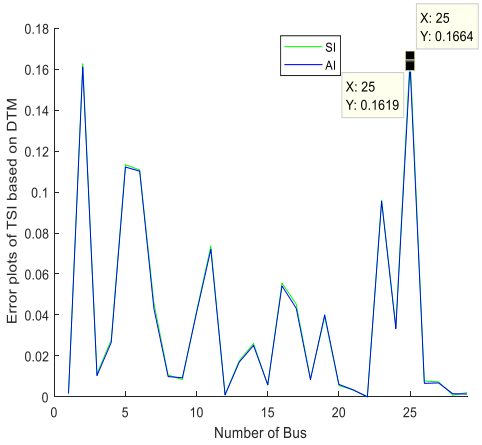

(**a**) Plots TSI evaluated based on DTM for fault clearing time of 150 ms

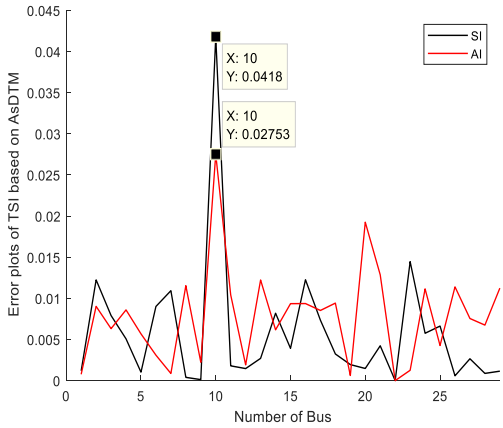

(**b**) Plots TSI evaluated based on AsDTM for fault clearing time of 150 ms

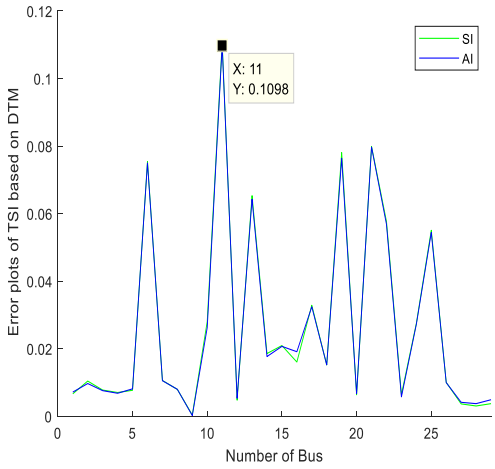

(**c**) Plots TSI evaluated based on DTM for fault clearing time of 250 ms

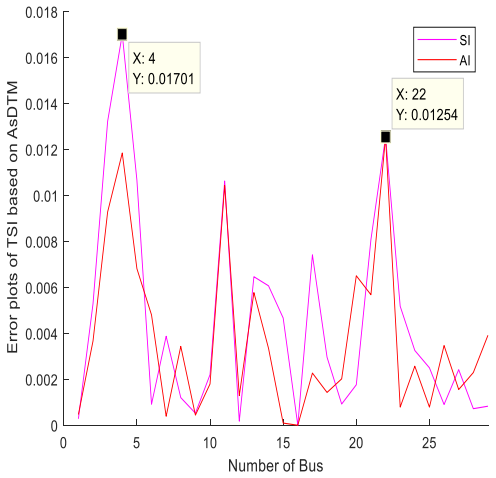

(**d**) Plots TSI evaluated based on AsDTM for fault clearing time of 250 ms

Figure 3-5 DTM- and AsDTM-based SI and AI error plots for 39-bus test system plots.

From Table 3-6, we can conclude that using the proposed AsDTM method in terms of the DTM method for contingency screening and ranking improves the accuracy of the TSI evaluation results by 74% up to 83% if the fault is cleared after 150 ms and by 84% up to 94% if the fault is cleared after 250 ms. All the test and analysis results given above prove that the proposed AsDTM method of contingency screen ranking provides more accurate results.

Validation of the Assessment Speed of the Proposed Method

Figure 3-6a,b,&c and 3-7a,b&c shows total elapsed time to evaluate TS indices for con-tingency screening and ranking based on AsDTM, DTM and Rk4 methods using both 39 bus and 9bus test system. The total assessment time required to evaluate TS indices based on AsDTM, DTM and Rk4 methods are 11.671sec, 20.962sec, and 65.65sec respectively for 9bus test system and 194.084sec, 279.047sec, and 768.062sec respectively for 39bus test system..

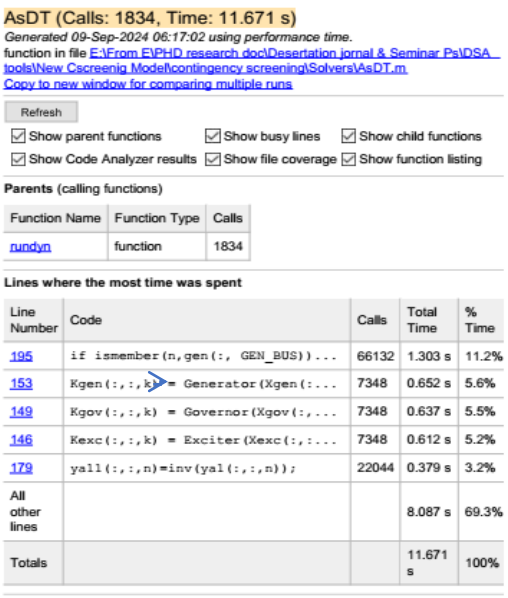

AsDT (Calls: 1834, Time: 11.671 s)

Generated 09-Sep-2024 06:17:02 using performance time.

function in file E:\From E\PHD research doc\Desertation jornal & Seminar Ps\DSA tools\New Cscreenig Model\contingency screening\Solvers\AsDT.m

Copy to new window for comparing multiple runs

Refresh

☑ Show parent functions ☑ Show busy lines ☑ Show child functions

☑ Show Code Analyzer results ☑ Show file coverage ☑ Show function listing

Parents (calling functions)

Function Name	Function Type	Calls
rundyn	function	1834

Lines where the most time was spent

Line Number	Code	Calls	Total Time	% Time
195	`if ismember(n,gen(:, GEN_BUS))...`	66132	1.303 s	11.2%
153	`Kgen(:,:,k) = Generator(Xgen(:...`	7348	0.652 s	5.6%
149	`Kgov(:,:,k) = Governor(Xgov(:,...`	7348	0.637 s	5.5%
146	`Kexc(:,:,k) = Exciter(Xexc(:,:...`	7348	0.612 s	5.2%
179	`yall(:,:,n)=inv(yal(:,:,n));`	22044	0.379 s	3.2%
All other lines			8.087 s	69.3%
Totals			11.671 s	100%

(a)

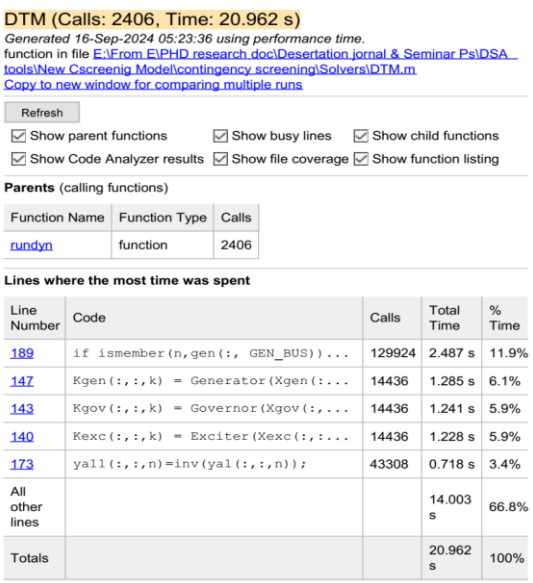

DTM (Calls: 2406, Time: 20.962 s)

Generated 16-Sep-2024 05:23:36 using performance time.

function in file E:\From E\PHD research doc\Desertation jornal & Seminar Ps\DSA tools\New Cscreenig Model\contingency screening\Solvers\DTM.m

Copy to new window for comparing multiple runs

Refresh

☑ Show parent functions ☑ Show busy lines ☑ Show child functions

☑ Show Code Analyzer results ☑ Show file coverage ☑ Show function listing

Parents (calling functions)

Function Name	Function Type	Calls
rundyn	function	2406

Lines where the most time was spent

Line Number	Code	Calls	Total Time	% Time
189	`if ismember(n,gen(:, GEN_BUS))...`	129924	2.487 s	11.9%
147	`Kgen(:,:,k) = Generator(Xgen(:...`	14436	1.285 s	6.1%
143	`Kgov(:,:,k) = Governor(Xgov(:,...`	14436	1.241 s	5.9%
140	`Kexc(:,:,k) = Exciter(Xexc(:,:...`	14436	1.228 s	5.9%
173	`yall(:,:,n)=inv(yal(:,:,n));`	43308	0.718 s	3.4%
All other lines			14.003 s	66.8%
Totals			20.962 s	100%

(b)

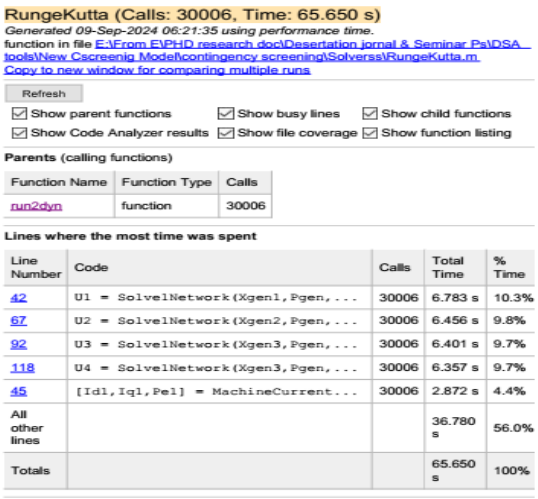

RungeKutta (Calls: 30006, Time: 65.650 s)

Generated 09-Sep-2024 06:21:35 using performance time.

function in file E:\From E\PHD research doc\Desertation jornal & Seminar Ps\DSA tools\New Cscreenig Model\contingency screening\Solverss\RungeKutta.m

Copy to new window for comparing multiple runs

Refresh

☑ Show parent functions ☑ Show busy lines ☑ Show child functions

☑ Show Code Analyzer results ☑ Show file coverage ☑ Show function listing

Parents (calling functions)

Function Name	Function Type	Calls
run2dyn	function	30006

Lines where the most time was spent

Line Number	Code	Calls	Total Time	% Time
42	U1 = SolvelNetwork(Xgen1,Pgen,...	30006	6.783 s	10.3%
67	U2 = SolvelNetwork(Xgen2,Pgen,...	30006	6.456 s	9.8%
92	U3 = SolvelNetwork(Xgen3,Pgen,...	30006	6.401 s	9.7%
118	U4 = SolvelNetwork(Xgen3,Pgen,...	30006	6.357 s	9.7%
45	[Idl,Iql,Pel] = MachineCurrent...	30006	2.872 s	4.4%
All other lines			36.780 s	56.0%
Totals			65.650 s	100%

C

Figure 3-6 Elapsed time (a) For AsDTM based TSI evaluation (b) For DTM based TSI evaluation (c) For Rk4 based TSI evaluation, of 9bus test system

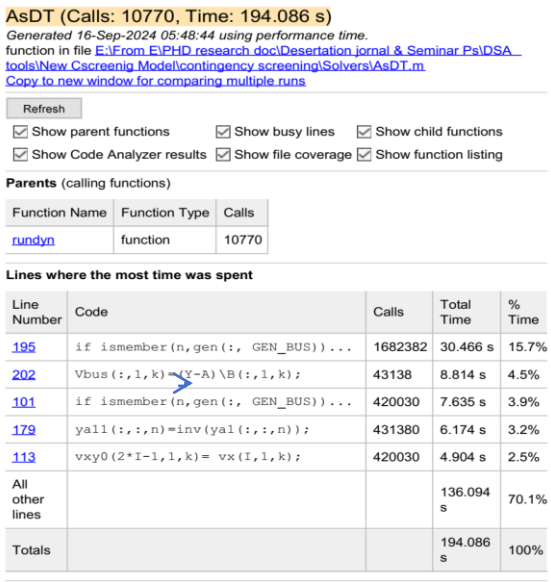

AsDT (Calls: 10770, Time: 194.086 s)

Generated 16-Sep-2024 05:48:44 using performance time.

function in file E:\From E\PHD research doc\Desertation jornal & Seminar Ps\DSA tools\New Cscreenig Model\contingency screening\Solvers\AsDT.m

Copy to new window for comparing multiple runs

Refresh

☑ Show parent functions ☑ Show busy lines ☑ Show child functions

☑ Show Code Analyzer results ☑ Show file coverage ☑ Show function listing

Parents (calling functions)

Function Name	Function Type	Calls
rundyn	function	10770

Lines where the most time was spent

Line Number	Code	Calls	Total Time	% Time
195	if ismember(n,gen(:, GEN_BUS))...	1682382	30.466 s	15.7%
202	Vbus(:,1,k)=(Y-A)\B(:,1,k);	43138	8.814 s	4.5%
101	if ismember(n,gen(:, GEN_BUS))...	420030	7.635 s	3.9%
179	ya11(:,:,n)=inv(ya1(:,:,n));	431380	6.174 s	3.2%
113	vxy0(2*I-1,1,k)= vx(I,1,k);	420030	4.904 s	2.5%
All other lines			136.094 s	70.1%
Totals			194.086 s	100%

(a)

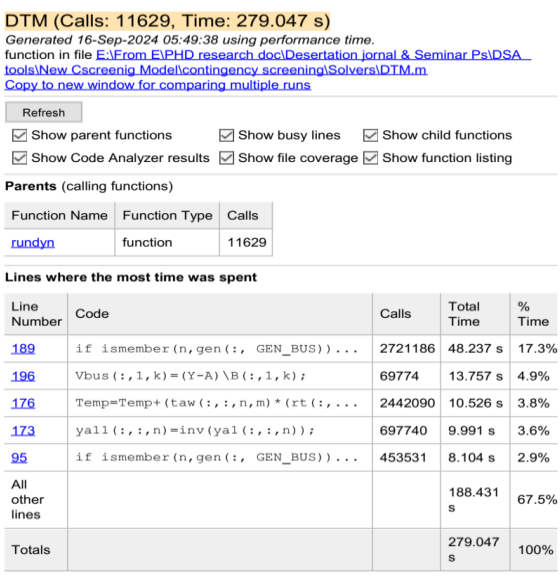

DTM (Calls: 11629, Time: 279.047 s)

Generated 16-Sep-2024 05:49:38 using performance time.

function in file E:\From E\PHD research doc\Desertation jornal & Seminar Ps\DSA tools\New Cscreenig Model\contingency screening\Solvers\DTM.m

Copy to new window for comparing multiple runs

Refresh

☑ Show parent functions ☑ Show busy lines ☑ Show child functions

☑ Show Code Analyzer results ☑ Show file coverage ☑ Show function listing

Parents (calling functions)

Function Name	Function Type	Calls
rundyn	function	11629

Lines where the most time was spent

Line Number	Code	Calls	Total Time	% Time
189	if ismember(n,gen(:, GEN_BUS))...	2721186	48.237 s	17.3%
196	Vbus(:,1,k)=(Y-A)\B(:,1,k);	69774	13.757 s	4.9%
176	Temp=Temp+(taw(:,:,n,m)*(rt(:,...	2442090	10.526 s	3.8%
173	ya11(:,:,n)=inv(ya1(:,:,n));	697740	9.991 s	3.6%
95	if ismember(n,gen(:, GEN_BUS))...	453531	8.104 s	2.9%
All other lines			188.431 s	67.5%
Totals			279.047 s	100%

(b)

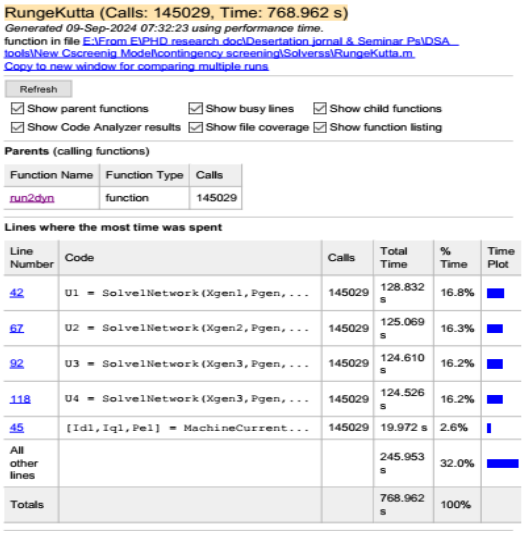

RungeKutta (Calls: 145029, Time: 768.962 s)

Generated 09-Sep-2024 07:32:23 using performance time.

function in file E:\From E\PHD research doc\Desertation jornal & Seminar Ps\DSA tools\New Cscreenig Model\contingency screening\Solverss\RungeKutta.m

Copy to new window for comparing multiple runs

Refresh

☑ Show parent functions ☑ Show busy lines ☑ Show child functions

☑ Show Code Analyzer results ☑ Show file coverage ☑ Show function listing

Parents (calling functions)

Function Name	Function Type	Calls
run2dyn	function	145029

Lines where the most time was spent

Line Number	Code	Calls	Total Time	% Time	Time Plot
42	`U1 = SolvelNetwork(Xgen1,Pgen,...`	145029	128.832 s	16.8%	
67	`U2 = SolvelNetwork(Xgen2,Pgen,...`	145029	125.069 s	16.3%	
92	`U3 = SolvelNetwork(Xgen3,Pgen,...`	145029	124.610 s	16.2%	
118	`U4 = SolvelNetwork(Xgen3,Pgen,...`	145029	124.526 s	16.2%	
45	`[Id1,Iq1,Pe1] = MachineCurrent...`	145029	19.972 s	2.6%	
All other lines			245.953 s	32.0%	
Totals			768.962 s	100%	

C

Figure 3-7 Elapsed time (a) For AsDTM based TSI evaluation (b) For DTM based TSI evaluation (c) For Rk4 based TSI evaluation, of 9bus test system

Capered with DTM and Rk4, the proposed AsDTM based contingency screening and ranking method improves the performance efficiency (performance speed) by 44.32% and 82.22% for 9 bus test system and 30.45% and 74.73% for 39bus test system respectively. Therefore, we can conclude that, the proposed contingency screening and ranking method is relatively faster.

Therefore from the above assessment and simulation results, compared to the con-ventional Range-kutta (Rk4) and the classical DTM methods of contingency screening and ranking the proposed method improves the assessment speed by more than 74.73% and 30.45% respectively. Compared to the classical DTM methods of contingency screening and ranking the proposed method improves the accuracy of the resulting transient stability indices by more than 74%. These results strongly approves that the proposed contingency screening and ranking method fast and robust.

CHAPTER FOUR: Fast Transient Stability Assessment

4.1. Introduction

Transient stability is the ability of the power system after exposure to large disturbance to transit to a stable state [**44**]. Transient stability analysis investigates the dynamic behavior of a power system for several seconds following a large disturbance. Inability to detect system instability behaviors in a sufficient time interval to launch the corrective actions could result in a system failure at one location on a system that can quickly degenerate to cascading failures, which is usually the mechanism for large collapses or blackout of the system. Fast and accurate assessment of transient stability is of great significance for safe and stable operation of power systems.

To identify any unstable system condition before it happens, assessment of transient stability shall be performed in near real-time operation environment. Traditional methods of transient stability analysis rely on numerical integration, such as the Runge–Kutta or Euler techniques in implicit and/or explicit form, to solve the differential algebraic equations governing power system dynamic behaviors. The methods are robust and commonly used in commercial software packages with small enough integration steps of typically one to a few milliseconds to meet accuracy requirements [**55**]. However, these methods are computationally intensive, especially for modern power system. The power system industry and the research community are seeking next-generation tools that are more powerful for power system near real-time transient stability assessments.

Several previous works have been explored different aspects of transient stability analysis and simulation. Generally we can group them in to the following 3 categories as direct methods, numerical integration methods, probabilistic methods, differential transformation methods, and Automatic Learning (AL) techniques as described in Chapter 2 Section 2.4.. Approaches such as a power system TDS based on numerical integrations provide accurate assessment results but are too slow due to their intensive computation requirement. Direct method such as transient energy function and hybrid (TDS and TEF) methods proposed by different authors may provide quantitative measures which indicate the degree of system stability based on the energy margin or stability indices but require model simplification and assumptions. Methods based on off-line databases, such as ANN, a decision tree, pattern recognition methods, etc, are suffering from multiple probable system operating states/scenarios [**37**].

4.2. Advanced fast and robust power system TDS

The most accurate method for assessing the transient stability of a power system is through time domain simulation. This approach can handle complex system modeling, allowing for the determination of stability conditions from electromechanical angular simulations [**44**]. However, transient stability analysis (TSA) is computationally intensive because it involves numerical integration to evaluate the system's behavior during significant disturbances. Advances in time domain simulation algorithms are required to improve computational efficiency and permit assessment of more contingencies in larger and complex power systems. In this dissertation, two novel, fast and robust dynamic simulation tools based on DTM are developed.

4.2.1. Power system TDS based on AsDTM

Adaptive step size DTM based fast power system transient stability simulation (AsDTM) method and tool is one of the simulation tools developed in this work. The proposed and developed AsDTM based simulation method solves complex power system DAE models using the DTM method at variable time steps. As described in Chapter two, section 2.4, the step size is varied based on the local truncation error control algorithm. The automatic controls of the step-size length is performed based on the principles that it reduces the time step length when the error is above the tolerable error limit, to improve the accuracy of simulation and increases the time step length when the error is below the tolerable error limit, to avoid unnecessary computational burden and improve the overall efficiency. It has been tested and validated using standard test systems by [**55**]. Test results revealed that AsDTM-based power system transient stability simulation increases simulation speed by 20–44.57% and 83–92% compared with the DTM and Rk4-based simulation methods, respectively. Furthermore, compared with the simulation speed of DTM-based simulation, the proposed AsDTM-based simulation improves simulation errors by more than 58%.

4.2.3. Power system TDS based on AOSDTM

Adaptive order and step size DTM based simulation (AOSDTM) is the second transient stability simulation method developed in this dissertation work. The developed AOSDTM based transient stability simulation method solves complex power system DAE models by adaptively varying DT order and step sizes of the DTM method. The automatic controls of DT order and step-size are performed based on the principles that it reduces the time step length and increase the order of the DTM when the error is above upper threshold limit during power system dynamic

simulation process, which improves the accuracy of simulation and increase the time step length and decrease the order of the DTM when the error is below the lower threshold limit during power system dynamic simulation process, which can avoid unnecessary computation burden and improve the overall efficiency. It has been tested and validated using standard test systems by [**77**]. Test results of the developed AOSDTM based power system transient stability simulation tool revealed that simulation speed improved by 14-34% and 70-80% compared with the simulation speed of DTM and Rk4 based simulations respectively. Additionally, compared with the DTM-based simulation, the AOSDTM-based power system transient stability simulation improved simulation results errors significantly by more than 77.84%. Similarly, the test result obtained indicated that compared with the AsDTM-based simulation method the developed AOSDTM-based power system transient stability simulation method improved the simulation speed by more than 17.44%.

4.2.4. Structure of the AsDTM based power system transient stability simulation

Power system transient stability simulation (TSS) tools based upon the developed adaptive step-size deferential transformation method (AsDTM) (explicit algorithm) have been applied at all system operating points during every credible contingency in order to assess power system transient stability. The power system transient stability calculation is a differential algebraic initial value problem with differential algebraic equations. Figure 4-1 presents the structure of the developed transient stability simulation tools based on AsDTM. This structure comprises blocks to represent synchronous machine's rotor electrical and mechanical differential equations, excitation system differential equations, turbine and governor differential equations, network interface machine variables, and stator and network algebraic equation. Overall, the model illustrates one of the synchronous generators and its controllers connected to the power system transmission network. It consists of a set of ordinary differential equations and a set of network algebraic equations, ensuring a comprehensive representation of system dynamics.

All synchronous generator models used for routine large scale studies are virtually based on Park's transformations, in which the machine electrical behavior may be represented by equivalent circuits in the rotor direct and quadrature axes. For transient stability simulation stator transients are neglected. Thus the stator equations are algebraic in common with the network equations.

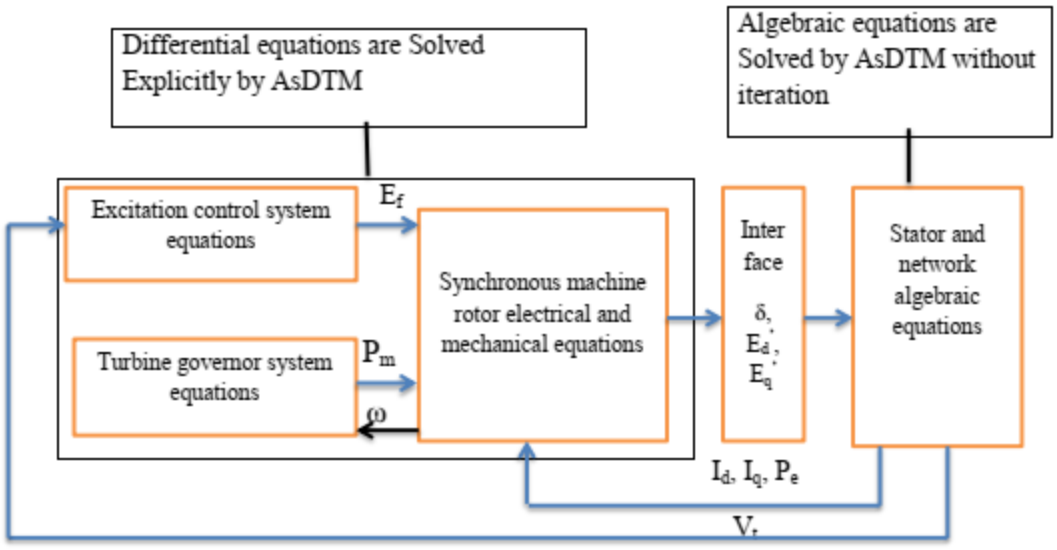

Figure 4-1 Structure of the developed TDS based on AsDTM

V_t, P_m, and E_{fdi} are the input variables to the dynamic models and the currents injected into the network from load and the generator (from solution of stator algebraic equations) buses are inputs of the algebraic network models. Where V_t represents complex terminal voltage, P_m represents the turbine mechanical power, and E_{fdi} represents the excitation voltage. The turbine governor controller block in Figure 4-1 contains dynamic model equations to represent the direct primary control of the turbine torque and the mechanical dynamics of the turbine itself. Similarly, the excitation system block contains dynamic model equations to represent voltage regulators and exciters. the dynamics of this excitation system depends on the nature of the feedback control arrangement and the nature of the source of DC voltage E_{fdi}. Since the proposed and developed TSS tools are flexible and scalable they can be adaptively used with power system different complexity and models detail levels. Thus, user-defined controller structures can be easily integrated on either the voltage or governor controller sides. This flexibility allows for enhanced analysis and simulation studies, enabling users to tailor the model to specific requirements and explore various scenarios effectively.

As given by the flowchart of Figure 2-3 of chapter 2, TDS based on AsDTM starts with solving load flow model or network algebraic equations shown at the right sides Figure 4-1 is solved without iteration to initialize the pre-disturbance state and provide the data corresponding to the pre-disturbance state. The post-disturbance dynamic behavior of the electrical signals are

determined by solving all the differential equations to the left sides of Figure 4-1 explicitly based on TDS by AsDTM . At each time step of simulation, the present state variables values are simply determined analytically as a power series of time from their respective 0 to K orders coefficient terms [**55**]. Similarly, the algebraic variables are updated analytically as a power series time from their respective 0 to K orders coefficient terms, refer Section 2-5 and [**55**]. At the instant of disturbance, the appropriate data must be modified accordingly. Then, the process repeated until the time of interest reached. The swing curves represent the evolution of rotor angle of each machine known at the end of each time step.

4.3. Critical Clearing Time (CCT)

The critical fault clearing time (CCT) is defined as the maximum duration of a fault that can occur without causing any generator to fall out of step or leading to other unacceptable repercussions in the power system, ensuring transient stability [**40**]. During significant disturbances, such as a three-phase short circuit, protective relays detect the disturbance and initiate the tripping of the nearest circuit breakers to isolate the fault. The time from the disturbance onset until the circuit breakers successfully isolate the fault is known as the fault clearing time (FCT). For a system to maintain stability, any generator must have a CCT greater than the FCT of the installed protection devices. Loss of connected generators can lead to severe consequences for the entire system. The total FCT comprises the operating time of the main protection system, along with signaling time, relay time, and breaker interrupting time. CCT serves as a key index for monitoring the transient stability of power systems during large disturbances, as referenced in various studies, including this thesis. An increased CCT provides better opportunities for protective relays and circuit breakers to isolate and clear disturbances. If the CCT is less than the operating time of the circuit breaker for the affected component, the system is deemed transiently unstable.

The acceptable CCT limit varies by system, but a common range is between 150 and 250 milliseconds, which is used in this dissertation for transient stability assessment. CCT is particularly beneficial compared to power limits evaluated using transient energy function (TEF). Transient stability analysis (TSA) utilizing CCT enables the screening and ranking of contingencies to identify the most severe scenarios and classify stability states as stable or unstable.

4.3.1. Transient Stability Assessment based on TDS by Cross cut Technique

Analyzing many contingencies have to be done iteratively in short period to evaluate system states. As briefly presented in Chapter 3 Section 3.2 above, in this thesis, lists of credible contingencies are analyzed and ranked based on their respective severity indices. At this stage the most severe contingency with respect to the operating state represented by the most current snapshot from the SCADA data is identified. Determining stabilizing solution for the most severe contingency requires its distance from transient stability limit or margin. In this thesis CCT is evaluated only for the worst contingency to represent the distance to stability boundary. Therefore, this CCT specifies the distance at this particular operating point from transient stability boundary.

TSS tool based on AsDTM, which introduced in section 2.3 of chapter 2 and section 4.2, is used to estimate the CCT in order to specify a quantified index for transient stability assessment. CCT is calculated by uniformly increase the fault clearing time until the system instability using traditional numerical integration based TDS [**78**]. TDS based on traditional numerical integration method, which is structurally complex & computationally intensive method, was proposed by [**78**]. To improve the computation speed of the proposed method the Authors have implemented TDS by bisection technic. However, still the traditional numerical integration method which is computationally intensive was there. In this thesis, the TDS based on the traditional numerical integration method is changed by the TDS based on the AsDTM , which provides significant improvements on computation speed i.e. by more than 90% (refer Section 2-5 of Chapter 2) when compared with the method proposed by [**78**] .

TDS based on novel AsDTM technique with cross cut is used to find the CCT for the worst fault in order to avoid the repetitive time-consuming with step increase fault duration and high computational burden by traditional numerical integration method. Figure 4-2 gives the developed algorithm for estimating CCT by cross cut method using TDS based on AsDTM.

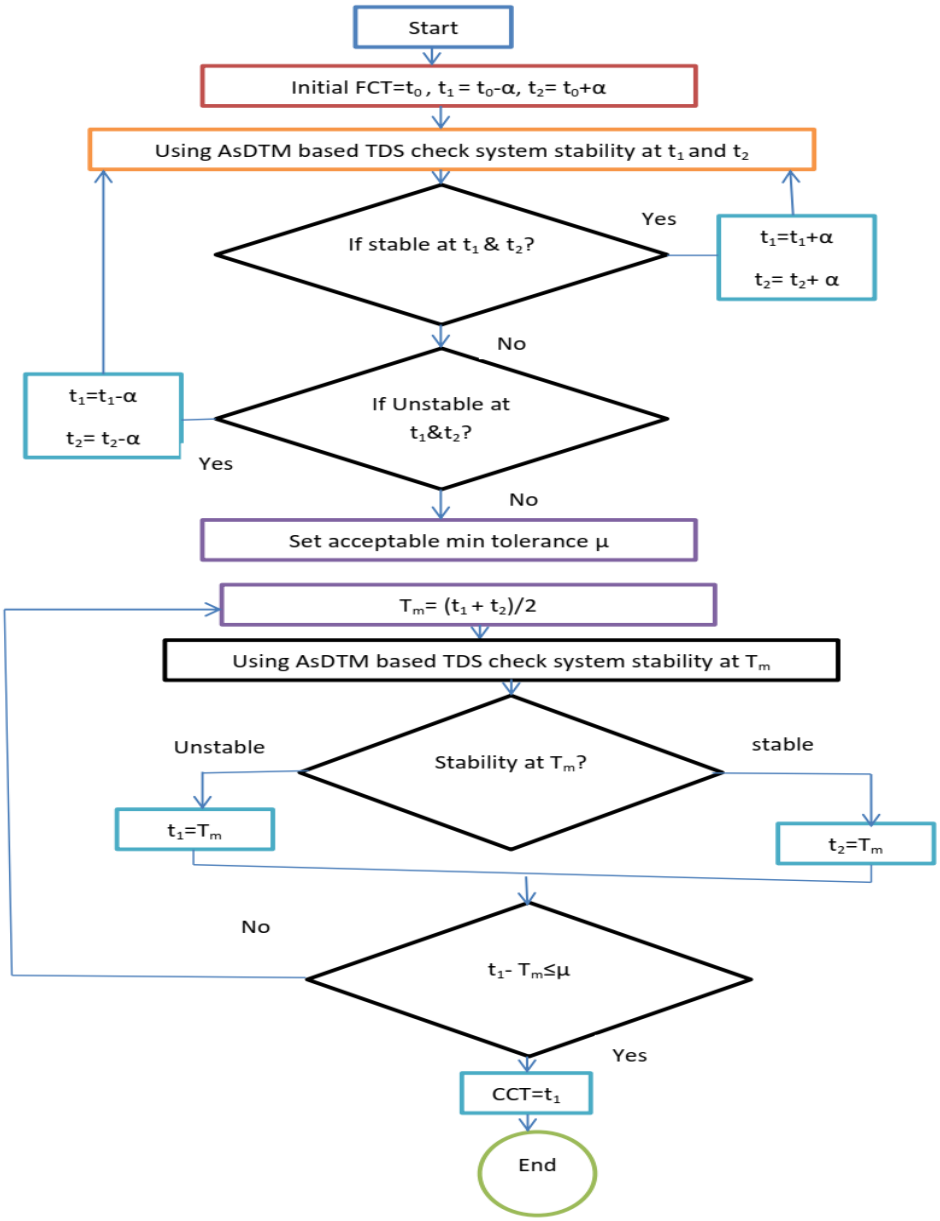

Figure 4-2 Evaluation of CCT using TDS by cross cut technique [78**]**

The proposed technique begins with an initial fault clearing time (FCT=to) and searches for the boundaries that include the critical fault clearing time (CCT). As illustrated in Figure 4-2, the initial time boundaries are set within (to ± α). If the CCT is found within these boundaries, the cross-cut technique is applied to evaluate the CCT. If not, the boundaries must be adjusted until the system demonstrates stability at one boundary and instability at the other, confirming that the CCT lies between these limits. The dynamic response of the system is then assessed at the midpoint (T_m) between the upper and lower limits. If the system is stable, the lower limit (t_1) is

updated to the mean value (T_m) .Conversely, if the system is unstable, the higher limit (t_2) is updated to (T_m) for the next calculation. This cross-cutting process continues until the acceptance tolerance (μ) between the limits is met, with the higher limit being selected as the CCT. The total computation time varies based on several parameters, including the chosen parameter σ, which should be sufficiently large to limit the number of simulations. Additionally, this value can be adapted between different contingencies to minimize overall simulation time.

4.4. Validation of the proposed TSA method using standard test systems

4.4.1. Test systems, cases, and assessment setup

Two test systems are employed to validate the proposed transient stability assessment approach. The first test system is the IEEE 9 bus system, which consists of nine bus and three machines. The second test system is the 11 bus system with 4 machines. Constant impedance load model is used with the TDS. A two axis model is used to represent synchronous generators, each with Type_1 automatic voltage regulation and primary speed control systems, as shown by Equations 2.12, 2-13 and 2-14 respectively. Figure 4-3 shows the single line diagrams of both test system. Dynamic data of all the machines with in both test cases are given in Appendix A. Three-phase bus faults are applied for both test systems. Three-phase short-circuit faults at bus 8 for IEEE 9 bus and at bus 6 for 11 bus test systems are considered during the assessment. A susceptance of 10−10 is enough to bring zero-impedance bus faults [**74**].

Transient stability assessment were conducted on a standard personal computer with the following properties: Intel CTM) i5-5200U CPU @ 2.20 GHz 2.20 GHz, 8 GB RAM, running on a 64-bit operating system, with a x64-based processor. The assessment was carried out using the TSA tools/codes developed on MATLAB R2017b [**75**]. MATPOWER 7.1 [**76**] version software was utilized. The CPU times included all steps of the simulation processes. MATPOWER is open-source power simulation software, used for power flow analysis and run on a MATLAB environment. This power system analysis software does not employ a graphical representation of a power system. Instead, the power system data were prepared in a table format specific to MATPOWER. Any functions of the MATPOWER can easily be accessed by functions developed on MATLAB editor. These include MATLAB functions that load and call for dynamic and static data file of simulation cases (case file), MATPOWER output interface functions, functions for initializing dynamic systems, model libraries for all dynamic systems,

solver functions file (algorithms for computation), and functions for plotting simulation results. Power flow analysis was performed using MATPOWER.

4.4.2. Assessment results and discussions

For validating the proposed AsDTM-based power system transient stability simulation, three-phase short-circuit faults on bus 8 of IEEE 9 bus and on bus 6 of 11 bus benchmark systems at 0.6 s and using AsDTM based bisection method described in subsection 4.2.2 above CCT for each case is estimated. In each case, the accuracy and performance of the proposed method was validated using the transient stability assessment results (CCT) based on the traditional numerical method (fourth-order Range–Kutta (Rk4) with step size h = 0.001 s) and total time cost (time for TS assessment) as benchmarks. For this purpose, differential transformation (DT) order of k = 7 for both test systems was used during assessment based on DTM and AsDTM methods.

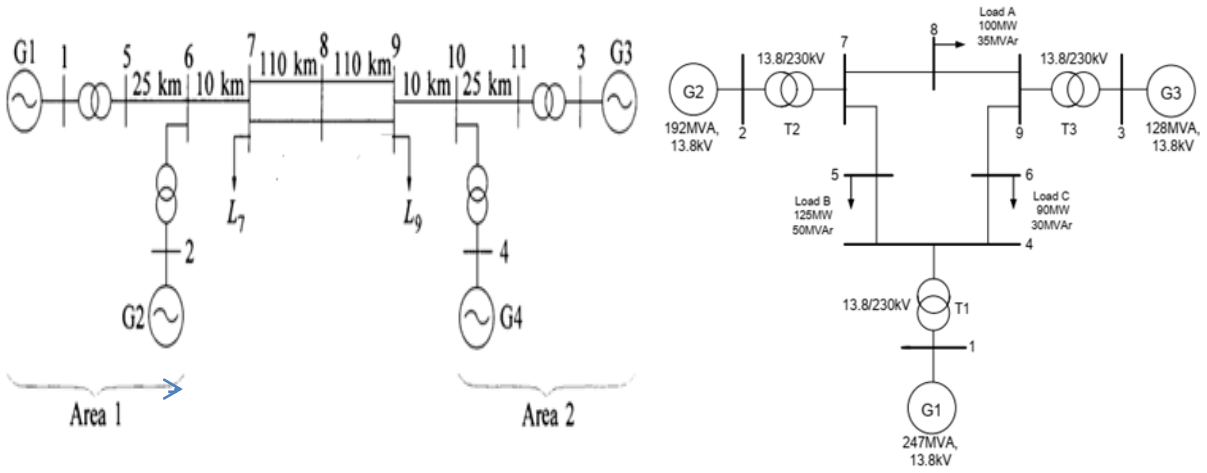

(a) (b)

Figure 4-3 Single line diagram of (a) 11 bus [1]; (b) IEEE 9 bus test systems [79].

From Figures 4-4a, b and 4-5a, b, we can observe the number of iterations and simulation time requirement relationships among AsDTM, DTM, and Rk4 simulation methods, respectively. The total number of steps required to determine CCT during three-phase fault using Rk4, DTM, and AsDTM methods are 45,000, 4984, and 2028 for the IEEE 9 bus test system and 65,000, 6520, and 3386 for the 11 bus test system, respectively. Similarly, the total assessment time cost for the same case using Rk4, DTM, and AsDTM methods are 76.14 s, 25 s, and 11.57 s, for the IEEE 9 bus test system and 127.2 s, 44.47 s, and 35.66 for the 11 bus test system, respectively. As we can see from the flowchart of the proposed transient stability assessment algorithm given by Figure 4.2, to obtain CCT of the contingency under assessment, a number of 5sec transient

stability simulation runs are required. The zigzag line pattern in the plots of total simulation time cost and number of time steps of Figures 4-4a, b and 4-5a, b, indicates the interpolation of the subtotal simulation time cost and number steps at every 5sec transient stability simulation run.

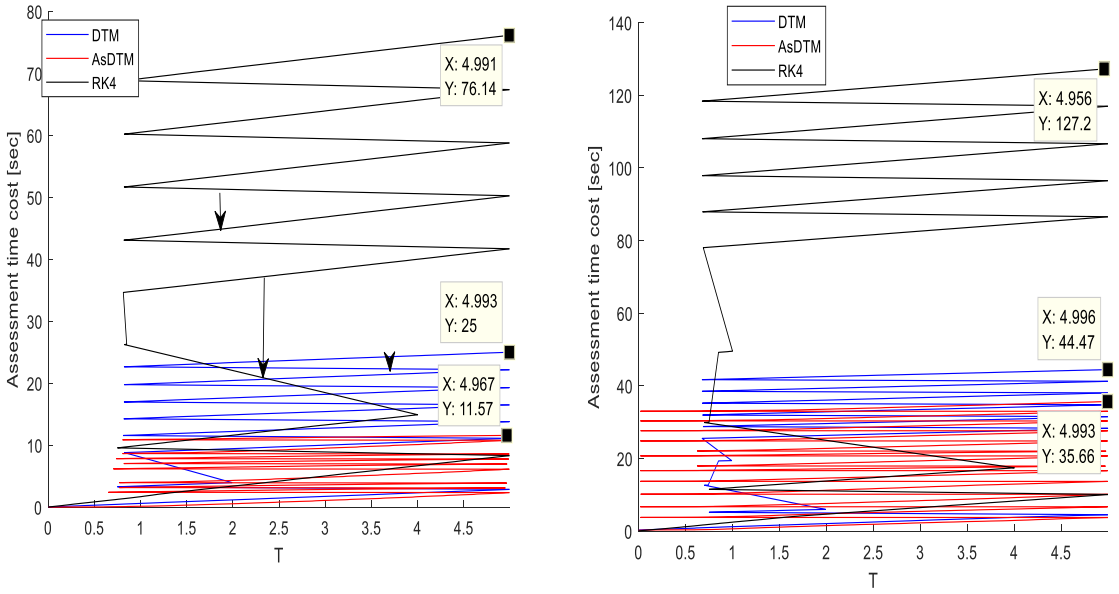

(a) (b)

Figure 4-4 Simulation time cost for (a) 9 bus and (b) 11 bus test systems.

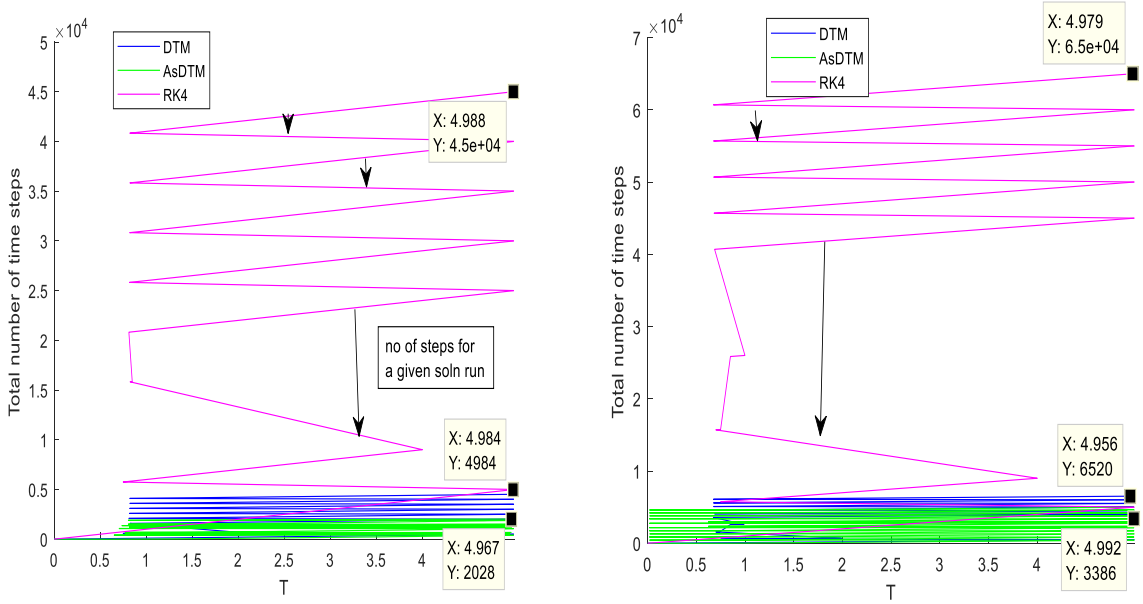

(a) (b)

Figure 4-5 Number of iterations for (a) 9 bus and (b) 11 bus test systems.

The CCT results of the contingency assessed from time domain simulations based on Rk4, AsDTM, and classical DTM methods are given in Table 4-1. Since time domain simulation based on Rk4 is used as a benchmark in this dissertation, the CCT results calculated based on AsDTM is the same as those calculated based on Rk4 for both 9bus and 11bus test systems.

Table 4-1 Transient Stability Assessment (TSA) results by different assessment methods

Assessment method	CCT(ms)		Remark
	For 9bus test system	For 11bus test system	
Rk4	223.4	170	
AsDTM	223.4	170	
DTM	226.5	173.05	

From the simulation results shown in Figures 4-4, 4-5, and Table 4-1

Compared with the DTM-based assessment: The proposed AsDTM improved/reduced the total assessment time cost and total number of iterations by 22% and 48.1.93% for the IEEE 11 bus test system and improved/reduced the total assessment time cost and total number of iterations by 53.72% and 59.31% for the IEEE 9 bus test system, respectively.

Compared with the Rk4-based assessment: The proposed AsDTM improved/reduced the total assessment time cost and total number of iterations by 72% and 94.8% for the 11 bus test system and improved/reduced the total assessment time cost and total number of iterations by 84.8% and 95.49% for the IEEE 9 bus test system, respectively.

Compared with the DTM-based assessment method, the proposed AsDTM assessment method also improves the accuracy the assessment results by 1.37% and 1.76% for IEEE 9 bus and 11bus test systems respectively.

Therefore, we can conclude that the proposed AsDTM-based power system transient stability assessment method increases the assessment speed by 22–59.31% and 72–95.49% when compared with the DTM, and Rk4-based assessments, respectively. The accuracy of the assessment results are improved by 1.37% - 1.76%, when compared with the classical DTM based assessment method .

CHAPTER FIVE: Transient Stability Based Optimal Generation Rescheduling To Enhance Power System Dynamic Security

5.1. Introduction

Security control is one of the prime concerns of planning and operation of modern power systems. The increase in size and complexity of modern interconnected power systems and the present trend towards deregulation has forced the electric utilities to operate their systems under stressed operating conditions closer to their security limits [**80**]. With this growing stress on present day power systems, they increasingly are facing the threat of transient stability problems. Transient stability or large disturbance rotor angle stability is deals with the capacity of the power system to stay intact when exposed to a critical disturbance, such as three phase short circuit. Instability that may result occurs in the form of increasing angular swings of some generators leading to their loss of synchronism with other generators ([**81**], [**1**]). When the transient security level falls below an acceptable level, preventive control actions can restore the system back to secure state of operation [**82**].

Preventive control aims at modifying the operating conditions of a power system so as to make it able to withstand severe contingencies that would drive it to instability, whenever they occur. These types of control measure include network switching, load curtailment, and reactive compensation, generation rescheduling. Preventive control is summoned up when the power system is still in normal status [**83**]. In the past many utilities have relied on preventive control in order to maintain system security at an acceptable level. This is due to the fact that with these control method time is available for decision making. Also, for the uncertain disturbances, the state of system is known in this control; therefore, it becomes easier to study dynamic behavior of the system. Maintaining a balance between supply and demand of electric power is one of the core tasks of power system operation. Since reactive power can be locally compensated, active power balance is the most important issue for power system operation.

In the literature survey generation rescheduling is reported as dominant preventive control method. Especially for transient stability control various generator rescheduling techniques have been proposed. In [**23**], the transient energy function (TEF) method is used to check the dynamic security of the system and the coherent behavior of generators is used to find a new generation configuration.

In [**84**], a coherency based sensitivity method is proposed for generation rescheduling. In [**85**], a coherency based generator rescheduling for preventive control of transient stability in power systems is proposed. In [**86**], dynamic security assessment and generation rescheduling method utilizing genetic algorithms (GAs) integrated with probabilistic neural networks (PNNs) and adaptive neuro-fuzzy inference systems (ANFISs) is proposed for the preventive control power systems against transient instabilities. A generation rescheduling approach for preventive control of power system is presented in [**87**] to reallocate power generation for multiple unstable contingencies based on graph theory. In [**88**], proposed a transient stability preventive control design that takes series compensation into account. A heuristic stability performance index (PI) was proposed to evaluate the gradient of the PI and determine the preventive control accordingly [**89**]. In [**90**], rescheduling of power systems constrained with transient stability limits in restructured power systems based on TEF is proposed. An optimal generation rescheduling with trajectory sensitivity-based transient stability constraints is presented in [**91**].

Generation rescheduling based upon the optimal result of multi-contingency transient stability constrained optimal power flow is suggested as preventive control of power systems in [**19**]. A real time preventive action for transient stability enhancement with a hybrid neural network optimization approach using derivatives of transient energy margin value is proposed in [**20**]. A technique using trajectory sensitivities to provide a preventive rescheduling scheme in dynamic security constrained power systems taking into account the economic aspect is proposed in [**21**].

In [**22**], trajectory sensitivities are used for multi-contingency preventive control. Iterative solution methodology and computer package for generation rescheduling is suggested in [**92**] The proposed approach in [**93**] considers generator shedding as the most effective discrete supplementary control for improving the dynamic performance of faulted power systems and preventing instabilities considering the sensitivity of the TEF with respect to changes in the amount of dropped generation which is used during the training phase of ANNs to assess the critical amount of generator shedding required to prevent the loss of synchronism. Decision tree (DT)-based preventive and corrective control methods are proposed in [**94**] to enhance the dynamic security of power systems against the credible contingencies causing transient instabilities. A radial basis function (RBF) neural network to assess the dynamic security status of the power system and to estimate the effect of a corrective control action applied in the event of a disturbance is proposed in [**95**] with optimal control action using particle swarm

optimization (PSO). In [**96**], an optimal power flow model with transient stability constraints is proposed for both dispatching and re-dispatching.

Methods those need training on data base, like as proposed by [**20**]. [**86**] [**87**] [**88**] [**93**] [**94**]. these approaches are not always be capable of correctly determining security and stability because such techniques require training on forecasted offline database, [**10**]. Methods based on off-line databases, such as ANN, a decision tree, pattern recognition methods, etc, are suffering from the a great extent of probable system operating states/scenarios. Approaches such as power system TDS based on energy function, numerical integrations, and probabilistic methods proposed in [**21**] [**22**] [**23**] and [**84**] [**85**] [**88**] [**89**] [**90**] provide a quantitative measure which indicate the degree of system stability based on energy margin or stability indices but required computational efforts and restrictions regarding modeling details. Therefore, there is need to improve and develop more robust and efficient preventive control method to enhance power system dynamic performances

This thesis introduces fast and robust power system transient stability based optimal generation rescheduling to improve power system dynamic security using combined particle swarm optimization (PSO) and power system time domain simulation (TDS). TDS Based on adaptive order and step size differential transformation (AOSDTM) methods [**77**] is proposed for this purpose. The proposed AOSDTM varies both order and step sizes of DTM adaptively to improve performance efficiency and accuracy of the simulation. The fault period for the unstable contingency under consideration is changed based on cross cut technique that further increases the performance efficiency of the method. Critical fault clearing time (CCT) is used as indicator for power system transient stability monitoring. Generation rescheduling is taken as a practical preventive or remedial control action to enable any transiently unstable contingency stable through increasing CCT without changing the required total generation. The relevant unstable equilibrium point (UEP) and the corresponding critical generators are determined using the proposed AOSDTM based power system time domain simulation by cross cut technique. The method have been tested on IEEE 9-bus, 3- generators and 11bus, 4- generators systems and the transiently insecure cases for certain contingencies are made secure by rescheduling the generation according to the proposed method. Test results show that proposed method is able to provide near optimal control solutions meeting dynamic security enhancement.

5.2. PSO based optimal generation rescheduling problem formulation

Effective operation of a power system requires the continuous supply of both active and reactive power while maintaining a stable voltage and constant frequency. In the event of significant disturbances, operators must implement strategies to prevent instability resulting from transient conditions. To address this, proactive control measures are essential to mitigate dynamic security risks linked to transient stability. These measures depend on a predetermined list of credible contingencies and their corresponding control actions. By adjusting operating conditions, these actions enhance transient stability while adhering to all specified constraints.

Various preventive control strategies have been explored in the literature, with power generation rescheduling emerging as a key method. This section outlines a framework and formulates the problem for optimally distributing generated power from each generator as a preventive measure aimed at bolstering transient stability and dynamic security in the face of credible contingencies that might breach stability limits. The goal is to improve transient stability through optimal rescheduling of power generation, utilizing a combination of AOSDTM-based transient dynamics simulation and Particle Swarm Optimization (PSO) techniques. This approach ensures a balance between power generation and load demand, avoids equipment overload, adheres to voltage limits, and minimizes power losses.

5.2.1. Particle Swarm Optimization (PSO) and its implementation

PSO is a population based stochastic optimization technique which is developed by Dr. Eberhart and Dr. Kennedy in 1995, and is inspired by social behavior of birds flocking or fish schooling that solves continuous and discrete optimizing problem of a large domain [**97**]. PSO learns from the scenario and uses it to solve the optimization problems while each individual shares the information with its neighbors. The particle is attracted towards the best position currently experienced by other particles that form its local neighborhoods and/or towards the best position found by any particle in the swarm so far. The individuals fly through the search space with velocities, which are adjusted dynamically according to their historical behaviors. Therefore, the particles have the tendency to fly towards the better and better search area over the course of search process until reach a stopping criterion.

Each individual, called particle, x_i, within the swarm is represented by a vector in multidimensional search space, which represents a potential solution of the entered problem and updates its position by adding the updated velocity, v_i .The updated velocity of each particle

influenced by the current velocity in addition to two terms based on the memorized best position it has explored and the global best position explored by the swarm in the feasible search space. To enhance the convergence capability of PSO, modifications such as introducing an inertia weight, crossover operations, and/or a constriction factor can be implemented [**45**] [**98**] [**99**] [**100**]. These enhancements help improve the algorithm's performance in finding optimal solutions. The original PSO equations define each particle, i as potential solution to a problem in D-dimensional space with a memory of its previous best position x_{ibest} and velocity vector of the swarm $v_{i,\ which}$ can be represented as:

$$\begin{aligned} x_i^T &= \left[x_{i1}, x_{i2} \ldots, x_{iD}\right] \\ x_{ibest}^T &= \left[x_{1best}, x_{2best} \ldots, x_{nbest}\right] \\ v_i^T &= \left[v_{i1}, v_{i2} \ldots, v_{iD}\right] \end{aligned} \qquad (5\text{-}1)$$

Particles' velocities can be clamped to a maximum velocity, serving as a constraint that controls the global explosion speed of the particles. This limitation restricts the maximum change in the particle's position, thereby adjusting the movement speed of the entire population within the hyperspace. Once the local and global best values are determined, the equations used to update the velocity and position of each particle can be represented as follows:

$$\begin{aligned} v_i(k+1) &= wv_i(k) + c_1 r_1 \left(x_{ibest}(k) - x_i(k)\right) + c_2 r_2 \left(x_{gbest}(k) - x_i(k)\right) \\ x_i(k+1) &= x_i(k) + \chi v_i(k+1) \end{aligned} \qquad (5\text{-}2)$$

In this context w denotes the inertia weight, which influences how much the previous velocity vector impacts the new velocity vector. It can be expressed as follows:

$$w = w_{\max} - \left(\frac{w_{\max} - w_{\min}}{iter_{\max}} \times iter\right) \qquad (5\text{-}3)$$

The constriction factor χ, utilized to restrict the velocity and enhance convergence, can be expressed as follows:

$$\chi = \frac{2}{|2 - \phi - \sqrt{\phi^2 - 4\phi}|} \; where: \phi = c_1 + c_2, \phi > 4 \qquad (5\text{-}4)$$

In this framework, c_1 and c_2 represent the positive acceleration coefficients for individual and social influences, respectively, governing how cognitive and social components affect the particle's velocity. The random values r1 and r_2 fall within the range (0, 1) and introduce randomness into the search process. $iter_{max}$ indicates the maximum number of iterations, while *iter* refers to the current iteration count. current number of iteration. x_{ibest} is the recorded local best position for particle i, and x_{gbest} represents the global best position for the entire swarm within the explored space. During optimization, if any variable exceeds its defined upper or lower limits, it is adjusted to the respective boundary using a method known as the "set to limit" approach. Each particle's performance is assessed through an objective function. The standard PSO algorithm can be succinctly implemented with a few lines of code as follows [**40**]:

- **Initialize** the inertia weight, constriction factor, and other necessary parameters.
- **Generate** the initial population and corresponding velocity vectors randomly within the feasible hypercube.
- **Evaluate** the fitness function for each particle based on its current position, taking into account any constraint violations.
- **Determine** the best position for each particle by comparing its current performance to its previous best.
- **Identify** the global best position for the swarm by comparing the best performances of each particle with the previous global best.
- **Update** the velocity and position of the particles according to the specified equations.
- If convergence is achieved or the stopping criteria are met, terminate the process and return the best solution along with its fitness value; otherwise, return to Step 3.

5.2.2. Transient stability assessment and monitoring based on CCT

The critical fault clearing time is defined as the maximum duration for which a fault can persist without resulting in any generator losing synchronism or causing other unacceptable consequences for the system. During this period, the power system remains transiently stable [**40**]. During large disturbances the protective relay detects the existence of disturbance and initiates the tripping of the nearest circuit breakers by closing the trip circuit to isolate the fault. The time duration from the instant the disturbance occurs until the circuit breakers isolate the fault is termed by fault clearing time (FCT). Therefore, any synchronous generators must have higher CCT than FCT of the protection devices installed in the transmission system to avoid a

loss of synchronism. Therefore, the corresponding CCT has been used as index to monitor the power system transient stability limit during faults.

Transient stability assessment (TSA) through the evaluation of critical clearing time (CCT) is defined by its capability to screen and rank a series of contingencies, identifying the most severe ones while categorizing stability scenarios as either stable or unstable. The assessment of power system transient stability is marked by intricate dynamic behavior resulting from the complexity of modeling and the interactions among individual components, along with the computational framework used to describe modern power systems. To effectively evaluate power system transient stability in terms of CCT, a mathematical model is used to represent the system. The representation consists of both static and dynamic characteristics and can be expressed by Differential Algebraic Equations (DAE). For the phenomena and timescales of interest ordinary differential equations are considered sufficient to describe power system dynamics. The general mathematical formulations used throughout this thesis are given by Equations 2-3 up to 2-12 of Chapter 2 Section 2.2.

5.2.3. CCT evaluation

In this thesis detailed power system time domain simulation based on AOSDTM is used to evaluate CCT. As the critical clearing time (CCT) increases, the system is afforded a greater opportunity to isolate and clear disturbances using protective relays and circuit breakers. Therefore, if the CCT is shorter than the operating time of the protection system for the affected electrical equipment, the system cannot be deemed transiently stable.

During optimization process, CCT is evaluated and used as key feature to monitor power system transient stability after each iteration step. To evaluate CCT after each iteration step, the following procedures are followed:

Step-1: update the power generated from each generator (PGi, QGi) in the power flow case data based on the optimal generation reschedule results

Step-2: perform power flow analysis (use Matpower)

Step-3: using the power flow results, initialize all the dynamic system

Step-4: evaluate CCT by using detail power system dynamic simulation (based on Equations (2-3 up to 2-12))

For every change in generated power of all the generators in the system under consideration after each iteration step of the optimization process, transient stability is assessed through evaluation of CCT. Therefore, we can express it as CCT ((PGi, QGi).

5.3. Problem Formulation

Optimal generation rescheduling in power systems may have different goals, such as minimizing total real power loss, enhancing transient stability, minimizing power generation/production cost and so on. In this paper, the goal of optimal generation rescheduling is to enhance dynamic security through stabilizing transiently unstable system operating conditions. This is based on maximizing critical clearing time. The problem formulation can be described as follows:-

i) Objective Function

The objective of optimal generation rescheduling here is to improve power system transient stability or to make the worst contingency identified during contingency screening ranking (Ch. 3) completely stable through maximizing critical clearing by rescheduling power generations. CCT is evaluated as function of PGi and QGi at each iteration step of the PSO algorithms, as described in the previous subsection and used to monitor the power system transient stability status. Therefore the objective function is expressed as given below [**78**] :

Maximizing Critical Clearing Time (CCT)

$$\max CCT_i\left(P_{Gi}, Q_{Gi}\right) and\ \min(P_{Li}) \qquad (5\text{-}5)$$

Subject to:-

Power flow equality constraints

The equality constraints are the power balance equations, which can be described by the equations below [**78**] :

$$\sum P_{Gi} - \sum P_{Di} - \sum P_{Li}\left(V_i, \theta_i\right) = 0$$
$$\sum Q_{Gi} - \sum Q_{Di} - \sum Q_{Li}\left(V_i, \theta_i\right) = 0 \quad (5\text{-}6)$$

Power flow inequality constraints

The inequality functions are the ranges of the bus voltage magnitudes constraints, Lines, cables and transformers flows constraints, total active power loss constraints, and active and reactive power generation constraints [**78**].

$$S_i\left(V_i, \theta_i\right) < S_{i\max}$$
$$V_{\min} \le V_i \le V_{\max}$$
$$P_{G\min} \le P_{Gi} \le P_{G\max} \quad (5\text{-}7)$$
$$Q_{G\min} \le Q_{Gi} \le Q_{G\max}$$
$$\sum P_{Li} \le \sum P_{iexist}$$

5.4. Description of the proposed dynamic security enhancement method

The overall framework of the developed dynamic security analysis tool is presented in Chapter 2 Section 2.5. The proposed contingency screening and security assessment is described and validated using two different standard test systems in the previous Chapters 3 and 4 respectively. Using the result of transient stability assessed for the worst contingency as an input, critical and noncritical machines cluster is identified including generator's sensitivity factors, as indicated Figure 5-2, flowchart of the algorithm for PSO based optimal generation rescheduling to enhance dynamic security. It shows the program flow to find a generation configuration with improved system dynamic behavior considering transient stability while satisfying operational constraints with minimum loss.

5.4,1, Power Generation Rescheduling and Optimization Process

In this thesis generation rescheduling is purposed to find the optimal amount of rescheduled power between generators with minimum power loss (PL) and maximum CCT. This process should restore all severely unstable contingencies to completely stable state at the same time. The sequence of optimization process can be summarized as follows:

- For each new operating point derived from the latest SCADA data snapshot, the power system is subjected to a set of selected credible contingencies.

- These contingencies are screened and ranked based on the methods described in Chapter 3, allowing for the identification of the worst contingency.
- Using the AOSDTM-based time domain simulation with a cross-cut technique, the CCT is estimated for this worst contingency.
- If the estimated minimum CCT is less than the specified minimum CCT limit, it is classified as an unstable contingency.

The rate of rotor angle variation is used as sensitivity index for generators response during the contingencies. If the system is transiently stable, rotor angle of each machine will move within certain border with respected to COA but if the system is transiently unstable, time response of rotor angles is used as sensitivity index to classify all generators into two groups. The first groups are generators with positive sensitivity and second groups are generators with negative sensitivity. Generators with positive sensitivity decrease their generation and generators with negative sensitivity increase their generation.

Particle Swarm Optimization (PSO) is employed to iteratively determine the optimal amount of power that needs to be shifted from critical machines (CM) to non-critical machines (NCM). The population in the PSO consists of multiple particles, with each particle represented by a dimensional vector x, This vector includes control variables, specifically the changes in rescheduled active power (ΔP) and reactive (ΔQ). Where Np1 and Np2 are the number of generators participating in active and reactive power rescheduling

$$\begin{aligned} x^T &= \left[\Delta P^T, \Delta Q^T\right] \\ \Delta P^T &= \left[\Delta P_1, \Delta P_2, ..., \Delta P_{Np1}\right] \\ \Delta Q^T &= \left[\Delta Q_1, \Delta Q_2, ..., \Delta Q_{Np1}\right] \end{aligned} \qquad (5\text{-}8)$$

The total shifted power can be distributed using various techniques based on technical or economic considerations. For example, distribution may occur equally among all or some critical machines, or it may be based on machine ratings or their response during critical contingencies. In this context, the total shifted power involves generators in each group, utilizing sensitivity factors derived from their inertia coefficients and rated capacities. The distribution of the shifted power from non-critical machines (NCM) to critical machines (CM) can be calculated based on the generators' capacities (S) and inertia (T). using Equation 5-9 [**78**].

The mathematical formulation of the necessary conditions is a system dynamic performance analysis based on Center of Angle (COA) that can be solved and simulated by Adaptive step-size based Differential Transformation Methods (AOSDTM). The output is the best control strategy with which to mitigate instabilities as shown in Figure 5-1.

$$\alpha_{iA} = \frac{T_{miA} s_{GiA}}{\sum_{i=1}^{N_A} T_{miA} s_{GiA}}, \qquad \alpha_{jB} = \frac{T_{mjB} s_{GjB}}{\sum_{j=1}^{N_B} T_{mjB} s_{GjB}}$$
$$\Delta P_{GiA} = \alpha_{iA} \Delta P, \qquad \Delta P_{GjB} = \alpha_{jB} \Delta P \qquad (5\text{-}9)$$
$$\sum_{i=1}^{N_A} \alpha_{iA} = 1, \qquad \sum_{J=1}^{N_B} \alpha_{jB} = 1$$

Where

α_{iA} and α_{jB} represent the factors used to distribute the shifted power among critical and non-critical machines

T_{miA} and T_{mjB} represent the inertia constant of generator i in group A and j in group B respectively

S_{GiA} and S_{GjB} represent capacity of generator i in group A and j in group B respectively

ΔP_{GiA} and ΔP_{GjB} represent the change of generated power from generator i in group A and generator j in group B respectively

The optimization process continues until specific stopping criteria are met. Two criteria are employed in this approach:

- **Global Best Fitness Movement**: The movement of the global best fitness is monitored. If the change in fitness falls below a certain threshold, the optimization program is terminated.
- **Distance Between Individuals**: The distance between the global best solution and each individual particle is evaluated. If the maximum distance is below a defined threshold value, the optimization process is also terminated.

These criteria ensure that the optimization ceases when further improvements are minimal, indicating that a near-optimal solution has been reached. The modeling and simulation results for

load flow and CCT calculations are accomplished using the simulation and assessment tools developed implemented and using MATLAB software with installed power flow analysis tool package, Matpower. The developed MATLAB code includes PSO implementation.

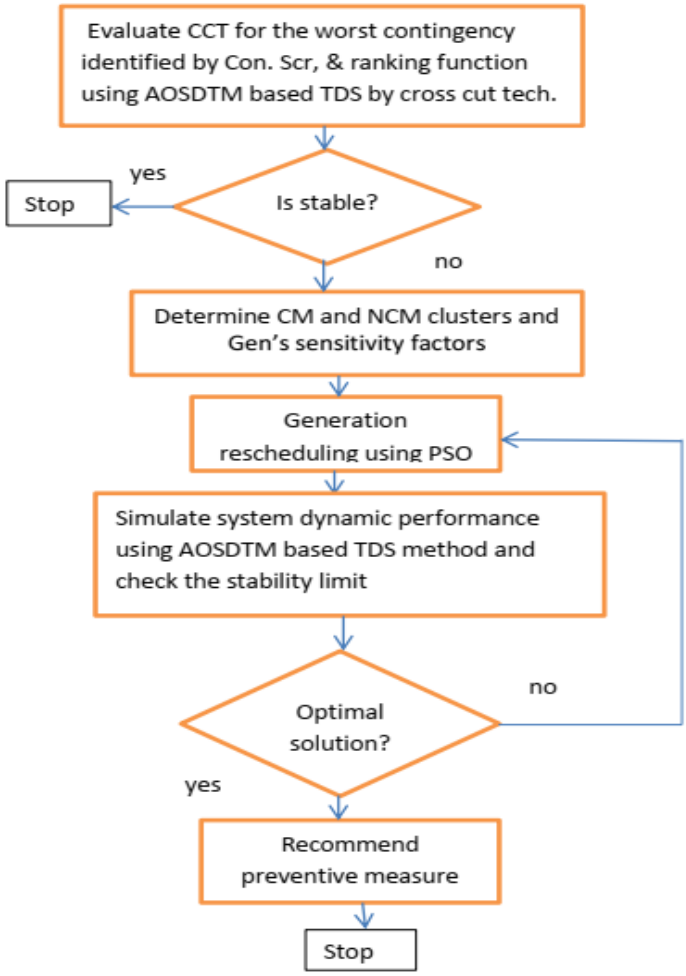

Figure 5-1 flowchart of the algorithm for PSO based optimal generation rescheduling to enhance dynamic security

In general the basic steps of the proposed transient stability based dynamic security enhancement can be summarized as follows:

- Based on the proposed Transient Stability Assessment (TSA) method, determine CCT for the identified contingency.
- If the security margin of the worst case is below an unacceptable level, run the proposed AOSDTM based TDS method, classify generators according to change of rotor angles from COA.

- Apply PSO technique to establish a power generation re-allocation to improve system transient stability.
- Check improvement of system dynamic performances, if no go to step 3

5.5. Test Results and Discussions

Two power systems are selected for testing the validation studies of the proposed algorithm: a four-machine two-area 11-bus benchmark system [**78**], and a three-machine 9-bus system [**57**]. The test systems are subjected to a set of contingencies and the contingency is always a three phase self-clearing faults to calculate CCT. In performing generation rescheduling, it is assumed that the total generation and loads are held constant. The change in system losses is compensated by slack bus.

5,5,1, Transient stability assessment results and discussion

Plots of the transient stability indices are evaluated for 3phase short circuit at all buses of both test systems (Figure 5.2a & b) step by step excluding the generator buses are given by Figure 5-2a and b.. The worst contingencies identified are 3phase short circuit at bus 8 and 6 for 9bus and 11bus test systems respectively.

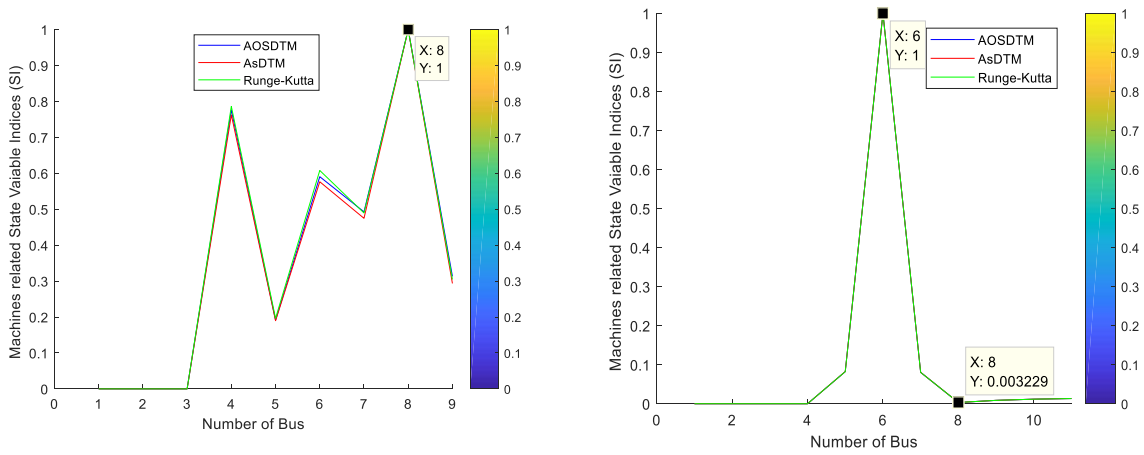

(**a**) (**b**)

Figure 5-2 TSI plots of (a) 9 bus and (b) 11 bus test systems.

Assessment results by RK4 are used as a bench mark and errors results of AsDTM and AOSDTM methods are considered as differences from the benchmark result. For AOSDTM based assessment DT order varies between k_min=6 and k_max=14 and the step-size varies adaptively between h_min=0.00425sec and h_max=0.2sec for both AsDTM and AOSDTM methods. kmax is used as a fixed DT order for AsDTM based assessment method.

The assessment time cost, total number of iteration, and accuracy of the assessment results by using the proposed method, for the identified worst contingencies, is validated in comparison with Rk4 and AsDTM methods. From Figures 5-3a, b and5-4a, b, one can observe that the total number of iterations and assessment time requirement relationships among Rk4, AsDTM, and AOSDTM based transient stability assessment (TSA) methods, to determine CCT during the worst contingency are 44,990, 10,840, and 10,650 for the IEEE 9 bus test system and 65,000, 27,720, and 19,270 for the 11 bus test system, respectively. Similarly, the total time required for the assessment for the same case are 75.83s, 9.844s, and 8.127s, for the IEEE 9 bus test system and 130.1s, 26.95s, and 16.63s for the 11 bus test system, respectively. As can be seen from the flowchart of the proposed transient stability assessment algorithm given by Figure 10, to obtain CCT of the contingency under assessment, a number of 5sec transient stability simulation runs are required. The zigzag line pattern in the plots of total assessment time cost and number of time steps of Figures 5-3a, b and 5-4a, b, indicates the interpolation of the subtotal simulation time cost and number of steps at every 5sec transient stability simulation run.

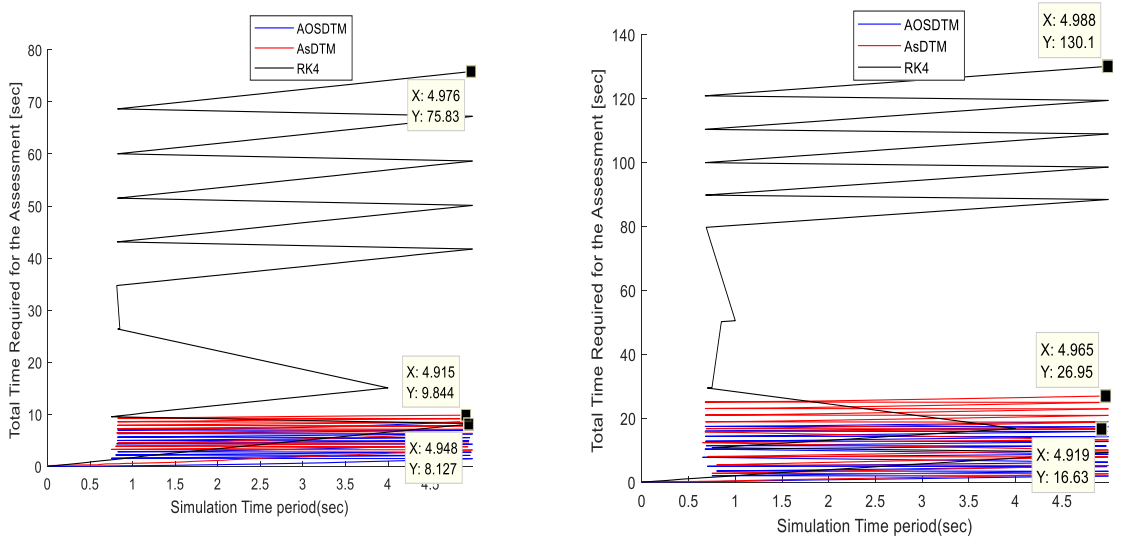

(**a**) (**b**)

Figure 5-3 Total Time required for the Assessment for (a) 9 bus and (b) 11 bus test systems.

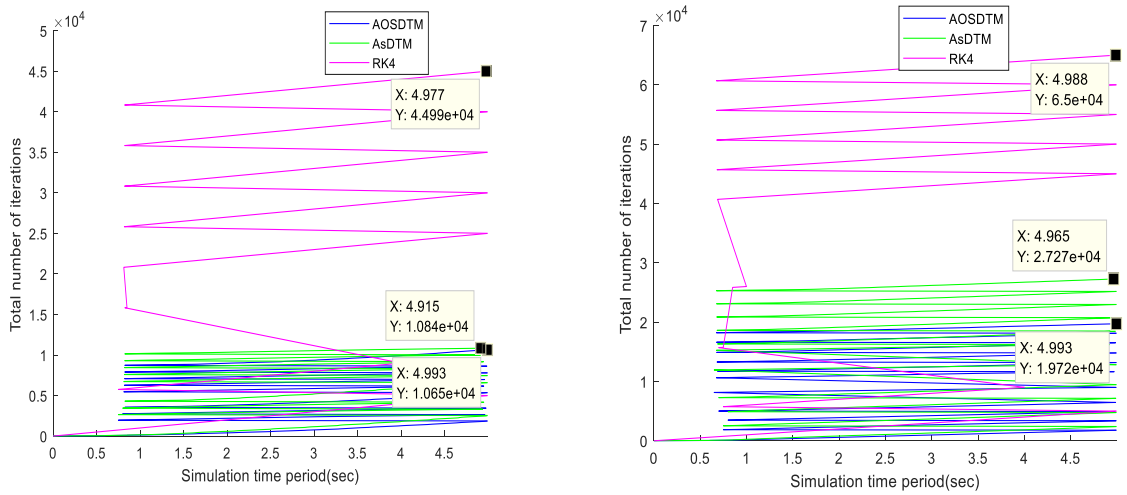

(**a**) (**b**)

Figure 5-4 Number of iterations for (a) 9 bus and (b) 11 bus test systems.

The CCT results of the contingency assessed from time domain simulations based on Rk4, AsDTM, and AOSDTM methods are given in Table 5-1. Since time domain simulation based on Rk4 is assumed accurate,it is used as a reference to validate the accuracies of the other methods in this paper, i.e. the CCT results calculated based on AOSDTM is the same as those calculated based on Rk4 for both 9bus and 11bus test systems.

Table 5-1 Transient Stability Assessment (TSA) results by different assessment methods

Assessment method	CCT(ms)				Remark
	For 9bus test system	Error (ms)	For 11bus test system	Error (ms)	
Rk4	223.4	0.0	75.80	0.0	
AOSDTM	223.4	0.0	75.80	0.0	
AsDTM	223.4	0.0	76.05	0.25	

From the simulation results shown in Figures 5-3a & b, 5-4a & b, and Table 5-1

Compared with the AsDTM-based assessment the proposed AOSDTM method improves the total assessment time required and total number of iterations by 38.59% and 30.48% for the IEEE 11 bus test system and improves by 17.44% and 17.63% for the IEEE 9 bus test system, respectively.

Compared with the Rk4-based assessment the proposed AOSDTM method improves the total assessment time required and total number of iterations by 78.65% and 92.34% for the 11 bus

test system and improved/reduced the total assessment time cost and total number of iterations by 85.34% and 96.74% for the IEEE 9 bus test system, respectively.

Compared with the AsDTM-based assessment method, the proposed AOSDTM assessment method also improves the accuracy the assessment results by up to 0.33% for 11bus test systems respectively.

Therefore, we can conclude that the proposed AOSDTM-based power system transient stability assessment method increases the assessment speed by 17.4–38.59% and 78.65–85.34% when compared with the AsDTM, and Rk4-based assessment methods, respectively. The accuracy of the assessment results are improved by 0.5% and 0.33%, when compared with the classical AsDTM based assessment method.

5.5.2. Results of the proposed transient stability based dynamic security enhancement method and discussion

The plots of TSI evaluated for 3phase short circuit at all buses excluding the generator buses, using the test systems, Figure 4-3a & b, is given by Figure 5-2a & b above. The worst contingencies identified are 3phase short circuit at bus 8 and 6 for 9bus and 11bus test systems respectively. Figure 5-5a and b shows the time response of rotor angles with respect to COA for all generators during the worst contingencies. In both systems the unstable equilibrium point is at FCT of 229.7 and 73 milliseconds and corresponding critical generators are G2 at bus 2 and G1 at bus 1 for IEEE 9 bus and 11bus test systems respectively. The system losses are 4.55 MW and 88 MW at unstable equilibrium point respectively.

As shown in Figure 5-5a and b, the generators are easily identified into two groups A & B, A (G2) and B (G1, G3) and A (G1, G2) and B (G3, G4) by their advanced angles at the UEP for both test systems respectively. PSO is applied to determine the optimal amount of generation to be coordinated between generators to improve the system transient stability. The results obtained with the optimization program show that the CCT increased to 246.1 and 184.4 milliseconds as shown by Figure 5-6a and b, and the losses reduced to 4.3 MW and 77.51 MW for IEEE 9 bus and 11bus test systems respectively as shown by Figure 5-7a and b.

. The results obtained with the optimization program show that in both cases the CCT is increased which clearly show that system stability is improved and at the same time the total active power loss is reduced as shown by Figure 5-7a and b.

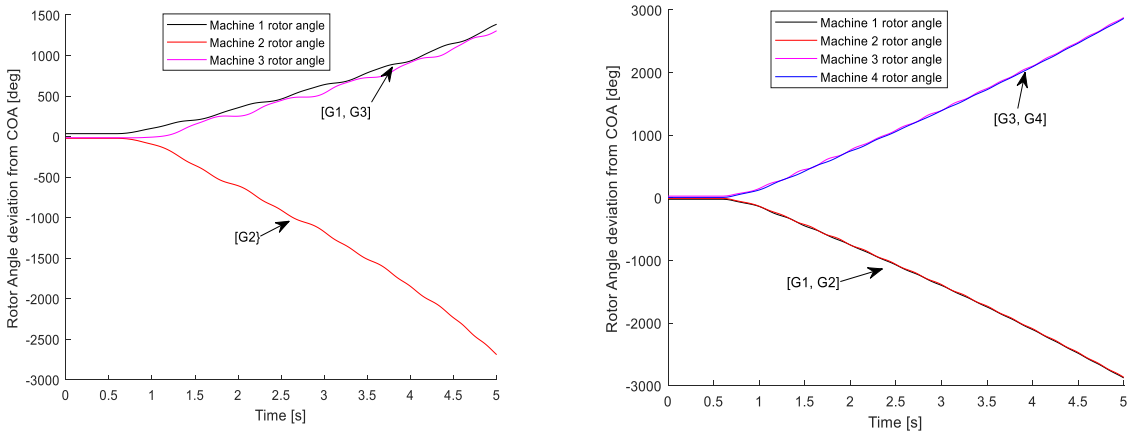

(**a**) (**b**)

Figure 5-5 Simulation of rotor angle deviation from COA with (a) 229.7ms FCT for IEEE 9bus test system and (b) 73ms FCTfor 11bus test system before generation rescheduling

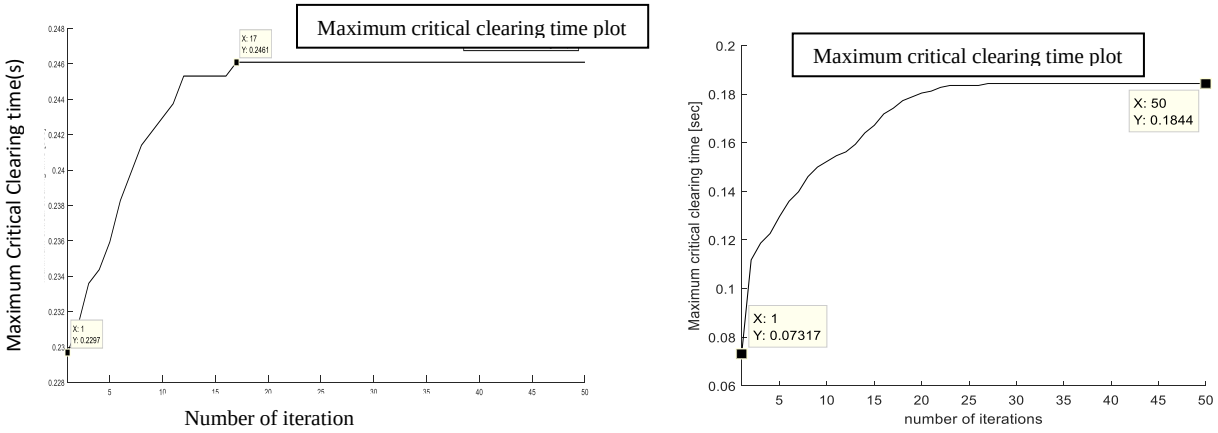

(**a**) (**b**)

Figure 5-6 CCT plots of (a) IEEE 9bus test system and (b) 11bus test system

Figure 5-8a and b shows changes in generated power after and before applying PSO to obtain optimal generation rescheduling for cases with both test system. As seen from the bar graphs, after PSO is applied, the power generated from critical generators/machines is reduced but the power generated from non-critical generators/machines is increased. Figure 5-9a and b show the dynamic response during 229.7-millisecond and 246.1milisecond for three phase fault at bus 8 (the most critical contingency before optimal generation rescheduling for 9bus test system) respectively. Similarly, Figure 5-10a and b show the dynamic response during 73 millisecond and 184.4milisecond for three phase fault at bus 6 (the most critical contingency before optimal generation rescheduling for 11bus test system) respectively. These Figures show that the system is transiently stable after generation is rescheduled.

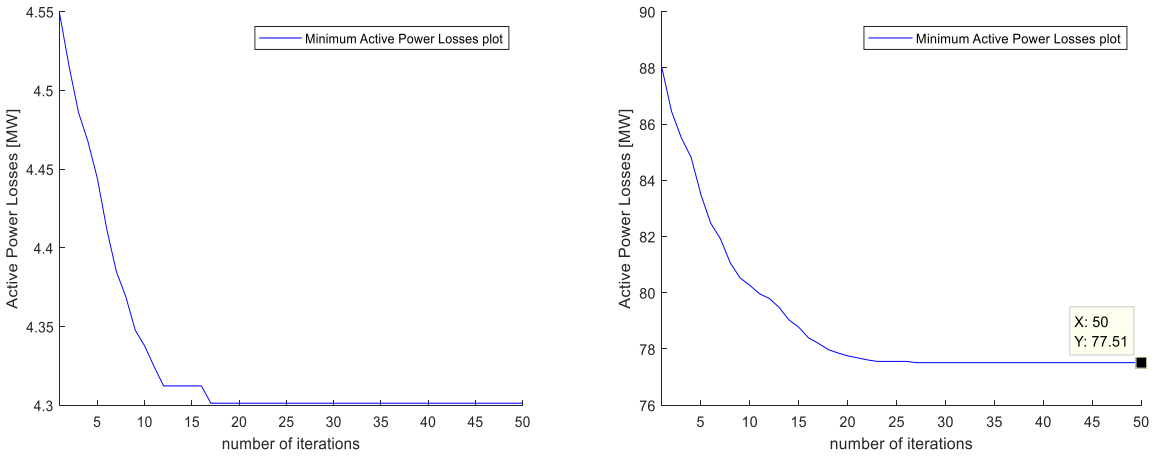

(**a**) (**b**)

Figure 5-7 Total active power loss plots of (a) IEEE 9bus test system, (b) 11bus test system

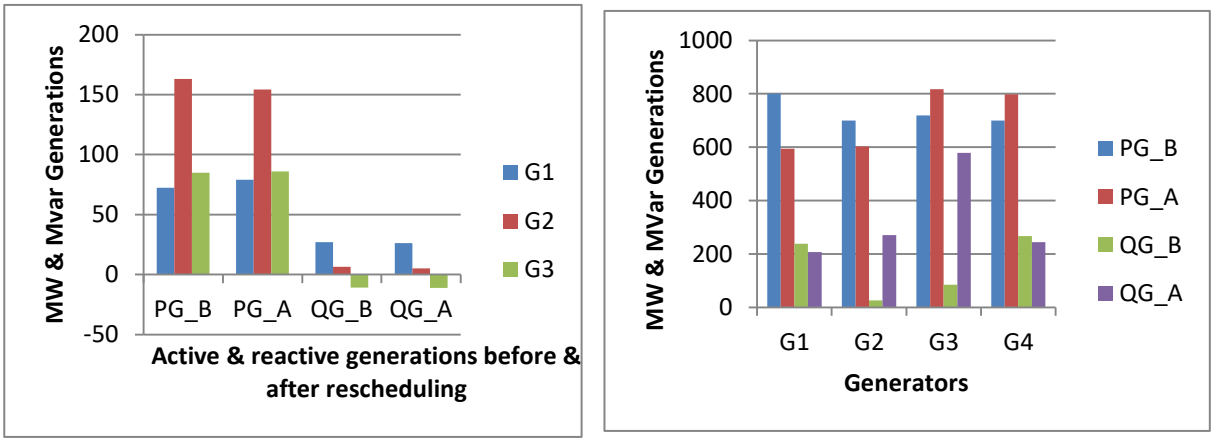

(**a**) (**b**)

Figure 5-8 Power generations before and after rescheduling for (a) IEEE 9bus test system (b) 11bus test system

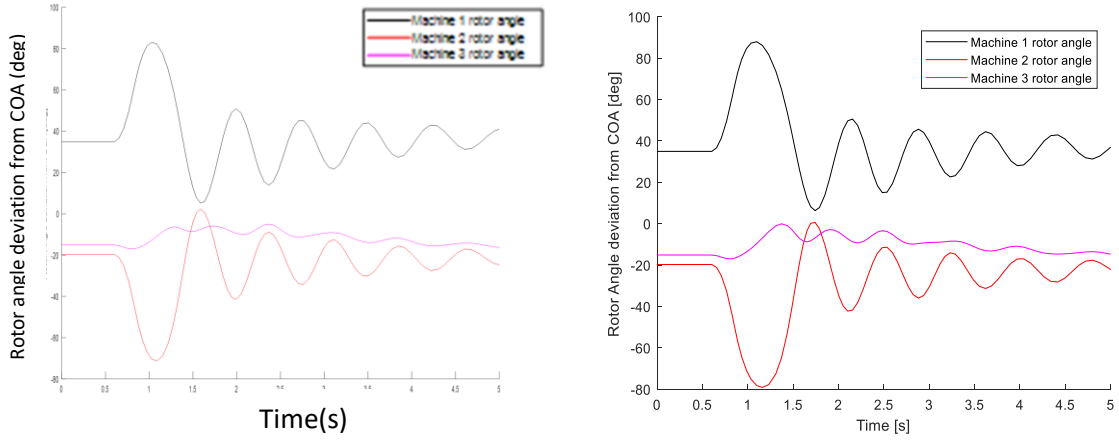

(**a**) (**b**)

Figure 5-9 (a) Simulation of rotor angle deviation from COA with 229.7ms FCT and (b) with 243ms FCT for IEEE 9bus test system after generation rescheduling

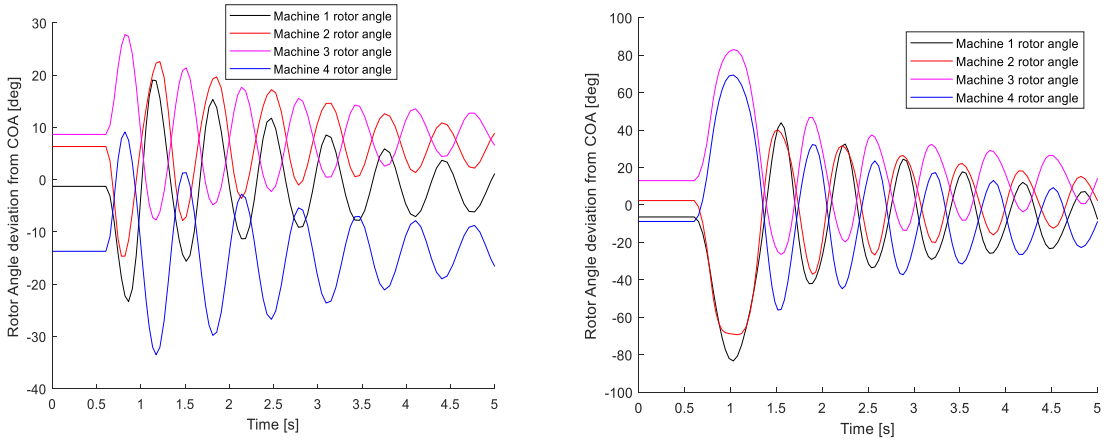

Figure 5-10 (a) Simulation of rotor angle deviation from COA with 73ms and (b) with 180ms FCT for 11bus test system after generation rescheduling

From the simulation results of assessment time cost per iteration given by Figure 5.3a&b and total number of iteration to achieve improved transient stability with constraints maintained in between the specified limits, the total assessment time cost is calculated for each assessment method as given in Table 5-1.

Table 5-2 total assessment time cost for transient stability improvement based on proposed method

Assessment method	Number of iterations	For 9bus test system		For 11bus test system		Remark
		Ass. time required/iter.(s)	Total ass. time required(s)	Ass. time required/iter.(s)	Total ass. time required(s)	
Rk4	50	74.85	3712.5	123.2	6160	
AOSDTM	50	10.98	549	26.3	1315	
AsDTM	50	16.23	811.5	44.25	2212.15	

Compared with Rk4 and AsDTM, using the proposed AOSDTM the total assessment time cost is improved by 85.2% and 32.35% respectively for 9bus test system. Similarly using the proposed AOSDTM improves the total assessment time cost by 78.65% and 40.56% respectively for 11bus test system. Therefore we can conclude that power system transient stability improvement based on optimal generation rescheduling using AOSDTM based power system time domain

simulation method proposed in this work is very fast and can be applied as a DSA tool in near real time power system operation environment.

In general, the proposed transient stability based power system dynamic security enhancement method consists of classifying critical and non-critical generators based on their transient behavior during the worst contingency and PSO was applied for allocating generation to improve system transient stability by maximize the critical fault clearing time under the condition of minimizing system power losses. Efficient and robust TSA technique is incorporated in order to speed up the transient stability border identification and reduce the consumed time in calculations. Numerical test results demonstrate that PSO based on power system transient stability simulation using AOSDTM method is effective for improving the transient stability status of power systems based on optimal generation rescheduling with a reasonable degree of accuracy and significant performance efficiency. The developed tools can be applied as a DSA tool in near real time power system operation environment.

CHAPTER Six: Conclusion and Outlook

The current power system is evolving into a complex dynamic system, increasingly interconnected with a significant amount of renewable energy resources. This transition necessitates higher utilization of existing power system equipment and a continuous adaptation to new operational situations. Identifying critical limits and instabilities within the power system, along with determining rapid corrective actions, is essential for ensuring grid security. This PhD project focuses on the investigation and development of dynamic security analysis tools for power systems. The developed tools and methods are based on advanced time-domain simulation (TDS) techniques, specifically designed to perform transient stability assessments. These tools will recommend enhancements or preventive mechanisms to restore the system in the event of any transiently unstable contingencies. This research aims to bolster the resilience and reliability of the power grid as it integrates more renewable energy sources.

6.1. Conclusion

This dissertation set out to develop power system dynamic security analysis (DSA) tools capable of real-time contingency screening, transient stability assessment, and recommending preventive measure to stabilize the system during transiently unstable situation. These objectives were systematically addressed through the development of advanced tools and methods leveraging the most current SCADA data, ensuring dynamic security assessments are based on real-time system conditions. This approach eliminated the reliance on offline-generated simulation databases, which are unsuitable for handling the unpredictability of stochastic generation and load variation.

The research successfully achieved its goals through the development of three core functional stages: contingency screening and ranking, detailed transient stability assessment for the worst contingencies, and dynamic security enhancement. The tools and methods developed include:

- Fast and robust transient stability simulation methods.
- Contingency screening and ranking tools for transient stability analysis.
- Tools for assessing transient stability that estimate proximity to stability boundaries.
- A machine clustering tool to identify critical and non-critical generator groups based on real-time SCADA snapshots.
- A DSA tool incorporating particle swarm optimization (PSO) to determine optimal remedial actions for improving transient stability.

The research objectives were met by introducing novel methodologies such as the **Adaptive Step-Size Differential Transformation Method (AsDTM)** and the **Adaptive Order and Step-Size Differential Transformation Method (AOSDTM)**. These methods significantly improved the computational efficiency and accuracy of transient stability simulations, enabling real-time analysis of large and complex power systems. For instance, AsDTM and AOSDTM-based tools demonstrated speed improvements of up to 92% and error reductions exceeding 77% compared to traditional simulation methods. These advancements directly address the need for faster and more accurate tools in modern power system operations.

The tools developed for contingency screening and ranking, using transient stability indices (TSI), further streamlined the identification of the most critical contingencies. This enhancement allowed operators to focus on the most severe scenarios, optimizing their response times. Additionally, the transient stability assessment tools, which incorporated the concept of Critical Clearing Time (CCT), provided operators with a clear measure of system resilience under worst-case conditions.

Beyond identifying instability, the research introduced a dynamic security enhancement tool that combined AOSDTM with PSO. This tool proposed optimal generation rescheduling strategies to restore system stability during severe contingencies, achieving rapid and efficient stabilization. Test results demonstrated that this approach improved assessment times by over 85% compared to traditional methods, making it highly suitable for near real-time applications.

The implications of this research are far-reaching. The developed tools offer power system operators the ability to perform dynamic security analysis in near real-time, enabling them to anticipate and mitigate transient instabilities effectively. This capability is crucial in modern grids where the integration of renewable energy sources and increasing system complexity introduce new challenges. Furthermore, the inclusion of optimization techniques like PSO demonstrates the potential for automation and intelligent decision-making in power system operations.

Finally, the research not only met its objectives by developing fast, robust, and accurate DSA tools but also provided a foundation for future advancements in real-time power system stability analysis. By addressing the challenges of computational efficiency and reliability, this work

contributes to the ongoing improvement of dynamic security in power system operations, paving the way for smarter and more resilient grids.

6.2. Outlook

The rapidly growing load and increasing complexity of the electric power industry compel power systems to operate near their stability limits, leading to various instabilities. Consequently, the assessment and enhancement of power system stability remain critical areas of active research. The ultimate goal of this research is to develop robust and rapid dynamic analysis (DA) tools that focus specifically on power system transient stability. This includes creating a comprehensive framework that can be utilized to enhance the transient stability of power systems. Test and validation results indicate that the developed DA tools significantly improve performance efficiency and accuracy compared to classical dynamic stability methods (DTM) and traditional numerical integration techniques. These advancements enable system operators to maintain situational awareness, allowing for accurate assessments of security risks (particularly regarding transient instability) and the initiation of necessary corrective measures in near real-time operational environments. Despite the speed and accuracy of these DA tools relative to existing tools based on time-domain simulations (TDS), several limitations remain that require further investigation. Addressing these limitations will be crucial for enhancing the effectiveness and reliability of dynamic stability assessments in the future.

Extension of the proposed DSA tools and methods: The proposed and developed tools to analyze power system dynamic security only in terms of transient stability, extending the method to assess other components of DSA, such as voltage stability, small signal stability, voltage transient sag, and etc, will need further works. Furthermore, in this work, both active and reactive power rescheduling are considered without taking into account the impact of distributed FACT devices and tap-changing transformers, extending the generation rescheduling by considering the effect of FACT, tap-changing transformers requires further investigations. This implies that a more comprehensive approach to stability will enhance overall system resilience against various disturbances, leading to a more reliable power supply. Improved rescheduling capabilities also can optimize energy distribution, reducing operational costs and improving efficiency.

Exploration of transient stability for various types of generators: The prevalence of generators that are not synchronously connected is increasing, particularly with the rise in wind

turbine installations. As a result, studying the transient stability of these generators could be beneficial, and it may be necessary to adapt existing transient stability assessment methods accordingly. This helps in understanding the stability of diverse generator types will facilitate greater integration of renewable energy sources, promoting sustainability and reducing reliance on fossil fuels. Improved adaptability can enhance grid stability as the energy mix evolves, supporting energy transition goals.

Viability of the proposed DSA tools and technique: For more advanced evaluation of the viability, testing of these tools on different and relatively large power systems should be conducted. The presented framework and developed tools next can be applied on large-scale power system where the system can be divided into multiple regions by considering the effect of stability of one region on the other. This implies that validating tools on large-scale systems enhances their credibility and encourages broader adoption by industry stakeholders. Insights into regional interactions can inform better grid management strategies and policy decisions, ultimately improving system reliability.

Further speed up of the proposed DSA tools and method: The performance efficiency of the developed DSA tools requires further improvement for online application in large systems. Therefore, in the future, use of high speed computing processors, parallel computing configuration or other different technics that can upgrade the performance efficiency of these tools shall be studied and investigated. Because of the fact that optimized tools can enable faster response times during emergencies, significantly improving grid reliability and stability. Enhanced performance can lower operational costs, making advanced stability assessments more accessible to system operators.

Appendix A

1. IEEE 9 Bus and New England 39 Bus Test Systems Generators and their controller's Data [**55**]

Table A-1 New England 39 bus test system generator data 1.

Bus #	Xd	Xq	X′d	X′q	Rs	T′do	T′qo	H	Dg
30	0.1000	0.0690	0.0310	0.0690	0.0002	10.200	0.020	42.000	0.0535
31	0.2590	0.2820	0.0700	0.1700	0.0002	6.5600	1.5000	30.300	0.0194
32	0.2500	0.2370	0.0530	0.0880	0.0002	5.7000	1.5000	35.500	0.06783
33	0.2620	0.2580	0.0440	0.1660	0.0002	5.6900	1.5000	28.500	0.01815
34	0.6700	0.6200	0.1320	0.1660	0.0002	5.4000	0.4400	26.000	0.0331
35	0.2540	0.2410	0.0500	0.0810	0.0002	7.3000	0.4000	35.00	0.06783
36	0.2950	0.2920	0.0490	0.1860	0.0002	5.6600	1.5000	26.500	0.01815
37	0.2900	0.2800	0.0570	0.0910	0.0010	6.7000	0.4100	24.300	0.0331
38	0.2110	0.2050	0.0570	0.0590	0.0002	4.7900	1.9600	34.500	0.06783
39	0.0200	0.0190	0.0060	0.0080	0.0002	7.0000	0.7000	31.0 00	0.01940

Table A-2 New England system generator controller's data

Bus #	Ke	Te	Aexc	Bexc	Ur_max	Ur_ min	Ka	Ta	Kf	Tf	Tch	Tg	Rg
30	1.0000	0.2500	0.0039	1.55	10	−10	20	0.06	0.04	1.0	0.1	0.05	0.05
31	1.0000	0.4100	0.0039	1.55	10	−10	20	0.05	0.06	0.5	0.1	0.05	0.05
32	1.0000	0.5000	0.0039	1.55	10	−10	20	0.06	0.08	1.0	0.1	0.05	0.05
33	1.0000	0.5000	0.0039	1.55	10	−10	20	0.06	0.08	1.0	0.1	0.05	0.05
34	1.0000	0.7900	0.0039	1.55	10	−10	20	0.02	0.03	1.0	0.1	0.05	0.05
35	1.0000	0.4700	0.0039	1.55	10	−10	20	0.02	0.08	1.25	0.1	0.05	0.05
36	1.0000	0.7300	0.0039	1.55	10	−10	20	0.02	0.03	1.0	0.1	0.05	0.05
37	1.0000	0.5300	0.0039	1.55	10	−10	20	0.02	0.09	1.26	0.1	0.05	0.05
38	1.0000	1.4000	0.0039	1.55	10	−10	20	0.02	0.03	1.0	0.1	0.05	0.05
39	0.0200	0.0190	0.0060	0.0080	0.0002	7.0	0.70	31.0	0.01940				

Table A-3. IEEE 9 bus test system generator data .

Bus #	Xd	Xq	X′d	X′q	Rs	T′do	T′qo	H	Dg
1	0.146	0.0969	0.0608	0.0969	0.004	8.96	0.31	23.000	0.0151
2	0.8958	0.8648	0.1198	0.1969	0.0026	6.00	0.535	6.400	0.001
3	1.3125	1.2578	0.1813	0.25	0.0035	5.890	0.6	3.010	0.0058

Table A-4. IEEE 9 bus test system generator controller's data

Bus #	Ke	Te	Aexc	Bexc	Ur_max	Ur_ min	Ka	Ta	Kf	Tf	Tch	Tg	Rg
1	1.0000	0.3140	0.0039	1.55	3	−3	20.0	0.20	0.0630	0.350	0.10	0.05	0.05
2	1.0000	0.3140	0.0039	1.55	3	−3	20.0	0.20	0.0630	0.350	0.1	0.05	0.05
3	1.0000	0.3140	0.0039	1.55	3	−3	20.0	0.20	0.0630	0.350	0.1	0.05	0.05

2. IEEE 9 Bus and New England 39 Bus Test Systems power flow Data

Table A-5 New England system power flow data I

Bus #	Voltage (p.u.)	Angle (degree)	*Pload*(MW)	*Qload*(MVAR)	*gen P*(MW)	*gen Q*(MVAR)
1	1.0436	-13.39	0.00	0.00	0.00	0.00
2	1.0378	-11.21	0.00	0.00	0.00	0.00
3	1.0056	-13.87	322.00	122.40	0.00	0.00
4	0.9864	-14.01	500.00	184.00	0.00	0.00
5	0.9924	-12.24	0.00	0.00	0.00	0.00
6	0.9956	-11.40	0.00	0.00	0.00	0.00
7	0.9851	-13.75	233.80	84.00	0.00	0.00
8	0.9843	-14.32	522.00	176.00	0.00	0.00
9	1.0233	-14.58	0.00	0.00	0.00	0.00
10	1.0060	-9.41	0.00	0.00	0.00	0.00
11	1.0013	-10.10	0.00	0.00	0.00	0.00
12	0.9876	-10.23	8.50	88.00	0.00	0.00
13	1.0014	-10.23	0.00	0.00	0.00	0.00
14	0.9947	-12.18	0.00	0.00	0.00	0.00
15	0.9909	-13.33	320.00	153.00	0.00	0.00
16	1.0043	-12.16	329.40	132.30	0.00	0.00
17	1.0076	-13.11	0.00	0.00	0.00	0.00
18	1.0055	-13.85	158.00	30.00	0.00	0.00
19	1.0432	-7.90	0.00	0.00	0.00	0.00
20	0.9938	-9.51	680.00	103.00	0.00	0.00
21	1.0122	-9.83	274.00	115.00	0.00	0.00
22	1.0387	-5.44	0.00	0.00	0.00	0.00
23	1.0322	-5.65	247.50	84.60	0.00	0.00
24	1.0029	-12.07	308.60	92.20	0.00	0.00
25	1.0461	-10.01	224.00	47.20	0.00	0.00
26	1.0299	-11.38	139.00	47.00	0.00	0.00
27	1.0136	-13.39	281.00	75.50	0.00	0.00
28	1.0308	-8.00	206.00	27.60	0.00	0.00
29	1.0318	-5.22	283.50	126.90	0.00	0.00
30	1.0475	-8.96	0.00	0.00	230.00	206.87
31	0.9820	0.00	0.00	0.00	722.53	274.61
32	0.9831	-1.58	0.00	0.00	630.00	254.00
33	0.9972	-2.84	0.00	0.00	612.00	152.86
34	1.0123	-4.50	0.00	0.00	488.00	236.74
35	1.0493	-0.58	0.00	0.00	630.00	290.62
36	1.0635	2.00	0.00	0.00	540.00	148.33
37	1.0278	-3.42	0.00	0.00	520.00	48.40
38	1.0265	1.74	0.00	0.00	810.00	138.33
39	1.0300	-14.68	1104.00	250.00	1000.00	123.30

Table A-6 New England system power flow data II

FromBus	ToBus	Resistance (p.u.)	Reactance (p.u.)	Line Charge (p.u.)	Tap Ratio
1	2	0.0035	0.0411	0.69870	0.00
1	39	0.002	0.05	0.37500	0.00
1	39	0.002	0.05	0.37500	0.00
2	3	0.0013	0.0151	0.25720	0.00
2	25	0.007	0.0086	0.14600	0.00
3	4	0.0013	0.0213	0.22140	0.00
3	18	0.0011	0.0133	0.21380	0.00
4	5	0.0008	0.0128	0.13420	0.00
4	14	0.0008	0.0129	0.13820	0.00
5	6	0.0002	0.0026	0.04340	0.00
5	8	0.0008	0.0112	0.14760	0.00

6	7	0.0006	0.009200	0.11300	0.00
6	11	0.0007	0.008200	0.13890	0.00
7	8	0.0004	0.004600	0.07800	0.00
8	9	0.0023	0.036300	0.38040	0.00
9	39	0.0010	0.025000	1.20000	0.00
10	11	0.0004	0.004300	0.07290	0.00
10	13	0.0004	0.004300	0.07290	0.00
13	14	0.0009	0.010100	0.17230	0.00
14	15	0.0018	0.021700	0.36600	0.00
15	16	0.0009	0.009400	0.17100	0.00
16	17	0.0007	0.008900	0.13420	0.00
16	19	0.0016	0.019500	0.30400	0.00
16	21	0.0008	0.013500	0.25480	0.00
16	24	0.0003	0.005900	0.06800	0.00
17	18	0.0007	0.008200	0.13190	0.00
17	27	0.0013	0.017300	0.32160	0.00
21	22	0.0008	0.014000	0.25650	0.00
22	23	0.0006	0.009600	0.18460	0.00
23	24	0.0022	0.035000	0.36100	0.00
25	26	0.0032	0.032300	0.51300	0.00
26	27	0.0014	0.014700	0.23960	0.00
26	28	0.0043	0.047400	0.78020	0.00
26	29	0.0057	0.062500	1.02900	0.00
28	29	0.0014	0.015100	0.24900	0.00
2	30	0.000	0.01810	0.000	1.025
6	31	0.00	0.050	0.00	1.070
6	31	0.00	0.050	0.00	1.070
10	32	0.00	0.020	0.00	1.070
12	11	0.0016	0.0435	0.00	1.006
12	13	0.0016	0.0435	0.00	1.0060
19	20	0.0007	0.0138	0.00	1.0600
19	33	0.0007	0.0142	0.00	1.0700
20	34	0.0009	0.018	0.00	1.0250
22	35	0.00	0.0143	0.00	1.0250
23	36	0.0005	0.0272	0.00	1.0000
25	37	0.0006	0.0232	0.00	1.0250
29	38	0.0008	0.0156	0.00	1.0250

Table A-7 IEEE 9bus system power flow Data I

Bus	Voltage		Generation		Load	
#	Mag(pu)	Ang(deg)	P (MW)	Q (MVAr)	P (MW)	Q (MVAr)
1	1.040	0.000*	71.64	27.05	-	-
2	1.025	9.280	163.00	6.65	-	-
3	1.025	4.665	85.00	-10.86	-	-
4	1.026	-2.217	-	-	-	-
5	1.013	-3.687	-	-	90.00	30.00
6	1.032	1.967	-	-	-	-
7	1.016	0.728	-	-	100.00	35.00
8	1.026	3.720	-	-	-	-
9	0.996	-3.989	-	-	125.00	50.00

Table A-8 IEEE 9bus system power flow Data II

Line		R [pu/m]	X [pu/m]	B [pu/m]
From Bus	**To Bus**			
4	5	0.0100	0.0680	0.1760
4	6	0.0170	0.0920	0.1580
5	7	0.0320	0.1610	0.3060
6	9	0.0390	0.1738	0.3580
7	8	0.0085	0.0576	0.1490
8	9	0.0119	0.1008	0.2090

REFERENCES

[1] P. Kundur, *Power System Stability and Control*.: McGraw-Hill Inc, 1994.

[2] P. W., Tomsovic, K. L. and Vittal, V. Sauer, "Dynamic Security Assessment, DOI: 10.1201/9781420009248," in *Dynamic Security Assessment, DOI: 10.1201/9781420009248*., May 2007, p. ch15.

[3] IEEE Power System Dynamic Performance Committee Task Force, "Stability Definitions and Characterization of Dynamic Behaviour in Systems with High Penetration of Power Electronic-Interfaced Technologies," Technical Report PES-TR77 April 2020.

[4] W. Lei, and P. Kundur K. Morison, "Power system security assessment," *IEEE Power and Energy Magazine*, vol. vol. 2, pp. pp. 30-39, 2004.

[5] Working Group Cigré C4.601, "Review of on-line dynamic security assessment tools and techniques," 2007.

[6] ENTSO-E RG-CE System Protection & Dynamics Sub Group, "SPD DSA Task Force Dynamic Security Assessment (DSA)," 2017.

[7] A. A. Fouad and Vijay Vittal, "Power System Transient Stability Analysis using the Transient Energy Function Method," 1992.

[8] Kundur et al, "Definition and classification of power system stability ," *IEEE Trans. Power Syst*, vol. vol. 19, no. 3, no. ieee/cigre joint task force on stability terms and definitions, pp. pp. 1387–1401, Aug 2004.

[9] http://mydocs.epri.com/docs/PublicMeetingMaterials/1202/MVNQQ2YVLLT/Lei_W ang.pdf.

[10] H. Jóhannsson, and J. Østergaard J. T. G. Weckesser, "On-line Dynamic Security Assessment in Power Systems," 2014.

[11] P. Donalek, et al. G. Andersson, "Causes of the 2003 Major Grid Blackouts in North America and Europe, and Recommended Means to Improve System Dynamic Performance," *IEEE Trans. on Power Systems*, vol. vol. 20, no. 4, November 2005.

[12] Loi Lei Lai, "Power System Restructuring and Deregulation," *John Wiley & Sons Ltd,England*, 2002.

[13] U.S.-Canada Power System Outage Task Force, "Final Report on the August 14, 2003 Blackout in the United States and Canada: Causes and Recommendations," U.S. Department of Energy, Washington DC, USA, technical report April, 2004.

[14] National Load Dispatch Centre of Ethiopia, "Partial and Total Blackouts Report, 2013-2015," National Load Dispatch Center, Ethiopian Electric Power, Ethiopia," EEP, Addis Ababa, Technical report 2017.

[15] Moges Alemu, "Study of Blackouts on Ethiopian Electric Power Network and Identification of System Vulnerabilities ," AAIT, Adis Ababa, Thesis report for partial fulfillment of MSC 2017.

[16] J. H. Eto and R. J. Thomas, "Computational needs for the next generation electric grid," *Department of Energy*, vol. vol. 593, 2011.

[17] & A. Bose, A. Chakrabortty, "Smart grid simulations and their supporting implementation methods," *Proceedings of the IEEE*, vol. vol. 105, no. 11, pp. pp. 2220-2243, Nov. 2017.

[18] D. Yang, "Power System Dynamic Security Analysis via Decoupled Time Domain Simulation and Trajectory Optimization ," Iowa State University: Ames, IA, USA, Thesis report 2006.

[19] L. Zuo, X. Yuan, J. Kubokawa, H. Sasaki, Y. Yuan, "A Novel Method for Power System Transient Stability Preventive Control," *IEEE/PES Trans-mission and Distribution Conference & Exhibition,China*, pp. pp.1-6, 2005.

[20] J.N. Fidalgo, J.A.P. Lopes, L.B. Almeida, V. Miranda, "Real Time Preventive Actions for Transient Stability Enhancement with a Hybrid Neural Network-Optimization Approach," *IEEE Transactions on Power Systems*, vol. Vol. 10(2), pp. pp. 1029-1035, 1995.

[21] Tony B. Nguyen and M. A. Pai, "Dynamic SecurityConstrained Rescheduling of Power Systems using Trajectory Sensitivities," *IEEE Transactions on Power Systems*, vol. Vol. 18(2), pp. pp. 848-854, 2003.

[22] Yuan WP, Chan KW, Liu MB. Li YH, "Coordinated Preventive Control of Transient Stability with MultiContingency in Power Systems using Trajectory Sensitivities," *Electrical Power and Energy Systems*, vol. Vol. 33(1), pp. pp. 147-53, 2011.

[23] A. Bose D. H. Kuo, "A Generation Rescheduling Method to Increase the Dynamic Security of Power Systems," *IEEE Transactions on Power Systems*, vol. Vol. 10 (1), pp. pp. 68-76, 1995.

[24] F.J., Ribbens-Pavella M. and Evans, "Direct methods for studying dynamics of large-scale electric powersystems—A survey," pp. Automatica, 21(1), 1–21, 1985.

[25] P. 1.Sarajcev, A. Kunac, G. Petrovic, and M. Despalatovic, "Power System Transient Stability Assessment Using Stacked Autoencoder and Voting Ensemble," *Energies*, vol. 14, 2021.

[26] Ed. Cham S. C. Savulescu, *Real-Time Stability in Power Systems*, 2nd ed.: Springer International Publishing, 2014.

[27] Y. Tada and H.-D. Chiang, "Design and Implementation of On-line Dynamic Security Assessment," *IEEJ TRANSACTIONS ON ELECTRICAL AND ELECTRONIC ENGINEERING*, vol. vol. 4, no. 3, pp. pp. 313–321, May 2009.

[28] C.-S. Wang, and Hua Li Chiang, "Development of BCU classifiers for on-line dynamic contingency screening of electric power systems," *IEEE Transactions on Power Systems*, vol. vol. 14, no. 2, pp. pp. 660–666, May 1999.

[29] A.Kurita, and K. Koyanagi Y. Tada, "BCU-guided time-domain method for energy margin calculation to improve BCU-DSA system," in *IEEE/PES Transmission and Distribution Conference and Exhibition*, vol. vol. 1. IEEE, 2002, pp. pp. 366–371.

[30] S. Likhate, V. Vittal, V. S. Kolluri, and S. Mandal K. Sun, "An Online Dynamic Security Assessment Scheme Using Phasor Measurements and Decision Trees," *IEEE Transactions on Power Systems* , vol. vol. 22, no. 4, pp. pp. 1935–1943, Nov. 2007.

[31] C. L. Bak, P. Thogersen, Z. Chen, C. Liu, K. Sun, and Z. H. Rathe P. Lund, "r A Systematic Approach for Dynamic Security Assessment and the Corresponding Preventive Control Scheme Based on Decision Trees," *IEEE Transactions on Power Systems*, vol. vol. 29, no.2, pp. pp. 717–730, 2014.

[32] V. Vittal, and J. Zhang M. He, "Online Dynamic Security Assessment With Missing PMU Measurements : A Data Mining Approach ," *Power Systems, IEEE Transactions on*, vol. vol. 28, no. 2, pp. pp. 1969–1977, 2013.

[33] U. D. Annakkage, B. Jayasekara, and B. Bagen A. Dissanayaka, "Risk-Based Dynamic Security Assessment," *IEEE Transactions on Power Systems* , vol. vol. 26, no. 3, pp. pp. 1302–1308, Aug. 2011.

[34] Miss Tingyan Guo, "On-line Identification of Power System Dynamic Signature Using PMU Measurements and Data Mining ," The University of Manchester, manchester, Thesis report May 2015.

[35] D. Ernst and D. Ruiz-Vega. M. Pavella, *Transient Stability of Power Systems: A Unified Approach to Assessment and Control*.: Kluwer Academic Publishers, 2000.

[36] Prem Kethavath, "Transient Stability Analysis for Power System Networks with Asynchronous Generation ," The University of Auckland, Thesis report 2015.

[37] J. Tilman G. Weckesser, "On-line Dynamic Security Assessment in Power Systems ," Department of Electrical Engineering Centre for Electric Power and Energy (CEE) , Technical University of Denmark, Thesis report 2014.

[38] Lei Tang, "Dynamic Security Assessment Processing System," Iowa State University , Ames, Iowa, Thesis report 2014.

[39] Michael Gerold Pertl, Johannes Tilman Gabriel Weckesser, Michel Maher Naguib Rezkalla, Kai Heussen, and Mattia Marinelli, "A Decision Support Tool for Transient Stability Preventive Control ," Technical University of Denmark, Thesis report 2017.

[40] Ayman Hoballah, "Power System Stability Assessment and Enhancement using Computational Intelligence ," Taif University, thesis report 2011.

[41] Yang Liu, "Solving Power System Differential Algebraic Equations Using Differential Transformation," 2019.

[42] E.R. El-Zahar, "Applications of Adaptive Multi Step Differential Transform Method to Singular Perturbation Problems Arising in Science and Engineering," *Appl. Math. Inf. Sci*, vol. 9, pp. 223–232,. 2015.

[43] G. Ahmet, M. Mehmet, and Y. Ahmet, "Adaptive multi-step differential transformation method to

solving nonlinear differential equations. ," *Math. Comp. Mod. Sci*, vol. 55, pp. 761–769, 2012.

[44] O.A. Bég, M. Keimanesh, M.M. Rashidi, M. Davoodi, and S.T. Branch, "Multi-step DTM Simulation of Magneto-Peristaltic Flow of a Conducting Williamson Viscoelastic Fluid.," *Int. J. Appl. Math Mech*, vol. 9, pp. 22–40, 2013.

[45] Roy billinton and Mahmud Fotuhi-Firuzabad, Saleh Aboreshaid, "Probabilistic Transient Stability Studies Using the Method of Bisection," *IEEE Transactions on Power Systems*, vol. vol. 11, no. 4, pp. pp. 1990–1995, Nov. 1996.

[46] P. Kundur and P. L. Dandeno, "Implementation of advanced generator models into power system stability programs," *IEEE Trans*, vol. Vol. PAS-102, pp. pp. 2047- 2052, July 1983.

[47] A. Bihain, J. Deuse and J. C. Baader, M. Stubbe, "STAG-A new unified software program for the study of the dynamic behavior of electrical power systems," *IEEE Trans*, vol. Vol. PWRS-4, No. 1, pp. pp. 129-138, 1989.

[48] J.J. Sanchez-Gasca, R. D'aquila, W.W. Price, and J.J. Paserba, "Variable time step, implicit integration for extended-term power system dynamic simulation," in *In Proceedings of the Power Industry Computer Applications Conference*, Salt Lake City, UT, USA, 7–12 May 1995.

[49] S. Kim and T. J. Overbye, "Optimal Subinterval Selection Approach for Power System Transient Stability Simulation," *Energies*, vol. vol. 8, pp. pp. 11871-11882, 2015.

[50] A.J.C. Laugier, "Adaptive Time Step for Fast Converging Dynamic Simulation System," in *In Proceedings of the IEEE/RSJ International Conference on Intelligent Robots and Systems*, vol. IROS '96, Osaka, Japan, 8 November 1996.

[51] M. A. Pai, "Energy Function Analysis for Power System Stability," 1989.

[52] K. Sun, C. Liu. B. Wang, "Fast power system Dynamic Simulation Using Continued Fractions," *IEEE Access*, vol. vol. 6, no. 1, pp. pp. 62687-62698, 2018.

[53] N. Duan, K. Sun, B. Wang, "A Time-Power Series Based Semi-Analytical Approach for Power System Simulation," *IEEE Trans. Power Syst.*, vol. vol. 34, No. 2, pp. pp. 841-851, March 2019.

[54] Kai Sun, Yang Liu, "Power System Time Domain Simulation Using a Differential Transformation Method ," Department of EECS, University of Tennessee, Knoxville, TN 37996 USA, Thesis report 2019.

[55] Teshome.L. Kumissa and F. Shewarega, "Fast Power System Transient Stability Simulation," *Energies*, vol. 16, 2023.

[56] G. Ahmet, M. Mehmet, and Y. Ahmet, "Adaptive multi-step differential transformation method to solving nonlinear differential equations. ," *Math. Comp. Mod. Sci.*, vol. 55, pp. 761–769, 2012.

[57] Peter W. Sauer, Vijay Vittal, Kevin L. Tomsovic, *Power System Stability and Control,* . London: Taylor and Francis Group, , 2006.

[58] Juan Manuel Gimenez Alvarez, "Critical Contingencies Ranking for Dynamic Security Assessment Using Neural Networks," in *Proceeding of Intelligent System Applications to Power Systems*, London, Nov. 2009, pp. 8 - 12.

[59] Kerin, E., Lerch, and G., Bizjak, U., "Power System Dynamic Security Inference Conceptual Solution," in *Proceeding of Power and Energy Society General Meeting* , Minneapolis, July 2010, pp. 25 - 29.

[60] J. Tilman G. Weckesser, "On-line Dynamic Security Assessment in Power Systems ," Department of Electrical Engineering Centre for Electric Power and Energy (CEE) , Technical University of Denmark, Thesis report. 2014.

[61] C. Fu. A. Bose, "Contingency ranking based on severity indices in Dynamic Security Assessment," *IEEE Trans. On Power Systems*, vol. Vol. 14. No. 3, pp. pp. 980-986, August 1999.

[62] S. Massucco, A. Pitto, F. Silvestro, S. Grillo, "Indices-based Voltage Stability Monitoring of the Italian HV Transmission System," in *Transmission & Distribution Conference and Exposition*, New Orleans, Louisiana, USA, April 19 – 22, 2010.

[63] S. Mandal, M. Y. Vaiman, M. M. Vaiman, , S. Lee, IEEE, and P. Hirsch V. Kolluri, "Fast Fault Screening Approach to As-sessing Transient Stability in Entergy's Power System," USA 2006.

[64] Ghadir Radman2 and Titus Oluwasuji Ajewole3 Waheed Ayinla Oyekanmi1, "Waheed Ayinla Oyekanmi1, Ghadir Radman2 and Titus Oluwasuji Ajewole3 Transient stability based dynamic security assessment indices".

[65] M. Pa, "i Energy Function Analysis for Power System Stability ," *Kluwer Academic Publishers*, 1989.

[66] V.G. K, N.V. Tomin, D.A. P. N.I. V, "Preventive and emergency control of intelligent power systems ," *IEEE PES Innovative Smart Grid Technologies* , Oct. 14-17 2012.

[67] C. Fu and A. Bose, "Contingency Ranking Based on Severity Indices in Dynamic Security Analysis," *IEEE Transaction on Power Systems*, vol. vol. 14, no. 3, p. pp. 980

[68] V. Vittal, G. C. Ejebe, G. D. Irisarri, J. Tong, G. Pieper, and M. McMullen V. Chadalavada, ",An On-Line Contingency Filtering Scheme for Dynamic Security Assessment," *IEEE Transaction on Power Systems*, vol. vol. 12, no. 1, pp. pp. 153–161, Feb 1997.

[69] S.-H. Kwon, J. Lee, H.-K. Nam, J.-B. Choo, and D.-H. Jeon, B. Lee, "Fast contingency screening for online transient stability monitoring and assessment of the KEPCO system," *IEEE Proc., Gener. Transm. Distrib*, vol. vol. 150, no. 4, pp. pp. 399-404, Jul 2003.

[70] Y. Xue and M. Pavella, ",Extended equal-area criterion: an analytical ultrafast method for transient stability assessment and preventive control of power systems," *International Journal of Electrical Power & Energy Systems*, vol. vol. 11, no. 2, pp. pp. 131–149.

[71] T. Huang, and F. Xue, Y. Xue, "Effective and Robust Case Screening for Transient Stability Assessment," *IREP Symposium* , no. Bulk Power System Dynamics and Control - IX Optimization,

Security and Control of the Emerging Power Grid., pp. pp. 1–8, 2013.

[72] P. Rousseaux, Z. Gao, L. Wehenkel, M. Pavella, R. Belhomme, E. Euxibie, and B. Heilbronn, Y. Xue, ""“Dynamic Extended Equal Area Criterion: ," *IEEE/NTUA Athens Power Tech Conference,* vol. vol. 71, no. 2, no. Part 1. Basic formulation, pp. pp.889-895, Sep. 1993.

[73] P. Rousseaux, Z. Gao, L. Wehenkel, M. Pavella, Y. Zhang, M. Trotignon, A. Duchamp, and B. Heilbronn Y. Xue, ", Dynamic Extended Equal Area Criterion," *IEEE/NTUA Athens Power Tech Conference*, no. Part 2. Embedding fast valving and automatic voltage regulation, pp. pp. 896-900.

[74] http://www.esat.kuleuven.be/electa/teaching/matdyn.

[75] (2017) MATLAB, T.M.I.2017b. The MathWorks Inc.

[76] R.D. Zimmerman, C.E. Murillo-Sanchez, and R.J. Thomas, "MATPOWER: Steady-State Operations, Planning, and Analysis Tools for Power Systems Research and Education. , ,.," *IEEE Trans. Power Syst.* , vol. 26, pp. 12–19, 2011.

[77] Teshome Lindi & Fekadu Shewarega, "Adaptive orderand step-size differential transformation method-based power system transientstability simulation," *Australian Journal of Electrical and Electronics Engineering*, Jun 2024.

[78] Ayman Hoballah and Istvan Erlich, "Generation coordination for transient stability enhancement using particle swarm optimization," *MEPCON’2008 IEEE*, March 2008.

[79] Peter W. Sauer and M. A. Pai, *POWER SYSTEM DYNAMICS*. Illinois, Urbana, 2006.

[80] D., Pavella, M. Ruiz-Vega, "A Comprehensive Approach to Transient Stability Control: Part I: Near Optimal Preventive Control, Part II: Open Loop Emergency Control," *IEEE Transactions on Power Systems*, vol. Vol.18, pp. pp.1446-1460, 2003.

[81] IEEE/CIGRE Joint Task Force, "Definition and classification of power system stability ," in *IEEE Transactions on Power Systems*, vol. Vol. 19 (2), 2004, pp. pp.1387-1401.

[82] K. R. Padiyar, *Power System Dynamics: Stability and Control,*. New York: Wiley, 1996.

[83] Pavella M., Wehenkel L, "Preventive vs. Emergency Control of Power Systems," in *IEEE/Power Energy Society Power Systems Conference & Exposition*, 2004, pp. pp. 1-6.

[84] A. Bose W. Li, "A Coherency Based Rescheduling Method for Dynamic Security," *IEEE Transactions on Power Systems*, vol. Vol.13 (3), pp. pp. 810-815, 1998.

[85] K. R. Niazi Kusum Verma, "A Coherency Based Generator Rescheduling for Preventive Control of Transient Stability in Power Systems," *Electrical Power and Energy Systems*, vol. Vol. 45 (1), pp. pp. 10-18, 2013.

[86] V.M.I. Genc, C.F. Kucuktezcan, "A New Dynamic Security Enhancement Method via Genetic Algorithms Integrated With Neural Network Based Tools," *Electric Power Systems Research*, vol.

Vol. 83, pp. pp. 1-8, 2012.

[87] K.S. Swarup, M. K. Maharana, "Graph Theoretic Approach for Preventive Control of Power Systems," *Electrical Power and Energy Systems*, vol. vol. 32 (4), pp. pp. 254-261, 2010.

[88] Y. J. Lin., "Prevention of Transient Instability Employing Rules Based on Back Propagation Based ANN for Series Compensation," *Electrical Power and Energy Systems*, vol. Vol. 3, pp. pp. 1776-1783, 2011.

[89] Yang X, Sun J, Yuan S, Zhang Y. Fang DZ, "An Optimal Generation Rescheduling Approach for Transient Stability Enhancement," *IEEE Transactions on Power Systems*, vol. Vol. 22(1), pp. pp. 386-394, 2007.

[90] M. Ehsan, R.Feuillet, N. HadjSaied, Kheradmandi, "Rescheduling of Power Systems Constrained with Transient Stability Limits in Restructured Power Systems," *Electric Power Systems Research*, vol. Vol. 81, pp. pp. 1-9, 2011.

[91] W. Sun, Z.Y. Xue, D.Z. Fang, "Optimal Generation Rescheduling With Sensitivity-Based Transient Stability Constraints," *IET Generation Transmission Distribution*, vol. Vol.4 (9, pp. pp.1044-1051, 2010.

[92] Z. Qu, H. Cai, X. Wang, D. Gan, "Methodology and Computer Package for Generation Rescheduling," *IEEE Proceedings Generation, Transmission & Distribution*, vol. Vol. 144(3), pp. pp. 301-307, 1997.

[93] D.J. Sobajic, Y.H. Pao, Djukanovic, "Neural Net Based Determination of Generator-Shedding Requirements in Electric Power Systems," *IEE ProceedingsC*, vol. Vol.139(5), pp. pp.427-436, 1992.

[94] R. Diao, V. Vittal, S. Kolluri, and S. Mandal, I. Genc, "Decision Tree-Based Preventive and Corrective Control Applications for Dynamic Security Enhancement in Power Systems," *IEEE Transactions on Power Systems*, vol. Vol. 25 (3), pp. pp. 1611-1619, 2010.

[95] N.D. Hatziargyriou, E.M. Voumvoulakis, "A Particle Swarm Optimization Method for Power System Dynamic Security Control," *IEEE Transactions on Power Systems*, vol. Vol. 25(2), pp. pp.1032-1041, 2010.

[96] T. V. Custem, F. Milano, A. J. Conejo, R. Minano, "Securing Transient Stability Using Time-Domain Simulations Within An Optimal Power Flow," *IEEE Transactions on Power Systems*, vol. Vol. 25(1), pp. pp. 243- 253, 2010.

[97] O.A. Bég, M. Keimanesh, M.M. Rashidi, M. Davoodi, and S.T. Branch, "Multi-step DTM Simulation of Magneto-Peristaltic Flow of a Conducting Williamson Viscoelastic Fluid.," *Int. J. Appl. Math Mech*, vol. 9, pp. 22–40., 2013.

[98] J. Kennedy and R.C Eberhart, "Particle swarm optimization," *IEEE International Conf*, vol. on Neural Networks, IV, pp. pp. 1942–1948, 1995.

[99] R. C. Eberhart and Y. Shi, "Comparing inertia weights and constriction factors in particle swarm

optimization," *IEEE Press*, no. 2000 Congress on Evolutionary Computation, pp. pp.84-88, 2000.

[100] T. K. Rasmussen, and T. Krink M. Lovbjerg, "Hybrid Particle Swarm Optimizer with Breeding and Subpopulations," in *The third Genetic and Evolutionary Computation Conference*, San Francisco, 2001, pp. pp.469-476.

[101] Louis A. Wehenkel, *Automatic Learning Techniques in Power System, ,*. Boston: Kluwer Academic Publishers, 1998.

[102] James A. Momoh and Mohamed E. El-Hawary, *Electric Systems, Dynamics, and Stability with Artificial Intelligence Applications*. Switzerland: Marcel Dekker, Inc., 2000.

energies

MDPI

Article

Fast Power System Transient Stability Simulation

Teshome Lindi Kumissa [1,*] and Fekadu Shewarega [2,*]

[1] Institute of Technology, School of Electrical and Computer Engineering (SECE), Hawassa University, Hawassa, Ethiopia
[2] Institutes of Electrical Power Systems, University of Duisburg-Essen, 47057 Duisburg, Germany
* Correspondence: teshomel@hu.edu.et (T.L.K.); fekadus@yahoo.com (F.S.); Tel.: +251-917824357 (T.L.K.)

Abstract: Power system transient stability simulation is of critical importance for utilities to assess dynamic security. Most of the commercially available tools use the traditional numerical integration method to simulate power system transient stability, which is computationally intensive and has low simulation speed. This makes it difficult to identify any insecure contingency before it happens. It is already proven that power system transient stability simulation achieved using the differential transformation method (DTM) requires less computational effort and has improved simulation speed, but it still requires further improvement regarding its accuracy and performance efficiency. This paper introduces a novel power system transient stability simulation method based on the adaptive step-size differential transformation method. Using the proposed method, the step size is varied based on the estimated local solution error at each time step. The accuracy and speed of the proposed simulation approach are investigated in comparison with the classical differential transformation method and the traditional numerical integration method using the IEEE 9 bus and 39 bus test systems. The simulation results reveal that the proposed method increases the simulation speed by 20–44.57% and 83–92% when compared with the classical DTM and traditional numerical-integration-based simulation methods, respectively. It is also proved that compared with the DTM-based simulation, the proposed method provides 45.27% to 58.85% and more than 90% accurate simulation results for IEEE 9 and IEEE 39 test systems, respectively. Therefore the proposed power system transient stability simulation method is faster and relatively more accurate and can be applied for online transient stability monitoring of power system networks.

Keywords: power system transient stability simulation; differential transformation method; adaptive step size

Citation: Kumissa, T.L.; Shewarega, F. Fast Power System Transient Stability Simulation. *Energies* **2023**, *16*, 7157. https://doi.org/10.3390/en16207157

Academic Editors: Alfeu J. Sguarezi Filho, Jen-Hao Teng, Kin-Cheong Sou and Lakshmanan Padmavathi

Received: 24 August 2023
Revised: 10 October 2023
Accepted: 16 October 2023
Published: 19 October 2023

1. Introduction

Modern society is very dependent on the availability of electric energy; therefore, reliable electricity supply is foundational to all economic and societal activities. To supply this continuously growing demand, the size and complexity of the power supply systems with stochastic generation (due to renewable energy systems) is increasing. This pushes power systems to operate more and more closely to stability limits [1]. The increase in the share of renewable energy system (RES) generations further results in the increased problem of reduced system inertia, which brings power systems to conditions of lower reliability, safety, and stability. This implies that stability, specifically transient stability, plays a significant role as an index of robustness of power systems, subject by its nature to faults and disturbances [2,3].

Transient stability is the ability of the power system after exposure to large disturbance to transit to a stable state [4]. Transient stability analysis investigates the dynamic behavior of a power system for several seconds following a large disturbance. Inability to detect system instability behavior in a sufficient time interval to launch the corrective actions could result in a system failure at one location on a system that can quickly degenerate to cascading failures, which is usually the mechanism for large collapses or blackout of the

system. Fast and accurate assessment of transient stability is of great significance for safe and stable operation of power systems.

To identify any unstable system condition before it happens, transient stability assessment is expected to be transitioned from offline or day-ahead studies to the online operation environment. Traditional methods of transient stability simulation rely on numerical integration, such as the Runge–Kutta or Euler techniques, to solve the differential algebraic equations governing power system dynamic behaviors. These solution methods, including implicit and explicit methods, are commonly used in commercial software packages with small enough integration steps of typically one to a few milliseconds to meet accuracy requirements [5]. However, these methods are computationally intensive, especially in large-scale systems with numerous contingencies. The power industry and the research community are seeking next-generation tools that are more powerful for power system online transient stability simulation.

Several previous works have been explored different aspects of transient stability analysis and simulation. For instance, ref. [6–8] used a coherency-based model reduction approach that aggregates a group of coherent generators in an equivalent generator, in which both the differential and algebraic equation models are simplified or reduced. Furthermore, to avoid solving nonlinear algebraic network equations separately from solving differential equations, many transient stability analysis and simulation tools assume all constant impedance loads and drive an ordinary differential equation model [6]. Such methods can result in substantial assessment and simulation errors. The parareal in time method by [9] involves parallel computers by decomposing a power system differential algebraic model or computation tasks to multiple processors to reduce simulation time. Similarly, the domain and multidecomposition methods by [10,11] involve parallel-computers-based computation tasks. But, still, the computation tasks are based on the traditional numerical algorithm to solve power system differential algebraic equations that require small enough integration steps and numerical iterations.

The semianalytical method proposed by [12–14] shifts some of the computation burdens from the online stage to the offline stage. In these methods, the offline drive approximates analytical solutions of differential equations for the purpose of online simulation. However, the network equations with power system differential algebraic model equations are still solved by traditional numerical iterations. The other semianalytical method proposed by [15,16], designed a differential transformation method (DTM)-based high-order semianalytical-based power system transient stability simulation scheme that allows significantly prolonged time steps to reduce simulation time compared to a traditional numerical approach. But this method assumes all loads as constant impedance so as to eliminate the network equations of a power system differential algebraic model and drive an ordinary differential equation model.

A variable time-step-based power system transient stability simulation was proposed by [17,18]. The integration time step control is performed based on the system behavior during the course of simulation. The method uses small time steps when the system variables are changing rapidly and large time steps when the system variables do not exhibit rapid variations. Solution error is estimated and the time step is adjusted to meet the specified tolerance threshold at each iteration step. This reduces the number of iterations and can also be used with more complex integration schemes. However, (1) at each iteration step, if the estimated solution error is greater than the specified tolerance threshold, the current solution is rejected and the solution procedures are repeated again using the new step size, which increases simulation time cost. (2) Still, algebraic equations are solved by iteration after each integration steps; this also has an impact on total simulation time cost.

An adaptive time step approach to dynamical simulation based on monitoring the conservation of energy was proposed by [19]. The method considers a physical object's velocity and positions error estimate to determine the next time step. Using this method, numerical stability and computational efficiency (speed) were improved when compared

with the traditional fixed-step numerical integration method. However, the method is independent of the system model equations describing its dynamic behaviors.

A differential transformation method (DTM)-based simulation algorithm proposed by [20], is fully analytical method. This method approximates the solution of complex power system differential algebraic model equations as a truncated power series of time. The approach is flexible in handling power system with any model detail without limitations. It also requires less computation effort and simulation time cost. However, differential transformation method gives a good approximation to the true solution in a very small region. To extend the region of solution convergence and improve accuracy of the results, DTM is applied at equal and fixed time interval as proposed by [21–24], up to the end of simulation period. In some cases, a very small sub division of interval is required with this method, which results in more computational effort and increased simulation time cost.

In this paper, an adaptive step size differential transformation method (AsDTM)-based power system transient stability simulation algorithm is proposed. This work introduces a novel step-size control algorithm based on local convergence error results at the end of each simulation time step by using the differential transformation method (DTM). The proposed novel power system transient stability simulation algorithm (1) is relatively robust and accurate, because it is flexible in handling power systems with any model detail and complexity without limitations; (2) improves simulation speed and accuracy based on control of local convergence error at each time step; (3) local solution error is estimated from only the last coefficient terms of the state and algebraic variables without any further calculations as in the variable step-size algorithm using traditional numerical integration methods; and (4) the solution obtained for the current simulation time step can be used during the next simulation time step without any limitations, such that the number of steps required to complete the transient stability simulation process reduces. These enable the proposed simulation scheme to be applied as an online transient stability simulation tool in small and medium-sized power systems.

The rest of the paper is organized as follows: Section 2 presents a description of the proposed method of power system transient stability simulation, Section 3 presents comparative analysis based on simulation results from the proposed method, traditional numerical integration method, and the classical DTM method, using IEEE test systems, and Section 4 presents conclusions and future work.

2. The Proposed Power System Transient Stability Simulation

2.1. Differential Transformation Method (DTM)

The differential transformation method (DTM) is a new emerging mathematical tool in power system analysis and simulation. The theory of the differential transformation method was originally established in [25] to derive approximate solutions of nonlinear differential equations and is defined below. Next, it was developed by researchers in the fields of mathematics and physics to obtain semianalytical solutions of various nonlinear dynamic systems. In [15,16,20–25], this method was examined for real-life complex network systems like power systems modeled by high-order nonlinear differential equations. DTM is defined as follows:

Definition: Consider a function x(t) of a real continuous variable t. The differential transformation (DT) of x(t) is defined by Equation (1), and the inverse DT of X(k) is defined by Equation (2), where k represents the order differential transformation (DT) [13–15].

$$\mathrm{X(k)} = \frac{1}{\mathrm{k!}}\left[\frac{\mathrm{d^k}x(t)}{dt^k}\right]_{\mathrm{(t=0)}} \tag{1}$$

$$x(t) = \sum_{k=1}^{\infty} X(k)t^k \tag{2}$$

The DT method provides various transformation rules for numerous generic functions [13–18], for both linear and nonlinear functions and for both simple and compositional functions, such that a differential equation in a continuous set about the variable t (time) is converted to a new set of difference equations in a discrete set about the variable k (the power series order) [25].

In power system simulation, DTM can be used as an explicit, fast, and robust solver of power system complex differential algebraic equations (DAEs). It is proved that the performance efficiency of a DTM is much better than that of the traditional numerical integration methods, because when using the DTM method, the iteration to solve algebraic equations after each integration step is eliminated and has a higher radius of convergence. To solve multimachine power system DAE models using the DTM method, the process is as follows: (1) transform power system DAE equations, (2) calculate the coefficients of state and algebraic variables, and (3) perform inverse transformation to determine state and algebraic variables as a function of time. Details of these procedures are presented in the following subsections.

2.2. Stability and Convergence Properties of the Proposed Method

In this paper, differential transformation method (DTM)-based fast power system transient stability simulation is introduced. In this subsection, the stability and convergence properties of the proposed method are demonstrated using the initial value problem.

Consider the following initial value problem, Equation (3), where $C \in R^m$ and $F : RxR^m \rightarrow R^m$:

$$\begin{aligned} &\tfrac{dy}{dt} = F(y(t), t),\ 0 \le t \le T, \\ &y(0) = c \end{aligned} \tag{3}$$

where y = (y_1, y_2, … y_n) and the interval [0, T] is partitioned into N subdomains with grid points expressed as t_0, t_1, …, t_{j-1}, t_j = T, such that $t_{j+1} = t_j + h$. Using the DTM solution approach, the first step is to determine the DTs of Equation (3), which is given as Equation (4) below, where K is the order of DT and m is the number of variables:

$$\begin{aligned} &Y_{m,n}(k) = \tfrac{1}{k}[F(k, t_n)] \\ &k = 0, 1, 2, \ldots, K \ \&\ n = 0, 1, 2, \ldots, N-1 \end{aligned} \tag{4}$$

By eliminating 1/k from the right side of Equation (4), we can rewrite it as Equation (5), where Y_{mn} and F are the transformed vector valued functions:

$$Y_{m,n}(k) = F(Y_{mn}(k-1), t_n) \tag{5}$$

As we can see from Equation (5) above, the coefficient terms $Y_{m,n}(k)$ can be explicitly determined from the lower-order coefficients terms recursively.

After all the coefficient terms from k = 0 up to k = K are known, the exact solution of Equation (3) at a point $t = t_{n+1} = t_n + h$ can be written in the form of Taylor expansion, considering m number of variables, as Equation (6), where h represents the step size:

$$y_m(t_{n+1}) = \sum_{k=0}^{\infty} Y_{mn}(k) h^k = \sum_{k=0}^{K} Y_{mn}(k) h^k + h\xi_n \tag{6}$$

where ξ_n is a local truncation error and n = 0, 1, 2, ... N − 1. The local truncation error can be expressed in the form of residual formula of Taylor series, considering m number of vectors of variable Y_n, and is expressed as Equation (7):

$$\begin{aligned} \xi_n &= Y_{mn}(k)h^k = h^k F(Y(k-1), t_c) \\ &= h^k \left[\frac{d^k f(y_m(t),t)}{dt^k}\right]_{t=t_c} \\ t_c &\in (t_n, t_{n+1}) \end{aligned} \tag{7}$$

This shows that the method approximates locally to the exact solution with order k. In this paper, the step size h is varied based on imposing the maximum of absolute value of the last coefficient terms to be lower than the admissible local error. This can be obtained by replacing ξ_n in Equation (7) by the admissible local error σ. Therefore, the new step size is calculated from Equation (8), where σ is the admissible local truncation error:

$$\begin{aligned} E &= \max|(Y_{mn}(k))| \\ \sigma &= Eh^k \rightarrow h_{new} = \left(\tfrac{\sigma}{E}\right)^{\frac{1}{k}} \leq h_{\max} \end{aligned} \tag{8}$$

To check the convergence properties of the proposed method, we need to have a bounded global error and thus know stability requirements of the method. Let us consider a linear system equation, Equation (9):

$$\frac{dy}{dt} = \mathrm{Ay(t)} + \mathrm{C(t)} \tag{9}$$

And let $\varepsilon_n = y(t_n) - y_n$ for n = 0, 1, 2,..., N. The DTM method for this equation yields the following discretization:

$$y_{n+1} = \sum_{k=0}^{K} Y_n(k)h^k \tag{10}$$

The DT of Equation (9) is given by Equation (11) by eliminating 1/k:

$$Y_{m,n}(k) = AY_{m,n}(k-1) + F(k-1) \tag{11}$$

where F(k) is DTs of C(t). With the recursive relation (11) the general term $Y_{m,n}(k)$ can be stated as Equation (12):

$$Y_{m,n}(k) = \frac{1}{k!}A^k Y_{m,n}(0) + \sum_{p=0}^{k-1} \frac{p!}{k!}F(p) \tag{12}$$

Subtracting Equation (10) from Equation (6) and using the general term (12) yields Equation (13):

$$\varepsilon_{n+1} = \sum_{k=0}^{k} \frac{1}{k!}A^k h^k \varepsilon_n + h\xi_n \tag{13}$$

where $\delta_n = h\xi_n$ and $\sum_{k=0}^{k} \frac{1}{k!}A^k h^k = e^{hA}$.

$$\varepsilon_{n+1} = e^{hA}\varepsilon_n + \delta_n \tag{14}$$

Note that the method is said to be consistent of order p if $\|\delta_n\| = O(h^{p+1})$. To relate global discretization error with the initial error ξ_0 and local discretization error, recursive relation (14) becomes Equation (15):

$$\varepsilon_n = e^{nhA}\xi_0 + \sum_{p=0}^{n-1} e^{(n-p-1)hA}\delta_p \tag{15}$$

Here, the stability of the method depends on the bound of the term e^{nhA} for all $(t_n + h) \leq T$. Therefore, considering the stability criterion $e^{nhA} \leq S$ (stability constant), for all $n \geq 0$ and $(t_n + h) \leq T$, the error norm bound is

$$\|\varepsilon_n\| \leq S\|\xi_0\| + S\sum_{p=0}^{n-1} \|\delta_p\| \tag{16}$$

Then, using the definition of local discretization error $\|\delta_p\| \leq Rh^k$ for all p and

$R = \max_{t\varepsilon[0,T]} \left(\left| \frac{dy^k(y(t),t)}{dt^k} \right| \right)$, and also assuming $y(0) = y_0$, leads to the following error norm inequality:

$$\begin{aligned} \|y(t_n) - y_n\| &\leq R^* h^k \\ R^* &= SRt_n \end{aligned} \tag{17}$$

for all n = 0, 1, 2, . . . N. Thus, whenever the exact solution is smooth and the stability criterion given above is satisfied, the proposed method converges to the exact solution.

2.3. Description of the Proposed Method

Power system transient stability simulation is one of the most critical functions of an online dynamic security assessment (DSA). Traditional numerical integration method is commonly used in commercially available power system transient stability simulation tools. Speed of computation remains the most critical challenge for its application in an online transient stability simulation. It was proved that the DTM-based transient stability simulation method reduces the impact of computation burden. For online application, the DTM-based simulation method still requires further improvement regarding its accuracy and performance efficiency. This paper focuses on developing a new and novel power system transient stability simulation algorithm that significantly improves simulation efficiency and accuracy.

For practical implementation of numerical methods of solving differential algebraic equations, the use of variable step-size length is a crucial issue because it allows us to automate the control of error. The proposed simulation method solves complex power system DAE models using the differential transformation method at variable time steps. The step size is varied based on the local truncation error control algorithm, as in Equation (8). The automatic controls of step-size length are performed based on the following principles:

- Reduce the time step length when the error is above the tolerable error limit, to improve the accuracy of simulation.
- Increase the time step length when the error is below the tolerable error limit, to avoid unnecessary computational burden and improve the overall efficiency.

Consider a power system with n bus and m machine DAE models in which generators are represented by a two-axis fourth-order model, all with a Type_1 excitation and voltage regulation system, as well as turbine/governor models, and all system loads are represented by constant impedance loads with both the network and stator algebraic equations represented by real matrices (expressed in rectangular form).

Consider also the state space representation of the power system DAE model equations as given by Equation (18), where x is the state vector, v is the vector of bus voltages, f represents a vector field determined by differential equations on dynamic devices such as synchronous generators and associated controllers, i is the vector valued function on current injections from all generators and load buses, and Y_{bus} is the network admittance matrix.

Figure 1 shows a flowchart of the proposed AsDTM-based transient stability simulation algorithm. In this subsection, each block of the proposed method of power system transient stability simulation will be described in more detail as follows:

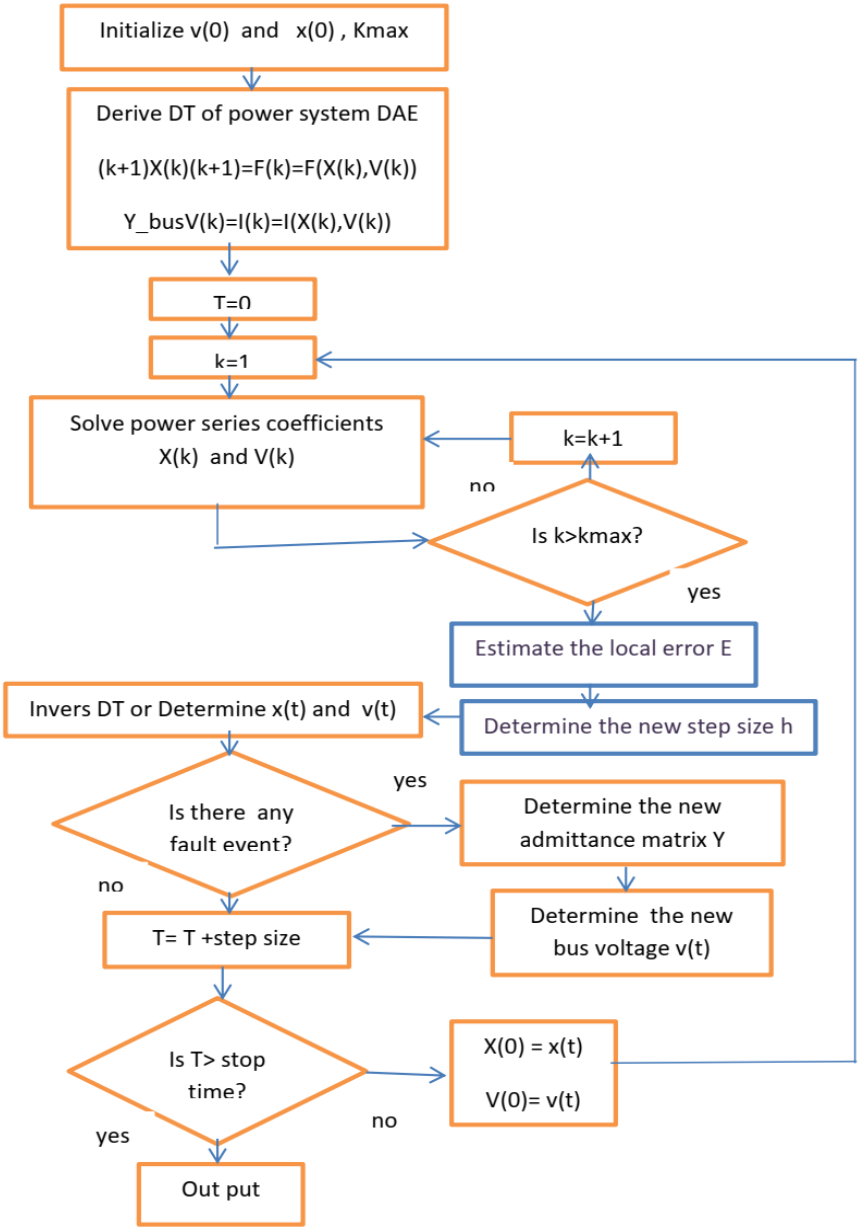

Figure 1. Flowchart of AsDTM-based fast power system transient stability simulation method.

$$\begin{aligned} \tfrac{dx_j}{dt} &= f(x_j, v_j) \\ Y_{bus} v_j &= i(x_j, v_j) \end{aligned} \tag{18}$$

where x(t) represents

$\delta_j(t), \omega_j(t), E'_{qj}(t), E'_{dj}(t), V_{rj}(t), V_{fj}(t), E_{fj}(t), P_{chj}(t),$ and $P_{svj}(t)$ and j = 1, 2, 3 . . . m, represent machine number.

Step 1. Derive DTs of power system DAEs:

Apply the differential transformation to functions given by Equation (18) on both sides, by using transformation to obtain Equation (19):

$$\begin{aligned} (k+1)X(k+1) &= F(X(m), V(m)), m = 0 \ldots k \quad \text{(a)} \\ Y_{bus} V(k) &= I(X(m), V(m)), m = 0 \ldots k \quad \text{(b)} \end{aligned} \tag{19}$$

where X represents $\delta_j, \omega_j, E'_{qj}, E'_{dj}, V_{rj}, V_{fj}, E_{fj}, P_{chj}$, and P_{svj}.

The vector valued function $i(x, v)$ in Equation (17) represents both generators and load current injections. But here, for this specific case, constant impedance loads are considered and are included in the network admittance matrix Y_{bus}. The differential transformation of the stator algebraic equation, Equation (20), can be derived and represented by Equation (22).

Let $y_a = \begin{pmatrix} r_a & -x'_q \\ x'_d & r_a \end{pmatrix}^{-1}$, $r = \begin{pmatrix} \sin\delta & \cos\delta \\ -\cos\delta & \sin\delta \end{pmatrix}$, $\tau = ry_a$, $\gamma = ry_a r'$, and the generator current injection equation is

$$\begin{bmatrix} I_x \\ I_y \end{bmatrix} = \left(\tau \begin{bmatrix} E'_d \\ E'_q \end{bmatrix} - \gamma \begin{bmatrix} V_x \\ V_y \end{bmatrix} \right) \tag{20}$$

Differential transformations of r, γ, and τ are given as

$$R(k) = \begin{pmatrix} \varphi(k) & \alpha(k) \\ -\alpha(k) & \varphi(k) \end{pmatrix} \tag{21}$$

where $\tau(k) = R(k)y_a$, $\gamma(k) = R(k)y_a R(k)'$.

Therefore, the differential transformation of the generator current injection equation is

$$\begin{bmatrix} I_x(k) \\ I_y(k) \end{bmatrix} = \left(\sum_{m=0}^{k} \tau(m) \begin{bmatrix} E'_d(k-m) \\ E'_q(k-m) \end{bmatrix} - \sum_{m=0}^{k} \gamma(m) \begin{bmatrix} V_x(k-m) \\ V_y(k-m) \end{bmatrix} \right) \tag{22}$$

The load current injection at each bus is represented by

$$\begin{bmatrix} I_x(k) \\ I_y(k) \end{bmatrix} = zeros(2,1) \tag{23}$$

Finally, DTs of the network algebraic equation are given as Equation (24):

$$\begin{bmatrix} I_{x1}(k) \\ I_{y1}(k) \\ \vdots \\ I_{xi(k)} \\ I_{yi}(k) \\ \vdots \\ I_{xN}(k) \\ I_{yN}(k) \end{bmatrix} = \begin{pmatrix} Y_{11} & \cdots & Y_{1i} & \cdots & Y_{1N} \\ \vdots & \ddots & \vdots & & \vdots \\ Y_{1i} & \cdots & Y_{ij} & \cdots & Y_{iN} \\ \vdots & & \vdots & \ddots & \vdots \\ Y_{N1} & \cdots & Y_{Nj} & \cdots & Y_{NN} \end{pmatrix} \begin{bmatrix} V_{x1}(k) \\ V_{y1}(k) \\ \vdots \\ V_{xi(k)} \\ V_{yi}(k) \\ \vdots \\ V_{xN}(k) \\ V_{yN}(k) \end{bmatrix} \quad I(k) = YV(k) \tag{24}$$

where $Y_{ij} = \begin{pmatrix} G_{ij} & -B_{ij} \\ B_{ij} & G_{ij} \end{pmatrix}$, $I(k) = \begin{bmatrix} I_{x1}(k) \\ I_{y1}(k) \\ \vdots \\ I_{xi(k)} \\ I_{yi}(k) \\ \vdots \\ I_{xN}(k) \\ I_{yN}(k) \end{bmatrix}$ $V(k) = \begin{bmatrix} V_{x1}(k) \\ V_{y1}(k) \\ \vdots \\ V_{xi(k)} \\ V_{yi}(k) \\ \vdots \\ V_{xN}(k) \\ V_{yN}(k) \end{bmatrix}$.

Step 2. Solve power series coefficients:

This step is initialized by the initial values of bus voltage V(0) and state variables X(0). The main task here is to solve power series coefficients X(k) and V(k) from the (k − 1)th-order coefficients, as indicated by the two circled numbers in Figure 2. Thus, any order coefficients are solvable from X(0),V(0).

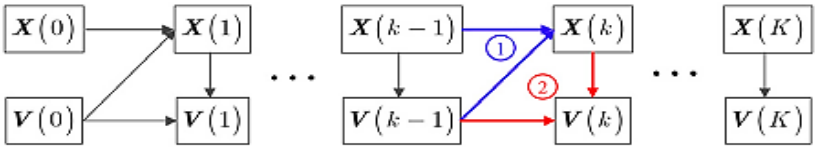

Figure 2. Recursive process to solve power series coefficients (source: [20]), where X(k) represents $\delta_j(k), \omega_j(k), E'_{qj}(k), E'_{dj}(k), V_{rj}(k), V_{fj}(k), E_{fj}(k), P_{chj}(k),$ and $P_{svj}(k)$ and j = 1, 2, 3 . . . m.

The coefficients of state variables X(k) for differential equations are derived from Equation (19a) recursively from X(1) up to X (k), as shown in Figure 2. But when solving the coefficients of algebraic variables, bus voltage V(k) is not straightforward since V(k) appears on both sides, as we can observe from Equation (19b). If ZIP load models are considered the current injunction equations for constant power, and constant current load portions of the ZIP load are nonlinear and will be turned into linear in terms of their coefficients, the proof is given by [20]. Since constant impedance load is considered in this paper, the DT of the generator current injection equation given by Equation (22) can be rewritten as Equation (25) below.

$$\begin{bmatrix} I_x(k) \\ I_y(k) \end{bmatrix} = \left(\sum_{m=0}^{k} \tau(m) \begin{bmatrix} E'_d(k-m) \\ E'_q(k-m) \end{bmatrix} - \sum_{m=1}^{k} \gamma(m) \begin{bmatrix} V_x(k-m) \\ V_y(k-m) \end{bmatrix} \right) - \gamma(0) \begin{bmatrix} V_x(k) \\ V_y(k) \end{bmatrix} \tag{25}$$

And let

$$\mathrm{B_g} = \sum_{\mathrm{m=0}}^{\mathrm{k}} \tau(m) \times \left[\frac{\mathrm{E'_d(k-m)}}{\mathrm{E'_q(k-m)}} \right] - \sum_{\mathrm{m=1}}^{\mathrm{k}} \gamma(\mathrm{m}) \times \left[\frac{V_{\mathrm{x}}(\mathrm{k-m})}{V_{\mathrm{y}}(\mathrm{k-m})} \right] \tag{26}$$

$$\begin{bmatrix} I_x(k) \\ I_y(k) \end{bmatrix} = A_g \begin{bmatrix} V_x(k) \\ V_y(k) \end{bmatrix} + B_g \; i.e \; I(k) = A_g V(k) + B_g \tag{27}$$

Since the load current injection is zero, letting A_l represent zeros (2,2), B_l represent zeros (2,1) at each of the n buses, $A = A_g + A_l$ & $B = B_g + B_l$ for machine buses, and $A = A_l$ & $B = B_l$ at (n − m) buses, then A represents (2 × n) by (2 × n) matrixes and B represents (2 × n) by 1 column vector. Therefore, the current injections into the network from all the buses can be

$$I(k) = AV(k) + B \tag{28}$$

where $I(k)$= $\begin{bmatrix} I_{x1}(k) \\ I_{y1}(k) \\ \vdots \\ I_{xi(k)} \\ I_{yi}(k) \\ \vdots \\ I_{xN}(k) \\ I_{yN}(k) \end{bmatrix}$ $V(k) = \begin{bmatrix} V_{x1}(k) \\ V_{y1}(k) \\ \vdots \\ V_{xi(k)} \\ V_{yi}(k) \\ \vdots \\ V_{xN}(k) \\ V_{yN}(k) \end{bmatrix}$.

The detailed derivation of matrix A and B for other types of load model is not the focus of this paper but it is available in [20]. Considering constant impedance loads, the coefficients of bus voltages V(k) for all the network buses and coefficients of state variables X(k) are solved from Equation (29) from a–c recursively from X(1) up to X(k) and V(1) up to V (k).

$$\begin{aligned} \mathrm{X(k)} &= \tfrac{1}{\mathrm{k}} \, \mathrm{F(X(m), V(m))}, \; \mathrm{m} = 0 \; \ldots \mathrm{k-1} && \text{(a)} \\ \mathrm{Y_{bus}} \; \mathrm{V} \; (\mathrm{k}) &= \mathrm{AV(k)} + \mathrm{B} && \text{(b)} \\ \mathrm{V(k)} &= (\mathrm{Y_{bus}} - \mathrm{A})^{-1} \, \mathrm{B} && \text{(c)} \end{aligned} \tag{29}$$

Step 3. Determine the new step size (h_{new}):

As described in the previous subsections, the proposed simulation method solves complex power system DAE models using the differential transformation method at variable time steps. The step size is varied based on the local truncation error control algorithm, as in Equation (8). The main term of this local truncation error is known in the form of $|Y(k)|t^k$ (see Equation (8) [22]), where t is the local time variable in subinterval $[t_m, t_{m+1}]$ and m is the number of subintervals between [0,T]. In this paper, the series term $|Y(k)|t^k$ is used as a local truncation error estimate of the power series of degree k. Therefore, without any further calculation, we can estimate the simulation step size that ensures the prescribed local admissible error by using just one of the coefficient terms [22,23]. The equation to calculate the step size (h) given by Equation (8) above is adopted and applied for power system transient stability simulation, as described below.

Let Mst, EXst, and TGst be matrix of generators, exciters, and turbine governor state variable, respectively. If m and N represent the number of machines and state variables, respectively, the size of each matrix is equal to m × N. Consider also the tolerable local solution error $\partial > 0$. The order of DTM, k, is given and fixed at the beginning of simulation. Therefore, since all order coefficient terms of state variables and all the network bus voltages are known at this stage, the new step size (h_{new}) will be determined as follows:

The admissible local solution error used. In this paper an admissible local solution error of $\partial = 10^{-6}$ per unit is considered. Therefore, we can calculate the new step size h using the following two steps:

1. Determine the maximum of absolute value of the last coefficient terms of all the variables as in Equation (30):

$$E = \max[\max(\max(|Mst(k)|), \max(\max(|EXst(k)|), \max(\max(|TGst(k)|), \max(|V(k)|)] \quad (30)$$

2. Next, evaluate the new step size h_{new} by using Equation (31):

$$h_{new} = \left(\left(\frac{\partial}{E}\right)^{\frac{1}{k}}\right) \leq \text{ max step size (hmax)} \quad (31)$$

Step 4. Inverse DT on X(k) and V(k).

Apply inverse DT to X(k) and V(k) to obtain the DTM-based solution of power system DEA in (32) a and b,

$$\begin{aligned} x_j(t) &= \sum_{m=0}^{k} X_j(m) {h_{new}}^m \quad \text{(a)} \\ v_j(t) &= \sum_{m=0}^{k} V_j(m) {h_{new}}^m \quad \text{(b)} \end{aligned} \quad (32)$$

where x(k) represents $\delta_j(k), \omega_j(k), E'_{qj}(k), E'_{dj}(k), V_{rj}(k), V_{fj}(k), E_{fj}(k), P_{chj}(k),$ and $P_{svj}(k)$.

Step 5. Check for disturbance or event, and if any, determine the new $(Y)_{matrix}$ and reinitialize bus voltages.

Step 6. Increment the simulation time t as $t_i + 1 = t_i + h_{new}$ (where i represents the number of time nodes, separated by the length of every time window).

Step 7. Using the time domain solutions x(t) and v(t) (step 4, above) as initial values of the state variables and bus voltages for the next simulation time window, respectively, repeat steps 2 to 6 until the end of the simulation period (T).

3. Case Studies and Results

3.1. Test System, Cases, and Setup

3.1.1. Test System

Two test systems are employed to validate the proposed online transient stability simulation approach. The first test system is the IEEE 9 bus system, which consists of nine bus and three machines. The second test system is the IEEE 39 bus system, which consists of 39 bus and 10 machines. The loads are modeled as constant impedances in the time

domain simulation. The generators are represented by a two-axis fourth-order model. They all have a Type_1 excitation and voltage regulation system as well as a turbine/governor model. Figure 3 shows the Single line diagrams of both test system. Dynamic data of all the machines with in both test cases are given in Appendix A.

3.1.2. Simulation Cases

For the purpose of testing the proposed power system transient stability simulation method, three-phase bus faults are simulated for both systems. Three-phase short-circuit faults at bus 1 for IEEE 9 bus and at bus 31 for 39 bus test systems are considered during simulation. A susceptance of 10^{-10} is enough to bring zero-impedance bus faults [26].

3.1.3. Simulation Setup

Simulations were carried out on a standard laptop with the following characteristics: Intel CTM i5-5200U CPU @ 2.20 GHz 2.20 GHz, 8 GB RAM, running on a 64-bit operating system, with a x64-based processor. The time domain simulations were carried out using the simulation tools/codes developed based on the proposed AsDTM on MATLAB R2017b [27]. MATPOWER 7.1 [28] version software was utilized. The CPU times included all steps of the simulation processes. MATPOWER is open-source power simulation software, used for power flow analysis and run on a MATLAB environment. This power system analysis software does not employ a graphical representation of a power system. Instead, the power system data were prepared in a table format specific to MATPOWER. Any functions of the MATPOWER can easily be accessed by functions developed on MATLAB editor. These include MATLAB functions that load and call for dynamic and static data file of simulation cases (case file), MATPOWER output interface functions, functions for initializing dynamic systems, model libraries for all dynamic systems, solver functions file (algorithms for computation), and functions for plotting simulation results. Power flow analysis was performed using MATPOWER.

3.2. Simulation Results and Discussion

For validating the proposed AsDTM-based power system transient stability simulation, three-phase short-circuit faults on bus 2 of IEEE 9 bus and on bus 31 of 39 bus test systems at 0.6 s and cleared after 0.2 s were simulated. In each case, the accuracy and performance of the proposed method was validated using the transient stability simulation results based on the traditional numerical method (fourth-order Range–Kutta (Rk4) with step size h = 0.001 s) and total time cost (time for TS simulation) as benchmarks. For this simulation purpose, differential transformation (DT) order k = 7 for IEEE 9 bus and k = 10 for 39 bus test systems were used with both DTM and AsDTM simulation methods.

Figure 4 shows the step-size variation of the AsDTM-based transient stability simulation under admissible local error of 10^{-6}. The step size varies adaptively between h_{min} = 0.00425 s and h_{max} = 0.2 s. The average step size h is equal to 0.01. For the DTM-based simulation, this average h = 0.01 was used as a fixed step size, shown in Figure 4.

From Figures 5a,b and 6a,b, we can observe the number of iterations and simulation time requirement relationships among AsDTM, DTM, and Rk4 simulation methods, respectively. The total number of iterations for simulating three-phase fault cleared after 0.2 s using Rk4, DTM, and AsDTM methods are 9995, 2345, and 1582 for the IEEE 9 bus test system and 9984, 3320, and 2260 for the IEEE 39 bus test system, respectively. Similarly, the total simulation time cost for the same case using Rk4, DTM, and AsDTM methods are 16.54 s, 2.331 s, and 1.292 s, for the IEEE 9 bus test system and 45.57 s, 9.614 s, and 7.692 for the IEEE 39 bus test system, respectively, from the simulation results shown in Figures 5 and 6.

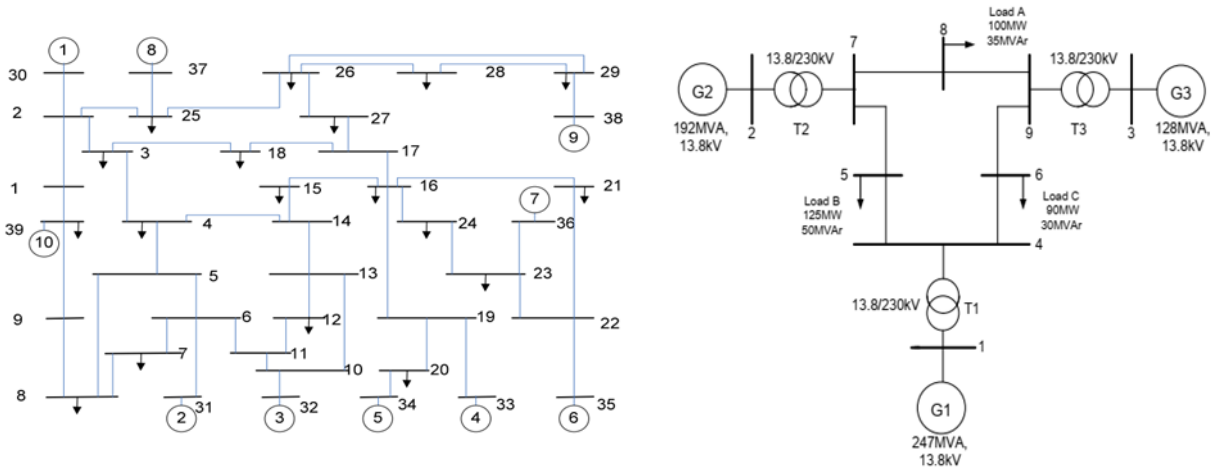

(**a**) (**b**)

Figure 3. One-line diagram of (**a**) New England 39 bus system; (**b**) IEEE 9 bus system [29].

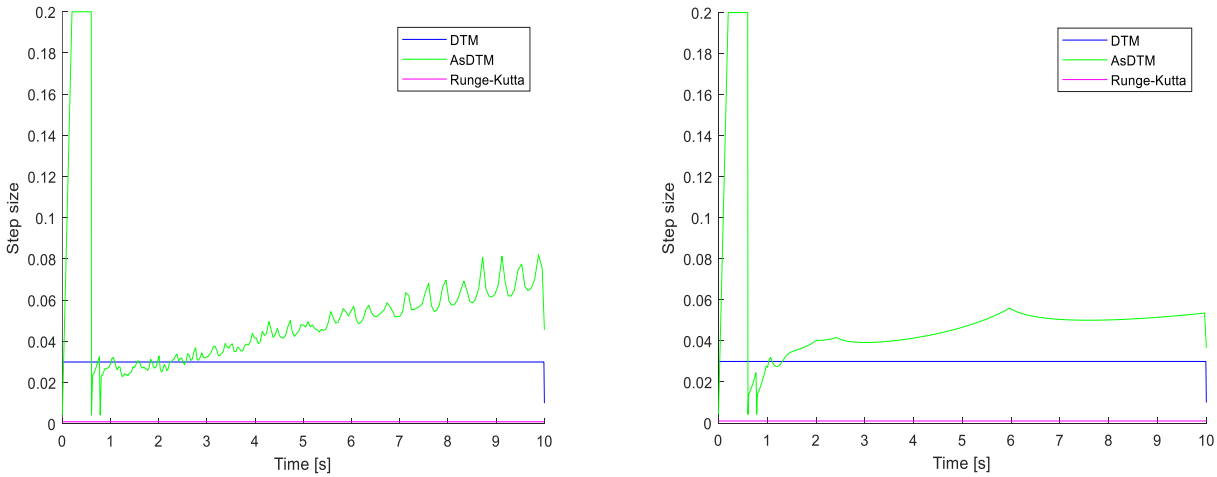

(**a**) (**b**)

Figure 4. Step-size variations during simulation for IEEE (**a**) 9 bus and (**b**) 39 bus test systems.

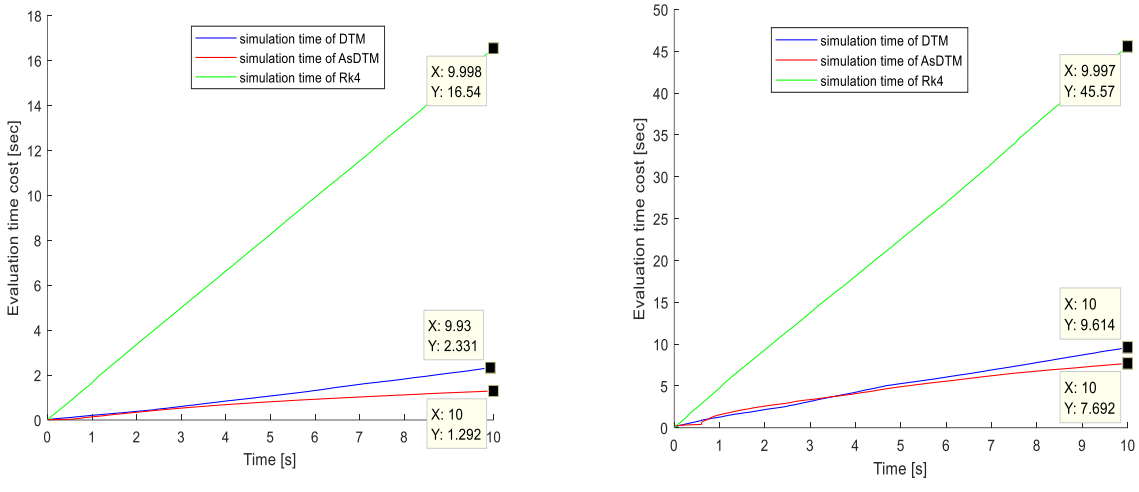

(**a**) (**b**)

Figure 5. Simulation time cost for IEEE (**a**) 9 bus and (**b**) 39 bus test systems.

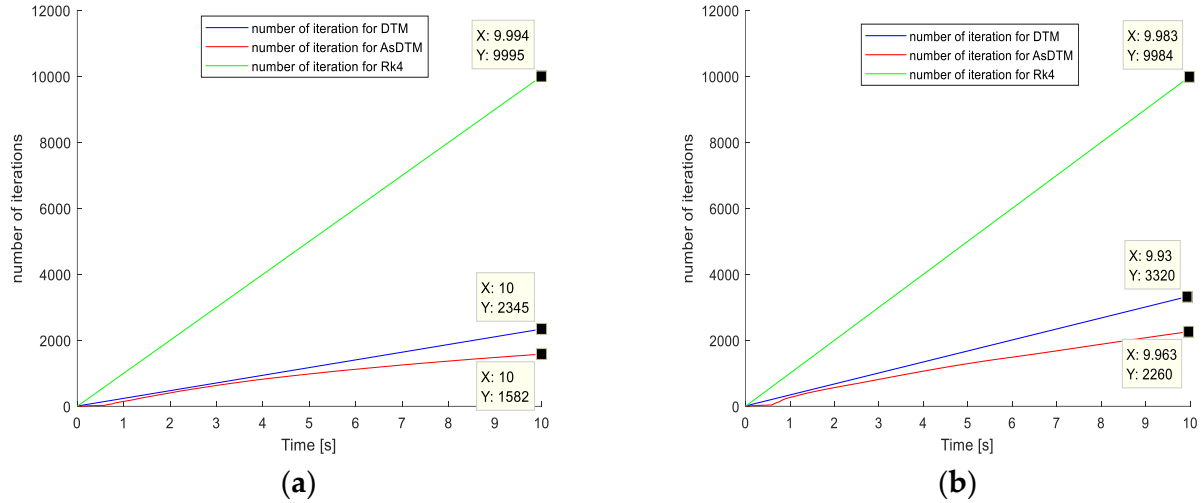

Figure 6. Number of iterations for IEEE (**a**) 9 bus and (**b**) 39 bus test systems.

- DTM-based simulation: The proposed AsDTM improved/reduced the total simulation time cost and total number of iterations by 20% and 31.93% for the IEEE 39 bus test system and improved/reduced the total simulation time cost and total number of iterations by 44.57% and 32.54% for the IEEE 9 bus test system, respectively.
- Rk4-based simulation: The proposed AsDTM improved/reduced the total simulation time cost and total number of iterations by 83% and 77.36% for the IEEE 39 bus test system and improved/reduced the total simulation time cost and total number of iterations by 92% and 84% for the IEEE 9 bus test system, respectively.

Therefore, we can conclude that the proposed AsDTM-based power system transient stability simulation method increases simulation speed by 20–44.57% and 83–92% when compared with the DTM- and Rk4-based simulations, respectively.

Figures 7a,b and 8a,b, show the rotor angle and speed errors simulation results. Error results relationships among AsDTM and DTM simulation methods are given in Table 1 below.

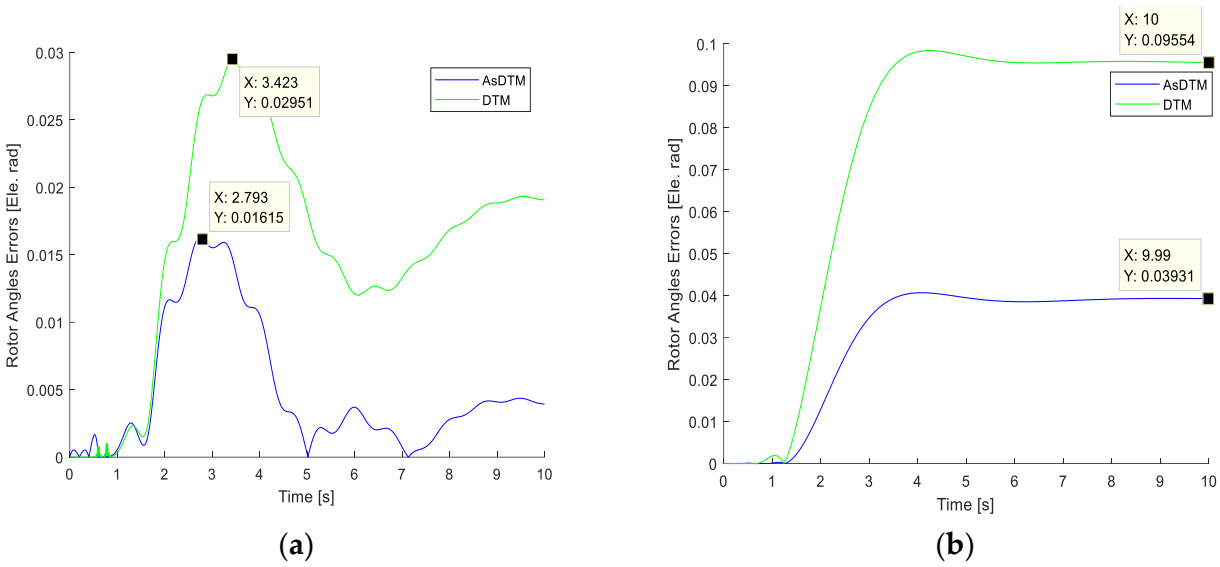

Figure 7. Rotor angle error for IEEE (**a**) 9 bus and (**b**) 39 bus test systems.

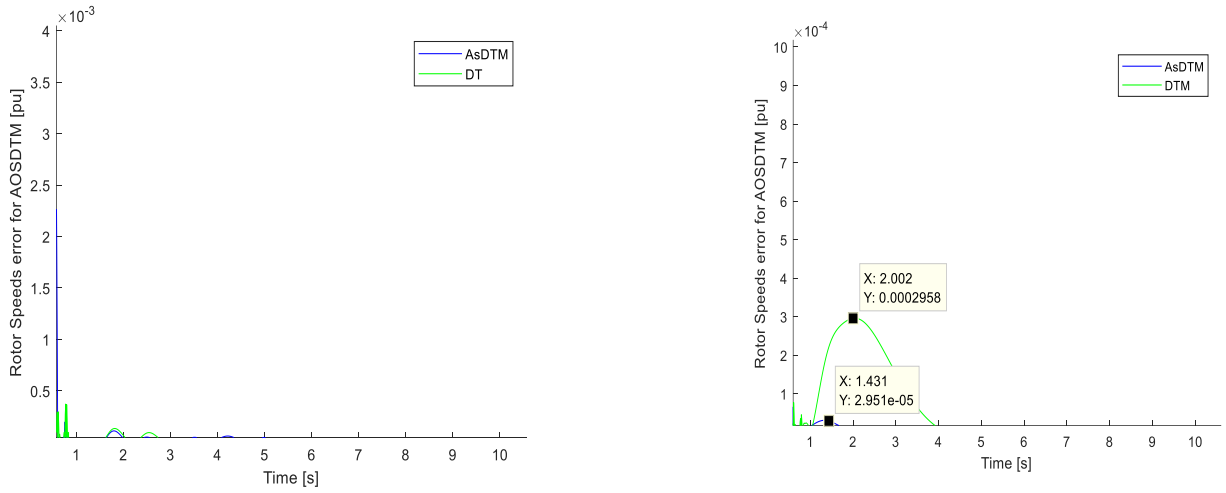

(**a**) (**b**)

Figure 8. Rotor speed error for IEEE (**a**) 9 bus and (**b**) 39 bus test systems.

Table 1. Rotor angle and speed errors simulation results relationships.

Method	Max Error			
	IEEE 9	IEEE 39	IEEE 9	IEEE 39
	Rotor Angle (rad)		Rotor Speed (pu)	
AsDTM	0.01615	0.03931	0.00005	0.00002951
DTM	0.02951	0.09554	0.0005	0.0002958

From the simulation results of Figures 7a,b and 8a,b and Table 1, compared with the DTM-based simulation, the proposed AsDTM-based power system transient stability simulation improves rotor angle error by 45.27% and 58.85% and improves rotor speed error by 90% for IEEE 9 and IEEE 39 test systems, respectively.

Figures 9a,b and 10a,b, represent the rotor angle and speed simulation results, where the quality of results obtained with AsDTM and DTM methods used the convergence criterion, the measure of which is the concurrency time of curves corresponding to two compared solutions. The best convergence was found for the AsDTM results. This implies that the AsDTM-based simulation gives more accurate results. However, since the shapes of the trajectories obtained by both DTM and AsDTM methods were the same as the reference trajectory obtained by the Rk4 method, we can conclude that both DTM and AsDTM methods are numerically stable.

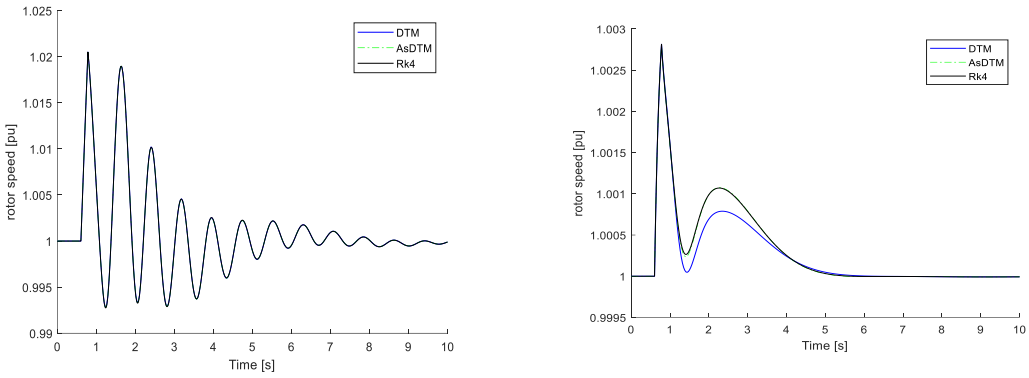

(**a**) (**b**)

Figure 9. Rotor speed simulation for IEEE (**a**) 9 bus and (**b**) 39 bus test systems.

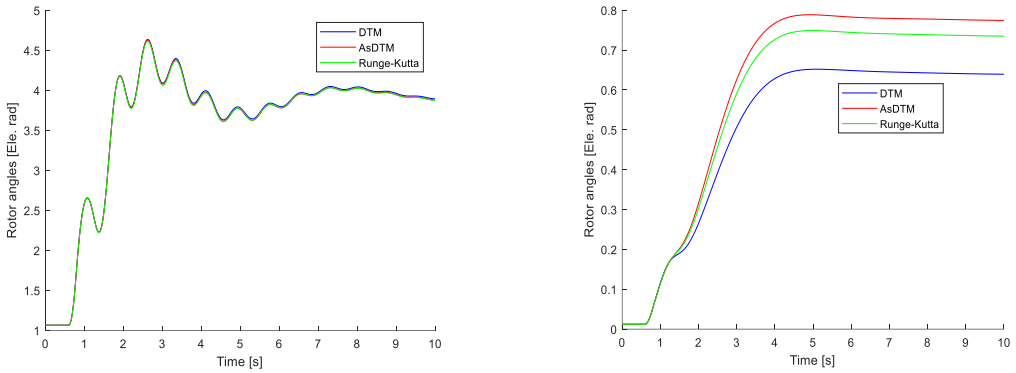

Figure 10. Rotor angle simulation for IEEE (**a**) 9 bus and (**b**) 39 bus test systems.

4. Conclusions and Future Work

In this paper, an AsDTM-based fast and accurate power system transient stability simulation is proposed. The validity of the method was proven successful by applying it to IEEE 3 machines 9 bus and New England 10 machines 39 bus test systems. The power system transient stability simulation results are presented in the figures for the given admissible local errors and fault locations. The results show that the method works successfully in handling the complex nonlinear power system differential algebraic equations with a reduced computation time cost and a wide interval of convergence.

As described in Section 4 above, the proposed approach improves the accuracy of simulation results by 45.27% to 58.85% and by 90% for IEEE 9 and IEEE 39 test systems, respectively, compared with the classical DTM. Furthermore, the proposed method also increases the simulation speed by 20–44.57% when compared with the classical DTM-based simulation. Therefore, by adaptively varying the step size of the differential transformation method, the speed and accuracy of the power system transient stability simulation is improved when compared with the classical DTM. Similarly, the simulation speed is improved significantly (by 83–92%) when compared with the traditional Rk4 simulation method. In general, the simulation results show that the proposed method is relatively accurate, fast, and efficient when compared with the classical fixed-step DTM-based simulation method. Therefore, we can conclude that the proposed method can be applied as an online transient stability simulation tool. Practical implementation of the proposed method in real-world power system operations is possible without any technical limitation, because the method is flexible enough to accommodate system models with any detail, and only requires the most recent snapshot from SCADA systems, generators, and their controllers' dynamic data.

Extending the approach for power system online contingency screening, which is the first stage of the online DSA session, will be our next focus of research.

Author Contributions: Conceptualization. methodology, software, formal analysis, investigation, resources, data curation, writing—original draft preparation, writing—review and editing, by T.L.K. Validation, visualization by T.L.K. and F.S. Supervision, project administration, by F.S. All authors have read and agreed to the published version of the manuscript.

Funding: This research received no external funding.

Data Availability Statement: All power flow data for the test cases are taken from Matpower software package cited in the reference. All dynamic data used for machines and their controllers given in the Appendix A Simulation codes are developed in Matlab 2017b environment.

Conflicts of Interest: The authors declare no conflict of interest.

Appendix A

IEEE 9 Bus and New England 39 Bus Test Systems Generators and their controller's Data.

Table A1. New England 39 bus test system generator data 1 [25].

Bus #	Xd	Xq	X'd	X'q	Rs	T'do	T'qo	H	Dg
30	0.1000	0.0690	0.0310	0.0690	0.0002	10.200	0.020	42.000	0.0535
31	0.2590	0.2820	0.0700	0.1700	0.0002	6.5600	1.5000	30.300	0.0194
32	0.2500	0.2370	0.0530	0.0880	0.0002	5.7000	1.5000	35.500	0.06783
33	0.2620	0.2580	0.0440	0.1660	0.0002	5.6900	1.5000	28.500	0.01815
34	0.6700	0.6200	0.1320	0.1660	0.0002	5.4000	0.4400	26.000	0.0331
35	0.2540	0.2410	0.0500	0.0810	0.0002	7.3000	0.4000	35.00	0.06783
36	0.2950	0.2920	0.0490	0.1860	0.0002	5.6600	1.5000	26.500	0.01815
37	0.2900	0.2800	0.0570	0.0910	0.0010	6.7000	0.4100	24.300	0.0331
38	0.2110	0.2050	0.0570	0.0590	0.0002	4.7900	1.9600	34.500	0.06783
39	0.0200	0.0190	0.0060	0.0080	0.0002	7.0000	0.7000	31.000	0.01940

Table A2. New England system generator controller's data [26].

Bus #	Ke	Te	Aexc	Bexc	Ur_max	Ur_min	Ka	Ta	Kf	Tf	Tch	Tg	Rg
30	1.0000	0.2500	0.0039	1.55	10	−10	20	0.06	0.04	1.0	0.1	0.05	0.05
31	1.0000	0.4100	0.0039	1.55	10	−10	20	0.05	0.06	0.5	0.1	0.05	0.05
32	1.0000	0.5000	0.0039	1.55	10	−10	20	0.06	0.08	1.0	0.1	0.05	0.05
33	1.0000	0.5000	0.0039	1.55	10	−10	20	0.06	0.08	1.0	0.1	0.05	0.05
34	1.0000	0.7900	0.0039	1.55	10	−10	20	0.02	0.03	1.0	0.1	0.05	0.05
35	1.0000	0.4700	0.0039	1.55	10	−10	20	0.02	0.08	1.25	0.1	0.05	0.05
36	1.0000	0.7300	0.0039	1.55	10	−10	20	0.02	0.03	1.0	0.1	0.05	0.05
37	1.0000	0.5300	0.0039	1.55	10	−10	20	0.02	0.09	1.26	0.1	0.05	0.05
38	1.0000	1.4000	0.0039	1.55	10	−10	20	0.02	0.03	1.0	0.1	0.05	0.05
39	0.0200	0.0190	0.0060	0.0080	0.0002	7.0	0.70	31.0	0.01940				

Table A3. IEEE 9 bus test system generator data.

Bus #	Xd	Xq	X'd	X'q	Rs	T'do	T'qo	H	Dg
1	0.146	0.0969	0.0608	0.0969	0.004	8.96	0.31	23.000	0.0151
2	0.8958	0.8648	0.1198	0.1969	0.0026	6.00	0.535	6.400	0.001
3	1.3125	1.2578	0.1813	0.25	0.0035	5.890	0.6	3.010	0.0058

Table A4. IEEE 9 bus test system generator controller's data.

Bus #	Ke	Te	Aexc	Bexc	Ur_max	Ur_min	Ka	Ta	Kf	Tf	Tch	Tg	Rg
1	1.0000	0.3140	0.0039	1.55	3	−3	20.0	0.20	0.0630	0.350	0.10	0.05	0.05
2	1.0000	0.3140	0.0039	1.55	3	−3	20.0	0.20	0.0630	0.350	0.1	0.05	0.05
3	1.0000	0.3140	0.0039	1.55	3	−3	20.0	0.20	0.0630	0.350	0.1	0.05	0.05

References

1. Sarajcev, P.; Kunac, A.; Petrovic, G.; Despalatovic, M. Power System Transient Stability Assessment Using Stacked Autoencoder and Voting Ensemble. *Energies* **2021**, *14*, 3148. [CrossRef]
2. Perilla, A.; Papadakis, S.; Rueda Torres, J.L.; van der Meijden, M.; Palensky, P.; Gonzalez-Longatt, F. Transient Stability Performance of Power Systems with High Share of Wind Generators Equipped with Power-Angle Modulation Controllers or Fast Local Voltage Controllers. *Energies* **2020**, *13*, 4205. [CrossRef]
3. Tina, G.M.; Maione, G.; Licciardello, S. Evaluation of Technical Solutions to Improve Transient Stability in Power Systems with Wind Power Generation. *Energies* **2022**, *15*, 7055. [CrossRef]
4. Kundur, P.; Paserba, J.; Ajjarapu, V.; Andersson, G.; Bose, A.; Canizares, C.; Vittal, V. IEEE/CIGRE Joint Task Force on Stability Terms and Definitions, Definition and Classification of Power System Stability. *IEEE Trans. Power Syst.* **2004**, *19*, 1387–1401.

5. Stott, B. Power system Dynamic response calculation. *Proc. IEEE* **1979**, *67*, 219–241. [CrossRef]
6. Chow, J.H. *Power System Coherency and Model Reduction*; Springer: New York, NY, USA, 2013.
7. Osipov, D.; Sun, K. Adaptive nonlinear model reduction for fast power system simulation. *IEEE Trans. Power Syst.* **2018**, *33*, 6746–6754. [CrossRef]
8. Milano, F. *Power System Modeling and Scripting*; Springer Science and Business Media: Berlin/Heidelberg, Germany, 2010.
9. Gurrala, G.; Dimitrovski, A.; Pannala, S.; Simunovic, S.; Starke, M. Parareal in Time for Fast Power System Dynamic Simulations. *IEEE Trans. Power Syst.* **2015**, *31*, 1820–1830. [CrossRef]
10. Zadkhast, S.; Jatskevich, J.; Vaahedi, E. A multi-decomposition approach for accelerated time domain simulation of transient stability problems. *IEEE Trans. Power Syst.* **2015**, *30*, 2301–2311. [CrossRef]
11. Aristidou, P.; Fabozzi, D.; Cutsem, T.V. Dynamic Simulation of Large Scale Power Systems Using a Parallel Schur-Compelement_Based Decomposition Method. *IEEE Trans. Parallel Distrib. Syst.* **2014**, *25*, 2561–2570. [CrossRef]
12. Liu, C.; Wang, B.; Sun, K. Fast power system simulation using semi-analytical solutions based on Pade approximation. In Proceedings of the 2017 IEEE Power & Energy Society General Meeting, Chicago, IL, USA, 16–20 July 2017; pp. 1–5.
13. Liu, C.; Wang, B.; Sun, K. Fast power system Dynamic Simulation Using Continued Fractions. *IEEE Access* **2018**, *6*, 62687–62698. [CrossRef]
14. Wang, B.; Duan, N.; Sun, K. A Time-Power Series Based Semi-Analytical Approach for Power System Simulation. *IEEE Trans. Power Syst.* **2019**, *34*, 841–851. [CrossRef]
15. Liu, Y.; Sun, K.; Yao, R.; Wang, B. Power System Time Domain Simulation Using a Differential Transformation Method. *IEEE Trans. Power Syst.* **2019**, *34*, 3739–3748. [CrossRef]
16. Liu, Y.; Sun, K. Power System Simulation Using a Differential Transformation Method. Ph.D. Thesis, University of Tennessee, Knoxville, TN, USA, 2022. Available online: https://trace.tennessee.edu/utk_graddiss/7073 (accessed on 28 August 2022).
17. Sanchez-Gasca, J.J.; D'aquila, R.; Price, W.W.; Paserba, J.J. Variable time step, implicit integration for extended-term power system dynamic simulation. In Proceedings of the Power Industry Computer Applications Conference, Salt Lake City, UT, USA, 7–12 May 1995. [CrossRef]
18. Kim, S.; Overbye, T.J. Optimal Subinterval Selection Approach for Power System Transient Stability Simulation. *Energies* **2015**, *8*, 11871–11882. [CrossRef]
19. Laugier, A.J.C. Adaptive Time Step for Fast Converging Dynamic Simulation System. In Proceedings of the IEEE/RSJ International Conference on Intelligent Robots and Systems, IROS '96, Osaka, Japan, 8 November 1996. [CrossRef]
20. Liu, Y.; Sun, K. Solving Power System Differential Algebraic Equations Using Differential Transformation. *IEEE Trans. Power Syst.* **2020**, *35*, 2289–2299. [CrossRef]
21. El-Zahar, E.R. An Adaptive Step-Size Taylor Series Based Method and Application to Nonlinear Biochemical Reaction Model. *Trends Appl. Sci. Res.* **2012**, *7*, 901–912.
22. El-Zahar, E.R. Applications of Adaptive Multi Step Differential Transform Method to Singular Perturbation Problems Arising in Science and Engineering. *Appl. Math. Inf. Sci.* **2015**, *9*, 223–232. [CrossRef]
23. Ahmet, G.; Mehmet, M.; Ahmet, Y. Adaptive multi-step differential transformation method to solving nonlinear differential equations. *Math. Comp. Mod. Sci.* **2012**, *55*, 761–769.
24. Bég, O.A.; Keimanesh, M.; Rashidi, M.M.; Davoodi, M.; Branch, S.T. Multi-step DTM Simulation of Magneto-Peristaltic Flow of a Conducting Williamson Viscoelastic Fluid. *Int. J. Appl. Math Mech.* **2013**, *9*, 22–40.
25. Pukhov, E.; Georgii, G. Differential transformation method and circuit theory. *Int. J. Circuit Theory Appl.* **1982**, *10*, 265–276. [CrossRef]
26. Available online: http://www.esat.kuleuven.be/electa/teaching/matdyn/ (accessed on 26 May 2020).
27. *MATLAB*, T.M.I.2017b; The MathWorks Inc.: Natick, MA, USA, 2017.
28. Zimmerman, R.D.; Murillo-Sanchez, C.E.; Thomas, R.J. MATPOWER: Steady-State Operations, Planning, and Analysis Tools for Power Systems Research and Education. *IEEE Trans. Power Syst.* **2011**, *26*, 12–19. [CrossRef]
29. Yang, D. *Power System Dynamic Security Analysis via Decoupled Time Domain Simulation and Trajectory Optimization*; Iowa State University: Ames, IA, USA, 2006.

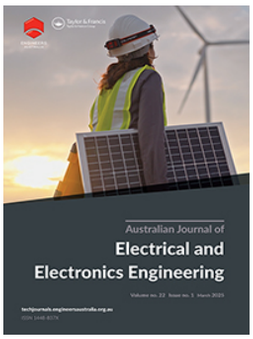

Taylor & Francis
Taylor & Francis Group

Australian Journal of Electrical and Electronics Engineering

ISSN: (Print) (Online) Journal homepage: www.tandfonline.com/journals/tele20

Adaptive order and step-size differential transformation method-based power system transient stability simulation

Teshome Lindi & Fekadu Shewarega

To cite this article: Teshome Lindi & Fekadu Shewarega (13 Jun 2024): Adaptive order and step-size differential transformation method-based power system transient stability simulation, Australian Journal of Electrical and Electronics Engineering, DOI: 10.1080/1448837X.2024.2359210

To link to this article: https://doi.org/10.1080/1448837X.2024.2359210

AUSTRALIAN JOURNAL OF ELECTRICAL AND ELECTRONICS ENGINEERING
https://doi.org/10.1080/1448837X.2024.2359210

Taylor & Francis
Taylor & Francis Group

RESEARCH ARTICLE

Adaptive order and step-size differential transformation method-based power system transient stability simulation

Teshome Lindi[a] and Fekadu Shewarega[b]

[a]School of Electrical and Computer Engineering (SECE), Hawassa University Institute of Technology, Hawassa, Ethiopia; [b]Institutes of Electrical Power Systems, University of Duisburg-Essen, Duisburg, Germany

ABSTRACT

Power system transient stability simulation is of critical importance for utilities to assess dynamic security. Most of the commercially available tools use traditional Forth order Rang-kutta (Rk4) method to simulate transient stability, which is computationally intensive. This made difficult to identify any insecure contingency before it happens. It is already proved that differential transformation method (DTM) requires less computational effort and has improved simulation speed. But, it still requires further improvement regarding its accuracy and performance efficiency. This paper introduces a novel power system transient stability simulation method based on adaptive order and step-size DTM. Using the proposed method, the order and step-size are varied based on the estimated local solution error at each time step. The accuracy and speed of the proposed simulation approach are investigated in comparison with classical DTM and Rk4method using IEEE 9 and 39-bus test systems. The simulation results reveal that the proposed method increases the simulation speed by 14–34% and 70–80% compared with the classical DTM and Rk4 based simulation, respectively. compared with the DTM-based simulation, the proposed method also provides 77.84% to 78.32% and more than 90% accurate simulation results for IEEE 9 and IEEE 39 bus test systems, respectively. Therefore, the proposed simulation method is faster and relatively accurate and can be applied for online transient stability monitoring power system network.

ARTICLE HISTORY
Received 22 July 2023
Accepted 19 May 2024

KEYWORDS
Power system transient stability simulation; differential transformation method; adaptive order & step-size; traditional numerical integration method; simulation speed & accuracy

SUBJECTS
Power & Energy engineering; Electrical and Electronic Engineering

1. Introduction

Modern society is very dependent on the availability of electric energy; therefore, reliable electricity supply is foundational to all economic and societal activities. To supply this continuously growing demand, the size and complexity of the power supply systems with stochastic generation (due to renewable energy systems (RESs)) is increasing. This pushes power systems to operate more and more closely to stability limits (Sarajcev et al. 2021). The increase in the share of RES generations further results in the increased problem of reduced system inertia, which brings power systems to conditions of lower reliability, safety, and stability. This implies that stability, specifically transient stability, plays a significant role as an index of robustness of power systems, subject by its nature to faults and disturbances (Perilla et al. 2020; Tina, Maione, and Licciardello 2022).

Transient stability is the ability of the power system after exposure to large disturbance to transit to a stable state (Kundur et al. 2004). Transient stability analysis investigates the dynamic behaviour of a power system for several seconds following a large disturbance. Inability to detect system instability behaviours in a sufficient time interval to launch the corrective actions could result in a system failure at one location on a system that can quickly degenerate to cascading failures, which is usually the mechanism for large collapses or blackout of the system. Fast and accurate assessment of transient stability is of great significance for safe and stable operation of power systems.

To identify any unstable system condition before it happens, transient stability assessment is expected to be transitioned from offline or day-ahead studies to the online operation environment. Traditional methods of transient stability simulation rely on numerical integration, such as the Runge – Kutta or Euler techniques, to solve the differential algebraic equations (DAEs) governing power system dynamic behaviours. These solution methods, including implicit and explicit methods, are commonly used in commercial software packages with small enough integration steps of typically one to a few milliseconds to meet accuracy requirements (Stott 1979). However, these methods are computationally intensive, especially in large-scale systems with numerous contingencies. The power system industry and the research community are seeking next-generation tools that are more powerful for power system online transient stability simulation.

Several previous works have been explored different aspects of transient stability analysis and

CONTACT Teshome Lindi teshelindi@gmail.com
Present affiliation for Teshome Lindi is Addis Ababa University, School of Electrical and Computer Engineering.
This article has been republished with minor changes. These changes do not impact the academic content of the article.

simulation. Generally, we can group them in to the following five categories: 1) model simplification, 2) parallel computing, 3) semi-analytical, 4) differential transformation methods (DTMs), and 5) variable or adaptive time step simulation. A coherency-based approach that aggregates a group of coherent generators in an equivalent generator, with simplified or reduced differential algebraic equation model is proposed by Chow (2013), Milano (2010), and Osipov and Sun (2018). Furthermore, to avoid solving nonlinear algebraic network equations separately from solving differential equations, many transient stability analysis and simulation tools assume all constant impedance loads and drive an ordinary differential equation model (Chow 2013). Such methods can result in substantial assessment and simulation errors.

The parareal in time method by Gurrala et al. (2015) involves parallel computers by decomposing a power system differential algebraic model or computation tasks to multiple processors to reduce simulation time. Similarly, the domain and multi-decomposition methods by Aristidou, Fabozzi, and Cutsem (2014) and Zadkhast, Jatskevich, and Vaahedi (2015) involve parallel-computers-based computation tasks. But still, the computation tasks are based on the traditional numerical algorithm to solve power system DAEs that require small enough integration steps and numerical iterations.

The semi-analytical method proposed by C. Liu, Wang, and Sun (2017, 2018) and Wang, Duan, and Sun (2019) shifts some of the computation burdens from the online stage to the offline stage. In these methods, the offline drive approximates analytical solutions of differential equations for the purpose of online simulation. However, the network equations with power system differential algebraic model equations are still solved by traditional numerical iterations. The other semi-analytical method proposed by Y. Liu and Sun(2022) and Y. Liu et al. (2019), designed DTM-based high-order semi-analytical power system transient stability simulation scheme that allows significantly prolonged time steps to reduce simulation time compared to a traditional numerical approach. But, this method assumes all loads as constant impedance so as to eliminate the network equations of a power system differential algebraic model and drive an ordinary differential equation model.

A variable time-step-based power system transient stability simulation was proposed by Kim and Overbye (2015) and Sanchez-Gasca et al. (1995). The integration time step control is performed based on the system behaviours during the course of simulation. The method uses small time steps when the system variables are changing rapidly and large time steps when the system variables do not exhibit rapid variations. Solution error is estimated and the time step is adjusted to meet the specified tolerance threshold at each iteration step. This reduces the number of iterations and can also be used with more complex integration schemes. However, (1) at each iteration step, if the estimated solution error is greater than the specified tolerance threshold, the current solution is rejected and the solution procedures are repeated again using the new step size, which increases simulation time cost. (2) Still, algebraic equations are solved by iteration after each integration steps; this also has an impact on total simulation time cost.

An adaptive time step approach to dynamical simulation based on monitoring the conservation of energy was proposed by Laugier (1996). The method considers a physical object's velocity and positions error estimate to determine the next time step. Using this method, numerical stability and computational efficiency (speed) were improved when compared with the traditional fixed-step numerical integration method. However, the method is independent of the system model equations describing its dynamic behaviours.

A DTM-based simulation algorithm proposed by Y. Liu and Sun (2020) is fully analytical method. This method approximates the solution of complex power system differential algebraic model equations as a truncated power series of time. The approach is flexible in handling power system with any model detail without limitations. It also requires less computation effort and simulation time cost. However, DTM gives a good approximation to the true solution in a very small region. To extend the region of solution convergence and improve accuracy of the results, DTM is applied at equal and fixed time interval as proposed by Ahmet, Mehmet, and Ahmet (2012), Bég et al. (2013) and El-Zahar (2012, 2015), up to the end of simulation period. In some cases, a very small subdivision of interval is required with this method, which results in more computational effort and increased simulation time cost.

In this work, an adaptive order and step-size differential transformation method (AOSDTM)-based power system transient stability simulation algorithm is proposed. A novel DT order and step-size control algorithms based on local convergence error results at the end of each simulation time step by using DTM is introduced in this paper. The proposed novel power system transient stability simulation algorithm (1) is relatively robust and accurate, because it is flexible in handling power systems with any model detail and complexity without limitations; (2) improves simulation speed and accuracy based on control of local convergence error at each simulation time step; (3) estimation of local solution error is only based on the last coefficient terms of the state and algebraic variables without any further calculations as in the variable step-size algorithm using traditional numerical integration methods; (4) the solution obtained for

the current simulation time step can be used during the next simulation time step without any limitations, consequently, the number of steps required to complete the transient stability simulation process reduces; and (5) the proposed simulation method can also handle the existing developed and validated generic models of large scale wind and PVs at the transmission level to perform simulation of combined conventional and renewable generation systems. These enable the proposed simulation scheme to be applied as an online transient stability simulation tool.

The rest of the paper is organised as follows: Section 2 describes the proposed power system transient stability simulation method; Section 3 validation of proposed simulation method, in comparison with traditional numerical integration method, and the classical DTM method is presented, using IEEE test systems; and Section 4 presents conclusions and future work.

2. The proposed fast power system transient stability simulation method

2.1. Differential transformation method

The theory of DTM is originally established in Pukhov and Georgii (1982) to derive approximate solutions of nonlinear differential equations and defined as follows.

Definition: Consider a function $\psi(t)$ of a real continuous variable t. The differential transformation (DT) of $\psi(t)$ is defined by Equation 1, and the inverse DT of $\psi(k)$ is defined by Equation 2, where k is the order.

$$\psi(k) = \frac{1}{k!}\left[\frac{d^k\psi(t)}{dt^k}\right]_{(t=0)} \tag{1}$$

$$\psi(t) = \sum_{k=1}^{\infty}\psi(k)t^k \tag{2}$$

Next,it is developed by researchers in the fields of mathematics and physics to obtain semi-analytical solutions of various nonlinear dynamic systems. In El-Zahar (2012), Y. Liu and Sun (2020, 2022), and Y. Liu et al. (2019), this method has been examined for real-life complex network systems like power systems modelled by high-order nonlinear differential equations.

DTM provides a set of transform rules. Some of these transform rules are listed below. Let $x(t)$, $y(t)$ and $z(t)$ are the original functions and X(k), Y(k) and Z(k) as their DTs, respectively, the following propositions hold, where c is a constant matrix, n is a nonnegative integer.

(a) $X(0) = x(0)$
(b) $y(t) = cx(t) \rightarrow Y(k) = cX(k)$
(c) $z(t) = x(t) \pm y(t) \rightarrow Z(k) = X(k) \pm Y(k)$
(d) $z(t) = x(t)y(t) \rightarrow Z(k) = \sum_{m=0}^{k} X(m)Y(k-m)$
(e) $Z(t) = \frac{y(t)}{h(t)}$ its DT
$$= \frac{1}{H(0)}\left(Y(k) - \sum_{m=0}^{k-1} H(k-m)Z(m)\right)$$
(f) $x(t)^T = X(k)^T$
(g) $dx/dt = (k+1)X(k+1)$ and if DT of $\sin\delta = \varphi(k)$ and DT of $\cos\delta = \alpha(k)$ then
(h) $\varphi(k) = \left(\sum_{m=0}^{k-1}\frac{k-m}{k}\alpha(m)\delta(k-m)\right)$
(i) $\alpha(k) = \left(-\sum_{m=0}^{k-1}\frac{k-m}{k}\varphi(m)\delta(k-m)\right)$

2.2. Description of the proposed method

Power system transient stability simulation is one of the most critical functions of an online dynamic security assessment (DSA). Traditional numerical integration method is commonly used in commercially available power system transient stability simulation tools. Speed of computation remains the most critical challenge for its application in an online transient stability simulation. It was proved that the DTM-based transient stability simulation method reduces the impact of computation burden. For online application, this method still requires further improvement regarding its accuracy and computation speed. This study focuses on investigating a new and novel power system transient stability simulation algorithm that significantly improves simulation speed and accuracy.

The proposed simulation method solves complex power system DAE models at variable DT order and step size using DTM. The automatic controls of DT order and step-size are performed based on the following principles:

- Reduce the time step length and increase the order of the DTM when the error is above upper threshold limit during power system dynamic simulation process, which improves the accuracy of simulation.
- Increase the time step length and decrease the order of the DTM when the error is below the lower threshold limit during power system dynamic simulation process, which can avoid unnecessary computation burden and improve the overall efficiency.

Figure 1 shows a flowchart of the proposed AOSDTM-based transient stability simulation algorithm. In this subsection, the proposed power system transient stability simulation method will be described step by step as follows:

Where $\psi_i(t)$ and $\psi_i(k)$ in Figure 1 denote state vector
$\delta(k), \omega(k), E_q'(k), E_d'(k), E_f(k), V_t(k), P_{CH}(k), P_{sv}(k), V_r(k), V_f(k) and \delta(t), \omega(t), E_q'(t), E_d'(t), E_f(t), V_t(t), P_{CH}(t), P_{sv}(t), V_r(t), V_f(t)$ respectively.
Consider n buses and m generators power system DAE model in which generators are represented by two-axis fourth-order model and all with **Type_1** excitation and voltage regulation system as well as turbine/governor models, all system loads are represented by constant impedance loads with both the network and stator algebraic equations are expressed in rectangular form. The state space representation of the complex power system DAE model equations are given by Equation 3, where ψ is the state vector, u is the vector of bus voltages, G represents a vector field determined by differential equations on dynamic devices such as synchronous generators and associated controllers, i is the vector valued function on current injections from all generators and load buses, and Y_{bus} is the network admittance matrix.

$$\begin{aligned} \frac{d\psi}{dt} &= G(\psi, u) \\ Y_{bus} u &= i(\psi, u) \end{aligned} \tag{3}$$

Where $\psi(t)$ represents & $\delta_i(t), \omega(t)_i E'_{qi}(t), E'_{di}(t), V, (t)$ $V_{fi}(t), P_{chi}(t), P_{svi}(t)$ and $E_{fi}(t) \& i = 1, 2, 3 \ldots \ldots$ m, represent machine number.

Step 1 Derive differential transforms of power system DAEs

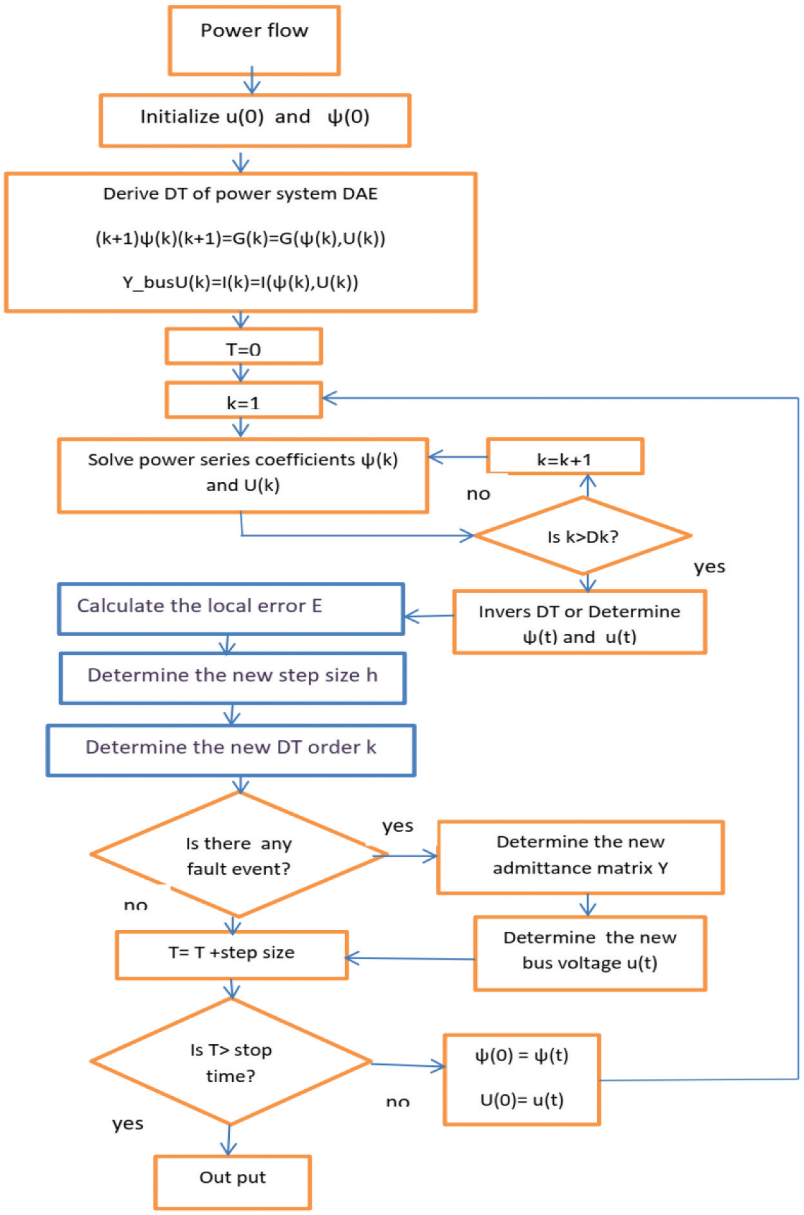

Figure 1. Flowchart of the proposed AOSDTM-based power system online transient stability simulation algorithm.

Apply the DT to functions given by Equation 3 on both sides, by using transformation rule **(g)**, to obtain Equation 4

$$\begin{aligned}(k+1)\psi(k+1) &= G(\psi(l),U(l)), l=0\ldots..k \quad (a)\\ Y_{bus}U(k) &= I(\psi(l),U(l)), l=0\ldots..k \quad (b)\end{aligned} \tag{4}$$

Whereψ *represent state variables* δ_i, ω_i, E'_{qi}, E'_{di}, E_{fi}, v_{ri}, v_{fi}, P_{chi}, *and* P_{svi}

The vector valued function $\boldsymbol{i}(\psi,\boldsymbol{u})$ in Equation 3 represents both generators and load current injections. But here, for this specific case, constant impedance loads are considered and it is included in network admittance matrix Y_{bus}. DT of stator algebraic equation can be derived as given below.

Let

$$y_a = \begin{pmatrix} r_a & -x'_q \\ x'_d & r_a \end{pmatrix}^{-1}, \rho = \begin{pmatrix} \sin\delta & \cos\delta \\ -\cos\delta & \sin\delta \end{pmatrix},$$

$\sigma = \rho y_a, \beta = \rho y_a \rho'$, and the generator current injection equation is given as Equation 5

$$\begin{bmatrix} I_x \\ I_y \end{bmatrix} = \left(\sigma \begin{bmatrix} E'_d \\ E'_q \end{bmatrix} - \beta \begin{bmatrix} U_x \\ U_y \end{bmatrix}\right) \tag{5}$$

Using transformation rule (h & i) DTs of ρ,β, and σ are given as:

$$\begin{aligned}\rho(k) &= \begin{pmatrix} \varphi(k) & \alpha(k) \\ -\alpha(k) & \varphi(k) \end{pmatrix}, \sigma(k) = \rho(k) y_a, \beta(k)\\ &= \rho(k) y_a \rho(k)'\end{aligned}$$

Similarly, using transformation rule **(d)**, DT of the generator current injection equation is

$$\begin{aligned}\begin{bmatrix} I_x(k) \\ I_y(k) \end{bmatrix} = &\left(\sum_{m=0}^{k} \sigma(m) \begin{bmatrix} E'_d(k-m) \\ E'_q(k-m) \end{bmatrix}\right.\\ &\left. - \sum_{m=0}^{k} \beta(m) \begin{bmatrix} U_x(k-m) \\ U_y(k-m) \end{bmatrix}\right)\end{aligned} \tag{6}$$

The load current injection at each bus is represented by

$$\begin{bmatrix} I_x(k) \\ I_y(k) \end{bmatrix} = zeros(2,1) \tag{7}$$

And finally, DTs of the network algebraic equations are

$$\begin{bmatrix} I_{x1}(k) \\ I_{y1}(k) \\ \vdots \\ I_{xi(k)} \\ I_{yi}(k) \\ \vdots \\ I_{xN}(k) \\ I_{yN}(k) \end{bmatrix} = \begin{pmatrix} Y_{11} & \cdots & Y_{1i} & \cdots & Y_{1N} \\ \vdots & \ddots & \vdots & & \vdots \\ Y_{1i} & \cdots & Y_{ij} & \cdots & Y_{iN} \\ \vdots & & \vdots & & \vdots \\ Y_{N1} & \cdots & Y_{Nj} & \cdots & Y_{NN} \end{pmatrix} \begin{bmatrix} U_{x1}(k) \\ U_{y1}(k) \\ \vdots \\ U_{xi(k)} \\ U_{yi}(k) \\ \vdots \\ U_{xN}(k) \\ U_{yN}(k) \end{bmatrix} I(k) = YU(k) \tag{8}$$

Where $i = 1, 2, 3 \ldots .N$, and I_{ix} & I_{iy} represent x and y component of bus i current, u_{ix} & u_{iy} represent x and y component of bus i voltage and

$$Y_{ij} = \begin{pmatrix} G_{ij} & -B_{ij} \\ B_{ij} & G_{ij} \end{pmatrix}, I(k) = \begin{bmatrix} I_{x1}(k) \\ I_{y1}(k) \\ \vdots \\ I_{xi(k)} \\ I_{yi}(k) \\ \vdots \\ I_{xN}(k) \\ I_{yN}(k) \end{bmatrix} U(k) = \begin{bmatrix} U_{x1}(k) \\ U_{y1}(k) \\ \vdots \\ U_{xi(k)} \\ U_{yi}(k) \\ \vdots \\ U_{xN}(k) \\ U_{yN}(k) \end{bmatrix}$$

Step 2 Solve power series coefficients

This step is initialised by the initial values of bus voltage U(0) and state variables ψ(0). The main task here is to solve power series coefficients $\boldsymbol{\psi}(k)$ and $\boldsymbol{U}(k)$ ($k \geq 1$) from the $(k\text{-}1)^{th}$ order coefficients, as indicated by two circled numbers in Figure 2. Thus, any order coefficients are solvable from $\boldsymbol{\psi}(0)$,$\boldsymbol{U}(0)$.

Where ψ(k) represent $\delta_i(k), \omega(k)_i, E'_{qi}(k), E'_{di}(k), E_{fi}(k), V, (k) V_{fi}(k), P_{chi}(k), and P_{svi}(k) \& i = 1, 2, 3 \ldots\ldots m$, represent machine number.

The coefficients of state variables ψ (k) for differential equations are derived from Equation 4 a recursively from ψ (1) up to ψ (k) as shown in Figure 2. But solving the coefficients of algebraic variables, bus voltage U(k) is not straightforward since U(k) appear on both sides as we can observe from Equation 4b. If ZIP load models are considered the current injunction equations for constant power and constant current load portions of the ZIP load are non-linear and these will be turned to linear in terms of their coefficients, its proof is given by Y. Liu and Sun (2020). Since constant impedance load is considered in this paper, the differential transforms of generator current injection given by Equation 8 can be rewritten as Equation below.

$$\begin{aligned}\begin{bmatrix} I_x(k) \\ I_y(k) \end{bmatrix} = &\left(\sum_{m=0}^{k} \sigma(m) \begin{bmatrix} E'_d(k-m) \\ E'_q(k-m) \end{bmatrix} - \sum_{k}^{\beta}(m) \begin{bmatrix} U_x(k-m) \\ U_y(k-m) \end{bmatrix}_{m=1}\right)\\ &- \beta(0) \begin{bmatrix} U_x(k) \\ U_y(k) \end{bmatrix}\end{aligned} \tag{9}$$

Let $B_g = \sum_{m=0}^{k} \sigma(m) * \begin{bmatrix} E'_q(k-m) \\ E'_q(k-m) \end{bmatrix} - \sum_{m=1}^{k} \beta(m)^* \begin{bmatrix} U_x(k-m) \\ U_y(k-m) \end{bmatrix} A_g = \beta(0)$

$$\begin{bmatrix} I_x(k) \\ I_y(k) \end{bmatrix} = A_g \begin{bmatrix} U_x(k) \\ U_y(k) \end{bmatrix} + B_g i.e I(k) = A_g U(k) + B_g \tag{10}$$

Since the load current injection is zero, let A_l represents zeros (2,2), B_l represents zeros (2,1) at each of the n buses, $A = A_g + A_l \& B = B_g + B_l$ for machine buses and $A = A_l \& B = B_l$ at (n-m) buses then A represents (2*n) by (2*n) matrices and B represents (2*n) by 1 column vector. Therefore the current injections in to the network from all the buses can be expressed as Equation 9 below.

$$I(k) = AU(k) + B \tag{11}$$

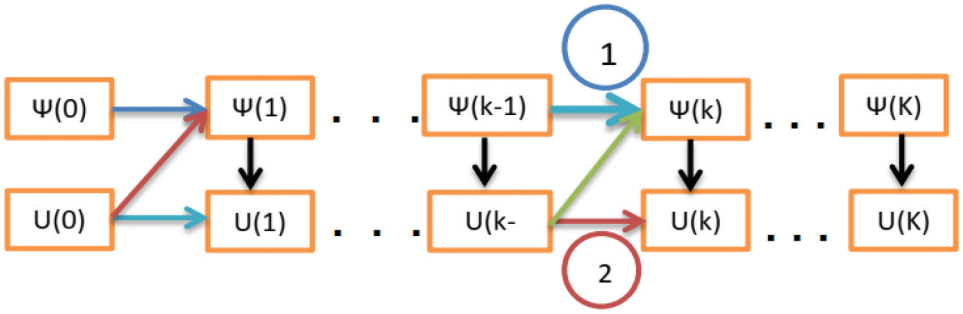

Figure 2. Recursive process to solve power series coefficients. Source: Y. Liu and Sun (2020).

Where

$$I(k) = \begin{bmatrix} I_{x1}(k) \\ I_{y1}(k) \\ \vdots \\ I_{xi(k)} \\ I_{yi}(k) \\ \vdots \\ I_{xN}(k) \\ I_{yN}(k) \end{bmatrix} \quad U(k) = \begin{bmatrix} U_{x1}(k) \\ U_{y1}(k) \\ \vdots \\ U_{xi(k)} \\ U_{yi}(k) \\ \vdots \\ U_{xN}(k) \\ U_{yN}(k) \end{bmatrix}$$

The detailed derivation of matrix A and B for other types of load model is not the focus of this paper but it is available in Y. Liu and Sun (2020). Considering constant impedance loads, the coefficients of bus voltages U(k) for all the network buses and coefficients of state variables ψ (k) are solved from Equation 10 from a-c recursively from ψ(1) up to ψ(k) and U(1) up to U (k).

$$\psi(k) = \frac{1}{k}\mathrm{G}(\psi(1), \mathrm{U}(1)), 1 = 0 \ldots .\mathrm{k} - 1 \quad \text{(a)}$$
$$\mathrm{Y\_busU(k)} = \mathrm{AU(k)} + \mathrm{B} \quad \text{(b)}$$
$$\mathrm{U(k)} = (\mathrm{Y\_bus} - \mathrm{A})^{-1}\mathrm{B} \quad \text{(c)} \quad (12)$$

Step 3 Inverse DT on ψ(k) and U(k)

Apply inverse DT to ψ(k) and U(k) to obtain the DTM-based solution of power system DEAs in (13) a&b., where ψ(k) and ψ(t) represent $\delta_i(\mathrm{k}), \omega(\mathrm{k})_i E'_{qi}(\mathrm{k}), E'_{di}(\mathrm{k}), V, (\mathrm{k}) V_{fi}(\mathrm{k}), P_{chi}(\mathrm{k}), P_{svi}(\mathrm{k})$ and $E_{fi}(\mathrm{k}) \& \delta_i(\mathrm{t}), \omega(\mathrm{t})_i E'_{qi}(\mathrm{t}), E'_{di}(\mathrm{t}), V, (\mathrm{t}) V_{fi}(\mathrm{t}), P_{chi}(\mathrm{t}), P_{svi}(\mathrm{t})$ and $E_{fi}(\mathrm{t})$*respectively*. & i = 1, 2, 3 . . . . . m, represent machine number.

$$\psi(t) = \sum_{m=0}^{k} \psi(m) t^m(a)$$
$$u(t) = \sum_{m=0}^{k} U(m) t^m(b) \quad (13)$$

Step 4 Evaluate the DT order and step-size

It was proved that DTM-based transient stability simulation method reduced the impact of computation burden on simulation speed. For online application, DTM-based simulation method still requires farther improvement regarding its computation speed. This paper focuses on developing new and novel power system transient stability simulation algorithm based on AOSDTM that significantly improves simulation efficiency and accuracy. Therefore, the proposed simulation method solves complex power system DAE models using the DTM at variable DT order and time steps.

The DT order and step size are varied based on the local truncation error control algorithm The main term of this local truncation error is known in the form of ψ(k) t^k (El-Zahar 2015), where t is the local time variable in subinterval $[t_m, t_{m+1}]$ and m is the number of subintervals between [0,T]. In this paper, the series term ψ(k) t^k is used as a local truncation error estimate of the power series of degree k. Therefore, without any further calculation, we can estimate the simulation step size that ensure the prescribed local admissible error limits by using just one of the coefficient terms (Ahmet, Mehmet, and Ahmet 2012; El-Zahar 2015). As investigated by Y. Liu and Sun (2022), the lowest order paired with the longest step size length leads to the largest error while the lowest error occurs at the highest order paired with the smallest step size length. Also, the error decreases rapidly with the increase of order when it is not too high. In this paper, DTM based power system transient stability simulation algorithm that adaptively changing both its order and step size based on estimated local solution error is developed.

Therefore, both DT order (k) and step-size length (h) can be changed based on estimated local error (E). Some parameters such as k_max = 20, k_min = 5, maximum and minimum DT order limit, respectively, the incremental to adjust the order of DT, dK = *1*, the upper tolerable error threshold value, $e_2 = 10^{-4}$, the lower tolerable error threshold value $e_1 = 10^{-8}$, minimum and maximum step size limit h_min = 0.00425 s, h_max = 0.2 s, and step-size adjustment factors $q_1 = 1.2$, $q_2 = 0.8$ are specifically used during simulation in this paper. Consider that Mst, EXst and TGst are matrix of machines, exciters and turbine governor state variable, respectively. If m and N represent the number of machines and state variables respectively, the size of each matrix is equal to ***m*** x ***N***. Therefore, the DT order and step size are adaptively determined as follows:

(1) Using the last coefficient terms of the state variables and bus voltages, estimate the local solution error, E

$$EE = \max[\max(\max(Mst(k)), \max(\max(EXst(k)), \max(\max(TGst(k)), \max(U(k))]E = EE * h^k \quad (14)$$

(2) Determine the next order and step-size

At the beginning of each simulation, time window local error E is estimated as described in previous sections. Therefore, if E<e_1, the new step-size and DT order for the next time window is determined by using Equation 12

$$k\_new = \max(k - dk, k\_\min)$$
$$h\_new = \min\left(q1^* \left(\frac{e_1}{EE}\right)^{\frac{1}{k}}, h\_min\right) \quad (15)$$

(3) If E > e_2, the new step-size and DT order for the next time window is determined by using Equation 13

$$k\_new = \min(k + dk, k\_\max)$$
$$h\_new = min\left(q_2^* \left(\frac{e_2}{EE}\right)^{\frac{1}{k}}, h\_max\right) \quad (16)$$

(4) If E is greater than the minimum tolerable local error threshold value (e_1) and less than the maximum tolerable local error threshold value (e_2), the order k and step size h will keep its current values during the next simulation time window.

Step 5 Checking for disturbance or event, determine the new Y_matrix and re-initialise bus voltages

In this step if there is any contingency event, the network admittance matrix is reconstructed and keeping the values of state variables, the network bus voltages are re-initialised.

The simulation process continues by incrementing the simulation time t as $t_i + 1 = t_i + h_$new. (where i represents the number of time nodes, separated by the length of every time window). The new time domain solutions x(t) and v(t) are used as initial values of the state variables and bus voltages for the next simulation time window, respectively, Therefore, solving coefficients, then applying inverse DT, determining the new DT order and step-size adaptively and checking for disturbance or event, are repeated at variable step size up to the end of simulation period, as shown in flowchart of Figure 1, in most cases, 5 to 10 s simulation period is required.

3. Case studies and results

3.1. Test system, cases and setup

3.1.1. Test system

Two test systems are employed to validate the proposed online transient stability simulation approach. The first test system is the IEEE 9-bus system, which consists of 9-bus and 3 machines. The second test system is the IEEE 39-bus system, which consists of 39-bus and 10 machines. The loads are modelled as constant impedances in the time domain simulation. The generators are represented by two axis fourth order model. They all have a Type_1 excitation and voltage regulation system as well as turbine/governor model. Figure 3 shows the Single line diagrams of both test system. Dynamic data of all the machines with in both test cases are given in Annex A.

3.1.2. Simulation cases

For the purpose of testing the proposed power system transient stability simulation method, three phase bus faults are simulated for both systems. Three phase short circuit fault at bus 1 for IEEE 9-bus and at bus 31 for 39-bus test systems are considered during simulation. A susceptance of 10^{-10} is enough to bring zero impedance bus faults.

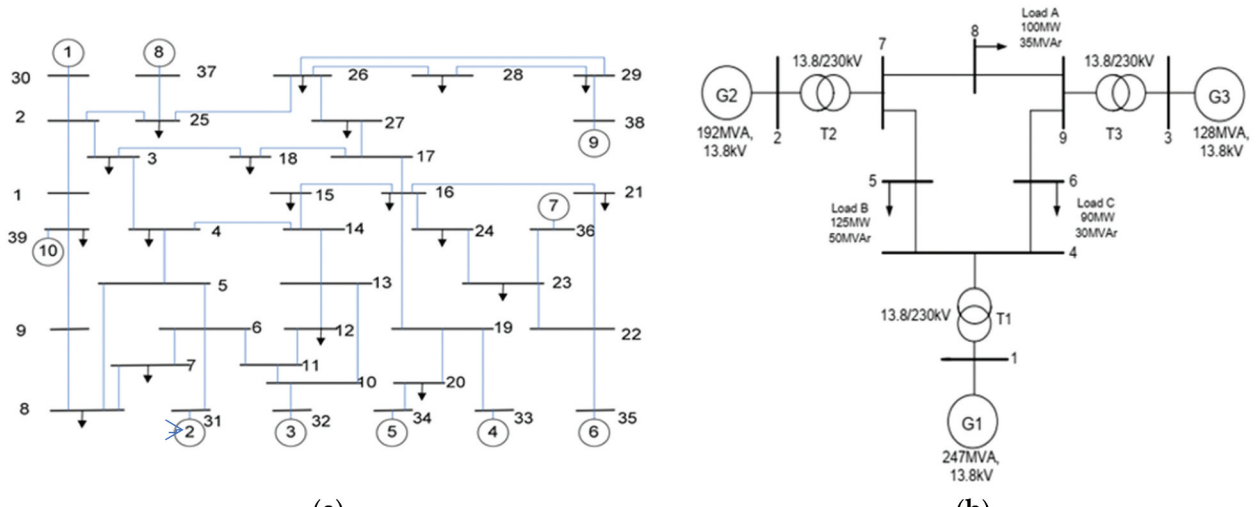

Figure 3. One-line diagram of (a) new england 3- bus system; (b) IEEE 9-bus system (Yang 2006).

3.1.3. Simulation setup

Simulations are carried out on standard laptop with the following characteristics: Intel(R) Core(TM) i5-5200 U CPU @ 2.20 GHz 2.20 GHz, 8GB RAM, running on 64-bit operating system, x64-based processor. The time domain simulations are carried out using the simulation tools/codes developed based on proposed AOSDTM on MATLAB R2017b (MATLAB, T.M. I.2017b 2017). MATPOWER 7.1 (Zimmerman, Murillo-Sanchez, and Thomas 2011) version software is utilised. The CPU times include all steps of the simulation processes. Matpower is open-source power simulation software, used for power flow analysis and run on a Matlab environment. This power system analysis software does not employ a graphical representation of a power system. Instead, the power system data is prepared in a table format specific to Matpower. Any functions of the Matpower can, easily, be accessed by functions developed on Matlab editor. These include Matlab functions that loads and call for dynamic and static data file of simulation cases (case file), Matpower output interface functions, functions for initialising dynamic system, model libraries for all dynamic systems, solver functions file (algorithms for computation), functions for plotting simulation results and others are developed on Matlab editor and power flow analysis is performed using Matpower.

3.2. Simulation results and discussion

For validating, the proposed AOSDTM-based power system transient stability simulation three-phase short circuit fault on bus 1 of IEEE 9 bus and on bus 31 of 39 bus test systems at 0.6 s and cleared after 0.2 s are simulated. In each case, the accuracy and simulation speed (performance efficiency) of the proposed AOSDTM based power system transient stability simulation is compared with the simulation results by using classical DTM and RK4. Simulation results by RK4 are used as a bench mark, since this method is already employed in commercially available stability analysis tools and also in use with an existing system, and Errors of DTM and AOSDTM methods are considered its differences from the benchmark result. The average step-size and DT order calculated from the variable step-size and order of AOSDTM based simulation results (from Figures 4 and5 below) is used for DTM based simulations, i.e. $h = 0.01$ and $k = 6$.

Figure 4 shows the variation in DT order during AOSDTM-based power system transient stability simulation and Figure 5(a) and (b) shows the relationship in step-size variation among AOSDTM-, DTM- and Rk4-based simulations in both cases. For AOSDTM-based simulation, DT order varies between $k\_min = 5$ and $k\_max = 10$ and the step-size varies adaptively between $h\_min = 0.00425$ s and $h\_max = 0.2$ s. The average order k and step-size h is equal 6 and 0.01, respectively. For the DTM-based simulation, these average k and h values are used as a fixed order and step-size as shown in Figure 4. An Rk4 method is used as a reference to compare the relative rotor angle and speed simulation errors by AOSDTM and DTM.

From Figures 6 and 7(a,b), we can observe that the number of iterations and simulation time requirement relationships among AOSDTM, DTM and Rk4 simulation methods, respectively. The total number of iterations for simulating 3 phase fault, cleared after 0.2 s, by using Rk4, DTM and AOSDTM methods are 9973, 5994 and 4180, for IEEE 9-bus test system and 9978, 6012 and 4885, for IEEE 39-bus test system, respectively. Similarly, the total simulation time cost required using Rk4, DTM and AOSDTM methods are 17.18, 5.178 and 3.377 s, for IEEE 9bus test system, and 42.38, 14.78 and 12.7s for IEEE 39-bus test system, respectively.

From the simulation results shown by Figure 5 up to 7 shown above, compared with:

- DTM-based simulation, the proposed AOSDTM improves/reduces the total simulation time cost and total number of iterations by 14.1% and

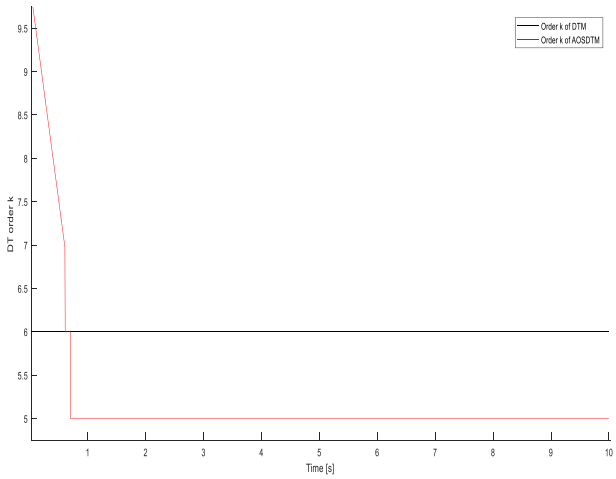

Figure 4. DT order variation during simulation for both cases.

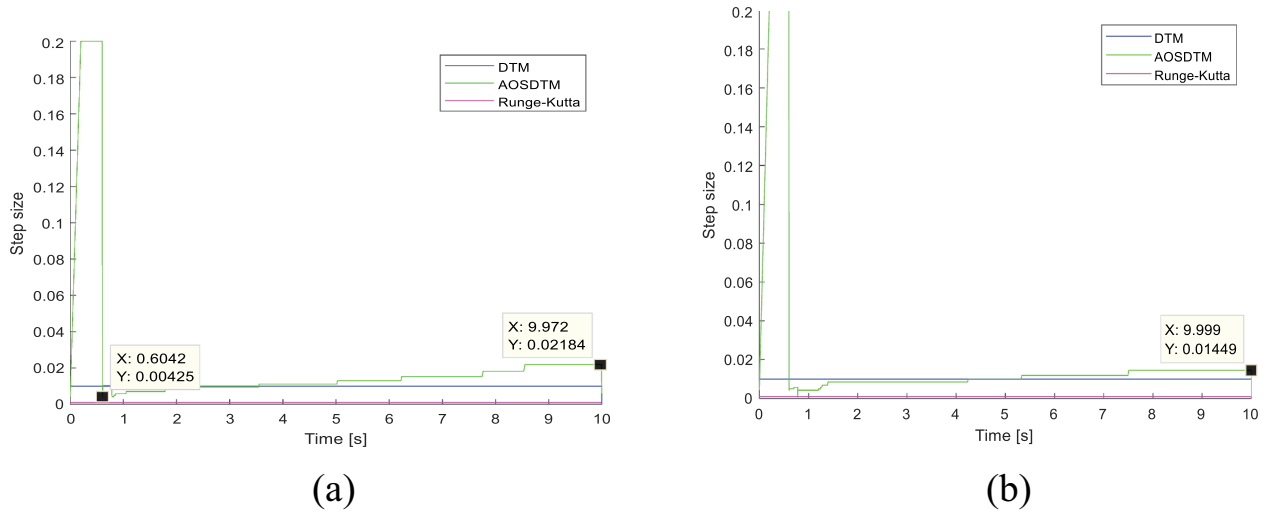

Figure 5. Step-size variations during simulation for IEEE (a) 9-bus and (b) 39-bus test system.

18.7% for IEEE 39-bus test system and improves/reduces the total simulation time cost and total number of iterations by 34.78% and 30.26% for IEEE 9-bus test system respectively.

- Rk4-based simulation, the proposed AOSDTM improves/reduces the total simulation time cost and total number of iterations by 70% and 51.04% for IEEE 39-bus test system and improves/reduces the total simulation time cost and total number of iterations by 80.34% and 58.08% for IEEE 9-bus test system respectively.

Therefore, we can conclude that the proposed AOSDTM-based power system transient stability simulation method increases simulation speed by 14–34% and 70–80% when compared with the DTM- and Rk4-based simulations, respectively.

Figures 8(a,b) and 9(a,b) show the rotor angle and speed errors simulation results. Error results relationships among AOSDTM and DTM simulation methods are given in Table 1.

From the simulation results of Figures 8a,b and 9(a,b) and Table 1, compared with the DTM-based simulation, the proposed AOSDTM-based power system transient stability simulation improves rotor angle error by 77.84% and 78.32% and improves rotor speed error by 90% for IEEE 9 and IEEE 39 test systems, respectively.

Figures 10(a,b) and Figure 11(a,b) represent the rotor angle and speed simulation results, where the quality of results obtained with AOSDTM and DTM methods used the convergence criterion, the measure of which is the concurrency time of curves corresponding to two compared solutions. The best convergence was found for the AOSDTM results. This implies that the AOSDTM-based simulation gives more accurate results. However, since the shapes of the trajectories obtained by both DTM and AOSDTM methods were the same as the reference trajectory obtained by the Rk4 method, we can conclude that both DTM and AOSDTM methods are numerically stable.

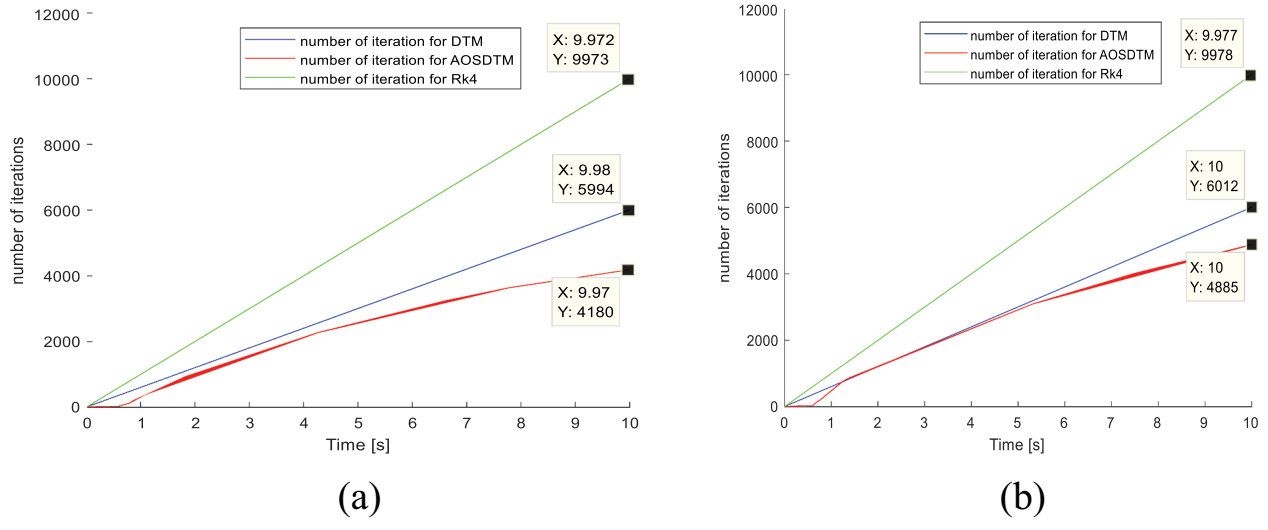

Figure 6. Number of iteration for IEEE (a) 9-bus and (b) 39-bus test system.

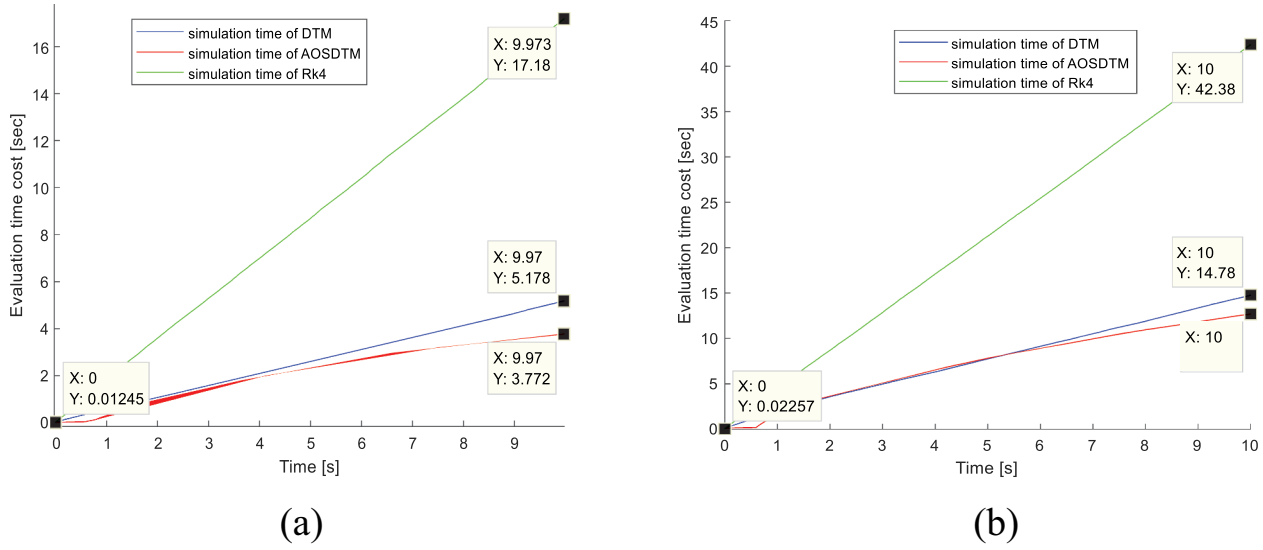

Figure 7. Simulation time cost for IEEE (a) 9-bus and (b) 39-bus test systems.

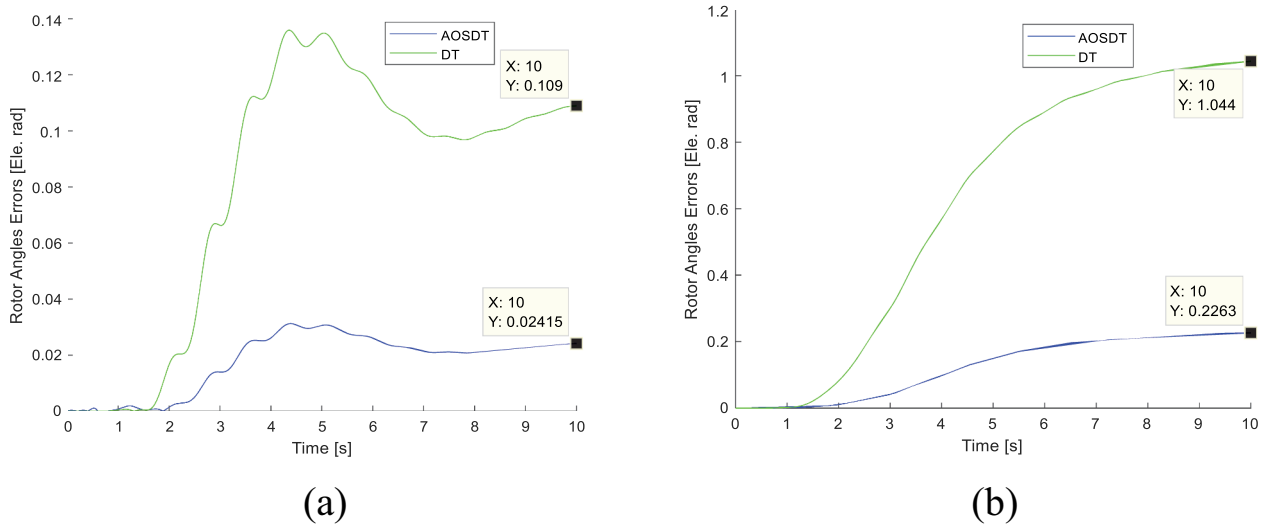

Figure 8. Rotor angle error for IEEE (a) 9-bus and (b) 39-bus test systems.

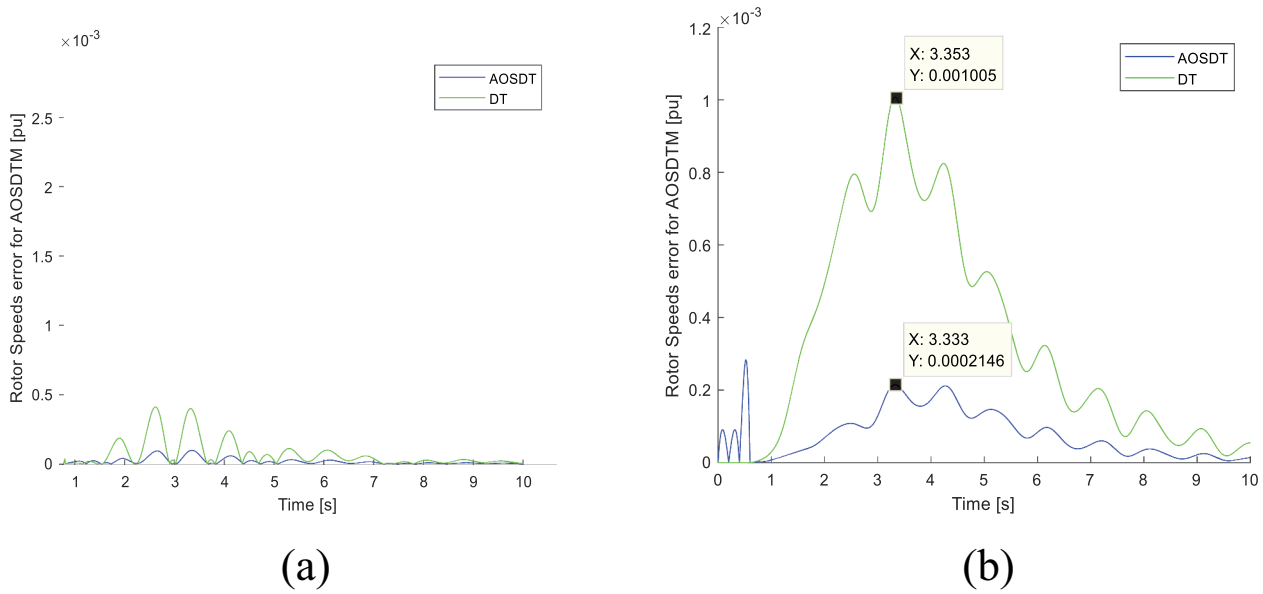

Figure 9. Rotor speed error for IEEE (a) 9-bus and (b) 39-bus test systems.

4. Conclusion and future work

In this paper, fast and accurate power system transient stability simulation based on AOSDTM is proposed. The validity of the method has been successful by applying it to IEEE 3 machines 9-bus and New England 10 machines 39-bus test systems. Power system transient stability simulation results are presented in figures for the given lower and upper threshold admissible local errors value and fault locations. The results show that the method works successfully in handling the complex non-linear power system DAEs with a minimum size of computations and a wide interval of convergence. The results show that the proposed method is an accurate, fast and efficient method for online transient stability simulation compared to classical fixed step DTM.

As described in section three above, the proposed approach improves the accuracy of simulation results by 77.84% to 78.32% and by 90% for IEEE 9 and IEEE 39 test systems, respectively, compared with the classical DTM simulation method. Furthermore, the proposed method also increases the simulation speed by 14–34% when compared with the classical DTM-based simulation. Therefore, by adaptively varying the step size and DT order of DTM the speed and accuracy of

Table 1. Rotor angle and speed errors simulation results relationships.

	Max Error			
	IEEE 9	IEEE 39	IEEE 9	IEEE 39
Method	Rotor angle (rad)		Rotor speed (pu)	
AOSDTM	0.02415	0.2263	0.00005	0.00021045
DTM	0.109	1.044	0.0005	0.001025

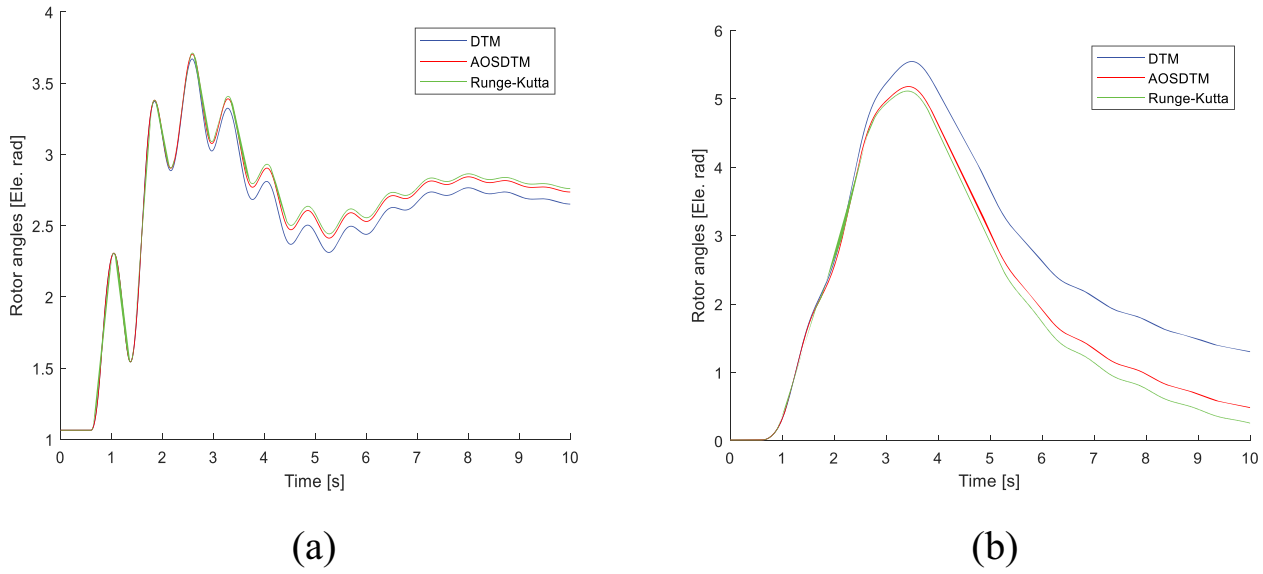

Figure 10. Rotor angle simulation for IEEE (a) 9-bus and (b) 39-bus test systems.

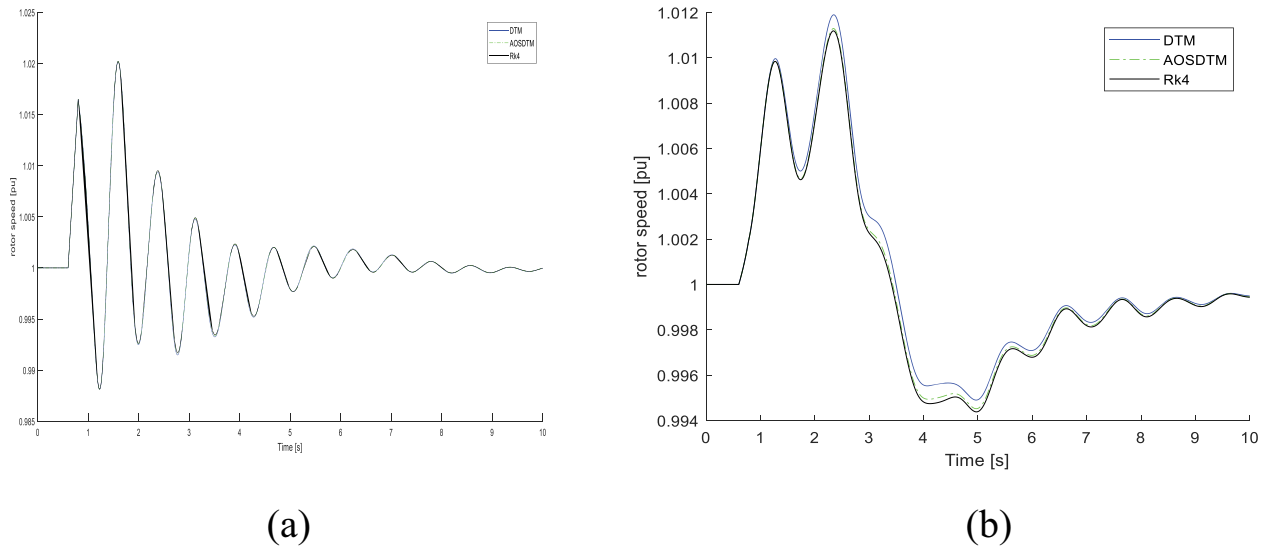

Figure 11. Angle simulation for IEEE (a) 9-bus and (b) 39-bus test systems.

power system transient stability simulation is improved when compared with the classical DTM and the simulation speed is improved significantly when compared with the traditional Rk4 simulation method (70–80%). Extending the approach for power system online contingency screening, which is the first stage of online DSA session, will be my next focus of research.

List of acronyms and symbols

AOSDTM	Adaptive order and step-size differential transformation method
CPU	Central processing unit
DAEs	Differential algebraic equations
DSA	Dynamic security assessment
DT	Differential transformation
DTM	Differential transformation method
E	Local error estimate
EE	Estimate of the maximum of power system state variable's & bus voltage's last order coefficient terms
GB	Giga bite
GHz	Giga hertz
RAM	Random access memory
RES	Renewable energy source
Rk4	Fourth Order Rangkuta
T	Simulation period
ZIP	Constant impedance, constant current, constant power Load
D	Damping constant
E'_d	D-axis machine internal voltage
E'_q	Q-axis machine internal voltage
E_{fd}	Field excitation voltage
H	Machine inertia constant
I_d	d-axis stator current
Iq	q-axis stator current
KA	Amplifier gain
K_E	Exciter constant
P	Active power
P_C	Speed governor input power setting
P_{CH}	Output power of steam chest
P_{SV}	Output power of steam valve
Q	Reactive power
R_f	Rate feedback in exciter
R_D	Speed regulation quantity (droop)
S	Complex power
S_E	Saturation constant
T_M	Mechanical torque
t	Time
U	Bus voltage
V_R	Exciter input
V_{ref}	Input reference voltage
X	Reactance
Y	Admittance
Z	Impedance
θ	Bus voltage angle
ω	Angular speed
Tg	Governor time constant
ω_s	Nominal angular speed
ψ	Time domain state variables
xd′	d-axis transient reactance
xq′	q-axis transient reactance
xd	d-axis steady state reactance
xq	q-axis steady state reactance
Tq′0	Stator transient q-axis time constant
Td′0	Stator transient d-axis time constant
Rs	Stator resistance
Rg	Droop
δ	Machine rotor angle
RES	Renewable energy system
PV	Photovoltaic
TS	Transient stability
Vf	Exciter feedback voltage
X	Transformed (k integer domain) state variables
Vt	Exciter terminal voltage

Disclosure statement

No potential conflict of interest was reported by the author(s).

Funding

The authors received no direct funding for this research.

References

Ahmet, G., M. Mehmet, and Y. Ahmet. 2012. "Adaptive Multi-Step Differential Transformation Method to Solving Nonlinear Differential Equations." *Mathematical and Computer Modelling* 55 (3–4): 761–769. https://doi.org/10.1016/j.mcm.2011.09.001.

Aristidou, P., D. Fabozzi, and T. V. Cutsem. 2014. "Dynamic Simulation of Large Scale Power Systems Using a Parallel Schur-Complement_based Decomposition Method." *IEEE Transactions on Parallel and Distributed Systems* 25 (10): 2561–2570. https://doi.org/10.1109/TPDS.2013.252.

Bég, O. A., M. Keimanesh, M. M. Rashidi, M. Davoodi, and S. T. Branch. 2013. "Multi-Step DTM Simulation of Magneto-Peristaltic Flow of a Conducting Williamson Viscoelastic Fluid." *International Journal of Applied Mathematics and Mechanics* 9:22–40.

Chow, J. H. 2013. *Power System Coherency and Model Reduction*. New York, NY, USA: Springer.

El-Zahar, E. R. 2012. "An Adaptive Step-Size Taylor Series Based Method and Application to Nonlinear Biochemical Reaction Model." *Trends in Applied Sciences Research* 7 (11): 901–912. https://doi.org/10.3923/tasr.2012.901.912 .

El-Zahar, E. R. 2015. "Applications of Adaptive Multi Step Differential Transform Method to Singular Perturbation Problems Arising in Science and Engineering." *Applied Mathematics and Information Sciences* 9 (1): 223–232. https://doi.org/10.12785/amis/090128.

Gurrala, G., A. Dimitrovski, S. Pannala, S. Simunovic, and M. Starke. 2015. "Parareal in Time for Fast Power System Dynamic Simula-tions." *IEEE Transactions on Power Systems* 31 (3): 1820–1830. https://doi.org/10.1109/TPWRS.2015.2434833.

Kim, S., and T. J. Overbye. 2015. "Optimal Subinterval Selection Approach for Power System Transient Stability Simulation." *Energies* 8 (10): 11871–11882. https://doi.org/10.3390/en81011871.

Kundur, P., J. Paserba, V. Ajjarapu, G. Andersson, A. Bose, C. Canizares, and V. Vittal. 2004. "IEEE/CIGRE Joint Task Force on Stability Terms and Definitions, Definition and Classification of Power System Stability." *IEEE Transactions on Power Systems* 19:1387–1401.

Laugier, A. J. C. "Adaptive Time Step for Fast Converging Dynamic Simulation System." In *Proceedings of the IEEE/710 RSJ International Conference on Intelligent Robots and Systems*. IROS '96, Osaka, Japan. 8 November 1996, https://doi.org/10.1109/IROS.1996.570806.

Liu, Y., and K. Sun. 2020. "Solving Power System Differential Algebraic Equations Using Differential Transformation." *IEEE Transactions on Power Systems* 35 (3): 2289–2299. https://doi.org/10.1109/TPWRS.2019.2945512.

Liu, Y., and K. Sun. 2022. Available online: Power System Simulation Using a Differential Transformation Method. Ph.D. Thesis, University of Tennessee, Knoxville, TN,

USA." Accessed August 28, 2022. https://trace.tennessee.edu/utk_graddiss/7073.

Liu, Y., K. Sun, R. Yao, and B. Wang. 2019. "Power System Time Domain Simulation Using a Differential Transformation Method." *IEEE Transactions on Power Systems* 34 (5): 3739–3748. https://doi.org/10.1109/TPWRS.2019.2901654.

Liu, C., B. Wang, and K. Sun. "Fast Power System Simulation Using Semi-Analytical Solutions Based on Pade Approximation." In *Proceedings of the 2017 IEEE Power & Energy Society General Meeting*, 1–5, Chicago, IL, USA, 16–20 July 2017.

Liu, C., B. Wang, and K. Sun. 2018. "Fast Power System Dynamic Simulation Using Continued Fractions." *IEEE Access* 6:62687–62698. https://doi.org/10.1109/ACCESS.2018.2876055.

MATLAB, T.M.I.2017b. 2017. "The MathWorks Inc."

Matpower. 2008. Accessed May 26, 2020. http://www.esat.kuleuven.be/electa/teaching/matdyn/ .

Milano, F. 2010. "Power System Modeling and Scripting; Springer Science and Business Media: Berlin/Heidelberg, Germany."

Osipov, D., and K. Sun. 2018. "Adaptive Nonlinear Model Reduction for Fast Power System Simulation." *IEEE Transactions on Power Systems* 33 (6): 6746–6754. https://doi.org/10.1109/TPWRS.2018.2835766.

Perilla, A., S. Papadakis, J. L. Rueda Torres, M. van der Meijden, P. Palensky, and F. Gonzalez-Longatt. 2020. "Transient Stability Per-Formance of Power Systems with High Share of Wind Generators Equipped with Power-Angle Modulation Controllers or Fast Local Voltage Controllers." *Energies* 13 (16): 4205. https://doi.org/10.3390/en13164205.

Pukhov, E., and G. Georgii. 1982. "Differential Transformation Method and Circuit Theory." *International Journal of Circuit Theory and Applications* 10 (3): 265–276. https://doi.org/10.1002/cta.4490100307.

Sanchez-Gasca, J. J., R. D'aquila, W. W. Price, and J. J. Paserba. "Variable Time Step, Implicit Integration for Extended-Term Power System Dynamic Simulation." In *Proceedings of the Power Industry Computer Applications Conference*, Salt Lake City, UT, USA, 7–12 May 1995. https://doi.org/10.1109/PICA.1995.515182.

Sarajcev, P., A. Kunac, G. Petrovic, and M. Despalatovic. 2021. "Power System Transient Stability Assessment Using Stacked Autoencoder and Voting Ensemble." *Energies* 14 (11): 3148. https://doi.org/10.3390/en14113148.

Stott, B. 1979. "Power System Dynamic Response Calculation." In *Proceedings of the IEEE*, 219–241. Vol. 67. IEEE.

Tina, G. M., G. Maione, and S. Licciardello. 2022. "Evaluation of Technical Solutions to Improve Transient Stability in Power Systems with Wind Power Generation." *Energies* 15 (19): 7055. https://doi.org/10.3390/en15197055.

Wang, B., N. Duan, and K. Sun. 2019. "A Time–Power Series-Based Semi-Analytical Approach for Power System Simulation." *IEEE Transactions on Power Systems* 34 (2): 841–851. https://doi.org/10.1109/TPWRS.2018.2871425.

Yang, D. 2006. "Power System Dynamic Security Analysis via Decoupled Time Domain Simulation and Trajectory Optimization." Appendix A. IEEE 9bus and New England Test System Generator Data, Ames, IA, USA, Iowa State University.

Zadkhast, S., J. Jatskevich, and E. Vaahedi. 2015. "A Multi-Decomposition Approach for Accelerated Time Domain Simulation of Transient Stability Problems." *IEEE Transactions on Power Systems* 30 (5): 2301–2311. https://doi.org/10.1109/TPWRS.2014.2361529.

Zimmerman, R. D., C. E. Murillo-Sanchez, and R. J. Thomas. 2011. "MATPOWER: Steady-State Operations, Planning, and Analysis Tools for Power Systems Research and Education." *IEEE Transactions on Power Systems* 26 (1): 12–19. https://doi.org/10.1109/TPWRS.2010.2051168.

Annex A

Table A1. IEEE 9-bus test system generator data 1.

	Bus numbers		
Parameters	1	2	3
Xd	0.146	0.8958	1.3125
Xq	0.0969	0.8648	1.2578
X'd	0.0608	0.1198	0.1813
X'q	0.0969	0.1969	0.25
Rs	0.004	0.0026	0.0035
T'do	8.96	6.00	5.890
T'qo	0.31	0.535	0.6
H	23.000	6.400	3.010
Dg	0.0151	0.001	0.0058

Table A2. New england system generator data 1 (Yang 2006).

	Bus numbers									
Parameters	30	31	32	33	34	35	36	37	38	39
Xd	0.1000	0.2590	0.2500	0.2620	0.6700	0.2540	0.2950	0.2900	0.2110	0.0200
Xq	0.0690	0.2820	0.2370	0.2580	0.6200	0.2410	0.2920	0.2800	0.2050	0.0190
X'd	0.0310	0.0700	0.0530	0.0440	0.1320	0.0500	0.0490	0.0570	0.0570	0.0060
X'q	0.0690	0.1700	0.0880	0.1660	0.1660	0.0810	0.1860	0.0910	0.0590	0.0080
Rs	0.0002	0.0002	0.0002	0.0002	0.0002	0.0002	0.0002	0.0010	0.0002	0.0002
T'do	10.200	6.5600	5.7000	5.6900	5.4000	7.3000	5.6600	6.7000	4.7900	7.0000
T'qo	0.020	1.5000	1.5000	1.5000	0.4400	0.4000	1.5000	0.4100	1.9600	0.7000
H	42.000	30.300	35.500	28.500	26.000	35.00	26.500	24.300	34.500	31.0 00
Dg	0.0535	0.0194	0.06783	0.01815	0.0331	0.06783	0.01815	0.0331	0.06783	0.01940

Table A3. IEEE 9-bus test system generator data 2.

	Bus numbers		
Parameters	1	2	3
Ke	1.0000	1.0000	1.0000
Te	0.3140	0.3140	0.3140
Se	0.0000	0.0000	0.0000
Ka	20.000	20.000	20.000
Ta	0.200	0.200	0.200
Kf	0.0630	0.0630	0.0630
Tf	0.350	0.350	0.350
Tch	0.1000	0.1000	0.1000
Tg	0.0500	0.0500	0.0500
Rg	0.0500	0.0500	0.0500

Table A4. New england system generator data 2 (Yang 2006).

	Bus numbers									
Parameters	30	31	32	33	34	35	36	37	38	39
Ke	1.0000	1.0000	1.0000	1.0000	1.0000	1.0000	1.0000	1.0000	1.0000	1.0000
Te	0.2500	0.4100	0.5000	0.5000	0.7900	0.4700	0.7300	0.5300	1.4000	1.0000
Se	0.0000	0.0000	0.0000	0.0000	0.0000	0.0000	0.0000	0.0000	0.0000	0.0000
Ka	20.000	40.000	40.000	40.000	30.000	40.000	30.000	40.000	20.000	20.000
Ta	0.0600	0.0500	0.0600	0.0600	0.0200	0.0200	0.0200	0.0200	0.0200	0.0200
Kf	0.0400	0.0600	0.0800	0.0800	0.0300	0.0800	0.0300	0.0900	0.0300	0.0300
Tf	1.0000	0.5000	1.0000	1.0000	1.0000	1.2500	1.0000	1.2600	1.0000	1.0000
Tch	0.1000	0.1000	0.1000	0.1000	0.1000	0.1000	0.1000	0.1000	0.1000	0.1000
Tg	0.0500	0.0500	0.0500	0.0500	0.0500	0.0500	0.0500	0.0500	0.0500	0.0500
Rg	0.0500	0.0500	0.0500	0.0500	0.0500	0.0500	0.0500	0.0500	0.0500	0.0500

electricity

Article

Transient Stability-Based Fast Power System Contingency Screening and Ranking

Teshome Lindi Kumissa [1,*] and Fekadu Shewarega [2]

[1] School of Electrical and Computer Engineering (SECE), Hawassa University Institute of Technology, Hawassa D-45117, Ethiopia
[2] Institutes of Electrical Power Systems, University of Duisburg-Essen, D-45117 Duisburg, Germany; fekadu.shewarega@uni-due.de
* Correspondence: teshomel@hu.edu.et

Abstract: Today's power systems are operated closer to their stability limits due to the continuously growing load demands, interface to open markets, and integration of more renewable energies. In order to provide operators with clear insight on the current system situation, near real-time power systems dynamic security assessment tools are required. One of the core elements of near real-time dynamic security assessment tools is contingency screening and ranking. Most of the commercially available tools screen and rank contingencies by using the traditional numerical integration or Transient Energy Functions (TEFs) or hybrid methods. The traditional numerical integration method is accurate but computationally intensive and has a slow assessment speed which makes it difficult to identify any insecure contingency before it happens. Despite the TEF method of transient stability analysis being relatively fast, it develops less accurate results due to models simplification and assumptions. This paper introduces transient stability based on fast and robust contingency screening and ranking using an Adaptive step-size Differential Transformation (AsDTM) method. Based on the most current snapshot from Supervisory Control and Data Accusation (SCADA) data, the proposed method triggers AsDTM-based transient stability simulation for each credible contingency and evaluates Transient Stability Indices (TSI) as the normalized weighted sum of squares of errors derived from state variables and complex bus voltages at every simulation time step. Finally, contingencies are ranked based on these TSI and the worst contingency is identified for the next detail assessment. The method is tested on IEEE 9 bus and 39 bus test systems. Test results reveal that the proposed method is faster, robust, and can be used in near real-time dynamic security assessment sessions.

Keywords: transient stability indices (TSI); dynamic security assessment (DSA); transient stability simulation; contingency screening

Citation: Kumissa, T.L.; Shewarega, F. Transient Stability-Based Fast Power System Contingency Screening and Ranking. *Electricity* **2024**, *5*, 947–971. https://doi.org/10.3390/electricity5040048

Academic Editor: Murilo E.C. Bento

Received: 19 September 2024
Revised: 11 November 2024
Accepted: 19 November 2024
Published: 25 November 2024

1. Introduction

A reliable electricity supply is foundational to all economic and societal activities in modern societies. Ensuring the secure operation of the system during widely varying loading scenarios or following possible unforeseen events represents an immense challenge to the system operator. To assess the security risk correctly and to initiate any necessary corrective measures, the operator needs to have situational awareness at all times. Most of the recent methods of stability assessment are based on extensive off-line computations and, consequently, may no longer be sufficient; hence, a near real-time DSA is significantly demanding [1]. The near real-time application of a DSA to a realistic network needs sufficient methods to screen and rank large number of contingencies to be investigated by DSA tools.

The goal of contingency screening and ranking is to shortlist critical contingencies for deeper evaluation of the power system. Since, in practice not every contingency will bring an instability problem to the power system, conformation of a critical contingencies list is created according to the comparisons of the performances of the power system [2,3]. The performances of the power system after being subject to each contingency are evaluated with respect to the capacities of the equipment, operating constraints, etc. During contingency screening, contingencies with a small influence on system operation are removed. Their exclusion from credible contingencies lists results in a significant reduction in information for near real-time operation, i.e., only a few potentially severe contingencies are considered to undergo detailed evaluation. Several broad approaches to contingency screening and ranking methods have been proposed [4].

The authors of [5,6] proposed some indices for contingency screening and ranking. However, they often require numerical integration for a significant interval after the fault clearance. Ref. [6] proposes heuristic individual and global transient instabilities indices based on combined numerical integration and direct methods (hybrid method) for contingency screening in an online DSA session. The method proposed by [7] is based on simplified modeling with assumptions which can result in substantial simulation errors. Transient stability simulation-based indices for contingency screening and ranking are proposed by [8], which solves both differential and algebraic equations of a power system numerically by a MATLAB ODE solver. Approaches, such as a numerical integration, direct (energy function methods), and combination of both methods, are explored by [9–11]. The conventional numerical integration-based methods are accurate but require intensive computations; but direct methods are the reverse.

In [12], various severity indices for dynamic security analysis and the ranking of contingencies are proposed. For the purpose of measuring the severity of a contingency, the authors propose several indices, which are based on coherency, transient energy conversion, and dot products of certain system states. Finally, the authors propose a composite index, which assigns different weights to the prior defined indexes and sums up their contributions. In this approach, a detailed time-domain simulation is carried out until 500 ms after fault clearance. Then, the indices are computed to determine stability and to rank the respective contingencies. However, the majority of the indexes do not obviously divide the contingencies into unstable and stable scenarios while tested being used with a particular test case. Power system contingency screening and a ranking method based on the TEF method was proposed by [13]. The method utilizes the transient energy function and aims at filtering out the non-severe disturbances. The TEF method has received a lot of attention and assessment methods based on it were continuously advanced.

Hybrid methods, like SIME [10], improve the transient stability simulation speed. The method consists of two blocks. The first block filters stable contingencies and the second block ranks and assesses the remaining possible harmful contingencies based on their estimated critical clearing times (CCTs). This requires running time-domain simulations twice per contingency. In [14], a fast power system contingency screening technique based on SIME was presented. A new index was introduced for grouping generators as well as a contingency classification based on the power angle shape of the one-machine infinite bus (OMIB) equivalent. For this purpose, the method requires running time-domain simulations one to three times per contingency with varying fault clearing times. Alternatively, contingency screening methods, which are executed periodically, and the deployment of wide-area measurement systems in power systems enabled transient stability prediction utilizing real-time synchronized phasor measurements.

A contingency screening method utilizing the extended equal area criterion (EEAC) as described in [15] was presented in [16]. The EEAC is a further development of the equal area criterion (EAC) to allow an application of the criterion to multi-machine systems. The authors derived a set of rules to effectively filter out the stable cases from a set of credible

contingencies. In order to identify and filter stable cases, just after fault clearance the stability margins determined from the static EEAC (SEEAC) and dynamic EEAC (DEEAC, as described in [17,18]) are computed. Then, the aforementioned rules are employed to identify if a case is stable and should be filtered out.

In [19], the authors propose a method to predict transient rotor swings using a fuzzy hyper-rectangular composite neural network and post-contingency phasor measurements to determine stability. Recently, a method for transient stability prediction and mitigation has been proposed by [20]. The method uses real-time measurements provided from phasor measurement units (PMUs) and an artificial neural network (ANN) to detect stability or instability of the power system. If instability is detected, a remedial action scheme is activated. This method improves the computation speed, but the detail system model is not supported. However, these methods require training on a forecast database and provide a certain degree of generalization that may not always be capable of correctly determining security and stability [4].

The review of works to advance power system contingency screening and ranking methods presented above can be summarized and grouped into four broad methods as a traditional numerical integration method of TDS, direct (TEF) methods, a hybrid of TDS and TEF methods, and automating learning methods (such as methods based on ANN). Approaches such as a power system TDS based on numerical integrations provide accurate assessment results but are too slow due to their intensive computation requirement. Transient energy function and hybrid methods proposed by different authors may provide quantitative measures which indicate the degree of system stability based on the energy margin or stability indices but require model simplification and assumptions. Since the generation and consumption pattern in the system become less predictable and dependent on forecasting accuracies, methods based on off-line databases, such as ANN, a decision tree, pattern recognition methods, etc, are going to be challenged by the vast amount of possible operating conditions [4]. It is likely that these very unpredictable situations are not part of the database and may even deviate significantly from the scenarios in the database.

To mitigate these problems, some advanced time-domain simulations have been proposed in different literatures. The analytical method of transient stability assessment recently proposed in [21] is a non-iterative method of solving complex power system differential algebraic model equations by using a differential transformation method. In this approach, a fully analytical solution method is used, no network simplifications are made, and loads are not assumed as a constant impedance load. However, the differential transformation method generates a series solution, actually a truncated series solution which does not exhibit the real behaviors of the problem but gives a good approximation to the true solution in a very small region. A multi-step differential transformation approach is required to extend the region of solution and improve the simulation speed and accuracy of the resulting solution [22,23]; in some cases, a very small sub-division of interval is required with this method, which actually results in a greater computational burden and more time.

To overcome the drawback of this differential transformation method, an adaptive step-size differential transformation method (AsDTM) is proposed by [24]. The proposed method introduces a novel step-size control algorithm based on local convergence error results at the end of each simulation time step. The method adaptively varies the step-size of classical DTM- based simulation method The step size is varied based on the local truncation error control algorithm. The automatic controls of the step-size length are performed based on the principles: (1) reduce the time step length when the error is above the tolerable error limit, to improve the accuracy of the simulation, and (2) increase the time step length when the error is below the tolerable error limit, to avoid an unnecessary computational burden and improve the overall efficiency.

This paper introduces a fast and robust power system contingency screening and ranking method, whose performance is suitable for a near real-time application and could be a part of a DSA toolbox. Power system transient stability analysis based on an AsDTM is used in this paper. TS indices are evaluated from the analysis results as normalized weighted sums of squares of error at every simulation time step for both state variables and complex bus voltages. This work has at least four major contributions: (1) It is relatively robust and accurate, because it is flexible in handling power systems with any model detail and complexity without limitations, for instance, complex high-order models of AVRs, turbine, governors, boilers, SVCs, and other items of plant can be used; (2) it improves simulation speed and accuracy based on the control of the local convergence error at each time step; (3) the local solution error is estimated from only the last coefficient terms of the state and algebraic variables without any further calculations as in the variable step-size algorithm using traditional numerical integration methods; and (4) the solution obtained for the current simulation time step can be used during the next simulation time step without any limitations, such that the number of steps required to complete the transient stability simulation process reduces. Therefore, using the AsDTM method reduces the time spent in filtering out the potentially severe contingencies and reduces the update time of the DSA system. These enable the proposed method to be applied in a near real-time DSA session. Using the proposed comprehensive methodology, case studies are performed on IEEE 9 bus and New England IEEE 39 bus test systems and validated.

The paper is organized as follows. Section II describes the proposed method; Section III presents test results of the proposed approach on IEEE 9 bus and New England IEEE 39 bus test systems, and Section IV presents conclusions and future work

2. The Proposed Contingency Screening and Ranking Method

In a near real-time DSA tool, power system contingency screening and ranking is expected to be executed periodically several times per day. In order that a large number of contingencies can be processed by a near real-time DSA system, it is necessary to include some form of contingency screening to filter out those contingencies which lead to little or no degradation of the system security [1]. This will reduce the time spent in filtering out the potentially severe contingencies and reduce the update time of the DSA system. At the same time, it is very important that all the contingencies that will lead to stability problems are identified, i.e., the screening process is accurate.

In this paper, contingency screening and ranking using an AsDTM-based power system transient stability analysis is proposed. The proposed method starts whenever the system operators require analyzing the impact of some set of selected contingencies for the purpose of a near real-time operation using the most current system operating state data as the basis. At each time step of the transient stability analysis for every credible contingency, the TSI (AI and SI) is evaluated as a weighted sum of squares of errors derived from state variables and complex bus voltages at every time step, during the process of transient stability simulations for each credible contingency. These indices are related by normalizing them with the largest of all and ranked. Finally, the worst contingency is identified for the next detail assessment. The TS indices evaluated based on the machine's state variables are represented as the machine's state variables indices (SI) and those evaluated based on the machine's bus complex bus voltages are represented as algebraic indices (AI).

Note that the method does not aim at predicting the transient response of the system after the occurrence of a fault; instead, the method carries out a contingency screening and ranking to ensure that the system is transiently stable with respect to a given set of credible contingencies. Figure 1 shows the flowchart diagram of the proposed contingency screening and ranking method assumed to be integrated into the near real-time DSA session. In the following subsections, each part of the proposed algorithm will be described in more detail.

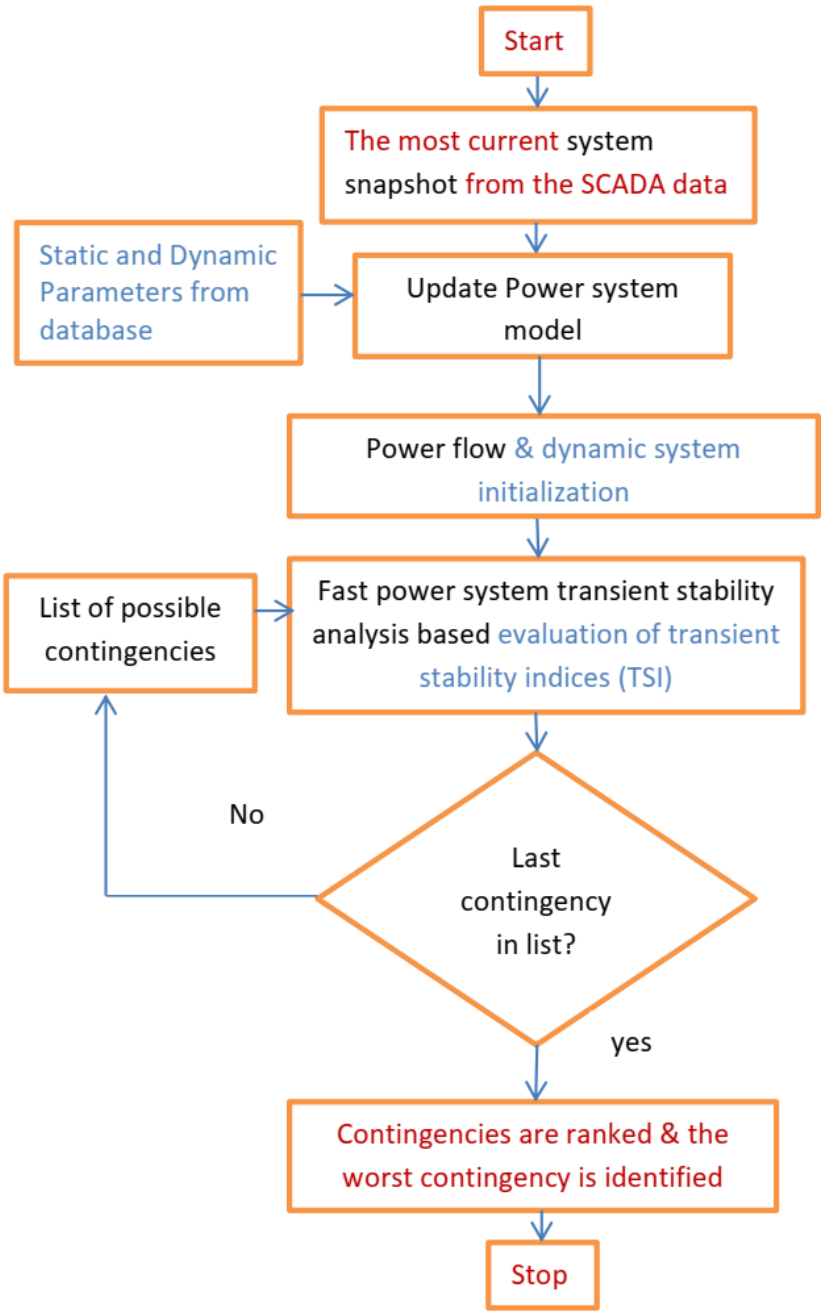

Figure 1. Flowchart diagram of the proposed power system contingency screening and ranking method integrated into a framework for near real-time application.

2.1. The Most Current System Snapshot from the SCADA Data

The most current system snapshots consisting of complex power flows through transmission lines, complex power injections (generation or demand at buses), and bus voltage magnitudes are read from Supervisory Control and Data Acquisition (SCADA) data. These data are used to represent the system's pre-fault condition so as to initialize the transient stability simulations.

2.2. Static and Dynamic Parameters from the Database

The static and dynamic data contain a system model parameter for all components in the monitored power system. The provided parameters are assumed to be enough to represent the power system components with proper detail to enable an accurate simulation

of the transient response. In this paper, the synchronous generator's rotor dynamics are represented by a fourth-order model.

2.3. Update Power System Models

The obtained most current system snapshot and the model database, which provide the required dynamic and static data and parameters of each component, are utilized to set up the power system models representing the current system state including the network admittance matrix Y.

2.4. Perform Power Flow, Initialize Dynamic System, and Prepare List of Credible Contingencies

Using the updated power system model, a power flow analysis is performed to represent the system's pre-fault steady state conditions and hence initialize the dynamic system for the next power system transient stability analysis-based evaluation of the TSI function based on the flowchart given by Figure 2. A list of credible contingencies is also generated for the system under consideration here.

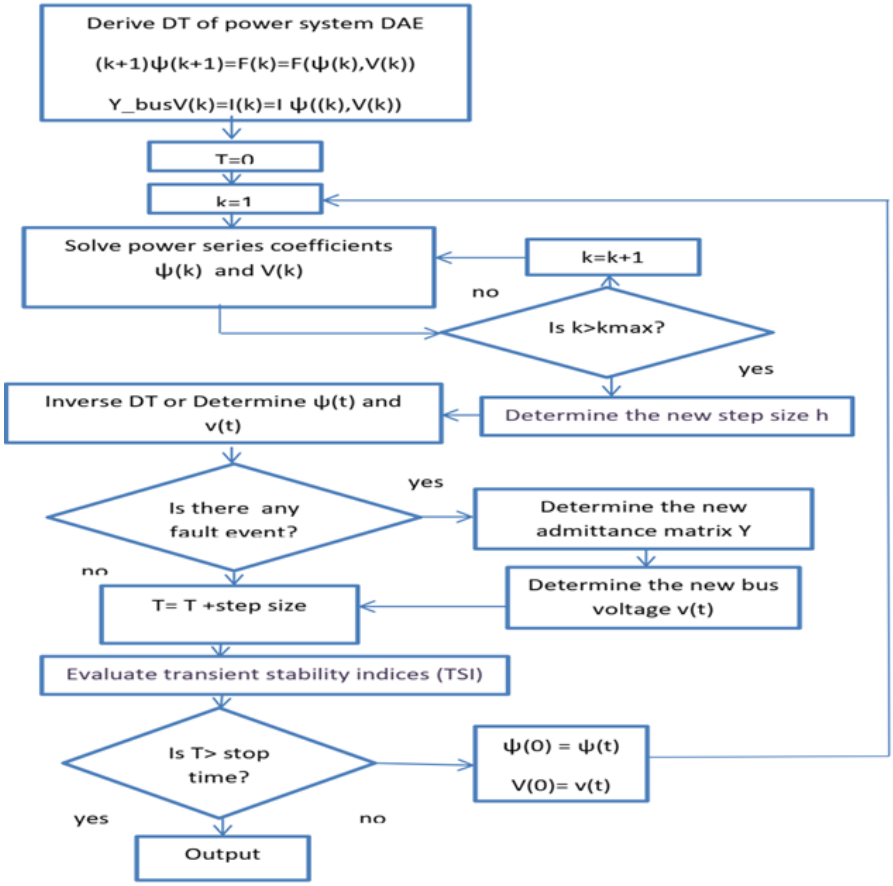

Figure 2. Flowchart of the algorithm for fast transient stability-based TSI evaluation.

2.5. Fast Power System Transient Stability Analysis-Based TSI Evaluations

2.5.1. Differential Transformation Method (DTM)

The theory of the differential transformation method is originally established in [25] to derive approximate solutions of nonlinear differential equations and is defined as below. Consider a function ψ(t) of a real continuous variable t. The differential transformation of ψ(t) is defined by Equation (1), and the inverse DT of ψ(k) is defined by Equation (2), where k is the order transformation.

$$\psi(\mathrm{k}) = \frac{1}{\mathrm{k!}}\left[\frac{\mathrm{d}^{\mathrm{k}}\psi(t)}{dt^{k}}\right]_{(\mathrm{t}=0)} \quad (1)$$

$$\psi(t) = \sum_{k=1}^{\infty} \psi(k) t^k \tag{2}$$

Next, it is developed by researchers in the fields of mathematics and physics to obtain semi-analytical solutions of various nonlinear dynamic systems. In [20,21], this method was examined for real-life complex network systems such as power systems modeled by high-order nonlinear differential equations. DTM provides a set of transform rules. Some of these transform rules are listed below. If we let x(t), y(t) and z(t) be the original functions and X(k), Y(k), and Z(k) their DTs, respectively, the following propositions hold, where c is a constant matrix and n is a nonnegative integer [26]:

(a) X(0) = x(0).
(b) y(t) = cx(t) → Y(k) = cX(k).
(c) z(t) = x(t) ± y(t) → Z(k) = X(k) ± Y(k).
(d) z(t) = x(t) y(t) → $Z(k) = \sum_{m=0}^{k} X(m)\, Y(k-m)$
(e) $Z(t) = \frac{y(t)}{h(t)}$ it sDT $= \frac{1}{H(0)}\left(Y(k) - \sum_{m=0}^{k-1} H(k-m) Z(m)\right)$
(f) $x(t)^T = X(k)^T$
(g) dx/dt = (k + 1)X(k + 1) and if DT of $\sin\delta = \varphi(k)$ and DT of $\cos\delta = \alpha(k)$ then
(h) $\varphi(k) = \left(\sum_{m=0}^{k-1} \frac{k-m}{k} \alpha(m)\delta(k-m)\right)$
(i) $\alpha(k) = \left(-\sum_{m=0}^{k-1} \frac{k-m}{k} \varphi(m)\delta(k-m)\right)$

The use of DTM as an explicit solver of power-system complex differential algebraic equations (DAEs) in power-system dynamic simulation presented by [21,24] introduces a significant advancement in power system dynamic simulation. It is proven that the performance efficiency of a DTM is much better than that of the traditional numerical integration methods, because when using the DTM method, the iteration to solve algebraic equations after each integration step is eliminated and has a higher radius of convergence. The procedures to solve multi-machine power system DAE models using the DTM method is as follows [21]: (1) transform power system DAE equations, (2) calculate the coefficients of state and algebraic variables, and (3) perform an inverse transformation to determine state and algebraic variables as a function of time.

Implementations of the DTM-based solution method is illustrated using an initial value problem as presented below.

Consider the following initial value problem: Equation (3), where $C \in R^m$ and $F : RxR^m \to R^m$:

$$\begin{aligned} &\frac{d\psi}{dt} = F(\psi(t), t)\ ,\ 0 \le t \le T, \\ &\psi(0) = c \end{aligned} \tag{3}$$

where ψ = (ψ1, ψ2, . . ., ψn) and the interval [0, T] is partitioned into N subdomains with grid points expressed as t0, t1, . . ., tj−1, tj = T, such that tj+1 = tj + h. Using the DTM solution approach, the first step is to determine the DTs of Equation (3), which is given as Equation (4) below, where K is the order of DT and m is the number of variables:

$$\begin{aligned} &\psi_{m,n}(k) = \frac{1}{k}[F(k, t_n)] \\ &k = 0, 1, 2, \ldots, K \ \&\ n = 0, 1, 2, \ldots, N-1 \end{aligned} \tag{4}$$

By eliminating 1/k from the right side of Equation (4), we can rewrite it as Equation (5), where ψmn and F are the transformed vector valued functions:

$$\psi_{m,n}(k) = F(\psi_{mn}(k-1), t_n) \tag{5}$$

As we can see from Equation (5) above, the coefficient terms ψm,n(k) can be explicitly determined from the lower-order coefficient terms recursively based on Figure 3.

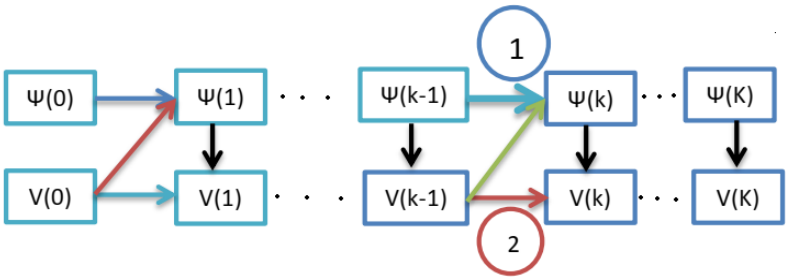

Figure 3. Recursive process to solve power series coefficients source [21].

After all the coefficient terms from k = 0 up to k = K are known, the exact solution of Equation (3) at a point $t = t_{n+1} = t_n + h$ can be written in the form of a Taylor expansion, considering m to be the number of variables, as in Equation (6), where h represents the step size:

$$\psi_m(t_{n+1}) = \sum_{k=0}^{\infty} \psi_{mn}(k)h^k = \sum_{k=0}^{K} \psi_{mn}(k)h^k + h\xi_n \tag{6}$$

where ξ_n is a local truncation error and n = 0, 1, 2, . . ., N − 1. The local truncation error can be expressed in the form of a residual formula of Taylor series, considering m to be the number of vectors of variable ψ_n, and is expressed as Equation (7):

$$\begin{aligned} \xi_n &= \psi_{mn}(k)h^k = h^k F(\psi(k-1), t_c) \\ &= h^k \left[\frac{d^k f(\psi_m(t), t)}{dt^k} \right]_{t=t_c} \\ t_c &\in (t_n, t_{n+1}) \end{aligned} \tag{7}$$

This shows that the DTM method approximates locally to the exact solution with the order k.

AsDTM-based analysis in which the step size h is varied based on imposing the maximum of absolute values of the last coefficient terms to be lower than the admissible local error [24] is applied in this paper. This can be obtained by replacing ξ_n in Equation (7) by the admissible local error σ. Therefore, the new step size is calculated from Equation (8), where σ is the admissible local truncation (solution) error:

$$\begin{aligned} E &= \max|(\psi_{mn}(k))| \\ \sigma &= Eh^k \rightarrow h_{new} = \left(\frac{\sigma}{E}\right)^{\frac{1}{k}} \leq h_{\max} \end{aligned} \tag{8}$$

Power system transient stability simulation-based on the AsDTM method was introduced for the first time by [24]. In using this mathematical tool, the local truncation error at each simulation time step is controlled by setting an acceptable minimum error per unit as illustrated and shown by Equation (8). This enables the AsDTM method to improve the performance efficiency and accuracy of the DTM-based transient stability analysis method. As presented by [24], the accuracy and speed of the transient stability simulation based on AsDTM are investigated in comparison with the classical differential transformation method and the traditional numerical integration method used for IEEE 9 and IEEE 39 test systems. The simulation results reveal that this method improves the simulation speed by 20–44.57% and 83–92% compared with the classical DTM and traditional numerical-integration-based simulation methods, respectively. It is also proven that compared with the DTM-based simulation, the method provides 45.27% to 58.85% and more than 90% accurate simulation results for IEEE 9 and IEEE 39 test systems, respectively.

2.5.2. Descriptions of the Proposed Transient Stability Analysis Based TSI Evaluations

Transient stability analysis-based TS indices evaluation of the scenario is triggered after the fault/event parameters (parameters that represent each credible contingency)

have been determined for all credible contingencies listed and the power system model is initialized. In this paper, an AsDTM-based transient stability analysis method is introduced and used to screen and rank contingencies. At every simulation time step, during the power system transient stability simulation considering each credible contingency, the TSI (AI and SI) is evaluated as the weighted sum of squares of errors derived from state variables and complex bus voltages. Indices evaluated for all listed credible contingencies are related by normalizing them with the largest of all and ranked. Finally, the worst contingency is identified for the next detail assessment. Application of this method significantly improves the performance efficiency as well as robustness of the assessment process. Figure 2 shows a flowchart of the proposed transient stability analysis-based TS indices evaluation algorithm and its descriptions will be presented step by step in this subsection as follows: Where ψ(k) = DT of ψ(t) and V(k) = DT of v(t).

Consider that the state space representation of the power system DAE model equations are as given by Equation (9), where ψ is the state vector, v is the vector of bus voltages, f represents a vector field determined by differential equations on dynamic devices such as synchronous generators and associated controllers, i is the vector valued function on current injections from all generators and load buses, and Y_bus is the network admittance matrix.

$$\begin{array}{l} \frac{d\psi_j}{dt} = f(\psi_j, v_j) \\ Y_{\text{-}bus} v_j = i(\psi_j, v_j) \end{array} \tag{9}$$

where ψ(t) represents the machines and respective controllers state variables such as $\delta_j(t), \omega_j(t), E'_{qj}(t), E'_{dj}(t), V_{rj}(t), V_{fj}(t), E_{fj}(t), P_{chj}(t),$ *and* $P_{svj}(t)$ and j = 1, 2, 3, . . ., m, represent the machine number.

Step 1 Derive DTs of power system DAEs:

Apply the differential transformation to functions given by Equation (9) on both sides, by using transformation rule (g) to obtain Equation (10)

$$\begin{array}{ll} (k+1)\psi(k+1) = F(k) = F(\psi(l), V(l)), l = 0.....k & (a) \\ Y_{bus} V(k) = I(k) = I(\psi(l), V(l)), l = 0.....k & (b) \end{array} \tag{10}$$

The vector valued function $i(\psi, v)$ in Equation (9) represents both generators and load current injections. But here for this specific case, constant impedance loads are considered and are included in the network admittance matrix $Y_{\_bus}$. Differential transformation of the network equations including the stator algebraic equation can be derived as given below:

$$\text{Let } y_a = \begin{pmatrix} r_a & -x'_q \\ x'_d & r_a \end{pmatrix}^{-1}, \rho = \begin{pmatrix} \sin\delta & \cos\delta \\ -\cos\delta & \sin\delta \end{pmatrix}, \sigma = \rho y_a, \\ \beta = \rho y_a \rho',$$

And the generator current injection equation is given as Equation (11)

$$\begin{bmatrix} I_x \\ I_y \end{bmatrix} = \left(\sigma \begin{bmatrix} E'_d \\ E'_q \end{bmatrix} - \beta \begin{bmatrix} V_x \\ V_y \end{bmatrix} \right) \tag{11}$$

Using the transformation rule (h & i), differential transformations of ρ, β, and σ are given:

$$\rho(k) = \begin{pmatrix} \varphi(k) & \alpha(k) \\ -\alpha(k) & \varphi(k) \end{pmatrix}, \ \sigma(k) = \rho(k) y_a, \ \beta(k) = \rho(k) y_a \rho(k)'$$

Similarly, using transformation rule (d), the differential transformation of the generator current injection equation is

$$\begin{bmatrix} I_x(k) \\ I_y(k) \end{bmatrix} = \left(\sum_{m=0}^{k} \sigma(m) \begin{bmatrix} E'_d(k-m) \\ E'_q(k-m) \end{bmatrix} - \sum_{m=0}^{k} \beta(m) \begin{bmatrix} V_x(k-m) \\ V_y(k-m) \end{bmatrix} \right) \tag{12}$$

The load current injection at each bus is represented by

$$\begin{bmatrix} I_x(k) \\ I_y(k) \end{bmatrix} = zeros(2,1) \tag{13}$$

And finally, the DTs of the network algebraic equations are

$$\begin{bmatrix} I_{x1}(k) \\ I_{y1}(k) \\ \vdots \\ I_{xi(k)} \\ I_{yi}(k) \\ \vdots \\ I_{xN}(k) \\ I_{yN}(k) \end{bmatrix} = \begin{pmatrix} Y_{11} & \cdots & Y_{1i} & \cdots & Y_{1N} \\ \vdots & \ddots & \vdots & & \vdots \\ Y_{1i} & \cdots & Y_{ij} & \cdots & Y_{iN} \\ \vdots & & \vdots & \ddots & \vdots \\ Y_{N1} & \cdots & Y_{Nj} & \cdots & Y_{NN} \end{pmatrix} \begin{bmatrix} V_{x1}(k) \\ V_{y1}(k) \\ \vdots \\ V_{xi(k)} \\ V_{yi}(k) \\ \vdots \\ V_{xN}(k) \\ V_{yN}(k) \end{bmatrix} I(k) = YV(k) \tag{14}$$

where i = 1, 2, 3, …, N, and I_{ix} and I_{iy} represent the x and y component of bus i current, v_{ix} & v_{iy} represent x and y component of bus i voltage and

$$Y_{ij} = \begin{pmatrix} G_{ij} & -B_{ij} \\ B_{ij} & G_{ij} \end{pmatrix}, I(k) = \begin{bmatrix} I_{x1}(k) \\ I_{y1}(k) \\ \vdots \\ I_{xi(k)} \\ I_{yi}(k) \\ \vdots \\ I_{xN}(k) \\ I_{yN}(k) \end{bmatrix} V(k) = \begin{bmatrix} V_{x1}(k) \\ V_{y1}(k) \\ \vdots \\ V_{xi(k)} \\ V_{yi}(k) \\ \vdots \\ V_{xN}(k) \\ V_{yN}(k) \end{bmatrix}$$

Step 2 Solve power series coefficients:

This step is initialized by the initial values of bus voltage V(0) and state variables ψ(0). The main task here is to solve power series coefficients ψ(k) and V(k) ($k \geq 1$) from the ($k-1$)th order coefficients, as indicated by two circled numbers in Figure 3. Thus, any order coefficients are solvable from ψ(0),V(0).

The coefficients of state variables ψ(k) for differential equations are derived from Equation (10)a recursively from ψ(1) up to ψ(k), as shown in Figure 3. But solving the coefficients of algebraic variables, bus voltage V(k) is not straightforward since V(k) appears on both sides as we can observe from Equation (10)b. If ZIP load models are considered, the current injunction equations for constant power and constant current load portions of the ZIP load are non-linear and these will be turned to linear in terms of their coefficients; the proof is given in [21]. Since the constant impedance load is considered in this paper, the differential transforms of generator current injection given by Equation (15) can be rewritten as Equation (16) below.

$$\begin{bmatrix} I_x(k) \\ I_y(k) \end{bmatrix} = \left(\sum_{m=0}^{k} \sigma(m) \begin{bmatrix} E'_d(k-m) \\ E'_q(k-m) \end{bmatrix} - \sum_{m=1}^{k} \beta(m) \begin{bmatrix} V_x(k-m) \\ V_y(k-m) \end{bmatrix} \right) \ldots \\ -\beta(0) \begin{bmatrix} V_x(k) \\ V_y(k) \end{bmatrix} \tag{15}$$

Let

$$B_g = \sum_{m=0}^{k} \sigma(m) * \begin{bmatrix} E'_d(k-m) \\ E'_q(k-m) \end{bmatrix} - \sum_{m=1}^{k} \beta(m) * \begin{bmatrix} V_x(k-m) \\ V_x(k-m) \end{bmatrix}$$

$$A_g = \beta(0)$$

$$\begin{bmatrix} I_x(k) \\ I_y(k) \end{bmatrix} = A_g \begin{bmatrix} V_x(k) \\ V_y(k) \end{bmatrix} + B_g \; i.e \; I(k) = A_g V(k) + B_g \tag{16}$$

Since the load current injection is zero, let A_l represent zeros (2,2), B_l represents zeros (2,1) at each of the n buses, $A = A_g + A_l$ & $B = B_g + B_l$ for machine buses and $A = A_l$ & $B = B_l$ at (n-m) buses then A represents (2 × n) by (2 × n) matrixes and B represents (2 × n) by 1 column vector. Therefore, the current injections into the network from all the buses can be expressed as Equation (17) below

$$I(k) = AV(k) + B \tag{17}$$

where I(k) and V(k) are as given for Equation (14)

Considering constant impedance loads, the coefficients of bus voltages V(k) for all the network buses and coefficients of state variables ψ(k) are solved from Equation (18) from a-c recursively from ψ(1) up to ψ(k) and V(1) up to V(k).

$$\begin{aligned} \psi(\mathrm{k}) &= \frac{1}{\mathrm{k}}\,\mathrm{F}(\psi(\mathrm{l}), \mathrm{V}(\mathrm{l})),\ \mathrm{l} = 0\ \ldots \mathrm{k}-1 && \text{(a)} \\ \mathrm{Y\_bus\ V}\ (\mathrm{k}) &= \mathrm{AV(k)} + \mathrm{B} && \text{(b)} \\ \mathrm{V(k)} &= (\mathrm{Y\_bus}\ -\ \mathrm{A})^{-1}\,\mathrm{B} && \text{(c)} \end{aligned} \tag{18}$$

Step 3 Inverse DT on ψ(k) and V(k).

Apply inverse DT to ψ(k) and V(k) to obtain the DTM-based solution of power system DEAs in (20) a&b, where ψ(k) and ψ(t) represent δ_i(k), ω(k)$_i E'_{qi}$(k), E'_{di}(k), V, (k) V_{fi}(k), P_{chi}(k), P_{svi}(k) and E_{fi}(k) & δ_i(t), ω(t)$_i E'_{qi}$(t), E'_{di}(t), V, (t) V_{fi}(t), P_{chi}(t), P_{svi}(t) and E_{fi}(t) respectively. & i = 1, 2, 3. . .. . .m, represent the machine number

$$\begin{aligned} \psi(t) &= \sum_{m=0}^{k} \psi(m) t^m && (a) \\ v(t) &= \sum_{m=0}^{k} V(m) t^m && (b) \end{aligned} \tag{19}$$

Step 4 Determine the new step size (hnew):

As described in Section 2.5.1 above, we can estimate the simulation step size that ensures the prescribed local admissible error by using just one of the coefficient terms without any further calculation. The equation to calculate the step size (h) given by Equation (8) above is adopted and applied for power system transient stability analysis, as described below.

Let M_{st}, E_{Xst}, and T_{Gst} be the matrix of generators, exciters, and turbine governor state variables, respectively. If m and N represent the number of machines and state variables, respectively, the size of each matrix is equal to m × N. Consider also the tolerable local solution error $\partial > 0$. The order of DTM, k, is given and fixed at the beginning of the simulation. Therefore, since all order coefficient terms of state variables and all the network bus voltages are known at this stage, the new step size (h_{new}) will be determined. In this paper, an admissible local solution error of $\partial = 10^{-6}$ per unit is considered. Therefore, we can calculate the new step size h using the following two steps:

I. Determine the maximum of the absolute value of the last coefficient terms of all the variables as in Equation (20):

$$\begin{aligned} E = Max[&Max(Max(|Mst(k)|), Max(Max(|EXst(k)|), \ldots \\ &Max(Max(|TGst(k)|), Max(|V(k)|)] \end{aligned} \tag{20}$$

II. Next, evaluate the new step size h_{new} by using Equation (21):

$$h_{new} = \left(\left(\frac{\partial}{E} \right) \frac{1}{k} \right)^{\leq \text{max step size (hmax)}} \tag{21}$$

Step 5 Check for disturbance or event, and if any, determine the new (Y)matrix and reinitialize bus voltages.

Step 6 Increment the simulation time t as ti + 1 = ti + hnew (where i represents the number of time nodes, separated by the length of every time window).

Step 7 Determining transient stability indices (TSI)

The TSI of each considered contingency is determined in terms of the dynamic performance response at each machine bus. The dynamic performance response at each machine bus is determined in terms of the machine state and algebraic variable values deviation from their respective steady-state conditions. When a power system is subjected to a large disturbance, the algebraic variables change instantly while the machine state variables may need some transient time to change values. Upon clearing, the variables are expected to return to their initial operating values or new and acceptable steady state values. However, this is not always the case due to the severity of that disturbance.

In this paper, transient stability index values, such as SI and AI representing the machine-related state variables and machine bus complex voltage deviations from steady state conditions, respectively, are used to identify and list contingencies according to their severity. For each contingency in the list, these deviations are expressed as the weighted sum of squares of error of the machine state and non-state variables, complex bus voltages at each simulation time step [8] as defined by Equation (22).

$$SI_{new} = SI_{prev} + \left(\frac{\sum_{i=1}^{m} \sum_{j=1}^{l} W_{ij}(\psi_{ij}(t) - \psi_{ij}(t_0))^2}{m} \right) * h$$
$$AI_{new} = AI_{prev} + \left(\frac{\sum_{i=1}^{m} \sum_{j=1}^{l} W_{ij}(v_{ij}(t) - v_{ij}(t_0))^2}{m} \right) * h \quad (22)$$

where:

h = the new step-size, v = complex machine bus voltage, ψ = machine's state variables

SI_{new} = new transient stability index values of machine related state variables

SI_{prev} = previous transient stability index values of machine related state variables

AI_{new} = new transient stability index values of machine bus complex voltage

AI_{prev} = previous transient stability index values of machine bus complex voltage

W_{ij} = weight associated with the state and algebraic variables

l = the number of the state or algebraic variables.

The transient stability index values of state and algebraic variables ψ and v, respectively, and the step-size (h) in the above equations are obtained from the power system transient stability simulation results at each simulation time step. These indices can be evaluated starting from any time as required during the simulation period. Finally, indices evaluated for all listed credible contingencies are related by normalizing them with the largest of all.

Step 8 Using the time domain solutions ψ(t) and v(t) (step 3, above) as initial values of the state variables and bus voltages for the next simulation time window, respectively, repeat steps 2 to 8 until the end of the simulation period (T).

2.6. Contingencies Are Ranked and the Worst Contingency Is Identified

For each considered contingency case, respective transient stability indices are evaluated. Finally, each of the transient stability indices are normalized with the largest of all the indices and listed in descending order. The contingency in the top position is the most critical contingency identified and the contingency in the bottom position is the least critical contingency.

3. Case Studies and Results

3.1. Test System, Cases, and Setup

3.1.1. Test System

Two test systems are employed to validate the proposed screening approach. The first test system is the 9-bus system, which consists of nine buses and three machines. The second test system is the 39-bus system, which consists of 39 buses and 10 machines, as shown by Figure 4 below. The loads are modeled as constant impedances in the time domain simulation. The generators are represented by a two-axis fourth-order model. They all have a Type_1 excitation and voltage regulation system as well as a turbine/governor model.

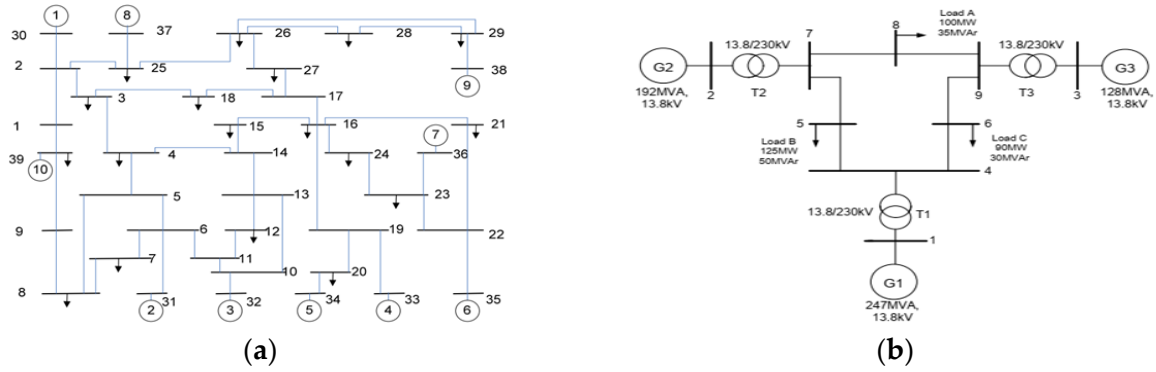

Figure 4. One-line diagram of (**a**) New England 39-bus system; (**b**) IEEE 9-bus system [24].

3.1.2. Test Cases

For the purpose of testing the proposed fast contingency screening method, a set of contingencies are defined. For both systems, three phase bus faults are considered. This located at 6 buses (non-generator buses) for the first test system and 29 buses (similarly, non-generator buses) for the second test system. A susceptance of 10^{-10} is considered enough to bring zero impedance bus faults [27]. This fault is added to the network admittance matrix for every non-generator bus in sequential order (one after the other). In this paper, the fault is cleared only by removing the added fault parameters from the respective bus admittance matrix without isolating the faulted bus itself so that the network structure is not changed.

3.1.3. Test Setup

The tests are carried out on a standard laptop with the following characteristics: Intel CTM) i5-5200U CPU @ 2.20 GHz 2.20 GHz, 8 GB RAM, running on a 64-bit operating system, with a x64-based processor. The transient stability analysis-based TSI evaluations were carried out using the tools/codes developed by using the proposed AsDTM on MATLAB R2017b [28]. MATPOWER 7.1 [29] version software was utilized. The CPU time included all steps of the transient stability analysis-based TSI evaluation processes. MATPOWER is open-source software for power flow analysis and run on a MATLAB environment. This power system analysis software does not employ a graphical representation of a power system. Instead, the power system data were prepared in a table format specific to MATPOWER. Any functions of the MATPOWER can easily be accessed by functions developed on MATLAB editor. These include MATLAB functions that load and call for dynamic and static data file of simulation cases (case file), MATPOWER output interface functions, functions for initializing dynamic systems, model libraries for all dynamic systems, solver functions file (algorithms for computation), and functions for plotting simulation results. Power flow analysis was performed using MATPOWER.

3.2. Assessment Results and Discussion

To validate the proposed contingency screening and ranking method, three-phase short-circuit faults located at 6 buses (non-generator buses) for IEEE 9-bus test system and 29 buses (similarly, non-generator buses) for the 39-bus test system are used. To analyze

their impacts, each fault is triggered at 0.6 s and cleared at two different fault clearing times. TSI for each faulted bus is evaluated, first by considering the 0.15 s (150 ms) fault clearing time and next by considering the 0.25 s (250 ms) fault clearing time. During both scenarios, the evaluated TSI are ranked and plotted. In both cases, the accuracy and performance of the proposed method are validated using the assessment results based on the traditional numerical method (fourth-order Range–Kutta (Rk4) with step size h = 0.001 s) as benchmarks. For this purpose, the differential transformation (DT) order k = 14 is used for both test systems with both DTM and AsDTM simulation methods.

Two types of TS indices are evaluated for each credible contingency during transient stability analysis at each assessment time step. These indices were evaluated based on the machine's state variables (as rotor angle deviations(δ),angular speed($\acute{\omega}$), etc.); analysis results are represented as state variable indices (SI) and those evaluated based on the machine's bus complex bus voltages (such as bus voltage magnitude (V) and voltage angle(θ)) analysis results are represented as algebraic variable indices (AI).

3.2.1. Validation of the Accuracy of the Proposed Method

In the following sub-section, the accuracy of the proposed method is validated with respect to the TS indices evaluated using transient stability analysis based on a traditional numerical method (fourth order Range–K utta (Rk4))) as a benchmark. Tests are performed considering two scenarios. During the first scenario, contingencies are analyzed and ranked considering a 150 ms fault clearing time and the next scenario by considering a 250 ms fault clearing time. The TSI evaluated based on a fourth order Range–K utta Rk4 (reference method), the proposed AsDTM, and the classical DTM methods using both test systems are plotted as shown by Figures 5a,b and 6a,b below. The TSI results evaluated based on the proposed method, and those evaluated from the classical DTM method (with a fixed step-size of h = 0.0125 s) are ranked and compared with the benchmark results as given in Tables 1–4 below. As one can clearly observe from the plots given by Figures 5a,b and 6a,b, the TSI (AI and SI) results evaluated based on the proposed method for the 150 ms fault clearing time indicate that the most and least critical situations are when there is a three phase short-circuit fault at buses 22 and 12, respectively, for the 39-bus test system and at buses 8 and 5, respectively, for the 9-bus test system. These results strongly agree with the most and least critical buses identified based on the Rk4 (benchmark) for both test cases as shown by Figures 5a,b and 6a,b below. But the plots of the TSI evaluated based on the classical DTM method indicate that the most and least critical situations are when there is a three-phase short-circuits fault at buses 22 and 9, respectively, for the 39-bus test system. This result shows that the least critical situation identified by using the classical DTM method is completely different from the benchmark result.

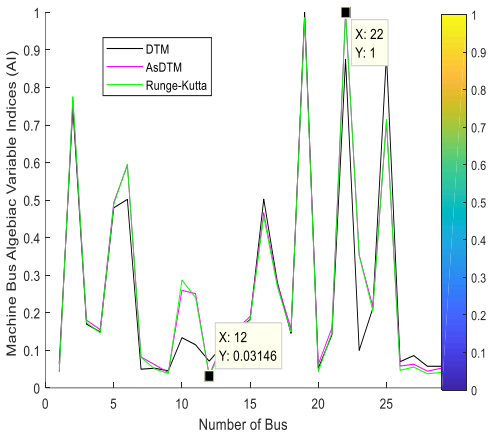

(**a**) SI plot for 150 ms fault clearing time

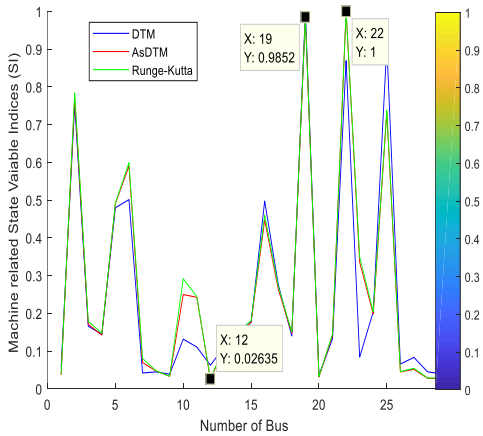

(**b**) AI plot for 150 ms fault clearing time

Figure 5. *Cont.*

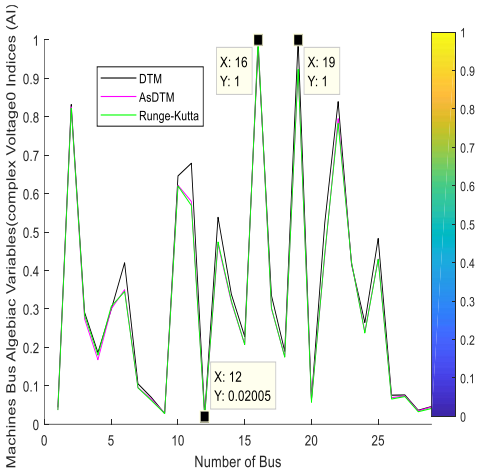

(**c**) SI plot for 250 ms fault clearing time

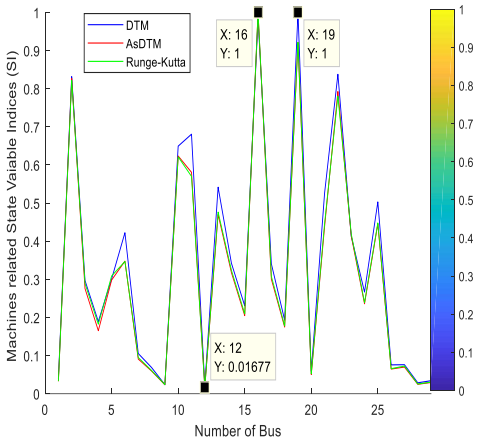

(**d**) AI plot for 250 ms fault clearing time

Figure 5. SI and AI plots of 39-bus test system.

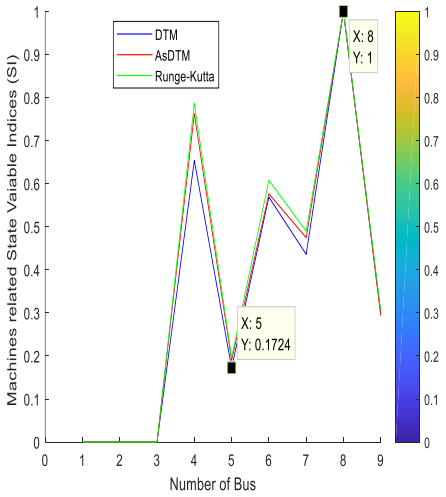

(**a**) SI plot for 150 ms fault clearing time

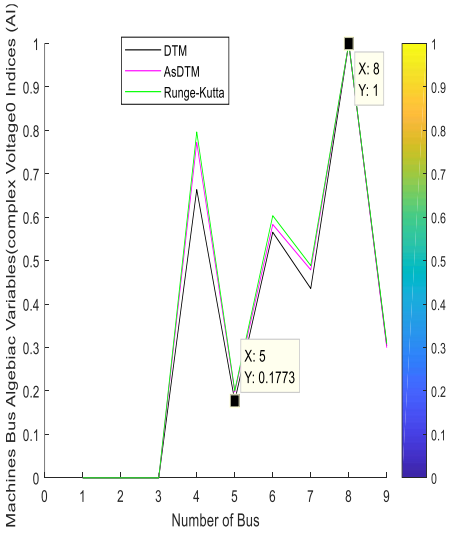

(**b**) AI plot for 150 ms fault clearing time

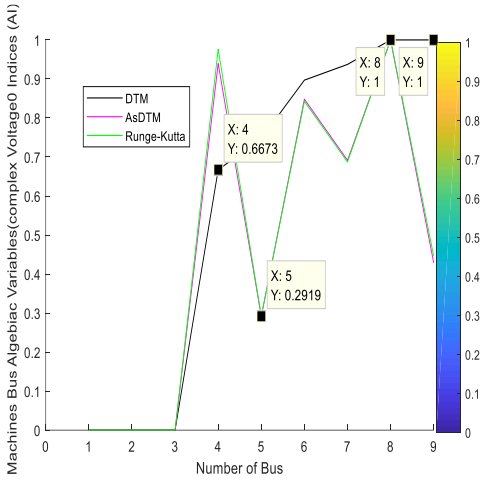

(**c**) SI plot for 250 ms fault clearing time

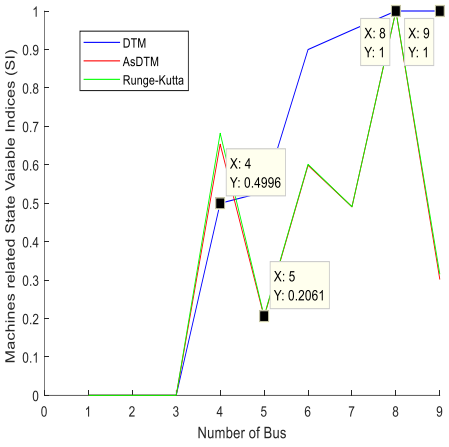

(**d**) SI plot for 250 ms fault clearing time

Figure 6. SI and AI plots of 9-bus test system.

Table 1. Three-phase short-circuit on each non-generator buses of 39-bus test system and each cleared after 150 ms.

Cont. Ranked Using TSI Evaluated Based on Numerical Integration Method (Benchmarks)		**Cont. Ranked Using TSI Evaluated Based on AsDTM Method**		**Con. Ranked Using TSI Evaluated Based on DTM Method**	
Bus No	Rank	Bus No	Rank	Bus No	Rank
Bus 22	1	Bus 22	1	Bus 22	1
Bus 19	2	Bus 19	2	Bus 19	2
Bus 2	3	Bus 2	3	Bus 2	3
Bus 25	4	Bus 25	4	Bus 25	4
Bus 6	5	Bus 6	5	Bus 6	5
Bus 5	6	Bus 5	6	Bus 16	6
Bus 16	7	Bus 16	7	Bus 5	7
Bus 23	8	Bus 23	8	Bus 23	8
Bus 10	9	Bus 10	9	Bus 10	9
Bus 17	10	Bus 17	10	Bus 17	10
Bus 11	11	Bus 11	11	Bus 15	11
Bus 24	12	Bus 24	12	Bus 11	12
Bus 15	13	Bus 15	13	Bus 24	13
Bus 3	14	Bus 3	14	Bus 3	14
Bus 14	15	Bus 18	15	Bus 21	15
Bus 18	16	Bus 14	16	Bus 18	16
Bus 4	17	Bus 4	17	Bus 14	17
Bus 21	18	Bus 21	18	Bus 4	18
Bus 13	19	Bus 13	19	Bus 13	19
Bus 7	20	Bus 7	20	Bus 27	20
Bus 27	21	Bus 27	21	Bus 26	21
Bus 8	22	Bus 8	22	Bus 8	22
Bus 26	23	Bus 26	23	Bus 1	23
Bus 1	24	Bus 1	24	Bus 7	24
Bus 9	25	Bus 9	25	Bus 29	25
Bus 20	26	Bus 20	26	Bus 28	26
Bus 28	27	Bus 28	27	Bus 12	27
Bus 29	28	Bus 29	28	Bus 20	28
Bus 12	29	Bus 12	29	Bus 9	29

Table 2. Three-phase short-circuit on each non-generator buses of 9-bus test system and each cleared after 150 ms.

Cont. Ranked Using TSI Evaluated Based on Numerical Integration Method (Benchmarks)		**Cont. Ranked Using TSI Evaluated Based on AsDTM Method**		**Con. Ranked Using TSI Evaluated Based on DTM Method**	
Bus No	Rank	Bus No	Rank	Bus No	Rank
Bus 8	1	Bus 8	1	Bus 8	1
Bus 4	2	Bus 4	2	Bus 4	2
Bus 6	3	Bus 6	3	Bus 6	3
Bus 7	4	Bus 7	4	Bus 7	4
Bus 9	5	Bus 9	5	Bus 9	5
Bus 5	6	Bus 5	6	Bus 5	6

Similarly, from the plots given by Figures 5c,d and 6c,d, the TSI (AI and SI) evaluated based on the proposed method for the 250 ms fault clearing time indicate that the most and least critical situations are when there is a three-phase short-circuit fault at buses 16 and 12, respectively, for the 39-bus test system and at buses 8 and 5, respectively, for the 9-bus test system. These results again strongly agree with the most and least critical buses identified based on the reference method for both test cases. But the plots of the TSI based

on the classical DTM method indicate that the most and least critical situations are when there is a three-phase short-circuit fault at buses 19 and 12, respectively, for the 39-bus test system and at buses 8 or 9 and 4, respectively, for the 9-bus test system. These results show that the most and least critical situations identified by using the classical DTM method are different from those identified by the benchmark method. Therefore, more accurate results are found by using the proposed contingency screening and ranking method.

Table 3. Three-phase short-circuit on each non-generator buses of 39-bus test system and each cleared after 250 ms.

Cont. Ranked Using TSI Evaluated Based on Numerical Integration Method (Benchmarks)		**Cont. Ranked Using TSI Evaluated Based on AsDTM Method**		**Con. Ranked Using TSI Evaluated Based on DTM Method**	
Bus No	Rank	Bus No	Rank	Bus No	Rank
Bus 16	1	Bus 16	1	Bus 19	1
Bus 19	2	Bus 19	2	Bus 16	2
Bus 2	3	Bus 2	3	Bus 22	3
Bus 22	4	Bus 22	4	Bus 2	4
Bus 10	5	Bus 10	5	Bus 11	5
Bus 11	6	Bus 11	6	Bus 10	6
Bus 13	7	Bus 13	7	Bus 13	7
Bus 25	8	Bus 25	8	Bus 21	8
Bus 21	9	Bus 21	9	Bus 25	9
Bus 23	10	Bus 23	10	Bus 6	10
Bus 6	11	Bus 6	11	Bus 23	11
Bus 14	12	Bus 14	12	Bus 14	12
Bus 5	13	Bus 5	13	Bus 17	13
Bus 17	14	Bus 17	14	Bus 12	14
Bus 3	15	Bus 3	15	Bus 3	15
Bus 24	16	Bus 24	16	Bus 24	16
Bus 15	17	Bus 15	17	Bus 15	17
Bus 4	18	Bus 18	18	Bus 18	18
Bus 18	19	Bus 4	19	Bus 4	19
Bus 7	20	Bus 7	20	Bus 24	20
Bus 27	21	Bus 27	21	Bus 27	21
Bus 26	22	Bus 26	22	Bus 26	22
Bus 8	23	Bus 8	23	Bus 8	23
Bus 20	24	Bus 20	24	Bus 20	24
Bus 1	25	Bus 1	25	Bus 1	25
Bus 29	26	Bus 29	26	Bus 29	26
Bus 28	27	Bus 28	27	Bus 28	27
Bus 9	28	Bus 9	28	Bus 9	28
Bus 12	29	Bus 12	29	Bus 12	29

Table 4. Three-phase short-circuit on each non-generator buses of 9-bus test system and each cleared after 250 ms.

Cont. Ranked Using TSI Evaluated Based on Numerical Integration Method (Benchmarks)		**Cont. Ranked Using TSI Evaluated Based on AsDTM Method**		**Con. Ranked Using TSI Evaluated Based on DTM Method**	
Bus No	Rank	Bus No	Rank	Bus No	Rank
Bus 8	1	Bus 8	1	Bus 8 & Bus 9	1
Bus 4	2	Bus 4	2	Bus 7	2
Bus 6	3	Bus 6	3	Bus 6	3
Bus 7	4	Bus 7	4	Bus 5	4
Bus 9	5	Bus 9	5	Bus 4	5
Bus 5	6	Bus 5	6	-	6

In addition, Figures 5a–d and 6a–d representing the SI and AI plots, where the quality of the plot results obtained with the AsDTM and DTM methods used the convergence criterion, the measure of which is the concurrency of trajectories rout corresponding to two compared solutions. The best convergence was found for the AsDTM-based SI and AI plots. This implies that the AsDTM-based TSI evaluation gives more accurate results. On the other hand, since the shapes of the trajectories obtained by both the DTM and AsDTM methods were the same as the reference trajectory for the first scenario (Figures 5a,b and 6a,b) we can conclude that both the DTM and AsDTM methods are numerically stable. However, when we observe the TSI plots for the second scenario (for the 250 ms fault clearing time), specially Figure 6c,d show that the DTM method is not numerically stable as the network complexity decreases and fault clearing time increases.

Tables 1–4 below give contingencies ranked using their respective TSI evaluated based on the benchmark, classical DTM and the proposed AsDTM methods considering both 150 ms and 250 ms fault clearing by using both test systems. From the summary and the results given in Table 5, in all cases the proposed AsDTM-based contingency screening and ranking method provides 93% accurate results.

Table 5. Summary of the accuracy of the ranked contingencies based on DTM and the proposed AsDTM methods compared with the benchmark results.

Fault Cleared	Accuracy of Contingencies Ranked Using TSI Evaluated Based on AsDTM Method in %		Accuracy of Contingencies Ranked Using TSI Evaluated Based on DTM Method in %	
	For 39-Bus Test System	For 9-Bus Test System	For 39-Bus Test System	For 9-Bus Test System
150 ms	93	100	41.38	100
250 ms	93	100	44.82	16.67

Compared with the benchmark results, the range of accuracy of assessment results based on the proposed AsDTM and the classical DTM methods are summarized as given in Table 5 below.

From the results summary given in Table 5 above, we can conclude that the proposed contingency screening and ranking method is more accurate compared with the DTM method. The increase in the fault clearing time also has no influence on the accuracy of the proposed AsDTM method. Further, as the complexity or sizes of the network decrease the proposed method is as accurate as the reference method. But we can simply observe from the assessment results given in Tables 1–5 that as the network size as well as the fault clearing time increase the probability that the classical DTM method can identify the most critical contingency is almost null.

Even though the most and least critical buses screened out based on the proposed method are the same as the benchmark results (evaluated based on the Rk4 method) in all cases, the magnitudes of the evaluated TS indices (SI and AI) for the three-phase short-circuit at all non-generator buses for both test cases are not the same as the benchmark results. Figures 7a–d and 8a–d below show the error plots of the AsDTM- and DTM-based evaluated transient stability indices. As can be seen from Figures 7 and 8a–d, the magnitudes of the generated SI and AI error by the DTM-based evaluation method are 0.1664 and 0.1619, respectively, for the 39-bus test system and 0.1327 for the 9-bus test system, when the fault is cleared after 150 ms in both cases. Similarly, the magnitudes of the generated SI and AI error by the proposed AsDTM-based evaluation method are 0.0418 and 0.02753, respectively, for the 39-bus test system and 0.03145 and 0.02427, respectively, for the 9-bus test system when the fault is cleared after 150 ms in both cases.

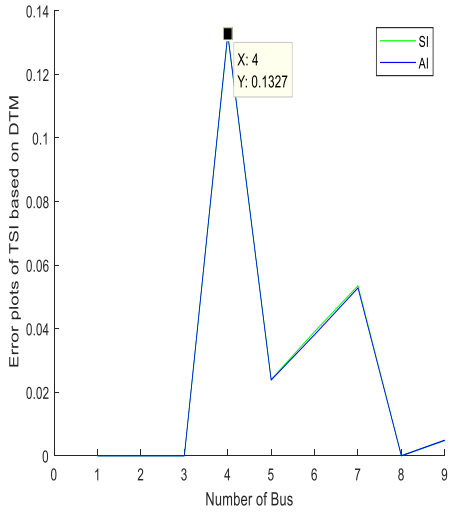

(**a**) Plots TSI evaluated based on DTM for fault clearing time of 150 ms

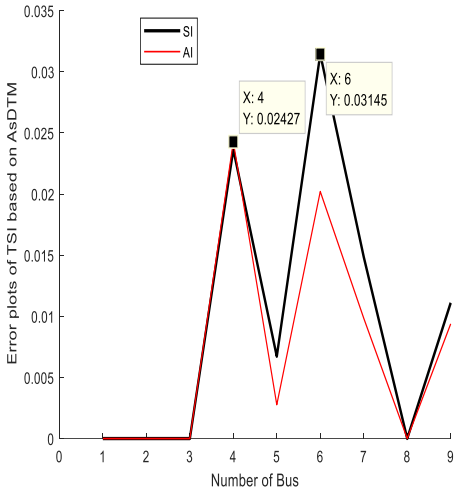

(**b**) Plots TSI evaluated based on AsDTM for fault clearing time of 150 ms

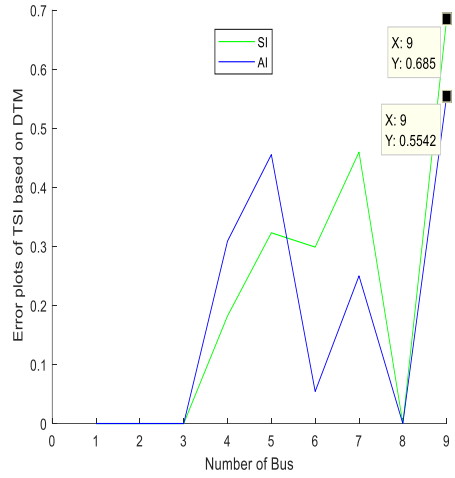

(**c**) Plots TSI evaluated based on DTM for fault clearing time of 250 ms

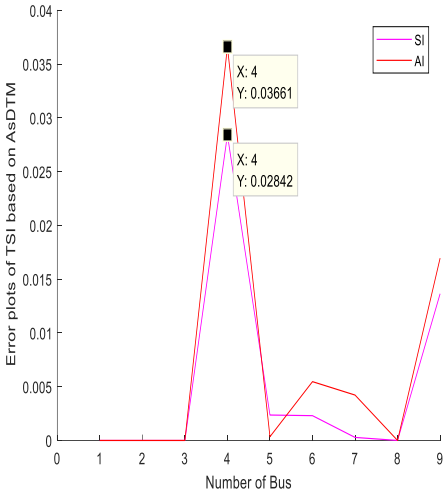

(**d**) Plots TSI evaluated based on AsDTM for fault clearing time of 250 ms

Figure 7. DTM- and AsDTM-based SI and AI error plots for 9-bus test system.

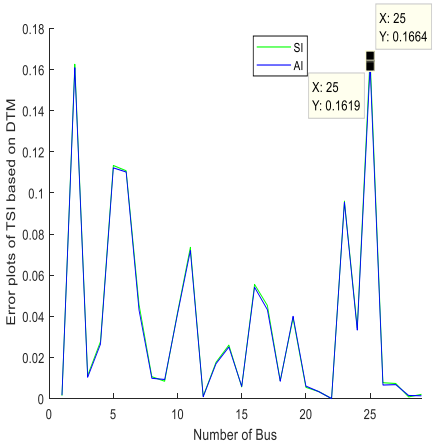

(**a**) Plots TSI evaluated based on DTM for fault clearing time of 150 ms

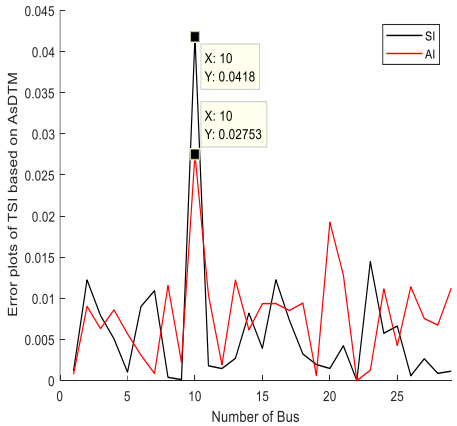

(**b**) Plots TSI evaluated based on AsDTM for fault clearing time of 150 ms

Figure 8. *Cont.*

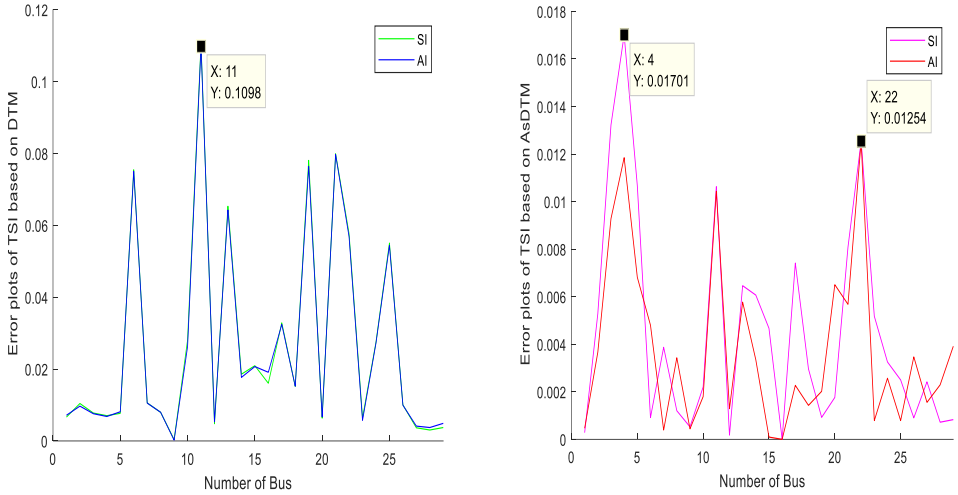

(**c**) Plots TSI evaluated based on DTM for fault clearing time of 250 ms

(**d**) Plots TSI evaluated based on AsDTM for fault clearing time of 250 ms

Figure 8. DTM- and AsDTM-based SI and AI error plots for 39-bus test system plots.

Similarly, when the fault is cleared after 250 ms, the magnitudes of the generated SI and AI error by the proposed AsDTM-based evaluation method are 0.01701 and 0.01254, respectively, for the 39-bus test system and 0.03661 and 0.02842, respectively, for the 9-bus test system and the magnitudes of the generated SI and AI error by the DTM-based evaluation method are 0.1098 for the 39-bus test system and 0.685 and 0.5542 for the 9-bus test system, respectively.

Compared to the proposed method, the magnitude of the SI and AI error generated by the classical DTM-based evaluation method is relatively greater. This shows that more accurate indices are evaluated based on the proposed AsDTM method. A summary of the TS indices error magnitude resulted from using AsDTM and DTM assessment methods relative to the benchmark results are given in Table 6 below.

Table 6. TSI error by AsDTM and DTM methods relative to the benchmark results.

Test System	Fault Cleared After	Assessment Method	Maximum TSI Error	
			SI	AI
9 bus	150 ms	AsDTM	0.03145	0.02427
		DTM	0.1327	0.1327
	250 ms	AsDTM	0.03661	0.02842
		DTM	0.685	0.5542
39 bus	150 ms	AsDTM	0.0418	0.02753
		DTM	0.1664	0.1619
	250 ms	AsDTM	0.01701	0.01254
		DTM	0.1098	0.1098

From Table 6, we can conclude that using the proposed AsDTM method in terms of the DTM method for contingency screening and ranking improves the accuracy of the TSI evaluation results by 74% up to 83% if the fault is cleared after 150 ms and by 84% up to 94% if the fault is cleared after 250 ms. All the test and analysis results given above prove that the proposed AsDTM method of contingency screen ranking provides more accurate results.

3.2.2. Validation of the Assessment Speed of the Proposed Method

Figures 9a–c and 10a–c show the total elapsed time to evaluate TS indices for contingency screening and ranking based on AsDTM, DTM, and Rk4 methods using both the 39-bus and the 9-bus test system. The total assessment times required to evaluate TS indices

based on AsDTM, DTM, and Rk4 methods are 11.671 s, 20.962 s, and 65.65 s, respectively, for the 9-bus test system and 194.084 s, 279.047 s, and 768.062 s, respectively, for the 39-bus test system.

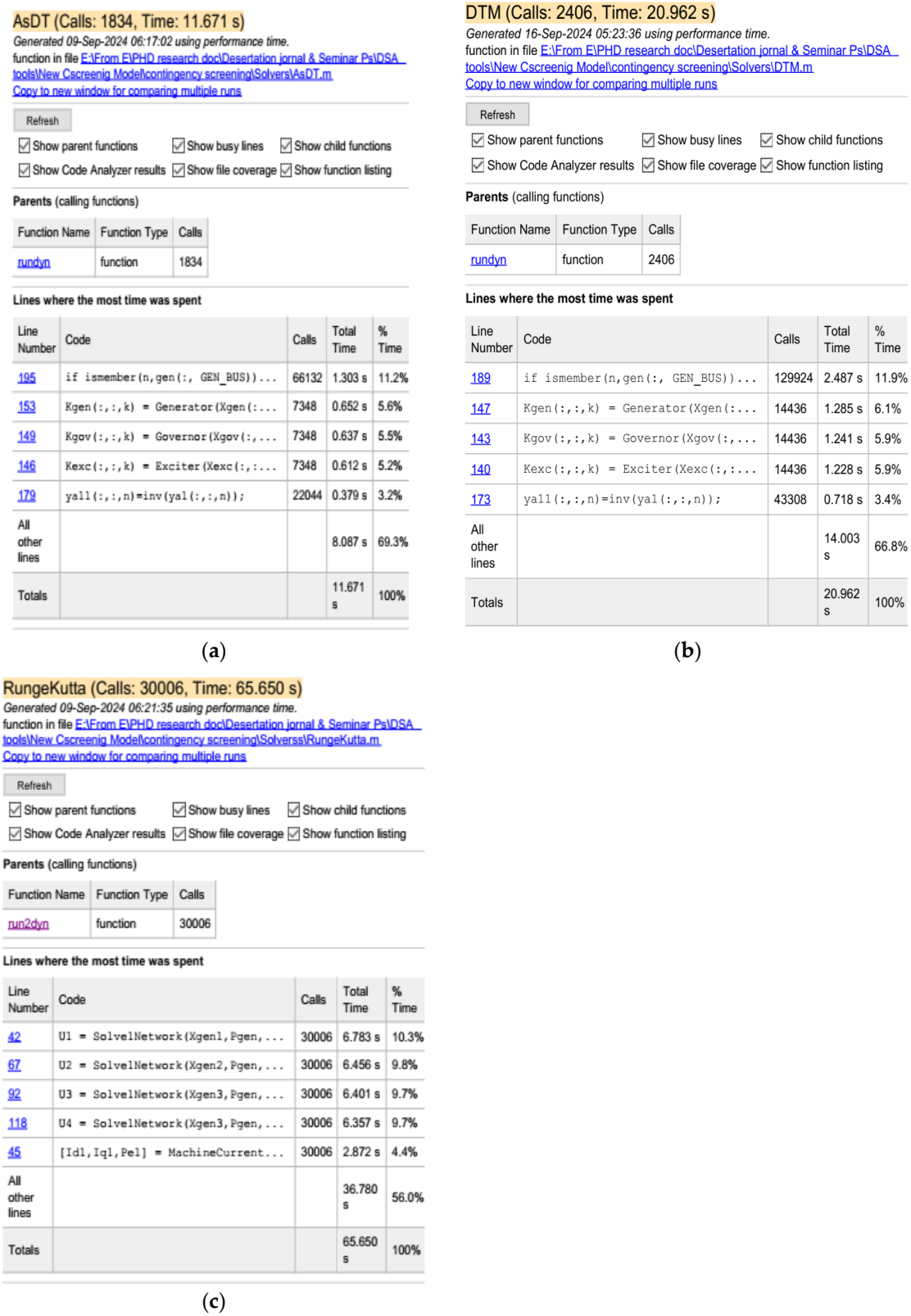

AsDT (Calls: 1834, Time: 11.671 s)

Generated 09-Sep-2024 06:17:02 using performance time.
function in file E:\From E\PHD research doc\Desertation jornal & Seminar Ps\DSA tools\New Cscreenig Model\contingency screening\Solvers\AsDT.m
Copy to new window for comparing multiple runs

Refresh

☑ Show parent functions ☑ Show busy lines ☑ Show child functions
☑ Show Code Analyzer results ☑ Show file coverage ☑ Show function listing

Parents (calling functions)

Function Name	Function Type	Calls
rundyn	function	1834

Lines where the most time was spent

Line Number	Code	Calls	Total Time	% Time
195	`if ismember(n,gen(:, GEN_BUS))...`	66132	1.303 s	11.2%
153	`Xgen(:,:,k) = Generator(Xgen(:...`	7348	0.652 s	5.6%
149	`Xgov(:,:,k) = Governor(Xgov(:,...`	7348	0.637 s	5.5%
146	`Xexc(:,:,k) = Exciter(Xexc(:,:...`	7348	0.612 s	5.2%
179	`yal1(:,:,n)=inv(yal(:,:,n));`	22044	0.379 s	3.2%
All other lines			8.087 s	69.3%
Totals			11.671 s	100%

(**a**)

DTM (Calls: 2406, Time: 20.962 s)

Generated 16-Sep-2024 05:23:36 using performance time.
function in file E:\From E\PHD research doc\Desertation jornal & Seminar Ps\DSA tools\New Cscreenig Model\contingency screening\Solvers\DTM.m
Copy to new window for comparing multiple runs

Refresh

☑ Show parent functions ☑ Show busy lines ☑ Show child functions
☑ Show Code Analyzer results ☑ Show file coverage ☑ Show function listing

Parents (calling functions)

Function Name	Function Type	Calls
rundyn	function	2406

Lines where the most time was spent

Line Number	Code	Calls	Total Time	% Time
189	`if ismember(n,gen(:, GEN_BUS))...`	129924	2.487 s	11.9%
147	`Xgen(:,:,k) = Generator(Xgen(:...`	14436	1.285 s	6.1%
143	`Xgov(:,:,k) = Governor(Xgov(:,...`	14436	1.241 s	5.9%
140	`Xexc(:,:,k) = Exciter(Xexc(:,:...`	14436	1.228 s	5.9%
173	`yal1(:,:,n)=inv(yal(:,:,n));`	43308	0.718 s	3.4%
All other lines			14.003 s	66.8%
Totals			20.962 s	100%

(**b**)

RungeKutta (Calls: 30006, Time: 65.650 s)

Generated 09-Sep-2024 06:21:35 using performance time.
function in file E:\From E\PHD research doc\Desertation jornal & Seminar Ps\DSA tools\New Cscreenig Model\contingency screening\Solverss\RungeKutta.m
Copy to new window for comparing multiple runs

Refresh

☑ Show parent functions ☑ Show busy lines ☑ Show child functions
☑ Show Code Analyzer results ☑ Show file coverage ☑ Show function listing

Parents (calling functions)

Function Name	Function Type	Calls
run2dyn	function	30006

Lines where the most time was spent

Line Number	Code	Calls	Total Time	% Time
42	`U1 = SolvelNetwork(Xgen1,Pgen,...`	30006	6.783 s	10.3%
67	`U2 = SolvelNetwork(Xgen2,Pgen,...`	30006	6.456 s	9.8%
92	`U3 = SolvelNetwork(Xgen3,Pgen,...`	30006	6.401 s	9.7%
118	`U4 = SolvelNetwork(Xgen3,Pgen,...`	30006	6.357 s	9.7%
45	`[Id1,Iq1,Pe1] = MachineCurrent...`	30006	2.872 s	4.4%
All other lines			36.780 s	56.0%
Totals			65.650 s	100%

(**c**)

Figure 9. Elapsed time (**a**) for AsDTM-based TSI evaluation (**b**) for DTM-based TSI evaluation (**c**) for Rk4-based TSI evaluation, of 9-bus test system.

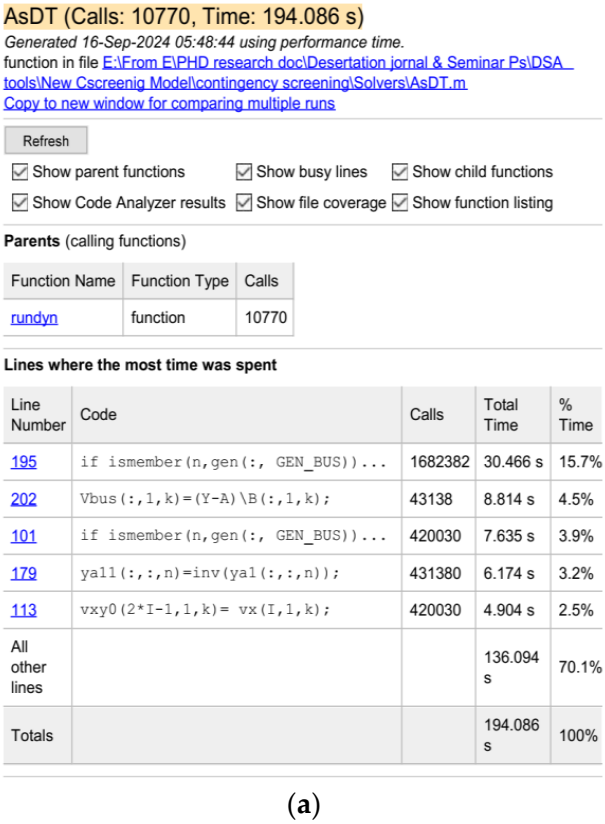

AsDT (Calls: 10770, Time: 194.086 s)

Generated 16-Sep-2024 05:48:44 using performance time.
function in file E:\From E\PHD research doc\Desertation jornal & Seminar Ps\DSA tools\New Cscreenig Model\contingency screening\Solvers\AsDT.m
Copy to new window for comparing multiple runs

Refresh

☑ Show parent functions ☑ Show busy lines ☑ Show child functions
☑ Show Code Analyzer results ☑ Show file coverage ☑ Show function listing

Parents (calling functions)

Function Name	Function Type	Calls
rundyn	function	10770

Lines where the most time was spent

Line Number	Code	Calls	Total Time	% Time
195	`if ismember(n,gen(:, GEN_BUS))...`	1682382	30.466 s	15.7%
202	`Vbus(:,1,k)=(Y-A)\B(:,1,k);`	43138	8.814 s	4.5%
101	`if ismember(n,gen(:, GEN_BUS))...`	420030	7.635 s	3.9%
179	`ya11(:,:,n)=inv(ya1(:,:,n));`	431380	6.174 s	3.2%
113	`vxy0(2*I-1,1,k)= vx(I,1,k);`	420030	4.904 s	2.5%
All other lines			136.094 s	70.1%
Totals			194.086 s	100%

(**a**)

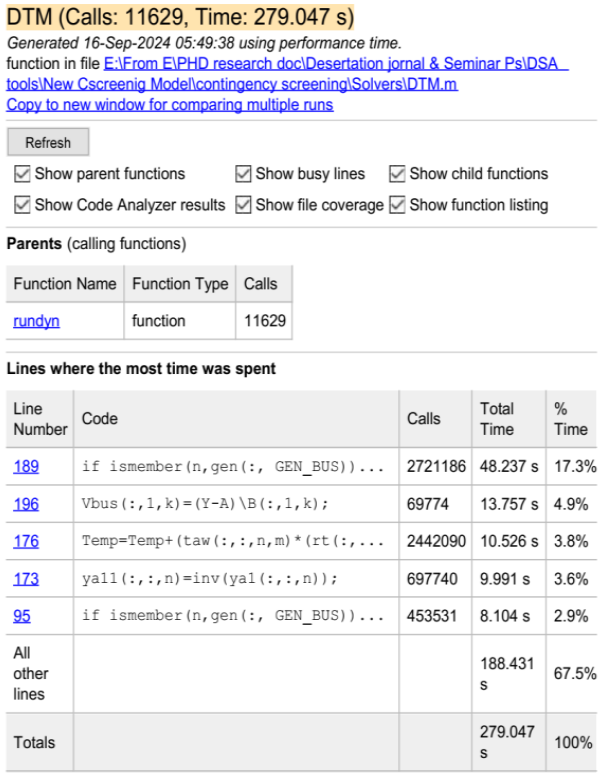

DTM (Calls: 11629, Time: 279.047 s)

Generated 16-Sep-2024 05:49:38 using performance time.
function in file E:\From E\PHD research doc\Desertation jornal & Seminar Ps\DSA tools\New Cscreenig Model\contingency screening\Solvers\DTM.m
Copy to new window for comparing multiple runs

Refresh

☑ Show parent functions ☑ Show busy lines ☑ Show child functions
☑ Show Code Analyzer results ☑ Show file coverage ☑ Show function listing

Parents (calling functions)

Function Name	Function Type	Calls
rundyn	function	11629

Lines where the most time was spent

Line Number	Code	Calls	Total Time	% Time
189	`if ismember(n,gen(:, GEN_BUS))...`	2721186	48.237 s	17.3%
196	`Vbus(:,1,k)=(Y-A)\B(:,1,k);`	69774	13.757 s	4.9%
176	`Temp=Temp+(taw(:,:,n,m)*(rt(:,...`	2442090	10.526 s	3.8%
173	`ya11(:,:,n)=inv(ya1(:,:,n));`	697740	9.991 s	3.6%
95	`if ismember(n,gen(:, GEN_BUS))...`	453531	8.104 s	2.9%
All other lines			188.431 s	67.5%
Totals			279.047 s	100%

(**b**)

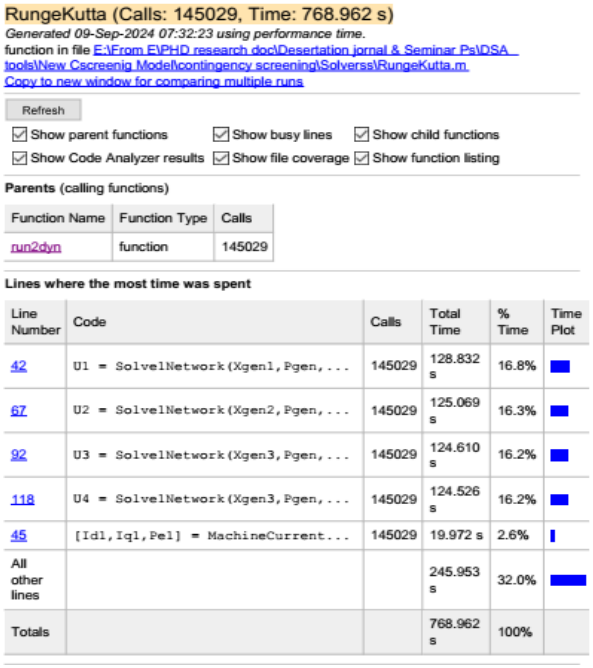

RungeKutta (Calls: 145029, Time: 768.962 s)

Generated 09-Sep-2024 07:32:23 using performance time.
function in file E:\From E\PHD research doc\Desertation jornal & Seminar Ps\DSA tools\New Cscreenig Model\contingency screening\Solverss\RungeKutta.m
Copy to new window for comparing multiple runs

Refresh

☑ Show parent functions ☑ Show busy lines ☑ Show child functions
☑ Show Code Analyzer results ☑ Show file coverage ☑ Show function listing

Parents (calling functions)

Function Name	Function Type	Calls
run2dyn	function	145029

Lines where the most time was spent

Line Number	Code	Calls	Total Time	% Time	Time Plot
42	`U1 = SolvelNetwork(Xgen1,Pgen,...`	145029	128.832 s	16.8%	
67	`U2 = SolvelNetwork(Xgen2,Pgen,...`	145029	125.069 s	16.3%	
92	`U3 = SolvelNetwork(Xgen3,Pgen,...`	145029	124.610 s	16.2%	
118	`U4 = SolvelNetwork(Xgen3,Pgen,...`	145029	124.526 s	16.2%	
45	`[Id1,Iq1,Pe1] = MachineCurrent...`	145029	19.972 s	2.6%	
All other lines			245.953 s	32.0%	
Totals			768.962 s	100%	

(**c**)

Figure 10. Elapsed time (**a**) for AsDTM-based TSI evaluation (**b**) for DTM-based TSI evaluation (**c**) for Rk4-based TSI evaluation, of 9-bus test system.

Capered with DTM and Rk4, the proposed AsDTM-based contingency screening and ranking method improves the performance efficiency (performance speed) by 44.32% and 82.22% for the 9-bus test system and 30.45% and 74.73% for the 39-bus test system, respectively.

Therefore, from the above assessment and simulation results, compared to the conventional Range–Kutta (Rk4) and the classical DTM methods of contingency screening and

ranking the proposed method improves the assessment speed by more than 74.73% and 30.45%, respectively. Compared to the classical DTM methods of contingency screening and ranking, the proposed method improves the accuracy of the resulting transient stability indices by more than 74%. These results strongly indicate that the proposed contingency screening and ranking method is fast and robust.

A near-real-time DSA cycle time should be short enough for the results to be still meaningful when the evaluation is completed, i.e., in the order of 10 to 15 min [1]. For example, performing a time domain simulation of 5000 contingencies using PowSim for 30 s each on the full UK National Grid Control (NGC) system takes approximately 11.5 h using one computing device. Using a similar computing device with the method of contingency screening proposed in this paper considering only 74% improvement in performance efficiency, the total assessment/simulation time is reduced to 4.14 h. This indicates that compared to the traditional numerical integration method, the proposed method performs with a smaller number of parallel computing devices to complete the whole assessment/simulation processes before the DSA cycle time. Therefore, we can conclude that the proposed contingency screening and ranking method is faster.

4. Conclusions and Future Work

Modern society is very dependent on the availability of electrical energy; therefore, a reliable electricity supply is foundational to all economic and societal activities. To supply this continuously growing demand, the size and complexity of the power supply systems with stochastic generation (due to renewable energy systems) are increasing. Ensuring secure operation of the system during widely varying loading scenarios or following possible unforeseen events represents an immense challenge to the system operator. Most of the recent methods of stability assessment are based on extensive off-line computations and, consequently, may no longer be sufficient; hence, a near-real-time DSA is significantly demanding. The near-real-time application of DSA to a realistic network needs sufficient methods to screen and rank large numbers of contingencies to be investigated by DSA tools.

In this paper, a transient stability-based fast and robust power system contingency screening and ranking method are proposed. Transient stability indices are generated from the AsDTM-based power system transient stability analysis results at each simulation time step. Two types of TS indices are evaluated. Those indices evaluated based on the analysis results of the machine's state variables (as rotor angle deviations (δ), angular speed ($\acute{\omega}$), etc) are represented as state variable indices (SI) and those evaluated based on the simulation results of the machine's bus complex bus voltages (such as bus voltage magnitude (V) and voltage angle (θ)) are represented as algebraic variable indices (AI). These indices are evaluated as the normalized weighted sum of squares of error at every simulation time step. As described in Section 3 above, compared with the classical DTM method the proposed AsDTM-based power system contingency screening and ranking method improves the accuracy of resulting indices by more than 74%. Similarly, compared with Rk4 and DTM the proposed AsDTM improves the total assessment time indices (evaluation + ranking) by more than 74.73% and 30.45%, respectively. This shows that the performance efficiency (performance speed) of the proposed method is significantly improved. The approach and indices are relatively simpler and can easily be integrated into an energy management system (EMS) or remedial action scheme (RAS) for determining the state of power system in case of large disturbances. Extending the approach for detail transient stability assessment of a near-real-time DSA session will be our next focus of research.

Author Contributions: Conceptualization. Methodology, software, formal analysis, investigation, resources, data curation, writing—original draft preparation, writing—review and editing, by T.L.K. Validation, visualization by T.L.K. and F.S. Supervision, project administration, by F.S. All authors have read and agreed to the published version of the manuscript.

Funding: This research received no external funding.

Data Availability Statement: All power flow data for the test cases are taken from the Matpower software package cited in the reference [29]. All dynamic data used for machines and their controllers are given in [24] Appendix A. Simulation codes are developed in a Matlab 2017b environment.

Conflicts of Interest: The authors declare no conflicts of interest.

References

1. Edwards, A.R. Detection of Instability in Power Systems Using Connectionism. Ph.D. Thesis, University of Bath, Bath, UK, 1995.
2. Tomsovic, K.L.; Sauer, P.W. *Vijay Vittal, Power System Stability and Control*; Taylor and Francis Group: London, UK, 2006.
3. Alvarez, J.M.G. Critical Contingencies Ranking for Dynamic Security Assessment Using Neural Networks. In Proceedings of the Intelligent System Applications to Power Systems, Curitiba, Brazil, 8–12 November 2009.
4. Tilman, J.; Weckesser, G. On-line Dynamic Security Assessment in Power Systems. Ph.D. Thesis, Department of Electrical Engineering Centre for Electric Power and Energy (CEE), Technical University of Denmark, Kongens Lyngby, Denmark, 2014.
5. Bose, A.; Fu, C. Contingency ranking based on severity indices in Dynamic Security Assessment. *IEEE Trans. Power Syst.* **1999**, *14*, 980–986.
6. Grillo, S.; Massucco, S.; Pitto, A.; Silvestro, F. Indices-based Voltage Stability Monitoring of the Italian HV Transmission System. In Proceedings of the Transmission & Distribution Conference and Exposition, New Orleans, LA, USA, 19–22 April 2010.
7. Kolluri, V.; Mandal, S.; Vaiman, M.Y.; Vaiman, M.M.; Lee, S.; Hirsch, P. Fast Fault Screening Approach to Assessing Transient Stability in Entergy's Power System. In Proceedings of the 2007 IEEE Power Engineering Society General Meeting, Tampa, FL, USA, 24–28 June 2007.
8. Oyekanmi, W.A.; Radman, G.; Ajewole, T.O. Transient stability based dynamic security assessment indices. *Cogent Eng.* **2017**, *4*, 1295506. [CrossRef]
9. Pai, M. *Energy Function Analysis for Power System Stability*; Kluwer Academic Publishers: London, UK, 1989.
10. Pavella, M.; Ernst, D.; Ruiz-Vega, D. *Transient Stability of Power Systems: A Unified Approach to Assessment and Control*; Kluwer Academic Publishers: London, UK, 2000.
11. Voropai, N.I.; Kurbatsky, V.G.; Tomin, N.V.; Panasetsky, D.A. Preventive and emergency control of intelligent power systems. In Proceedings of the 2012 IEEE PES Innovative Smart Grid Technologies (ISGT Europe), Berlin, Germany, 14–17 October 2012.
12. Fu, C.; Bose, A. Contingency Ranking Based on Severity Indices in Dynamic Security Analysis. *IEEE Trans. Power Syst.* **1999**, *14*, 980–985. [CrossRef]
13. Chadalavada, V.; Vittal, V.; Ejebe, G.C.; Irisarri, G.D.; Tong, J.; Pieper, G.; McMullen, M. An On-Line Contingency Filtering Scheme for Dynamic Security Assessment. *IEEE Trans. Power Syst.* **1997**, *12*, 153–161. [CrossRef]
14. Lee, B.; Kwon, S.H.; Lee, J.; Nam, H.K.; Choo, J.B.; Jeon, D.H. Fast contingency screening for online transient stability monitoring and assessment of the KEPCO system. *IEEE Proc. Gener. Transm. Distrib.* **2003**, *150*, 399–404. [CrossRef]
15. Xue, Y.; Pavella, M. Extended equal-area criterion: An analytical ultrafast method for transient stability assessment and preventive control of power systems. *Int. J. Electr. Power Energy Syst.* **1989**, *11*, 131–149. [CrossRef]
16. Xue, Y.; Huang, T.; Xue, F. Effective and Robust Case Screening for Transient Stability Assessment. In Proceedings of the 2013 IREP Symposium Bulk Power System Dynamics and Control—IX Optimization, Security and Control of the Emerging Power Grid, Rethymno, Greece, 25–30 August 2013; pp. 1–8.
17. Xue, Y.; Rousseaux, P.; Gao, Z.; Belhomme, R.; Euxible, E.; Heilbronn, B. Dynamic Extended Equal Area Criterion: Part 1. Basic formulation. In Proceedings of the IEEE/NTUA Athens Power Tech Conference, Athens, Greece, 5–8 September 1993; Volume 71, pp. 889–895.
18. Xue, Y.; Zhang, Y.; Gao, Z.; Rousseaux, P.; Wehenkel, L.; Pavella, M.; Trotignon, M.; Duchamp, A.; Heilbronn, B. Dynamic Extended Equal Area Criterion Part 2. Embedding fast valving and automatic voltage regulation. In Proceedings of the IEEE/NTUA Athens Power Tech Conference, Athens, Greece, 5–8 September 1993; Volume 71, pp. 896–900.
19. Liu, C.W.; Su, M.C.; Tsay, S.S.; Wang, Y.J. Application of a Novel Fuzzy Neural Network to Real-Time Transient Stability Swings Prediction Based on Synchronized Phasor Measurements. *IEEE Trans. Power Syst.* **1999**, *14*, 685–692.
20. Hashiesh, F.; Mostafa, H.E.; Khatib, A.R.; Helal, I.; Mansour, M.M. An intelligent wide area synchrophasor based system for predicting and mitigating transient instabilities. *IEEE Trans. Smart Grid* **2012**, *3*, 645–652. [CrossRef]
21. Liu, Y.; Sun, K. Solving Power System Differential Algebraic Equations Using Differential Transformation. *IEEE Trans. Power Syst.* **2019**, *35*, 2289–2299. [CrossRef]
22. El-Zahar, E.R. An Adaptive Step-Size Taylor Series Based Method and Application to Nonlinear Biochemical Reaction Model, Trends. *Appl. Sci. Res.* **2012**, *7*, 901–912.
23. El-Zahar, E.R. Applications of Adaptive Multi Step Differential Transform Method to Singular Perturbation Problems Arising in Science and Engineering. *Appl. Math. Inf. Sci.* **2015**, *9*, 223–232. [CrossRef]
24. Kumissa, T.L.; Shewarega, F. Fast Power System Transient Stability Simulation. *Energies* **2023**, *16*, 7157. [CrossRef]
25. Pukhov, E.; Georgii, G. Differential transformation method and circuit theory. *Int. J. Circuit Theory Appl.* **1982**, *10*, 265–276. [CrossRef]
26. Lindi, T.; Shewarega, F. Adaptive order and step-size differential transformation method-based power system transient stability simulation. *Aust. J. Electr. Electron. Eng.* **2024**, 1–14. [CrossRef]

27. Available online: http://www.esat.kuleuven.be/electa/teaching/matdyn/ (accessed on 26 May 2020).
28. The MathWorks Inc. *MATLAB (R2017b)*; The MathWorks Inc.: Natick, MA, USA, 2017.
29. Zimmerman, R.D.; Murillo-Sánchez, C.E.; Thomas, R.J. MATPOWER: Steady-State Operations, Planning, and Analysis Tools for Power Systems Research and Education. *IEEE Trans. Power Syst.* **2011**, *26*, 12–19. [CrossRef]